CORRELATION OF MEMBRANE SURFACE CHARACTERISTICS AND SOLUTION ENVIRONMENT WITH ULTRAFILTRATION MEMBRANE PERFORMANCE

A THESIS

SUBMITTED TO THE

UNIVERSITY OF POONA

FOR THE DEGREE OF

DOCTOR OF PHILOSOPHY

IN CHEMISTRY

By

DEEPAK A. MUSALE

UNDER THE GUIDANCE OF

Dr. S.S. KULKARNI

POLYMER SCIENCE AND ENGINEERING GROUP

CHEMICAL ENGINEERING DIVISION

NATIONAL CHEMICAL LABORATORY

PUNE 411 008

NOVEMBER 1996

DECLARATION

Certified that the work incorporated in the thesis **"CORRELATION OF MEMBRANE SURFACE CHARACTERISTICS AND SOLUTION ENVIRONMENT WITH ULTRAFILTRATION MEMBRANE PERFORMANCE"** submitted by Mr. Deepak A. Musale was carried out by the candidate under my supervision. Such material as has been obtained from other sources has been duly acknowledged in the thesis.

Sudhir Kulkarni

National Chemical Laboratory
Pune 411 008

(Dr. S.S. Kulkarni)
Research Guide

Dedicated to

my parents and teachers

"Death ends a life, but it doesnot end a relationship, which struggles on in the survivor's mind towards some resolution which it may never find."

Erich Segal

Acknowledgments

I would like to express my deep sense of gratitude to my thesis supervisor, Dr. S.S. Kulkarni without whose support this thesis would not have been possible. I am grateful to him for his constant encouragement and kindness shown by him.

I am thankful to Director, NCL, who permitted me to present the work in the form of thesis.

The research fellowship awarded to me by CSIR, New Delhi is gratefully acknowledged.

I would like to thank Dr. B.D. Kulkarni, Head, C.E. div., Dr M.G. Kulkarni, Head, PSE group, and Mr. S. Nene, Head, Bio. Eng. group, who permitted me to avail of the research facilities in the division.

I am greatful to Dr. A.P. Joshi, Dr. S.G. Joshi and Dr. A.M. Bodhe for the fruitful discussions on various topics of my research work with them. I would also like to thank them for their generous help in my everyday work.

Dr. (Mrs) N.R. Deshpande (S.P. College Pune) and Dr. S.K. Kamat (NCL) who taught me various practical techniques in the early stages of my research career are greatfully acknowledged.

I would like to thank my colleagues Dr. Pandit, Dr. Deshmukh, Dr. Kharul and Bhagyashree for their help at various stages of my work.

My thanks are due to Sandeep and Anuj, with whom I had very frequent discussions on novel ideas on my research topic as well as on various topics in science. I would like to specially thank Sandeep, who taught me various aspects of chemical engineering and computer science.

It would be unfair if I fail to thank my parents, brothers and sister for their patience and unstinted support during the course of this work.

I must thank my colleagues Jaya, Arvi, Madhuri, Prasad, Vidya, Leena, Deepak, Ajit, Mahendra and Soraj without whose help my thesis completion would have been really a difficult task. I am grateful to them.

I must not forget to thank my friends Raju, Amolak, Vilas, Vijay and Prabhakar whose moral support made me comfortable during the course of my studies.

I would like to thank Dr. Badrinarayanan and Mr. Sanjay Patil for their help in getting ESCA and SEM spectral data.

Deepak A. Musale

C O N T E N T S

List of figures

List of Tables

Chapter 6

Abbreviations

AN	Acrylonitrile
AOT	Aorosol-OT
AW	Acid whey
BSA	Bovine serum albumin
CTAB	Cetyl trimethyl ammonium bromide
CW	Cheese whey
DMF	Dimethyl formamide
DMSO	Dimethyl sulfoxide
EDS	Energy dispersive spectroscopy
ESCA	Electron spectroscopy for chemical analysis
EVA	Ethylene-vinyl acetate
EVAL	Ethylene-vinyl alcohol
FR	Flux recovery
FTIR-ATR	Fourior transform infrared -attenuated total reflection
Hb	Hemoglobin
HBA	Hydroxybutyl acrylate
HEA	Hydroxyethyl acrylate
HEMA	2-Hydroxyethyl methacrylate
IEP	Isoelectric point
IgG	Immunoglobin G
LB	Langmuir-Blodgett
MC	Methyl cellulose
MWCO	Molecular weight cut-off
PAN	Poly(acrylonitrile)
PEEK	Poly(etheretherketone)
PEG	Polyethyleneglycol
PEI	Polyetherimide / Polyethyleneimine
PES	Polyethersulfone

PI	Polyimide
PVA	Polyvinylalcohol
PVP	Polyvinylpyrrolidone
RF	Relative flux
RO	Reverse osmosis
SEM	Scanning electron microscopy
SW	Shrikhand whey
TIRF	Total internal reflection fluorescence
UF	Ultrafiltration
VCF	Volume concentration factor

List of Symbols

A	Membrane area (cm^2)
a, c	Adjustable parameters (eqn. 3.14)
b	Ratio of frictional force of moving solute to that of bulk solution (eqn. 3.6) / adjustable parameter (eqn. 3.14)
$\overline{B}$	Constant (eqn. 3.7)
C	Solute concentration (mg/ml)
D_∞	Solute diffusivity in bulk solution ($cm^2\ s^{-1}$)
d_h	Hydraulic diameter (cm)
d_i	Internal diameter of tube (cm) (eqn. 3.34)
d_s	Solute diameter (cm)
d_w	Diameter of water / solvent molecule (cm)
E	Represents potential function for long range interactions
I_a	Applied current (mA)
I	Ionic strength (M)
J	Flow rate ($cm^3\ s^{-1}$)
J_∞	Limiting flux ($cm\ s^{-1}$)
J_i	Flow rate of protein molecules to membrane surface due to protein-membrane electrostatic interaction ($cm^3\ s^{-1}$)(eqn. 3.22)
J_v	Volumetric flow rate ($cm^3\ s^{-1}$)
J_w	Pure water flux ($cm\ s^{-1}$)
$\overline{J_s}$	Overall solute flux ($cm\ s^{-1}$) (eqn. 3.8)
k	Mass transfer coefficient ($cm\ s^{-1}$)
K_C	Hindrance factor for convective transport (eqn. 3.9)
K_D	Hindrance factor for diffusion (eqn. 3.9)
K_L	Hydrodynamic coefficient representing solute velocity lag
K_w	Hydrodynamic coefficient representing drag on solute from pore walls
l	Membrane thickness (cm)

l_c	Cake layer thickness (cm)
n	Exponential factor in van't Hoff relation (eqn. 3.24)
n_i	No. of pores per unit area (eqn 4.4)
P	Applied pressure (kPa)
P'	Local solute permeability (eqn. 3.17)
Pe	Peclet no. (J_v/k)
P_m	Solute permeability
r	Radius (cm)
R	Intrinsic rejection of membrane
$\boldsymbol{R}$	Gas constant
r_a	Effective reduced pore radius (cm) (eqn. 3.7)
R_{bl}	Boundary layer resistance ($cm^{-1)}$
R_c	Cake layer resistance (cm^{-1})
r_c	Specific cake resistance (cm^{-1})
Re	Reynolds no. (vd_h/ν)
R_m	Membrane resistance (cm^{-1})
R_a	Resistance due to adsorption on pore walls (cm^{-1})
R_{cp}	Resistance due to concentration polarization (cm^{-1})
R	Observed solute rejection
R_{osm}	Resistance due to osmotic pressure (cm^{-1})
r_p	Pore radius (cm)
r_s	Radius of solute particle (cm)
r_h	Hydraulic radius of stirred cell (cm)
Sc	Schmidt no. (ν/D)
Sh	Sherwood no.
T	Absolute temperature (°K)
V	Permeate volume (cm^3)
v	Solvent velocity ($cm\ s^{-1}$)
v_l	Lift velocity (eqn. 3.41)
ΔP	Hydrostatic pressure difference across membrane

X_{AB}	Constant relating the frictional force between solute and solvent to their relative velocity (eqn. 3.6)
$Y(r)dr$	Number of pores with size between r and $r+dr$ (eqn. 3.5)

Subscripts

c	Cake layer
d	Deposited layer
eo	Electro-osmotic
f	Feed
g	Gel layer
i	Initial / species i / internal
l	Liquid
p	Permeate
r	Retentate
s	Solute / Polymer (eqn. 4.2)

Superscripts

d	Dispersion force component of surface free energy (eqn. 4.2)
p	Polar force component of surface free energy (eqn. 4.2)

Greek letters

δ	Boundary layer thickness (cm)
τ	Observed solute transmission
τ'	True solute transmission
η	Permeate viscosity (dyne s cm^{-2})
λ	Ratio of solute radius to pore radius (r_s / r_p)
$\phi(r)$	Potential function for the force exerted by the pore wall on the solute
ν	Kinematic viscosity ($cm^2\ s^{-1}$)
σ	Staverman reflection coefficient
σ'	Interfacial tension (dynes cm^{-1})

π	Osmotic pressure (kPa)
$\Delta\pi$	Osmotic pressure difference across the membrane (kPa)
ρ	Density (g cm^{-3})
ξ	Zeta potential (mV)
λ_0	Specific conductivity of electrolyte solution (mS cm^{-1})
ε	Cake porosity (eqn. 3.36) / Permittivity of electrolyte solution (mC^2 $dyne^{-1}$ cm^{-2}) (eqn. 4.6)
θ	Contact angle (°)
γ	Surface free energy (erg cm^{-2})
$\dot{\gamma}$	Shear rate (s^{-1})
μ	Proportionality factor accounting for drag forces (eqn. 3.34)

ABSTRACT

Membrane based separation techniques such as ultrafiltration (UF) are being increasingly used in protein purification, concentration and fractionation applications. The viability of UF is frequently adversely affected by membrane fouling and concentration polarization. An important aspect of the fouling process is related to the interactions of the membrane surface with solute molecules. These interactions also affect protein transmission and permeate flux. This thesis studies the effect of changing the membrane surface chemistry (hydrophilicity, surface energy and surface electrostatic charge) and solution environment (pH, concentration) on the membrane filtration characteristics.

Experimental

Membranes were prepared from commercially available acrylonitrile homopolymer (PAN) and from copolymers with 12 - 30 mole % acrylamide prepared by solution polymerization. Membranes were cast from dimethyl formamide solutions of each polymer using water as the coagulating agent. The membrane hydrophilicity and surface charge (in terms of zeta potential) were determined by the contact angle and electroosmosis method, respectively. The pore size distribution was determined by the modified bubble point method and confirmed by neutral solute rejections and water permeation measurements.

The ultrafiltration of bovine serum albumin (BSA), hemoglobin (Hb), BSA-Hb solutions and acid whey (AW), cheese whey (CW) and shrikhand whey (SW) were carried out at 200 kPa and 27-29°C in a stirred cell at various pH values and volume concentration factors. The data was collected in terms of permeate flux, rejection, flux recovery and separation factor (in the case of BSA-Hb).

Results and discussion

The casting conditions were varied so that membranes made from both types of polymers had similar pore sizes. Since steric effects are similar, differences in the UF performance can be ascribed to differences in the membrane surface chemistry. Membranes made from poly(acrylonitrile-*co*-acrylamide) were more hydrophilic, had a lower dispersion component of surface energy and a lower negative surface charge than

those made from poly(acrylonitrile). Since the acrylamide incorporation increases hydrophilicity and decreases surface electrostatic negative charge, it is possible to delineate the relative importance of these effects during UF.

BSA and Hb have similar molecular sizes but Hb is more hydrophobic than BSA and also has an higher isoelectric point (IEP) (pH 6.8 compared to pH 4.8 for BSA). The UF data with these standard proteins can be used to understand the more complex case of whey UF.

Single protein UF (BSA or Hb) :

The permeate fluxes and flux recoveries (in case of BSA UF) increase with increasing pH for both homopolymer and copolymer membranes. This is attributed to decreasing electrostatic attraction, as pH increases up till the IEP, and increasing repulsion above the IEP between protein and membrane. In the case of Hb UF through PAN, a flux minima was also observed at its IEP (pH 6.8), which is attributed to the lack of repulsive interactions at this pH. The permeate fluxes and the flux recoveries were generally higher, at any given pH value, for the copolymer membranes, due mainly to their higher hydrophilicity and reduced dispersive surface energy. The data could be interpreted in terms of protein adsorption on the pore wall and consequent narrowing of the pore size.

In the case of both BSA and Hb UF, the rejection remained constant with pH for the homopolymer membrane because of its hydrophobic nature, while it decreased after the IEP for the copolymer membranes. This is attributed to the higher hydrophilicity and lower negative charge on the copolymer membrane. Hb rejections were higher compared to BSA at any pH value, due to the higher hydrophobicity of Hb.

The UF data with the single proteins can be correlated with hydrophilic and electrostatic interactions between the protein and membrane surface. Electrostatic interactions are important with the hydrophilic copolymer membrane surfaces and with the more hydrophilic protein (BSA). In the case of Hb UF through the PAN membrane, hydrophobic interactions dominate the electrostatic effects.

Binary protein UF (BSA-Hb) :

Because of its hydrophobicity, Hb is expected to be preferentially adsorbed on the membrane surface. This may explain why the permeate flux behaviour with the mixed

proteins is similar to that of Hb alone. The mixed protein data can be explained by the same mechanisms operational for pure Hb UF in combination with BSA-Hb attractive interactions at pH values between the IEPs of BSA and Hb.

BSA rejections in the mixture are higher than with BSA alone. BSA rejection increases initially from pH 4.0 to 5.5 and then remains constant with increasing pH. This is explained mainly by BSA-Hb and protein-membrane electrostatic interactions at these pH values. The Hb rejections trends are similar except for a small decrease after the Hb IEP. This is because of electrostatic repulsion between BSA, Hb and membrane, since all three are negatively charged above the Hb IEP.

Whey Ultrafiltration :

The whey UF data are complex as a result of the multicomponent and non ideal nature of these solutions. All three wheys contain similar proteins with IEP values ranging from pH 5-7. Both AW and SW contain more ash content than CW. SW contains a significantly higher amount of lactic acid than the other two wheys.

The dependence of flux on pH for all three types of natural wheys resembles that seen with mixed protein UF data. The clarification of natural wheys by precipitation at pH 7.5 reduces both salt and protein content, resulting in increased permeate flux and decreased protein rejection. SW clarification results in a marked loss of protein (~ 50%), which may be attributed to the interactions of lactic acid with proteins.

The change in the UF characteristics of clarified wheys can be correlated with the change in protein content / composition. Immunoglobulins are most prone to precipitate at the clarification pH. Thus, in clarified wheys, protein-protein electrostatic interactions can only be repulsive and the flux dependence on pH is similar to pure protein (BSA) UF. The protein rejection trend is also similar to BSA UF.

The copolymer membranes do not show consistently higher fluxes or protein transmissions during whey UF. This may be attributed to the higher protein concentrations in the whey.

Chapter 1

INTRODUCTION

Protein purification, concentration and fractionation are important process steps in food, dairy, biotechnology, downstream processing and pharmaceutical industries. These process steps can be performed by conventional techniques such as centrifugation or precipitation as well as membrane based separation techniques. For example, in downstream processing, cells and cell debris are traditionally removed from the fermentation broth by centrifugation. The recovery of protein from the cell free extract is usually carried out by ammonium sulfate precipitation (Scopes, 1987). Further fractionation / purification is carried out by gel filtration, ion-exchange or affinity chromatography (Asenjo and Patrick, 1990). All of the above separations can also be achieved by microporous membrane based processes such as microfiltration, ultrafiltration and nanofiltration. In recent years these microporous membrane based separations are becoming widely used in such protein process applications.

Ultrafiltration (UF) is considered to be size-exclusion based, pressure-driven process. Typical membrane pore sizes are in the range of 30-1000 Å for UF. UF is mainly used for clarification, concentration and fractionation of macromolecules (Kulkarni et al, 1992a). Thus, the large scale applications of UF are in industries such as food and dairy (Cheryan, 1986; Mohr et al, 1989), downstream processing, biotechnology (Michaels and Matson, 1985; McGregor, 1986), pulp and paper, electronics, wastewater / effluent treatment, tanning and leather, textile, medical and therapeutics (Cheryan, 1986, Kulkarni et al, 1992d).

Definitions :

The viability of UF processing depends primarily on the membrane productivity (flux) and selectivity (rejection). The volumetric flux (J_v) through the membrane is defined as the permeate volume per unit membrane area per unit time. The observed solute rejection (R) is given as :

$$R = 1 - C_p / C_r \tag{1.1}$$

where C_p and C_r are the solute concentrations in the permeate and retentate, respectively. The transmission (τ) of solute through the membrane is defined as (1 - R). If the actual

solute concentration at the membrane surface is C_m ($> C_r$), the true rejection through the membrane is R', given by :

$$R' = 1 - C_p / C_m \qquad (1.2)$$

UF membranes are generally characterized by their molecular weight cut-off (MWCO) value, which is defined as the smallest molecular weight of the species for which the membrane has more than 90% rejection. The typical MWCO values of UF membranes range between 0.5-500 kD (kD = 10^3 daltons).

Although, UF is primarily a size-exclusion based separation process, various solute-membrane interactions are also important in many applications. Membrane performance i.e. flux and rejection, depends not only on membrane porosity but also on membrane characteristics such as surface charge, surface roughness, pore tortuosity etc. and solution properties such as ionic strength, concentration and pH. The isoelectric point (IEP) is defined as the pH at which the net charge on the protein is zero i.e. the number of positive and negative charges on a solute molecule are equal. The ionic strength (I) is defined as :

$$I = \frac{1}{2}\sum_i C_i Z_i^2 \qquad (1.3)$$

where C_i and Z_i are the molar concentration and the valency of the ion respectively.

Advantages of UF :

UF processing has several advantages over conventional methods :

i) Product quality : Since no additional chemicals are typically required in these membrane processes, product purity is maintained. During processing, changes in the temperature, pH and ionic strength of the product can be minimized. This is important while processing biomolecules like proteins and enzymes, which are sensitive to changes in solution environment. Hence, the purity of the product with membrane processes is usually better than that from conventional processes.

ii) Modular configuration : Since UF membranes are assembled in modular form, scale-up is easier. Space requirements are limited.

iii) Processing cost : UF operates at relatively low pressures (2-10 bars) and ambient temperatures with no phase change. Usually, the operating costs of this membrane process is less than those with conventional methods, although the capital investment may be higher.

Limitations of UF :

The major limitations for the use of membrane filtration in many applications are low membrane productivity and insufficient selectivity. These limitations can be blamed on two distinct phenomena : concentration polarization (CP) and membrane fouling. Both of these occur due to rejection of solute molecules at the membrane surface. Fouling necessitates frequent cleaning which can reduce membrane life as well as process productivity. The increased membrane replacement cost and the cleaning cost can make membrane processing uneconomical. Hence, additional understanding of the flux decline mechanism is of great importance.

The membrane process flux is affected by several mass transfer resistances. These are schematically depicted in Figure 1.1. R_m refers to the mass transfer resistance due to the membrane phase itself. Due to membrane selectivity, solute molecules which do not pass through the membrane accumulate at the membrane surface. The mass transfer resistance arising out of this phenomena is called the concentration polarization resistance (R_{cp}). If the solute concentration at the membrane surface approaches the solubility limit, the solute may precipitate or gel; the added mass transfer resistance due to this layer deposited on the membrane surface is R_g. Two additional resistances R_a and R_p refer to the additional mass transfer resistance vis-a-vis a clean membrane with a given pore size. The pore diameter can decrease either due to adsorption on the pore walls or blockage / precipitation of solute within the pores. These additional resistances are referred to as R_a and R_p respectively.

Concentration polarization refers to the increase in concentration of rejected solute at the membrane surface. CP sets in over very short time periods and is considered to be a reversible phenomenon. CP can be reduced mainly by changing physical parameters such

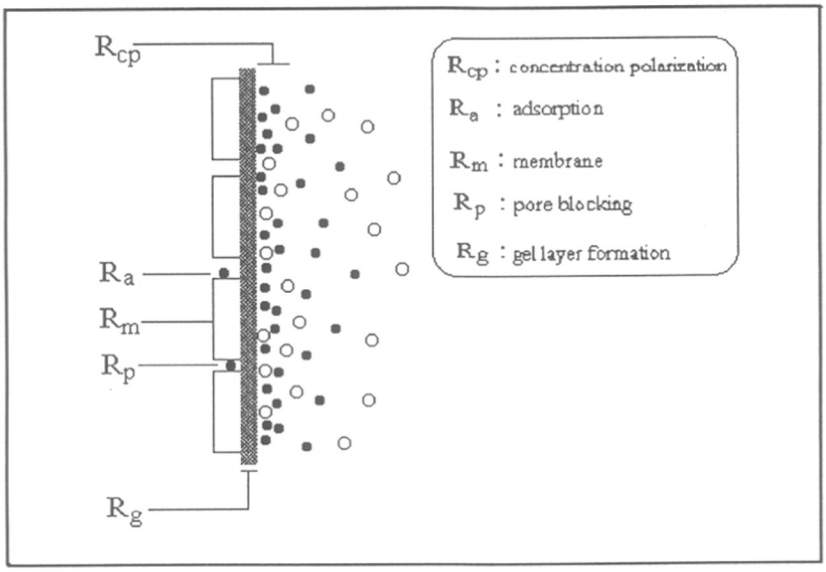

Figure 1.1: Depiction of resistances in membrane filtration.

as module design and system hydrodynamics. These methods are described in section 3.4.2

Fouling is defined as the adsorption or deposition of some of the feed components on the membrane surface (surface fouling) or within the membrane pores (internal fouling).

Fouling results in a long term flux decline with time. It is generally irreversible by physical means, though its effect can be reduced by various techniques related to control of concentration polarization. Fouling can also be reduced by optimizing membrane chemistry and solution environment. Internal fouling which includes solute adsorption on the pore walls can be reduced by backflushing the membranes (only with cylindrical geometry) or membrane cleaning. These methods are described in sections 3.4.3 and 3.4.4.

While both concentration polarization and fouling reduce the flux, they affect solute rejection in different ways. Rejection is either constant or increases after fouling, while it decreases due to concentration polarization. This can decrease concentration efficiency or the extent of fractionation / purification.

Thesis outline :

The thesis is organized in six chapters :

Chapter 1 : Introduction

This chapter deals with the growing importance of UF as an alternative to conventional methods for protein purification, concentration and separation. The importance of fouling in determining the applications of these membrane processes is highlighted. The organization of the thesis is presented and various terms are defined.

Chapter 2 : Problem statement and objectives

In this chapter, the problem areas addressed in this thesis are defined. The objectives of the present work are outlined. The focus of this thesis is on studying the effect of various membrane surface parameters and solution environment variables on filtration characteristics. This involves UF of standard proteins (bovine serum albumin and hemoglobin) and various wheys through poly(acrylonitrile) (PAN) and poly(acrylonitrile-*co*-acrylamide) membranes.

Chapter 3 : Literature review

This chapter reviews the literature on transport through UF membranes, various techniques for control of concentration polarization and fouling, and factors affecting the fouling and transmission of proteins through membranes. The literature relating to UF through modified PAN membranes are also specifically summarized and the limitations pointed out.

Chapter 4 : Experimental

In this chapter, the experimental techniques for polymer preparation and characterization are described along with the membrane fabrication and characterization methods. The methodology of the permeation studies of these membranes with various protein containing solutions are described.

Chapter 5 : Results and discussion

This chapter discusses the experimental results, in terms of permeate flux, solute rejection, flux recovery and protein separation, for the filtration of various test solutions through poly(acrylonitrile) based UF membranes. The permeation characteristics are discussed with reference to the surface properties (hydrophilicity, surface charge / energy) of the membranes and the solution environment (pH, concentration). The results are interpreted in terms of various protein-protein and protein-membrane interactions.

Chapter 6 : Conclusions and recommendations for the future work.

This chapter summarizes the thesis results and data interpretation. It also suggests areas for further work.

Chapter 2

PROBLEM STATEMENT AND OBJECTIVES

The major limitation for application of UF processes is the membrane fouling and concentration polarization phenomena that occur due to rejection of solute molecules at the membrane surface. Concentration polarization can be controlled by changing module design and system hydrodynamics. Fouling depends mainly on various solute-membrane interactions, membrane morphology and solute-solute interactions. Studies of the membrane surface chemistry and solution environment, which are responsible for solute-membrane interactions are important for understanding fouling and its effect on membrane performance.

There are several membrane characteristics and solution parameters which are known to affect membrane performance and fouling behaviour. These are discussed in detail in chapter 3. It is reported in the literature that hydrophilic membranes tend to adsorb less protein, and exhibit higher fluxes and slower flux declines than hydrophobic membranes with similar other characteristics. Also, it is known that electrostatic charges on both protein and membrane affect the permeate flux, protein transmission and the fouling mechanism. The pH, concentration and ionic strength of the protein containing solution is known to affect flux and protein transmission through membranes. The protein solution filtration characteristics are also affected by the electrostatic and hydrophobic interactions between the proteins themselves and between protein and membrane.

It is obvious from the above, that in addition to pore size, several other factors also affect membrane performance and fouling characteristics. Since several factors are involved, it is sometimes difficult to identify specific factors responsible for observed membrane performance in a given application. Furthermore, some variables such as pH could have opposing effects on membrane flux and transmission. For example, charge repulsion between membrane and solute may cause increased rejection due to charge exclusion; however, it may also cause reduced rejection due to less adsorption and consequently less pore narrowing. Increasing or decreasing pH away from the protein IEP can increase repulsive interactions between protein molecules; however, at the same time this may lead to attractive interactions between positively charged protein and negatively charged membrane surfaces. These effects could also affect membrane performance in

opposing manners. The relative importance of membrane hydrophilicity and membrane charge in various solution environments is also not clear.

The membrane pore size is generally expected to be a principal factor affecting rejection and flux. The nature of the solute-membrane interactions are expected to be particularly important as the solute size : pore size ratio increases (section 3.5.1). Therefore it is of interest to study the transport of similar sized solutes through membranes with similar pore sizes where other variables such as electrostatic charge, surface energy and hydrophilicity have been varied.

Scope of thesis

The present work involves study of the *fouling* characteristics of poly(acrylonitrile) (PAN) based UF membranes. The membrane performance has been studied in terms of membrane surface chemistry (hydrophilicity, surface charge and surface energy) and solution environment (pH and solute concentration).

The PAN based membranes were prepared from poly(acrylonitrile) and poly(acrylonitrile-*co*-acrylamide) with varying acrylonitrile : acrylamide ratios. The membranes made from the copolymers were more hydrophilic, less negatively charged and had a lower dispersion force component of surface free energy than those made from the homopolymer. The ultrafiltration characteristics of these membranes were studied with standard proteins such as bovine serum albumin (BSA), hemoglobin (Hb) and with different wheys. BSA and Hb have similar molecular sizes but Hb is more hydrophobic than BSA. BSA has an IEP of 4.8 while Hb is positively charged upto pH 6.8. The feed solution pH was varied so that data could be obtained when the proteins were both positively charged, neutral as well as negatively charged.

Objectives

The broad objective of this thesis was to study the effect of changing the membrane surface chemistry (hydrophilicity, surface charge and surface energy) and solution environment (pH and concentration) on the membrane filtration characteristics. The detailed objectives are explained below :

A) To synthesize copolymers of acrylonitrile with varying amounts of acrylamide (12-30 mole %) and to characterize both homopolymer and copolymers in terms of hydrophilicity and surface energy.

B) To fabricate ultrafiltration membranes from poly(acrylonitrile) (PAN) and poly(acrylonitrile-*co*-acrylamide) and characterize these for pore size and surface electrostatic charge.

C) To investigate ultrafiltration characteristics such as permeate flux, protein transmission and flux recovery at different pH values for bovine serum albumin (BSA) ultrafiltration through PAN and copolymer based membranes. The BSA charge varies as a result of changing pH. Since the membranes were prepared so as to have similar pore sizes, this study allows an evaluation of the effect of increased hydrophilicity combined with reduced negative charge in the case of copolymer based membranes.

D) To compare hemoglobin (Hb) ultrafiltration characteristics with those of BSA ultrafiltration in PAN and copolymer membranes. While BSA and Hb are of similar size, Hb is more hydrophobic and is positively charged upto pH 6.8 while BSA is positively charged only below pH 4.8. This study allows an evaluation of the effect of the above protein charge and hydrophilicity characteristics on the performance of PAN and copolymer based membranes.

E) To study the effect of protein-protein interactions between BSA and Hb during ultrafiltration of solutions containing both proteins through PAN and copolymer membranes.

F) To study the effect of interactions between various solution components (salts, proteins) on the ultrafiltration performance of wheys from various sources (acid, cheese and shrikhand).

Chapter 3

LITERATURE REVIEW

In this chapter, the literature relevant to transport through UF membranes is reviewed. The literature review is divided into four main sections;

i) theoretical background of transport through UF membranes,

ii) techniques for the control of concentration polarization and fouling and,

iii) factors affecting the fouling and protein transmission through membranes, and

iv) summary and limitations of previous UF studies with modified poly(acrylonitrile) membranes.

3.1 TRANSPORT THROUGH MICROPOROUS MEMBRANES

In the simplest terms, transport through microporous membranes can be thought of as flow through pores, where the flow is modified by factors such as pore size and pore size distribution, pore tortuosity and interactions of the feed components with themselves and the membrane (Kulkarni et al, 1992b).

Idealizing the pore structure by assuming a uniform pore radius (r_p) and pore length (l), the volumetric flow rate can be given by Hagen-Poiseuille's equation as,

$$J_v = \frac{n\pi r_p^4}{8\eta l}\Delta p \tag{3.1}$$

where n is the no. of pores per unit area, η is the permeate viscosity and Δp is the applied pressure.

The solute rejection (R') defined in eqn. (1.2) can be related to the ratio (λ) of radii of the solute, r_s, and the pore, r_p, by the Ferry equation (Ferry, 1936),

$$R' = [\lambda(2-\lambda)]^2 \qquad \text{for } \lambda < 1 \tag{3.2}$$

$$R' = 1 \qquad \text{for } \lambda \geq 1 \tag{3.3}$$

Zeman and Wales (1981) have extended this expression to take into account the solute velocity lag. This more accurate expression for the observed solute rejection is given as :

$$R' = 1 - \left\{1 - [\lambda(2-\lambda)]^2\right\} \exp(-0.7146\lambda^2) \tag{3.4}$$

This correction factor is particularly significant for λ values greater than 0.5.

Hagen-Poiseuille's equation (eqn. 3.1) does not take into account any membrane characteristics other than pore radius. A more comprehensive model (Surface force - Pore flow) developed by Matsuura and Sourirajan (1981) takes into account solute size, pore diameter, solute/membrane friction and solute/membrane interactions. According to this model, the solute rejection is given as,

$$R' = 1 - \frac{1}{C_f} \frac{\int_{-\infty}^{\infty} Y(r)[\int_0^r C_p(r')v(r')r'dr']dr}{\int_{-\infty}^{\infty} Y(r)[\int_0^r v(r')r'dr']dr} \tag{3.5}$$

where $Y(r)dr$ is the number of pores with pore sizes between r and $r+dr$, C_f and C_p are the feed and permeate solute concentrations respectively, and v is the solvent velocity which is calculated from the following equation :

$$\frac{d^2v}{dr^2} + \frac{1}{r}\frac{dv}{dr} + \frac{\Delta P}{\eta l} + \frac{\boldsymbol{R}T}{\eta l}(C_p - C_f)\left[1 - \exp(-\frac{\phi(r)}{\boldsymbol{R}T})\right] - \left\{\frac{(b-1)X_{AB}C_p v}{\eta}\right\} = 0 \tag{3.6}$$

where at $r = 0$, $dv/dr = 0$ and at $r = r_p$, $v = 0$. η is the viscosity, X_{AB} is a constant relating the frictional force between solute and solvent to their relative velocity, b is the ratio of frictional force of moving solute to that of the bulk of the solution, $\boldsymbol{R}$ is the gas constant, T is the absolute temperature and $\phi(r)$ is the potential function for the force exerted by the pore wall on the solute. The electrostatic and van der Waals interactions which affect $\phi(r)$ are expressed in terms of constants $\bar{A}$ and $\bar{B}$ which can be determined by HPLC (Matsuura and Sourirajan, 1981). For example, the governing equation for $\phi(r)$ in terms of van der Waals interactions is :

$$\phi(r) = -\frac{(\bar{B}/r_a^3)}{\left[(r_p/r_a) - r\right]^3} \tag{3.7}$$

where r_a is an effective reduced radius ($r_a = r_p - d_w$) and d_w is the diameter of a water / solvent molecule.

Deen (1987) and Anderson and Quinn (1974) described a comprehensive hindered transport model which models the transport of solute through the pores in terms of diffusive and convective factors. The diffusive and convective transport parameters have been calculated as a function of pore geometry and various solute-pore wall interactions. For example, Smith and Deen (1980) include the effect of electrostatic and dispersion forces. According to this theory, the overall solute flux is given as :

$$\overline{J_s} = K_C \bar{v} C_f \frac{1-(C_p / C_f)\exp(-Pe)}{1-\exp(-Pe)} \tag{3.8}$$

where,

$$Pe = \frac{\bar{v} l}{D_\infty}\left(\frac{K_C}{K_D}\right) \tag{3.9}$$

and $K_D(K_W, \lambda, E)$ is the hindrance factor for diffusion, $K_C(K_L, \lambda, E)$ is the corresponding hindrance factor for convective transport, $\bar{v}$ is the average solvent velocity in the pore, D_∞ is the solute diffusivity in bulk solution, K_W and K_L are the hydrodynamic coefficients which represent drag on the solute from the pore walls and the solute velocity lag, respectively, and E represents the potential function for long range interactions.

3.2 CONCENTRATION POLARIZATION

Concentration polarization is defined as the build up of rejected solute at the membrane surface. It has been modeled by many researchers by (i) resistance in series models or (ii) osmotic pressure models. These models have been reviewed by van den Berg and Smolders (1990), Fane (1986), Gekas and Hallström (1990) and Mulder (1995). These two classes of models are summarized below.

3.2.1 RESISTANCES IN SERIES MODELS

The observed flux decline in microporous membranes has been attributed to the additional resistances to permeate flow offered by either a boundary layer, cake layer or

gel layer formed at the feedside surface of the membrane (see Figure 1.1). Models which take these additional resistances into account are reviewed below.

3.2.1.1. *Boundary layer (Film) model*

This model has been used by many investigators to analyze flux reduction phenomena in a variety of membrane separation processes (Michaels, 1968; Brian, 1965; Kozinski and Lightfoot, 1972; Blatt et al, 1970; Belfort and Nagata, 1985). A schematic of this model is shown in Figure (3.1). Solute rejection at the membrane surface leads to a buildup in concentration of that solute at the membrane surface. This results in diffusive back transport through a hypothetical boundary layer to the bulk solution.

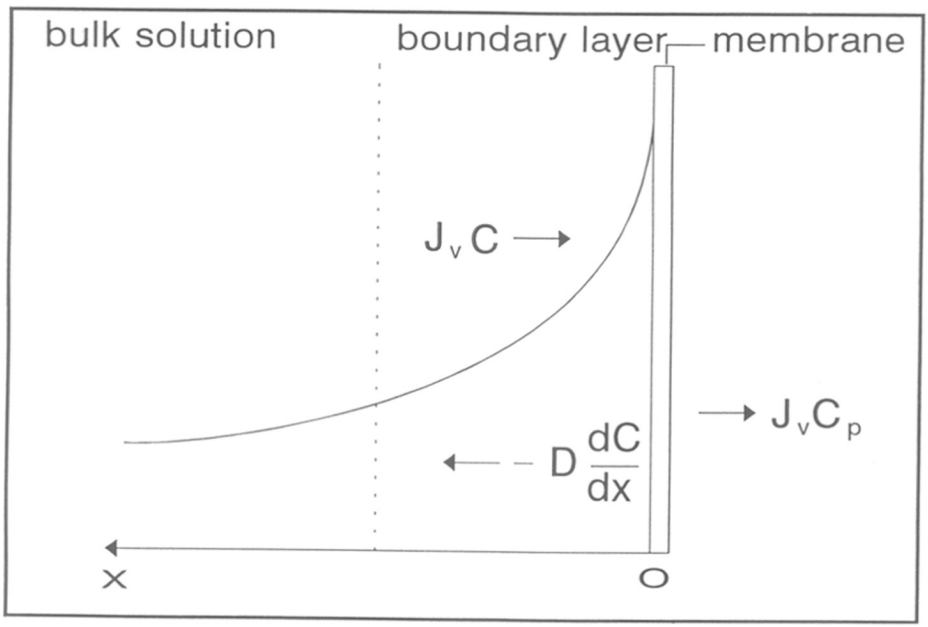

Figure 3.1 : Schematic of boundary layer model

At steady state conditions, transport of solute to the membrane surface by convective flow is balanced by diffusive back transport plus the solute flux in the permeate :

$$J_v C = J_v C_p - D\frac{dC}{dx} \qquad (3.10)$$

Integrating eqn. 3.10 across the boundary layer of thickness δ with the conditions that at $x = 0$, $C = C_m$ and at $x = \delta$, $C = C_f$ results in the well known film model,

$$J_v = k \ln \frac{(C_m - C_p)}{(C_f - C_p)} \tag{3.11}$$

where $k = D/\delta$ is the mass transfer coefficient and C_m is the solute concentration at the membrane surface. The mass transfer coefficient depends strongly on the hydrodynamics of the system. Equation (3.11) can be rearranged as:

$$\ln \frac{\tau}{(1-\tau)} = \frac{J_v}{k} + \ln \frac{\tau'}{(1-\tau')} \tag{3.12}$$

where, $\tau' = C_p / C_m$ is the true transmission and $\tau = C_p / C_f$ is the observed transmission. This equation predicts an increase in τ with increasing J_v, the observed transmission tending to unity as J_v increases. For a perfectly retentive membrane, the permeate concentration (C_p) becomes negligible and equation (3.11) takes the form,

$$\frac{C_m}{C_f} = \exp\left[\frac{J_v}{k}\right] \tag{3.13}$$

where J_v / k is the Peclet number (Pe).

The mass transfer coefficient, k is related to the Sherwood number (Sh) based on Chilton-Colburn analogy (Bennett and Myers, 1982) as :

$$Sh = kd_h / D = aRe^b Sc^c \tag{3.14}$$

where Re is the Reynolds number ($Re = v_f d_h / \nu$) and Sc is the Schmidt number ($Sc = \nu / D$), ν the kinematic viscosity, d_h the hydraulic diameter, v_f is the feed flow velocity, D is the solute diffusion coefficient and a, b and c are adjustable parameters. Since D cannot be increased significantly (except by increasing temperature), k can only be increased by increasing feed velocity and by changing the module design. Porter (1972) has given the following correlation for k in laminar flow, in terms of the shear rate ($\dot{\gamma}$).

$$k = 0.816 \dot{\gamma}^{0.33} D^{0.67} L^{-0.33} \tag{3.15}$$

where $\dot{\gamma} = 8v_f / d_i$ for tubes with diameter d_i

$\dot{\gamma} = 6v_f / h$ for rectangular channels of height h

In protein containing solutions, it has also been shown that D is a function of solution parameters such as ionic strength, pH, concentration etc. Besides increasing flow velocity, mass transfer can also be improved by other methods such as using turbulence promoters, corrugated membranes or pulsatile flow. These methods are discussed in section 3.4.2.

The solute concentration at the membrane surface may attain the solubility limit and form a gel layer, in which case $C_m = C_g$. Then, eqn. (3.13) can be written as :

$$\frac{C_g}{Cf} = \exp\left[\frac{J_\infty}{k}\right] \tag{3.16}$$

where, J_∞ is the limiting flux. Eqn. (3.16) is known as the gel polarization model (Bixler et al, 1968; Blatt at al, 1970; Porter, 1972). The gel concentration (C_g) depends on the nature of the solute but is considered to be independent of the feed concentration and pressure. This allows an apriori conservative estimate of the membrane limiting flux in certain applications.

The gel polarization model has some limitations. C_g is expected to be independent of bulk concentration and flow velocity, however, in some cases (Nakao et al, 1979) it has been found to be affected by these variables. While C_g is expected to be an intrinsic property of a solute-solvent system, differing values of C_g have been reported for a given solute (Dejmek et al, 1975). Although proteins form a gel readily, many other macromolecules like dextrans do not form gels even at higher concentrations. Despite these limitations, it is still considered as a simple and useful model.

3.2.1.2 *Combined concentration polarization - irreversible thermodynamics model*

Kedem and Katchalsky (1958) derived the following equation for transport through a membrane phase, based on non-equilibrium thermodynamics :

$$J_s = -P'\frac{dC}{dx} + (1-\sigma)CJ_v \tag{3.17}$$

where σ and P' are the Staverman reflection coefficient and the local solute permeability respectively. Since the solute flux $J_s = J_v C_p$, integrating eqn. (3.17) over the membrane thickness, l, gives the following expression for $\tau'(= C_p / C_m)$:

$$\tau' = \frac{(1-\sigma)\exp(Pe)}{(\exp(Pe)-\sigma)} \tag{3.18}$$

where Pe ($= J_v$ (1-σ) / P_m) is the membrane Peclet number and P_m (= P'/l) is the solute permeability. According to eqn.(3.18), τ' decreases exponentially from unity with increasing J_v and asymptotically approaches a value of (1-σ)..

Opong and Zydney (1991) have combined the concentration polarization model with the Kedem-Katchalsky model. Substituting the expression for τ' from eqn. (3.18) into the concentration polarization eqn.(3.12) gives :

$$\ln\frac{\tau}{1-\tau} = \frac{J_v}{k} + \ln\frac{(1-\sigma)\exp(Pe)}{\sigma(\exp(Pe)-1)} \tag{3.19}$$

In the case of small Pe (low J_v), eqn.(3.19) becomes :

$$\frac{1}{\tau} = \frac{1}{(1-\sigma)} - \frac{\sigma}{(1-\sigma)}\exp[-J_v(1-\sigma)/P_m] \tag{3.20}$$

For large Peclet no., eqn.(3.19) becomes

$$\ln\frac{\tau}{1-\tau} = \frac{J_v}{k} + \ln\frac{(1-\sigma)}{\sigma} \tag{3.21}$$

3.2.1.3 *Modified concentration polarization - charged solute migration model*

Balakrishnan et al (1993) modified the concentration polarization model to take into account migration of protein molecules (J_i) to the membrane surface due to electrostatic interactions between charged protein and the membrane surface. With this additional transport term, the mass balance at the boundary layer can be written as :

$$J_v C + J_i - D\,dC/dx = J_v C_p \tag{3.22}$$

Integrating this equation across the boundary layer thickness (δ) and rearranging gives :

$$\frac{1}{\tau} = \frac{J_v}{J_v + J_i} + \left(\frac{1}{\tau'} - \frac{J_v}{J_v + J_i}\right)\exp\left[-(J_v + J_i)/k\right] \tag{3.23}$$

The value of J_i can be positive or negative depending upon whether overall protein-membrane interactions are attractive or repulsive. For positive J_i , this model predicts a maximum (τ > 1) in the τ vs. J_v curve at low J_v followed by a decrease in τ to unity at

large J_v. For negative J_i , this model predicts a monotonic increase in τ which asymptotically approaches unity at large J_v.

3.2.2 OSMOTIC PRESSURE MODEL

Because of high fluxes, high rejections or low mass transfer coefficient values, the concentration of macromolecules at the membrane surface becomes high. This leads to an increase in the osmotic pressure on the feed side of the membrane, which reduces the driving force for filtration (Wijmans et al, 1984 and 1985; Goldsmith, 1971; Vilker et al, 1981a; Johnsson, 1984, van den Berg and Smolders, 1989a).

For dilute solutions, the osmotic pressure π can be related to solute concentration by the van't Hoff type relation,

$$\pi = \boldsymbol{R}TC^n \tag{3.24}$$

where $\boldsymbol{R}$ is the gas constant, T is the absolute temperature and n is an exponential factor which is usually 1 for low molecular weight species and dilute solutions. For higher concentrations / non-ideal systems, π is expressed as a power series in C as :

$$\pi = \boldsymbol{R}T\sum_{n=1}^{N} a_n C^n \tag{3.25}$$

where a_n are constants. According to this model, the permeate flux is given as :

$$J_v = \frac{\Delta P - \Delta\pi}{\eta R_m} \tag{3.26}$$

where $\Delta\pi$ is the osmotic pressure difference across the membrane.

Applying this osmotic pressure effect to the concentration at the membrane surface (C_m) and combining eqn. (3.26) with the simplified boundary layer model (eqn. 3.13), the flux can be expressed as :

$$J_v = \frac{\Delta P - a\boldsymbol{R}TC_f^n \exp\left[\frac{nJ_v}{k}\right]}{\eta R_m} \tag{3.27}$$

Differentiating eqn. (3.27) with respect to ΔP and using eqn (3.26), leads to the following dependence of flux on pressure (Mulder, 1995) :

$$\frac{\partial J_v}{\partial \Delta P} = \frac{1}{\eta R_m}\left[1+\frac{\Delta \pi n}{\eta R_m k}\right]^{-1} \tag{3.28}$$

which predicts that J_v initially increases linearly with pressure and finally attains a limiting value :

$$\frac{\partial J_v}{\partial \Delta P} \rightarrow (\eta R_m)^{-1} \qquad \text{for } \Delta\pi \rightarrow 0$$

$$\frac{\partial J_v}{\partial \Delta P} \rightarrow 0 \qquad \text{for very high } \Delta\pi$$

Similarly, the concentration dependence of the flux is expressed as :

$$\frac{\partial J_v}{\partial \ln(C_f)} = -k\left[1+\frac{R_m k \eta}{\Delta \pi n}\right]^{-1} \tag{3.29}$$

3.2.3 COMBINED OSMOTIC PRESSURE - GEL LAYER MODEL

Bhattacharjee and Bhattacharya (1992) proposed a combined model to unite the concepts of osmotic-pressure control and gel-layer control. This model is based on the integral theory of Probstein et al (1978) and the work of Trettin and Doshi (1980). It first calculates flux decline by a osmotic-pressure controlled mechanism :

$$J_v = \frac{\Delta P}{\eta R_m}\left(1-\frac{\sigma \Delta \pi}{\Delta P}\right) \tag{3.30}$$

Subsequently, depending on the tendency of solute to form a gel-layer, flux decline is calculated by the gel-layer controlled mechanism :

$$J_v = \frac{\Delta P - \sigma \Delta \pi_f}{\eta (R_{ma} + R_p)} \tag{3.31}$$

where R_{ma} (= R_m + R_a) and R_p (= R_{osm} + R_g) are functions of time. R_a and R_{osm} are the mass transfer resistances due to solute adsorption and osmotic pressure respectively.

3.3 FOULING

Fouling is defined as the adsorption or deposition of solute molecules on the membrane surface or on the pore walls. It has been modelled by many researchers on the basis of pore plugging and adsorption phenomena. These models have been reviewed by

Davis (1992), Gekas and Hallström (1990) and Belfort and Nagata (1985) and will be described here briefly. These models can be classified as particle models, surface fouling models and internal fouling models.

PARTICLE MODELS :

3.3.1 *Inertial lift model* (*tubular pinch effect*)

This model describes the enhanced back-transport of particles from the membrane surface, in which the particles in the boundary layer are lifted away from the surface towards the bulk, due to inertial effects (Green and Belfort, 1980; Altena and Belfort, 1984; Drew et al, 1991, Porter, 1972). At steady state the flux is given as :

$$J_v = v_l/(1-\delta)^m \tag{3.32}$$

where m = 4 and 6 for two dimensional channel and tubular configurations respectively, δ is the dimensionless thickness of deposit and v_l is the lift velocity for a clean tube or channel. For a spherical particle near the wall of a two-dimensional channel, the maximum lift velocity is :

$$v_l = 0.577\frac{\rho r_s^3 \dot{\gamma}^3}{16\eta} \tag{3.33}$$

where ρ is the particle density and $\dot{\gamma}$ is the shear rate.

3.3.2 *Frictional force model*

This model is based on the frictional force balances on a solute particle (Rautenbach and Schock, 1988; Balman et al, 1990). Drag force due to convective flow deposits the particles on the membrane surface, while drag forces due to crossflow-velocity move them along the membrane surface. If the latter force exceeds the former, deposition does not occur. Rautenbach and Schock (1988) have derived the following relationship for the flux in a tubular membrane :

$$J_v = 0.22\mu^{-1}\,\mathrm{Re}^{1.26}\left(\frac{\eta}{\rho d_i}\right)\left(\frac{d_s}{d_i}\right) \tag{3.34}$$

where μ is a proportionality constant which accounts for the drag forces; and d_i and d_s are the diameters of the tube and the solute respectively.

Futselaar (1993) compared the applicability and limitations of various fouling models in MF processing as a function of the particle size. He concluded that the frictional force model gave the best predictions over the entire particle range.

SURFACE FOULING MODELS :

As described in section 3.2.1.1, the concentration of rejected solute builds up at the membrane surface. If the surface concentration exceeds the solubility limit of solute, a gel may form or the solute may form aggregate to form a cake on the surface. A deposited surface layer may also build up due to adsorption. The gel layer fouling model has already been discussed in section 3.2.1.1. as an extension of the boundary layer model describing concentration polarization.

All these surface phenomena can be modelled as an additional resistance in series with the membrane resistance. These models are exemplified by the cake filtration models described below.

3.3.3 *Cake-filtration model*

In this concept, solute particles deposited at the membrane surface are considered to form a 'cake' which forms an additional resistance (R_c) in series with the membrane resistance (R_m) (Vilker et al, 1981a) :

$$J_v = \frac{\Delta P}{\eta(R_m + R_c)} \tag{3.35}$$

R_c is defined as the specific cake resistance (r_c) times the cake layer thickness (l_c). The specific cake resistance (r_c) is expressed by the Kozeny-Carman relationship,

$$r_c = 180\frac{(1-\varepsilon)^2}{(d_s)^2\varepsilon^3} \tag{3.36}$$

where ε is the porosity of the cake layer and d_s is the solute diameter. The cake layer thickness depends on the type of solute, operating conditions and time. For unsteady-state dead-end filtration, the cake layer thickness can be obtained by a mass balance as,

$$C_f R' V = C_m l_c A \tag{3.37}$$

where V is the total permeate volume, C_f and C_m are solute concentrations in the bulk and at the membrane surface, respectively, and R' is the intrinsic rejection of the membrane.

The cake filtration model concept has been used to analyze cross-flow, stirred and unstirred dead-end filtration of various solutes (Howell, 1980; Baker et al, 1985; Fane 1984; Chudacek and Fane, 1984)

3.3.4 *Modified cake filtration model*

Schulz and Ripperger (1989) modified the cake filtration model by taking into account the wall shear stress. For turbulent flow, the flux is given as :

$$J_v = \left[\frac{K_2 \Delta P(\rho_p - C_f)\rho}{r_c C_f}\right]^{0.5} \frac{v_s}{\eta} \tag{3.38}$$

where K_2 is a constant, ρ_p is the particle density and v_s is the solute velocity. For laminar flow, the flux is proportional to the square root of the solute velocity as :

$$J_v = \left[\frac{K_3 \Delta P(\rho_p - C_f)v_s}{\eta d_i r_c C_f}\right]^{0.5} \tag{3.39}$$

where d_i is the internal diameter of the capillary and K_3 is a constant.

INTERNAL FOULING MODEL :

3.3.5 *Pore restriction model*

The pore size may narrow due to adsorption of solutes on the membrane pore walls or due to precipitation of solutes within the pores. This model has been used to model adsorptive fouling (Brites et al, 1993; Flora, 1993, Dejmek and Nilsson, 1989, Dal-Cin et al, 1995). According to Hagen-Poiseuille's equation (eqn. 3.1), the permeate flux is proportional to the fourth power of the pore radius. Thus if the pore radius decreases from initial radius (r_{pi}) to a smaller radius (r_{pi} - l_d), where (l_d) is the deposited layer thickness, the final flux (J_v) is related to the initial flux (J_v) by :

$$\frac{J_{vf}}{J_{vi}} = (1 - l_d / r_{pi})^4 \tag{3.40}$$

Eqn. (3.40) assumes that other parameters e.g. η do not change during processing. If pure water fluxes are measured before and after processing, the ratio J_{wf} / J_{wi} (known as the flux recovery, FR) can be used to estimate the extent of internal fouling. This ratio can also be used to assess the efficacy of membrane cleaning.

3.4 TECHNIQUES FOR CONTROL OF CONCENTRATION POLARIZATION AND FOULING

Various methods have been used to control concentration polarization and fouling; these are reviewed by several authors (Cheryan, 1986; Kulkarni et al, 1992c; Nyström and Howell, 1993; Mulder, 1995; Gupta, 1996; Jagannadh and Murlidhara, 1996). The various methods of limiting flux loss can be classified as :

i) identification of foulants and feed pretreatment,

ii) module design and solution hydrodynamics,

iii) membrane cleaning, and

iv) modification of membrane properties itself.

Each of these methods is described below.

3.4.1 IDENTIFICATION OF FOULANTS AND FEED PRETREATMENT

Feed pretreatment is a very important method of improving membrane productivity for applications in food, dairy and beverage industries. Identification of foulants is a prerequisite for designing an appropriate feed treatment. Foulants can be classified as either mineral (salts), organic (proteins) or particulate materials.

3.4.1.1 *Identification of foulants*

Various physical and chemical methods have been routinely used to characterize various foulants on the membrane surface and within the membrane pores. These methods are listed in Table 3.1.

Table 3.1

Methods for identification of foulants

Method	UF system	Foulant identified	Reference
Atomic force microscopy (AFM)	Whey	Proteins	Gésan et al, 1993,
Contact angle	BSA, dextran Peptide mixtures	BSA, dextran Peptide mixtures	Oldani and Schock, 1989 Gourley et al, 1994
Energy dispersive spectroscopy (EDS)	Protein	Protein	Bansal et al, 1991
Electron paramagnetic resonance (EPR)	Protein	BSA, Lysozyme	Oppenheim et al, 1994
Electron spectroscopy for chemical analysis (ESCA)	BSA, dextran Whey	BSA, dextran Proteins	Oldani and Schock, 1989 Labbé et al, 1990
Fourier transform infrared - attenuated total reflectance (FTIR-ATR)	BSA, dextran Whey	BSA, dextran Proteins	Oldani and Schock, 1989 Gésan et al, 1993, Labbé et al, 1990
Radiolabeling (Ca^{45} and P^{32})	Whey	Ca salts	Hanemaaijer et al, 1989
Scanning electron microscopy (SEM)	Milk Whey	Proteins Proteins, Ca salts	Glover and Brooker, 1974 Vetier et al, 1988 Lee and Merson, 1975 and 1976
Total internal reflection fluorescence (TIRF)	Protein	Immunoglobulin - G	Grabbe, 1993

3.4.1.2 *Feed Pretreatment methods*

Depending on the identification of the foulant type, specific feed pretreatment processes have been found to be effective. These are discussed below in the case of whey processing by membranes.

i) Ca salts : Calcium phosphate is a well known foulant in whey processing (Merin, 1979; Patocka and Jelen, 1987; Lee and Merson, 1976; Labbé et al, 1990; Taddei et al, 1988). Pretreatment of whey to reduce the calcium phosphate concentration drastically reduces membrane fouling. Flux increases have been observed after removal of Ca by chelation with EDTA for acid whey (Patocka and Jelen, 1987; Lee and Merson, 1976), by chelation with citrate for acid (Patocka and Jelen, 1987) or sweet cheese whey (Taddei et al , 1988) , or by replacement of Ca by Na for acid whey (Patocka and Jelen, 1987).

ii) Proteins : Heat treatment of whey at 85°C for 15s has also been shown to improve flux (Delaney and Donnelly, 1977). Since proteins are know to form aggregates at their isoelectric points (IEP) (Saksena and Zydney, 1994; Fane et al, 1983), the adjustment of the feed solution pH away from the protein IEP has been shown to improve the flux for acid whey (Patocka and Jelen, 1987; Muller et al, 1973; Hayes et al, 1974), whey protein solutions (Heinemann et al, 1988) as well as in BSA UF (Fane et al, 1983).

iii) Particulates : Whey clarification by microfiltration has also been shown to increase UF flux (Lee and Merson, 1976; Maubois et al, 1987). Removal of suspended particles and fat by high-speed centrifugation is a standard pretreatment in the dairy industry (Delaney and Donnelly, 1977). Gravity settling and filtration can also be used to clarify whey (Marshall, 1982).

3.4.2 MODULE DESIGN AND SOLUTION HYDRODYNAMICS

As described in section 3.2.1.1, the mass transfer coefficient at the membrane surface, k, can be increased by increasing Re or γ i.e. by increasing feed velocity or decreasing the module channel height. Both of these methods are limited by the pumping costs and the module mechanical stability. Recently, studies have identified new module

designs which result in improved hydrodynamic conditions at the membrane surface to reduce concentration polarization and fouling in membrane processing. Applications of these techniques have been reviewed by Mulder (1995), van den Berg and Smolders (1990), Gupta (1996), Nyström and Howell (1993), Marshall et al (1993) and Kulkarni et al (1992c).

3.4.2.1. *Rotating modules / filters*

These devices contain two concentric cylinders, of which the inner one supporting a membrane sheet is rotated, causing flow instability due to formation of Taylor vortices in the annulus. The major advantage of a rotating module is that permeate flux becomes independent of circulation flow, as the shear rate at the membrane surface is controlled by the rotational velocity (Nyström and Howell, 1993). Thus, feed solutions with higher concentrations or higher viscosities can be treated in a single pass, reducing circulation pumping costs. Hallström and López-Leiva (1978) have observed significant flux increase with increasing rotational speed. However the major drawback of this device is the mechanical complexity and cost of the system which limits large scale application.

Rolchigo et al (1989) compared the UF of protein solutions containing myoglobin, BSA and Ferritin, in cross-flow and rotary systems. They observed that in the rotary module, the permeate flux of a hydrophilic membrane approached 90% of the initial water flux; this permeate flux was significantly higher than that of a hydrophobic membrane. By contrast, fluxes for both membranes were low in the cross-flow system. Kroner and Nissinen (1988) also observed higher protein recovery through permeable UF membranes in the rotary module. Rebsamen and Ziegler (1986), Goldinger et al (1986), Kroner et al (1987), Riesmeir et al (1990) and Tobler (1982) have also found similar advantages in using an axially rotating filter for biotechnological applications.

In another type of rotary module, Lee et al (1995) observed a dramatic flux improvement for microfiltration of recombinant yeast cells using a rotating disc filtration system. Flux enhancement was attributed to minimal cake buildup and reduced membrane fouling.

3.4.2.2 *Corrugated membranes*

Corrugations at the membrane surface promote feed side turbulence which decreases concentration polarization (van der Waal and Rácz, 1989a). An optimal distance between corrugations is required. If the distance between adjacent corrugations is too small, the fluid streamline will not approach the membrane surface and the improvement in mass transfer is limited. If the distance is too large, the effect of the corrugation also diminishes. Jeffree et al (1981) has observed 6x increase in the UF flux for bovine whole blood using corrugated membranes. Similar results were obtained by van der Waal et al (1987, 1988, 1989b).

Combining this technique with flow pulsing (discussed in section 3.4.2.6), for harvesting of microorganisms using a 0.2 μm polysulfone membrane, Wyatt et al (1987) obtained 51 and 75% of the initial water fluxes for a flat and corrugated membrane, respectively. However, without flow pulsing, the permeate flux was only 25% of the initial water flux for both flat and corrugated membranes.

3.4.2.3 *Transverse flow module*

In this module design, hollow fiber or capillary membranes with the separating surface at the outer diameter are used and the feed flows perpendicular to the fibers (Baudet, 1976; Yang and Cussler, 1986, Knops et al, 1992). This results in a large increase in the mass transfer compared to the conventional design in which feed flows through the fiber bore (lumen) as the fibers act as feed flow turbulence promoters. In addition to UF, MF and RO, this type of design is also applicable to pervaporation, liquid membranes and membrane contactors where the boundary layer resistance can be very severe.

Futsellar (1993) and Knops et al (1992) have shown for that for filtration of oil-in-water emulsions, the permeate fluxes improved in transverse flow compared to flow through the fiber bore, for a given energy consumption.

3.4.2.4 *Other module designs*

Various module designs have used turbulence promoters in order to increase the rate of mass transfer of rejected species from the membrane surface to the bulk and to remove deposited layers from the membrane surface. Turbulence can be created by inserting baffles, static mixers, particles etc. in the feed flow path. These techniques are explained below.

Baffles : Various types of baffles have shown promising results with different feed solutions. Finnigen and Howell (1989) showed an increase in permeate flux when doughnut or disc shaped baffles were incorporated in a tubular membrane system, under both steady and pulsed flow conditions. Colman and Mitchell (1990) investigated vortex mixing at the surface of a flat sheet membrane, generated by pulsed flow in a baffled rectangular channel. The spacing between the baffles was optimized for maximum mass transfer. A mass transfer coefficient, equivalent to a steady flow Reynolds number $>10^4$ was achieved in baffled channels at low mean flows (Re = 100-200) (Colman and Mitchell, 1991). Flux improvements by 3x over steady flow in an unbaffled channel was reported during UF of dextran solutions. Flux improvements using baffles have also been shown by Gupta et al (1994b) and Hiddink et al (1980).

Gupta et al (1994a) observed a flux increase of more than 50% by incorporating helical baffles in a tubular mineral membrane for processing of yeast cell solution. Rotational flow around the baffle axis increased the mixing and migration of rejected particles from the membrane surface. Field et al (1995) and Gupta et al (1995) have found a 'critical flux' below which fouling does not occur.

The effect of turbulence promoters during the UF of whey protein concentrate has been studied by Dejmek et al (1974). Probstein et al (1978) demonstrated that the limiting flux could be raised 3x at the same flow rate by using strip type turbulence promoters.

Particles / beads : Montlohuc et al (1985) and Rios et al (1987) reported 5x increase in permeate flux for UF of gelatin / milk solutions when 3 mm diameter stainless steel beads were used as free turbulence promoters. They concluded that the presence of these particles not only introduced turbulence in the system, but also caused continuous mechanical erosion of the protein deposit at the membrane surface. Mateus and Cabral

(1989) observed a substantial increase in flux while recovering 6-α-methylprednisolone from culture broth using microsized charged particles in plate - frame as well as hollow fiber units. De Boer et al (1980) also used fluidized beds of glass, steel and lead as turbulence promoters during reverse osmosis processing of food liquids in tubular membranes. They found that glass beads caused less damage to the membranes. Lowe and Durkee (1971) observed 3x improvement in the flux as well as a lower flux decline rate for reverse osmosis concentration of orange juice, using plastic spheres as turbulence promoters.

More recently, Lee et al (1993) observed a flux enhancement for crossflow MF/UF of E. *coli* and B. flavum cells, by introducing air slugs into the crossflow stream. These air slugs, disturbed the cell sublayer formation as they moved along the flow and thus reduced the polarization on the membrane surface. In a similar experiment, Cui and Wright (1996) used a gas-liquid two-phase crossflow system with tubular membranes, in which air was injected into the feed. They observed flux increases upto 3x for dextran filtration in laminar flow, due to development of secondary flow induced by the gas bubbles; however, in turbulent flow, significant flux enhancement was not observed. In a similar study, Bellara et al (1996) obtained flux increases of 20-50% for dextran UF and 10-60% for albumin UF in a hollow fiber pilot plant system. In the hollow fiber membrane case, the flux enhancement was attributed to physical removal of the concentration polarized layer by the flowing bubbles.

Others :

Winzeler (1990) developed a crossflow filtration module in which the retentate system swept the membrane surface through spiral wound channels of semi-circular cross-section. This arrangement was characterized by uniform velocity at a very low pressure drop. This module showed higher flux rates than a plate and frame module, at comparatively lower power consumptions. Using a similar device, Moulin et al (1996) attributed the mass transfer improvement to Deen vortices.

3.4.2.5 *Flow pulsation*

Flow pulsation is a promising method to control concentration polarization, which can be used with conventional modules. Pulsed flow can be obtained by various techniques as explained below. Flow pulsation can refer to periodic changes in either the feed velocity or pressure or in the permeate pressure.

Transmembrane pressure pulsing either on the feed side or permeate side has been reported to show flux improvements.

Permeate side transmembrane pressure pulsing has been shown to decrease concentration polarization (Rodgers and Sparks, 1992 and 1993) and fouling (Rodgers and Sparks, 1991). In the former study, cross-flow ultrafiltration of 1% BSA at pH 7.4 was carried out upto 140 kPa transmembrane pressures with a YM-30 cellulosic membrane. Transmembrane pressure pulsing was generated by increasing the filtrate pressure 5 - 10 kPa above the operating pressure at frequencies ranging from 0 - 5 Hz. The flux increase was attributed to the altered concentration boundary layer due to translation of body forces through the membrane and slight but significant membrane motion. Flux enhancement due to pulsing was sensitive to changes in feed concentration; however, pH and ionic strength variation had little effect. Flux increase of 100x during UF of albumin - γ-globulin was obtained by negative transmembrane pressure pulsing (Rodgers and Sparks, 1991).

Nikolov et al (1993) investigated the effect of simultaneous pulsating pressures in the feed and permeate solution on the performance of a tubular UF membrane. The frequency of the pulsation was synchronized in such a way that the minimum pressure in the feed corresponded to the maximum pressure in the permeate. They reported that synchronous pulsations in the feed and the permeate led to a better performance than independent pulsation alone and could even eliminate gel layer formation.

Jaffrin et al (1994) introduced feed side pressure pulsing using a piston-in cylinder pump which produced periodic bursts of velocity and pressure along the membrane at frequencies between 0.5 and 1.5 Hz. This system was employed for red wine clarification using ZrO_2 membranes. Energy analysis showed that this technique was more efficient as

compared to the superimposition of pulsations on a steady flow. Similarly, Arroyo and Fonade (1993) used a pneumatically controlled valve to generate intermittent jets from the main flow, causing the formation of large vortices moving downstream along a tubular membrane.

For whey MF, Bauser et al (1982) applied a periodic sequence of pumping pulses keeping mean flow constant by simultaneous adjustment of the frequency and amplitude. With this system, they found 25% flux increase after 1 hour and 38% after 2-3 hours. In another study, Bauser et al (1986) applied a pulsatile negative pressure from the filtrate side of the module during whey UF and found 150% gain in flux.

Ilias and Govind (1990) modelled the performance of a tubular membrane module under oscillatory flow conditions. An analysis of the extra power requirement for flow oscillation showed that the gain in transmembrane flux outweighs the cost of the extra power, which was only a minute fraction of the power required to maintain steady flow.

Spiazzi et al (1993) have developed a new unsteady-state flow generator for tubular membranes. It consists of a perforated rotary distributor disc placed in front of the entrance plate of a tubular membrane bundle. The main feature of this design is that pulsatile flow is generated only in the membrane module; no variation in flow or pressure occur elsewhere in the equipment. With this design, they observed a 50% reduction in cross-flow velocity for the same power consumption per unit permeate flux compared to steady crossflow filtration of aqueous bentonite suspensions.

Najarian and Bellhouse (1996) found an increase in selectivity for albumin while filtering bovine plasma due to transmembrane pressure pulsing.

3.4.2.6 *Application of an external field / centrifugal forces* :

Coupling of UF with electrophoresis has been shown to reduce solute concentration buildup at the membrane surface and thus improve permeate flux (Silva et al, 1991; Robinson et al, 1993; Lentsch et al, 1993; Hong and Lee, 1986; Lee and Hong, 1987). Lentsch et al (1993) applied this concept for BSA-PEG separation where the presence of an electric field, normal to the membrane, reduced BSA buildup and enhanced PEG transport. Robinson et al (1993) used a pulsed electric field across the membrane

during BSA UF, thereby imposing a discontinuous electrophoretic velocity upon the molecules being concentrated. This resulted in a 25-40% decrease in the solute related resistance compared to the case without an electric field.

Bowen et al (1989) used intermittent electric field pulses to clean membranes without interruption of the separation process. Increase in permeation rates by 10x were obtained with only a modest electric energy requirement for cross-flow microfiltration of dispersions of baker's yeast or TiO_2.

Ahner et al (1993) reported the use of piezoelectric transducers / ultrasonic horns to improve flux by promoting local turbulence on fouled UF membranes. They observed significant increases in the permeate flux for polysulfone and regenerated cellulose membranes fouled with dextran and PEG when the piezoelectric transducer was operated periodically for 20-90 s. The flux was increased by 8x within seconds and the increased flux remained stable for upto 3 hours. Wakeman et al (1991) studied the effect of application of an electric field and ultrasound, either individually or in combination, on the permeate flux of china clay and anatase clay suspensions. They found that flux was increased when an electric field (50 V cm^{-1}) alone was applied but no significant flux increase was observed when an ultrasonic field (1.7 W cm^{-2} cm^{-1}) alone was applied. However, the combination of electric field and ultrasonic field increased flux higher than that with the electric field alone.

Vigo et al (1990) found flux improvements for oil / water ultrafiltration by applying low frequency vibrations tangential to the membrane surface by means of a mechanical coupling. They observed that at low frequencies (5,10 Hz), the flux attained the limiting value at 100 kPa, while at very high frequency, the flux increased with pressure over a wider pressure range (50 - 900 kPa). At low amplitudes, the flux increased gradually with increasing frequency; whereas at higher amplitudes, the flux increased rapidly with a small increase in frequency.

Robertson et al (1982) found a reduction in concentration polarization for casein UF with a centrifugally driven membrane. In this device, the centrifugal force vector is perpendicular to the membrane surface and acts in the opposite direction as the permeate flow. Destabilization of the polarization layer at 100-600g centrifugal field strengths

improved the permeate flow rate by 3-15x times depending upon the combination of protein concentration and applied centrifugal force. This unit was found to be particularly suited for systems with a tendency to form gel layers.

Iritani et al (1992) suggested dead-end upward UF for preventing flux decline, particularly for fragile bioproducts that may be denatured by heat / cavitation in a circulating pump. Here, the polarization layer was destabilized by the action of gravity.

3.4.3 MEMBRANE CLEANING

Although the methods described in section 3.4.2 reduce fouling to some extent, membrane cleaning is found to be an essential step in practice. Membrane cleaning can be done by four methods, viz. i) hydraulic cleaning, ii) mechanical cleaning, iii) chemical cleaning and iv) electrical cleaning as explained below.

3.4.3.1 *Hydraulic cleaning*

Hydraulic cleaning can be done by backflushing the membrane with a small quantity of permeate, by periodically reversing the flow direction or by using pulsatile flow.

Backflushing the membrane (applicable only to membranes with cylindrical geometry) with a small quantity of permeate has met varied results. Breslau et al (1975) obtained 90% flux recovery after city water ultrafiltration when the membrane was backflushed with 1% chlorine solution. . Bhattacharyya et al (1979) suggested that flux reduction can be minimized with short term membrane depressurization during UF of oil-detergent-water systems. van Gassel and Ripperger (1985) showed that during wine UF, the long term permeate flux could be doubled by 2 second backflushes every 2 minutes. Kuruzovich and Piergiovanni (1996) concluded that flux declines more slowly with increasing backflushing time. However, while processing raw whole milk with a 1.8 μm Ceraver membrane, Piot et al (1986) observed that backflushing the membrane resulted in an immediate improvement in the permeate flux, but the improvement was very short-lived with the permeate flux returning to the original flux almost immediately. van der Horst and Hanemaaijer (1990) found that backflushing had no effect on the permeate flux

obtained with various MF membranes used for the removal of fat from whey. While processing raw water in a membrane bioreactor, Urbain et al (1996) obtained only 8% flux recovery by backwashing twice an hour, coupled with chlorination once a day.

Porter (1988) suggested that if fouling is caused by accumulation of particles on the membrane surface or in the pores, these particles can be removed by intermittent backflush pulses. However, if fouling is due to protein being strongly adsorbed or bound to the membrane surface, backflushing is not effective.

Fane and Fell (1987) have discussed a novel backwashing approach which is feasible only with hollow fiber membranes with a relatively low bubble point. A feed suspension was pumped across the outside of the fiber and filtrate passed through the lumen. The flux decline due to deposition of colloids on and within the membrane was reversed by pulsing the lumen with gas (air, nitrogen etc.) and backwashing with a gas/permeate mixture. The gas pulse expands the fiber and open the pores allowing material to be flushed out.

Goel and McCutchan (1976) used periodic flow reversal to reduce fouling in tubular reverse osmosis systems with river water. About 10-15% higher fluxes were obtained with reduced flux decline. They attributed these improvements to added turbulence due to flow reversal. The effect of flow pulsation on flux has already been described in section 3.4.2.5.

3.4.3.2 *Mechanical cleaning*

Mechanical cleaning can be done by oversized sponge balls to physically wipe away the foulant layer. This technique is useful only in relatively large diameter tubular membrane systems. The use of beads added to the feed solution for disrupting the foulant layer has been discussed in section 3.4.2.4.

3.4.3.3 *Chemical cleaning*

Chemical cleaning is the most important method for restoring flux after fouling. The concentration of the cleaning chemicals, hydrodynamics, and the cleaning time and temperature are important parameters. The chemicals mainly used are acids (strong acids

such as H_3PO_4 or weak acids such as citric acid), alkalis (NaOH), detergents (usually non-ionic), enzymes (lipases, proteases), complexing agents (EDTA) and disinfectants (H_2O_2 or NaOCl).

Whittaker et al (1984) found that a combination of anionic and chaotropic cleaning agents was most effective for removing biofilm in spirally wound cellulose-acetate reverse osmosis membranes.

Razavi et al (1996) obtained almost 100% flux recovery for UF of soy flour extract by successive cleaning of the membrane by sodium hydroxide, protease detergent, sodium hypochlorite and flushing with water.

Daufin et al (1991) showed that, membrane cleaning after whey protein concentration or milk UF was done effectively by a HNO_3-NaOCl cleaning sequence For milk UF, cleaning with either HNO_3-NaOCl or NaOCl alone was able to restore membrane permeability while HNO_3 alone was not effective. The -ClO^- ion acts on polymeric membranes as a swelling agent, which promotes the release of fouling material within the pores.

Cross (1991) studied the cleaning of PM10 membrane fouled by E. *coli* broth in flat sheet and hollow fiber configurations. The cleaning sequence included the initial rinsing of the membrane with water, followed by addition of detergent to 0.4% NaOH solution and circulation for 60 min. at 60°C. Cleaning by nonionic surfactants was not beneficial. The highest flux recovery (76%) was obtained with a cleaning formulation based on surfactant, chelants and dispersants. Flat sheet membranes were easier to clean than hollow fiber membranes. Also, among two hollow fiber systems, the anisotropic membrane was easier to clean than the homogeneous membrane.

Kim et al (1993) studied various parameters related to cleaning of both retentive and partially permeable UF membranes fouled by BSA. The greatest fouling resistance removal was achieved with HCl or NaOH rather than surfactants when the membranes were fouled at pH 5. For membranes fouled at pH 7, the cationic surfactant CTAB was most effective. Thus, electrostatic interactions play an important role in the cleaning of membranes. Increase in cleaner concentration by 10 fold improved the cleaning only marginally. Cleaners which permeated through the membrane showed only slightly higher

resistance removal than surface cleaning. Both excessive cleaning or too infrequent cleaning resulted in lower productivity, indicating the need for an optimum cleaning protocol..

Munoz-Aguado et al (1996) have suggested combined enzymatic and detergent cleaning to be an effective method for increasing the flux recovery of polysulfone ultrafiltration membranes fouled by BSA or whey.

Other researchers have investigated cleaning procedures for membranes used in dairy (Parkin and Marshall, 1976; Smith and Bradley, 1987) and biotechnology (Taeymans and Lenges, 1989) applications.

3.4.3.4 *Electrical cleaning*

Murlidhara and Huffman (1988) and Bowen et al (1989) have suggested the use of a pulsed electric field, which results in the movement of charged particles or molecules away from the membrane. A drawback of this method is the necessity of electrically conducting membranes and a special module design. The principle of this type of cleaning has been explained in section 3.4.2.6.

3.4.4 MEMBRANE MATERIAL CHARACTERISTICS

Various solute-membrane interactions are known to affect ultrafiltration performance. It is well documented that biomolecules such as proteins, enzymes etc. adsorb more on hydrophobic surfaces than hydrophilic surfaces (Persson et al, 1993; Sheldon et al, 1991; van den Berg and Smolders, 1990; Fell et al, 1990; McDonogh et al, 1990; Matthiasson, 1984). Protein-membrane electrostatic interactions also affect membrane performance (Nakao et al, 1988, Nyström and Lindström, 1988; Nyström, 1989). Therefore, modification of membrane material / surface in order to increase hydrophilicity or to modify surface charge has been investigated for reducing adsorption/fouling of ultrafiltration membranes by biomolecules. The techniques investigated for this purpose include : i) using hydrophilic polymers / copolymers, ii) blending of hydrophilic or charged polymers with hydrophobic polymers or iii) surface modification of the membrane surface itself. These techniques are explained below.

3.4.4.1 *Hydrophilic polymers / copolymers*

A large variety of commercial membranes are based on cellulosics which have good fouling resistance due to their low adsorption of hydrophobic solutes. However, the disadvantage with these materials is their restricted chemical or thermal stability. Therefore, new hydrophilic membranes have been investigated based on more stable materials. Polyamide based membranes are found useful as microfilters (Pall, 1982); however, their residual positive charge can be detrimental in some applications. Sulfonation of hydrophobic polysulfone by sulphuric acid, chlorosulfonic acid or by SO_3 - triethyl phosphate complex (Nakao et al, 1988) gives a negatively charged hydrophilic material. Since sulphuric acid may cause polymer degradation, the other two reagents are preferred. Similarly, polyetheretherketone (PEEK), which is extremely chemically stable but rather hydrophobic, is modified by partial sulfonation to get a more hydrophilic polymer (Mulder, 1993).

Miyama et al (1988) grafted sodium p-styrene sulfonate on bromine containing polyacrylonitrile (PANBr). They found that membranes made from grafted PANBr (Poly(acrylonitrile)-g-sodium styrene sulfonate) (PAN-g-SSS) showed higher separation of BSA and γ-globulin at pH 4.3 than those made from PANBr. This was attributed to the negatively charged PAN-g-SSS membrane attracting positively charged protein, which increases the permeation of the albumin compared to that of γ-globulin.

Copolymers of acrylonitrile (AN) with hydroxyethyl (HEA) acrylate or hydroxybutyl acrylate (HBA) have been prepared by Silva et al (1990) as suitable hydrophilic materials for dialysis and UF membranes.

Kobayashi et al (1994) prepared charged UF membranes of poly(acrylonitrile-*co*-sodium styrene sulfonate) followed by ion exchange of Na with amphiphilic counter ions such as stearyltrimethyl ammonium chloride. They found that the flux for dextran UF increased as a result of this ion-exchange. Also, the UF separation of dextran / dextran sulfate was enhanced by increasing the content of the styrene sulfonate group in the membrane.

3.4.4.2 *Polymer blends*

Blending of mutually miscible hydrophilic polymers with chemically and thermally stable polymers is another method to prepare more stable hydrophilic polymers. However, the choice of polymers is limited since only a few polymers are miscible with each other. Krause (1978) has reviewed the compatibility of various polymers.

Polyvinylpyrrolidone (PVP) which is a hydrophilic polymer, is known to form blends with polysulfone (PSF) (Tam et al, 1993), polyethersulfone (PES), polyimide (PI) and polyetherimide (PEI) (Roesink, 1989). Membranes from homogeneous blends of these polymers e.g. PVP/PSF or PVP/PES can be prepared by phase inversion. Recently Chen et al (1996) have prepared mechanically stable, partially charged hydrophilic membranes from blends of aminated polysulfone or sulfonated polysulfone with polysulfone.

3.4.4.3 *Surface modification methods*

Another widely investigated method is to modify the surface of an existing hydrophobic membrane. Various modification methods are reviewed by Mulder (1993), Nyström and Howell (1993) and Garg et al (1996). These methods include chemical reaction, plasma treatment and adsorption coating.

Chemical reaction :

Hydrophobic surfaces can be chemically modified by the introduction of charged and / or hydrophilic groups such as carboxylic, amino, hydroxyl, sulfonic or quaternary ammonium groups. Generally, hydrophobic membranes such as polyvinylidene fluoride (PVDF), polyolefins, PAN or PSF membranes are modified by this technique. Examples of this technique are discussed below.

Stengaard (1988) reported that ether or amine groups can be introduced onto a PVDF surface by reaction with a hydroxyl group (R-OH) or a primary amine ($R\text{-}NH_2$) in the presence of a strong base (NaOH).

Polysulfone membranes have been modified by the introduction of hydroxyl groups (Higuchi et al, 1990, 1991, 1993), or sulfonate group (Chang et al, 1987) or by surface

fluorination (Le Roux et al, 1992, Sedath et al, 1993). Higuchi et al (1991) found increased separation between BSA and γ-globulin after surface modification of polysulfone membranes with propylene oxide. They attributed the increase in separation to the balance of hydrophobic and hydrophilic segments on the surface of the modified membrane.

Godjevargova and Dimov (1992) studied the permeability of Vitamin B12 through surface modified, charged membranes of acrylonitrile copolymer. They found that surface modification by NaOH and hydroxylamine increases the hydrophilicity of the membrane and thereby, the permeability of Vitamin B12. However, modification with diethylaminoethyl methacrylate and further quaternization with dimethyl sulfate results in an increase in Vit. B12 permeability only upto 1.6 % degree of grafting, while above this level, the permeability decreased. This decrease was attributed to decreased pore volume in the skin layer of the modified membrane.

Ulbricht et al (1996b) studied grafting of hydrophilic monomers such as acrylic acid, 2-hydroxy ethyl methacrylate (HEMA) and various poly(ethylene glycol) methacrylates on polyacrylonitrile UF membranes by either simultaneous or sequential UV irradiation methods. They found that for UF membranes with sufficient degree of modification (degree of grafting > 400 $\mu g/cm^2$), very little protein (γ-globulin, BSA and cytochrome C) adsorption occurred and almost no fouling due to BSA adsorption was observed.

Garg et al (1996). studied surface modification of polypropylene membranes (Celgard® 2400 and 2500) by hydroxylation with potassium peroxydisulfate solution followed by grafting with acrylamide using cerric ammonium nitrate as an initiator. Subsequently, the acrylamide groups at the membrane surface were partially hydrolyzed to carboxyl groups.

Kim et al (1994) showed that nonselective adsorption of BSA and γ-globulin on polyethylene microfiltration membranes can be reduced by hydrophilizing the membranes by radiation induced grafting of hydrophilic monomers such as HEMA, vinyl acetate and glycidyl methacrylate. Radiation induced grafting of hydrophilic monomers has also been reported using polypropylene hollow fiber membranes (Kim et al, 1996).

Plasma treatment :

Dudley et al (1993) modified 0.2 μm PVDF membranes by first introducing hydroxyl groups by oxygen plasma etching, followed by grafting of 2-methacryloyloxyethyl phosphoryl choline using cerric ammonium nitrate as an initiator. They found that the treated membrane had increased flux and lower rate of flux decline for BSA UF. Similar results were obtained by Akhtar et al (1995) for cellulose acetate MF membranes. Plasma treatment followed by grafting of hydrophilic monomers such as acrylic acid and methacrylic acid on polyacrylonitrile and polysulfone membranes has been shown to improve permeate fluxes for BSA ultrafiltration (Ulbricht and Belfort, 1996a). Surface modification by plasma treatment has also been studied by Wolff et al (1988), Karakelle and Zdrahala (1989), Vigo et al (1988) and Lai and Chao (1988).

Adsorption coating :

In this method, membranes are made hydrophilic by pretreatment with hydrophilic polymers, surfactants etc.

i) Pretreatment with hydrophilic polymers :

Preadsorption or coating of UF or MF membranes with hydrophilic polymers generally results in improved permeate fluxes and reduced protein adsorption.

Adsorption coating of two hydrophilic polymers, poly(vinyl methyl ether) and methyl cellulose, on polycarbonate (Nuclepore) and polysulfone membranes led to reduced protein adsorption within the membrane pores (Brink et al, 1993). This was attributed to the polymers preoccupying the protein adsorption sites. Also, the coated polymer partly seals off the pore entrance and prevents internal protein adsorption due to increased steric hindrance.

Nyström (1989) found decreased flux reduction for ovalbumin UF due to adsorption coating of polysulfone membranes with polyethyleneimine (PEI). He attributed this to the increase in hydrophilicity rather than to charge modification. Surface coating of polyethersulfone membranes by polyurea / polyurethane showed improved permeate fluxes

and flux recoveries for BSA, dextran and PEG ultrafiltration, compared to standard polysulfone membranes (Hvid et al, 1990).

Kim et al (1988) studied the effect of pretreating PM30 membranes with hydrophilic polymers such as methyl cellulose (MC), polyvinyl alcohol (PVA) and polyvinyl pyrrolidone (PVP) by passive or convective adsorption methods. Average flux improvements of 20-40% relative to untreated membranes were obtained for BSA UF. In multiple usage cycles, MC treated membrane showed 100% higher flux after 5 cycles.

Brink and Romijn (1990) studied the effect of preadsorbing polysulfone membranes with anionic, non-ionic and cationic polymers and surfactants, on the adsorption of whey proteins and flux stability. They concluded that application of non-ionic hydrophilic polymers (poly(ethylene glycol), poly(acrylamide), PVP and poly(vinyl methyl ether)) was effective in reducing protein adsorption as well as membrane resistance during ultrafiltration. The application of other surfactants and ionic polymers PEI, poly(acrylic acid), carboxymethyl cellulose and poly(sodium 4-styrene sulfonate) (PSSNa)) was generally less successful.

Bauser et al (1982) found that permeate fluxes for UF of bovine blood serum were increased by 2x and 3x after coating a 0.4 μm Nuclepore membrane with polyacrylonitrile and isotropic carbon, respectively.

ii) Pretreatment with surfactants :

Pretreatment of membranes with ionic or non-ionic surfactants have also been shown to improve permeate fluxes and reduce flux decline.

Coating of alcohols and nonionic surfactants on polysulfone UF membranes showed reduced fouling during UF of model fermentation broths containing either antifoam agents or yeast extract and glucose (Yamagiwa et al, 1994). Nonionic surfactants were generally more effective than alcohols in reducing antifoam agent fouling.

Chen et al (1992) studied the effect of various surfactant coatings on the performance of PM30 membranes used in protein UF. They observed that in contrast to long chain nonionic surfactants, the small anionic surfactant (AOT) reduces protein adsorption by altering protein-membrane electrostatic interactions. AOT was less

effective at reducing flux decline at pH values below the BSA IEP. When AOT was used in conjuction with other nonionic surfactants or with polyethylene oxide, significant flux improvement for BSA UF was observed compared to that when either AOT or a nonionic surfactant was used alone.

Fane et al (1985) observed flux increases for BSA UF after treatment of various membranes with nonionic surfactants. Kim et al (1989) showed that membranes pretreated with non-ionic surfactant monolayers by the Langmuir-Blodgett (LB) technique exhibited 30% higher flux increase than untreated membranes for albumin ultrafiltration. They attributed this effect to the increase in membrane smoothness and homogeneity rather than the increase in hydrophilicity, because similar flux improvement was also observed with a coating of strongly hydrophobic stearic acid.

iii) Other pretreatment methods :

Dumon and Barnier (1992) showed that the presence of negatively charged phosphate or citrate groups on the surface of zirconia membranes, prior to ovalbumin UF, favoured low adsorption of ovalbumin, while nitrate groups favoured high adsorption of this protein.

Howell and Velicangil (1980) suggested increasing flux by enzyme immobilization on the membrane surface to hydrolyze adsorbed solute. They immobilized various proteases and papain on PM-10 membranes and showed flux improvements for BSA, hemoglobin and cheese whey ultrafiltration. The net protein loss due to cleavage of filtered albumin by active enzyme was found to be between 5-7% of the total protein processed.

3.5 FACTORS AFFECTING FOULING AND PROTEIN TRANSMISSION IN ULTRAFILTRATION

Fouling and protein transmission in ultrafiltration is affected by:

i) membrane characteristics such as pore size, surface roughness, hydrophilicity, surface charge and energy,

ii) protein solution characteristics such as pH, ionic strength and concentration, and
iii) membrane system operating parameters.
These factors are reviewed here briefly.

3.5.1 MEMBRANE CHARACTERISTICS

3.5.1.1 *Pore size / pore size distribution*

It is well documented that increasing the membrane pore size and hence reducing the intrinsic membrane resistance, results in increased membrane fouling. For example, while processing isoelectric soy protein precipitate suspensions, Devereux and Hoare (1986) found that the flux decline of a 0.2 μm MF membrane was greater than that of a PM-50 UF membrane. Gatenholm et al (1988) also found higher flux decline for fermentation broth (E. *coli.*) filtration with a 0.2 μm MF membrane than with a 100 kD UF membrane. Attia et al (1988, 1991b) while processing skim milk with alumina MF membranes found higher permeate fluxes with a 0.2 μm membrane than with a 0.8 μm membrane.. While removing yeast cells from apple cider broths using various MF membranes, Scott (1986) found that fluxes increased with increasing pore size; however, flux decline was higher as the pore size increased. Higher fouling in MF membranes than UF membranes has also been observed by Defrise and Gekas (1988) for cell debris removal and cell recycle. Tarleton and Wakeman (1993) found that steady state filtrate fluxes during suspension filtration decreased with increasing pore size, indicating fouling in pores.

Mueller and Davis (1996) studied the effect of surface porosities on the fouling of track-etched polycarbonate (PC), polysulfone (PSF), cellulose acetate (CA) and polyvinylidene fluoride (PVDF) membranes. The low-surface porosities of PSF and PVDF membranes leads to almost immediate external fouling; while with the higher surface porosity PC and CA membranes, internal fouling is more important. Protein transmission remained constant or decreased only slightly due to internal fouling, while significantly decreased protein transmission was observed with external fouling.

The membrane pore size also affects protein transmission. This has already been discussed in section 3.1. Pore size distribution can also be important in some applications.

For example, Urase et al (1996) studied the transmission of Coliphage QB and T4 viruses through membranes with various pore sizes. They found leakage of viruses through some membranes, which they attributed to some pores being considerably larger than the average pore size. Some MF membranes showed higher virus rejection than UF and NF membranes.

The theoretical basis for the dependence of solute permeability and flux on membrane porosity was described in section 3.1.

3.5.1.2. *Hydrophilicity*

Though membrane hydrophilicity is not the only factor affecting fouling (van der Horst and Hanemaiijer, 1990), it is definitely important. It is well documented that hydrophilic membranes tend to adsorb less protein than hydrophobic ones (Reihanian et al, 1983; Matthiasson 1983, 1984; Osada et al, 1986; Lee and Ruckenstein, 1988; Gölander and Kiss, 1988; Hanemaiijer et al, 1989; van den Berg and Smolders, 1990; Sheldon et al, 1991; Persson et al, 1993). Correspondingly, higher permeate fluxes have been achieved when the membrane surface is more hydrophilic (Fane et al, 1985, 1987; Aimar et al, 1988; Stengaard et al, 1988, Hanemaiijer et al, 1989, Kim et al, 1995).

The hydrophobicity of the membrane surface can also influence the nature of the deposited protein. For example, Sheldon et al (1991) considered the adsorption of BSA on 10 kD polysulfone and regenerated cellulose membranes using various TEM techniques. They found that the tertiary protein structure of the globular protein was disrupted and distorted by interactions between BSA and polysulfone.

Membrane hydrophilicity also affects protein transmission. Rolchigo et al (1989) considered the behaviour of a protein solution (myoglobin, BSA and ferritin) with two 100 kD Ultrafilic™ membranes; one which had a contact angle of 4° and an unmodified precursor with a contact angle of 46°. They found that BSA and myoglobin transmissions were higher with the hydrophilic membrane in both crossflow and rotary systems. Higuchi et al (1993) compared the separation of γ-globulin and BSA through surface modified and unmodified polysulfone membranes. They observed that the transmission of γ-globulin was higher than BSA at pH 7.2 and 9.0, although the molecular weight of γ-globulin is higher

than that of BSA. They attributed this to the balance of hydrophilic and hydrophobic segments on the surface of modified membranes, rather than to charge repulsion or sieving mechanisms.

Additional literature on the effect of membrane hydrophilicity on ultrafiltration performance has been cited in Sec. 3.4.4.

3.5.1.3 *Surface roughness / surface energy*

The influence of surface roughness on flux and fouling has been investigated by Fane and Kim (1988), who found greater flux loss with increase in surface roughness. Kim et al (1989) also found that the smoothing of the surface by application of Langmuir-Blodgett layers decreased flux loss and fouling.

Larsson (1980) stated that any increase in surface roughness increases the surface free energy, which in turn could be expected to increase the tendency for adhesion of surface active molecules.

Fell et al (1990) suggested that surface roughness will affect the transverse flow of the feed with a strong likelihood of high local concentration polarization at the pore entrance. They attributed this to liquid stagnation in the surface depressions where pores usually exist.

3.5.1.4 *Surface charge*

Generally, higher permeate fluxes are obtained if the membrane is of similar charge to that of the protein being ultrafiltered (Nyström and Lindström, 1988; Heinemann et al, 1988; Nyström, 1989; Brink and Romijn, 1990). The electrostatic charges on a membrane are dependent upon the membrane material, the pH and the ionic strength of the feed solution. Polymeric membranes are generally negatively charged at neutral pH. For example, polysulfone PM10 and Dynel XM-300 membranes carry negative charges at pH 2-10 while cellulosic YC-05 membranes have an isoelectric point at pH 9 (Lee and Hong, 1988). By contrast some inorganic membranes such as alumina which has an IEP at pH 4 are positively charged at neutral pH.

Bowen and Hughes (1990) found that adsorption of BSA on alumina membranes decreased below pH 4 due to electrostatic repulsion between positively charged membrane and protein. Dumon and Barnier (1992) reported that the presence of negatively charged phosphate or citrate groups at the surface of the zirconia membranes favours low ovalbumin. adsorption. Godjevargova and Dimov (1992) also found less BSA adsorption and higher permeability with membranes based on hydrolyzed poly(acrylonitrile) (containing carboxyl groups) than on poly(acrylonitrile) itself at pH 7.4.

The electrical charge on the membrane has also been used to enhance the separation of charged proteins / solutes. For example, Nakao et al (1988) measured the transmission of myoglobin and cytochrome C (which are of similar sizes) through positively and negatively charged polysulfone membranes. They found that rejection of proteins of the same charge as the membrane (either positive or negative) was high. The rejection of both proteins at their IEP was low, despite a reduction in pore size due to increased protein deposition at this pH. Kontturi et al (1996) achieved separation of HSA and hemoglobin (which are again of similar sizes) by convective electrophoresis using ion exchange membranes. They found that the HSA/Hb separation factor increases with decreasing pH in the range of 7.2 - 5.2, where the negative charge on BSA decreases while HSA becomes more positive. Kobayashi et al (1994) reported that the separation of dextran over dextran sulfate by charged ultrafiltration membranes of poly(acrylonitrile-*co*-styrene sulfonate) with stearyl trimethyl ammonium chloride as a counterion, increases as the styrene sulfonate group content in the membrane increases. For BSA-γ-globulin separation Miyama et al (1988) obtained a higher separation factor with negatively charged poly(acrylonitrile)-*graft*-poly(sodium-p-styrene sulfonate) membranes compared to that for poly(acrylonitrile) at pH values both above and below IEP of BSA (pH 4.8) and below IEP of γ-globulin (pH 7.0).

3.5.2 SOLUTION ENVIRONMENT

3.5.2.1 *Effect of pH*

The solution pH determines the net charge on the protein; thereby, it affects membrane-protein interactions, protein-protein interactions and the solubility of proteins

and salts in the feed solution. Thus, it affects the amount of protein adsorption on the membrane surface, the protein fractionation properties and the permeate flux..

i) Protein-membrane interactions : It is generally observed that the permeate flux is minimum at the protein isoelectric point (Muller et al, 1973; Hayes et al, 1974; Fane et al, 1983a, 1983b; Nyström, 1989; Palecek et al, 1993; Kim et al , 1995; Iritani et al, 1995b). The decrease in flux at the protein IEP is generally attributed to increased adsorption or deposition of protein at this condition where the net charge on the protein is zero (Reihanian et al, 1983; Fane et al, 1983a; Fane et al, 1985; Bowen and Hughes, 1990; McDonogh et al, 1990; Clark et al, 1991; Kim et al , 1995). However, Matthiasson (1983), in static adsorption studies with polysulfone and cellulose acetate membranes in an unstirred cell, found that BSA adsorption increased continuously with decreasing pH with maximum adsorption at the lowest pH (pH 3) i.e. when the protein and membrane are oppositely charged.

Pouliot et al (1994) studied the UF of negatively charged whey proteins in a pH range of 4.8 - 6.7 through positively charged alumina membranes. They found that the permeate flux decreased as the pH approached the protein IEP. For the ultrafiltration of ovalbumin through GR61PP and GS61PP membranes, Nyström (1989) found that the flux was high at pH 8, where both protein and membrane are negatively charged. However, at pH 3-4, where protein and membrane are oppositely charged the flux was still high, which cannot be explained by protein-membrane interactions alone. Hence the effect of pH on the protein itself must also be considered. When a protein is charged, its solubility / stability increases and the affinity for the membrane material decreases (Marshall et al, 1993).

Hanemaaijer (1985) found a slight decrease in rejection of whey proteins as the pH was decreased from 6.5 to 5.5. However, in another study on β-lactoglobulin ultrafiltration, Hanemaaijer et al (1988, 1989) found that maximum rejection occurred around pH 4, which corresponded to the point of maximum protein deposition.

ii) Protein-protein interactions : In a study of unstirred, dead-end ultrafiltration of BSA through 30 kD polysulfone membranes, Iritani et al (1991) found that the average cake porosity was minimum and the average specific filtration resistance was maximum at

the BSA IEP. In a study of BSA-Lysozyme ultrafiltration with 10 kD polysulfone membranes, Iritani et al (1995a) found that the average cake porosity decreased and the average specific filtration resistance increased with increasing pH. They attributed this effect to the maximum electrostatic repulsion between both proteins at pH 4, since both proteins are positively charged at this pH. At higher pH values BSA becomes negatively charged while lysozyme remains positively charged.

Miyama et al (1988) obtained higher separation factors for BSA-γ-globulin UF through poly(acrylonitrile)-*graft*-(styrene sulfonic acid) membranes below the BSA IEP than above IEP. BSA transmission through the negatively charged membrane was higher when BSA was positively charged.

Attia et al (1988) studied the effect of acidifying milk on the performance of a Ceraver 0.2 μm alumina membrane. Acidification from pH 5.9 to 5.6 resulted in a significant decrease in flux. Further decrease in pH from 5.6 to 4.6 resulted in higher initial fluxes; however the flux rapidly declined to a value less than that seen with milk at its normal pH (6.7). Attia et al (1991a) studied the foulant layer by SEM and found that the foulant structure became increasingly compact with decreasing pH, with maximum compactness at pH 5.6. Below pH 5.2, the deposit consisted of individually clumped particles (identified as demineralised casein micelles) which formed an increasingly open structure. Thus, the nature of protein deposited during UF at various pH values affects the permeate flux.

iii) Precipitation of solutes : Precipitation of solutes other than proteins at certain pH values also affects UF performance. For example, while studying the UF of whey on zirconium oxide membranes, Labbé et al (1990) observed calcium phosphate precipitation when the feed pH was increased from 5.6 to 6.9. This resulted in decreased permeate flux above pH 5.6.

3.5.2.2 *Effect of Ionic strength*

The ionic strength (I) of protein solutions modifies the charge on the protein and thereby affects permeate fluxes, protein rejections and the amount of protein adsorption on the membrane surface.

For BSA ultrafiltration through XM100A membrane, Fane et al (1983a, 1983b) and Kim and Fane (1995) found that increasing I at pH values above and below the IEP results in decreased flux due to shielding of electrostatic charges. At the IEP, flux increased with increasing I due to anion binding. Palecek et al (1993) also observed similar results at pH values other than the IEP. At the BSA IEP, they found flux to be independent of I. By contrast with the above results Iritani et al (1995c) found that the UF flux of a BSA-lysozyme solution increased with increasing I upto 0.3 M and then remained constant upto 0.6 M.

Nel et al (1994) studied the UF of BSA-IgG through 100 kD cellulosic membranes. They found that hydraulic permeability, after the UF run decreases with increasing salt concentration in the protein feed from 0.01 to 0.15 M. They attributed this effect to increased protein binding to the membrane at higher I.

Changing I is known to affect the protein transmission in reverse modes i.e. transmission can either increase or decrease with increasing I. For example, during ultrafiltration of a BSA-lysozyme mixture at pH 7 through 30 kD polysulfone membranes, Iritani et al (1995c) found that lysozyme transmission increases with increasing I (0-0.6 M). Renner and Abd El-Salam (1991) also showed that the transmission of β-lactoglobulin and α-lactalbumin increased as NaCl was added to the feed during UF of whole milk. However, Nel et al (1994) found that BSA transmission through a 100 kD cellulosic membrane at pH 5.8 was higher at 0.01 M NaCl than at 0.15 M NaCl. This trend was slightly reversed at pH 8.5. Millesime et al (1994) also studied the ultrafiltration of BSA-lysozyme mixture at pH 7 through 100 kD membranes prepared from sulfonated polysulfone (negatively charged) as well as sulfonated polysulfone modified with quaternized polyvinylimidazole (positively charged). At lower I (0-0.1 M), they found significant differences in the rejection of positively charged lysozyme and negatively charged BSA when the proteins and membrane were oppositely charged. However, at higher I (0.1-1 M), protein rejection and membrane flux with both positive and negatively charged membranes were similar due to protein adsorption on the membranes and the interactions of adsorbed protein with free protein.

The calcium content in milk or whey has been shown to affect ultrafiltration performance. Hayes et al (1974) reported that addition of calcium to cheese whey reduced the flux at pH 6.2. In a complementary study, Patocka and Jelen (1987) showed that cheese whey pretreatments which removed free calcium, resulted in improved flux . Vetier et al (1988) performed UF trials with milk having various calcium contents and found that increased calcium levels resulted in increased fouling due to calcium phosphate precipitation. They suggested that calcium acts as a "cement" between micelles and the alumina membrane and between the micelles themselves.

The effect of changing *I* has also been studied for protein fractionation. Recently, Eijndhoven et al (1995) showed that during BSA-hemoglobin (Hb) ultrafiltration through 100 kD polysulfone membranes, the Hb/BSA selectivity increased from 2.5 to 70 as the solution ionic strength was reduced from 0.1 to 0.0023 M.

3.5.2.3 *Effect of Feed concentration*

Increasing the feed concentration during UF generally results in a decrease in the permeate flux. Generally, flux decreases with log concentration as predicted by concentration polarization theory (see section 3.2). However, the linear relationship between flux and log concentration does not necessarily hold at high concentrations. While processing E. *coli* at high concentrations, Tuntunjian (1984) found that the rate of flux decline with concentration was higher than expected from the semi-log relationship. On the other hand, Le et al (1984) found higher permeate fluxes than expected with high feed concentrations, and in one case, the permeate flux has even been reported to increase with increasing concentration (Pritchard, 1990). Scott (1988) showed that at high velocities ($> 50\ l\ h^{-1}$), increasing concentration did not reduce flux significantly although at low velocities ($< 50\ l\ h^{-1}$) flux reduced with increasing concentration.

In the case of surface fouling, increasing feed concentration has been shown to increase the total membrane resistance (Taddei et al, 1988; Daufin et al, 1991b). However, Daufin et al (1991b) found that whereas concentration polarization increased with concentration, irreversible fouling remained unaffected. In spite of the decrease in flux, rejections do not generally vary with increasing feed concentration, suggesting that the

surface fouling does not affect transmission markedly (Taddei et al, 1988; Matsumoto et al, 1988; Bennasar et al, 1982).

On the other hand, in case of internal fouling, increasing concentration resulted in more rapid flux decline (Bowen and Gan, 1991). This may be attributed to the increased exposure of the membrane to solute (increased adsorption) with increasing concentration. McDonogh et al (1990) showed that BSA adsorption on polysulfone powder increases with increasing concentration at various pH values in a range from 3 - 11. The only exception was at pH 6.5, at which the adsorption remained constant with increasing concentration. Similarly, Persson et al (1993) found increased β-lactoglobulin adsorption on various membranes with increasing log concentration.

The feed solution concentration also affects the rejection. For example, for BSA ultrafiltration through three Membralox membranes of varying pore sizes, Clark et al (1991) found that at low protein concentrations (0.1 g/L), BSA rejection decreased as pore size increased. However, at high concentrations (1 g/L), the rejection was the same for all three membranes and was also independent of feed pressure and velocity.

The concentration of one component in the binary mixture affects the rejection of other components. Usually, rejection of smaller components of the mixture is increased by increasing concentration of the larger component, as found by Iritani et al (1995c) for UF of BSA-lysozyme. In a study of BSA-IgG ultrafiltration through 100 kD cellulosic membranes, Nel et al (1994) found that at either pH 5.8 and 0.15 M NaCl or pH 8.5 and 0.01 M NaCl, introduction of 0.07% IgG caused an increase in BSA rejection.

3.5.3 OPERATING PARAMETERS

Various operating parameters such as transmembrane pressure, temperature and crossflow velocity also affect ultrafiltration performance.

3.5.3.1 *Effect of transmembrane pressure*

Increasing transmembrane pressure generally results in increased flux. However, pressure is ineffective beyond a certain level because of i) the limiting flux caused by concentration polarization and ii) increased fouling. Limiting flux effects during UF of

BSA or whey solution have been reported by Daufin et al (1992), Attia et al (1988), Bentham et al (1988), Meireles et al (1991) and Taddei et al (1986, 1988). The dependence of flux on pressure predicted by the concentration polarization - osmotic pressure model was discussed in section 3.2.2.

Taddei et al (1986, 1988) found that the pressure induced flux increase was accompanied by increased membrane fouling. Similar behavior was observed by Bowen and Gan (1991) for BSA microfiltration and Gésan et al (1993) and Labbé et al (1990) for whey microfiltration and ultrafiltration respectively. Nakanishi and Kessler (1985) found that reducing the transmembrane pressure during ultrafiltration considerably increases the rate of removal of the deposited layer during rinsing, even though the transmembrane pressure had little effect on the flux during ultrafiltration.

Kroner et al (1987, 1988) investigated the separation of cell debris from enzymes and found that enzyme transmission decreases rapidly with increasing transmembrane pressure. Kim et al (1992) found that with a 100 kD polysulfone membrane, BSA rejection increased rapidly at 1 bar to around 70% after 40 min. By contrast at 0.5 bar, the rejection remained constant for 20 minutes before increasing more slowly to around 35%.

An extensive study on the flux and transmission of lysozyme, ovalbumin and myoglobin as a function of transmembrane pressure in a rotary filter has been carried out recently for UF of single proteins (Balakrishnan and Agarwal, 1996a). They found increase in both flux and transmission with increase in pressure (10-90 kPa) during protein UF.

3.5.3.2 *Effect of temperature*

Increasing temperature generally increases flux in both UF and MF by i) reducing permeate viscosity, and ii) increasing solute diffusivity, which assists dispersion of the concentration polarized layer (Attia et al, 1991; Scott, 1988). The dependence of flux on these parameters was discussed in section 3.1 and 3.2.1.

Piot et al (1984) and van Boxtel et al (1991) found with cheese whey UF that the rate of flux decline increases with increasing temperature. Piot et al (1984) attributed the

increased fouling rate to the precipitation of calcium phosphate. Vetier et al (1988) also saw a distinct increase in calcium and phosphate fouling with skim milk at 50°C than at 20°C. They attributed this mainly to the increased flux at 50°C.

Protein rejection can decrease with increasing temperature (Attia et al, 1991b, 1988). However, Piot et al (1984) suggested that the reduction in protein rejection may be due to increased concentration polarization as a result of higher membrane fluxes rather than to a reduction in membrane fouling.

Increasing temperature also affects protein stability and solubility. For example, during BSA ultrafiltration at pH 7 through a 100 kD polysulfone membrane, Meireles et al (1991) showed that solution turbidity increased with time when the solution was ultrafiltered at temperatures greater than 8°C. HPLC and light scattering confirmed the presence of polymeric species, probably protein aggregates, above 8°C.

3.5.3.3 *Effect of crossflow velocity*

As discussed in section 3.2.1.1, increase in crossflow velocity results in increased mass transfer coefficient, and hence, increased permeate fluxes.

Increasing crossflow velocity also affects protein stability, and hence, can result in increased adsorption on the membranes. While processing soy protein precipitate suspensions, Devereux and Hoare (1986) found that greater pore obstruction occurred at high shear rates due to break-up of precipitate aggregates by higher pump speeds.

3.6 POLY(ACRYLONITRILE) BASED MEMBRANES.

This section summarizes the literature related to protein UF through PAN based membranes. The limitations of previous studies are also pointed out.

PAN or modified PAN based polymers are commonly used for fabricating UF membranes. Such membranes are commercially available from several manufacturers such as Asahi, Rhone-Poulenc, Akzo-Enka, Membrex, Daicel and PCI. PAN based membranes can be used in a number of applications within a pH range of 3-10 and a high temperature operating limit of 60°C. PAN based membranes can be made in a form compatible for blood processing. These membranes also have a fairly wide range of solvent compatibility.

In order to optimize their UF performance, commercially available PAN membranes have proprietary copolymer or even terpolymer compositions as reported in the patent literature (Brun and Angleraud, 1992). Several more systematic studies with PAN based membranes are also reported in the open literature.

Hydrolysis of PAN has been used as a method to modify the membrane surface. Introduction of hydrophilic and / or charged functional groups on the membrane surface by this method has been attempted in order to obtain membranes with reduced fouling / protein adsorption. For example, Godjevargova and Dimov (1992) found less BSA adsorption and higher UF membrane permeability on hydrolyzed poly(acrylonitrile) (containing carboxyl group) than on poly(acrylonitrile) itself at pH 7.4. One problem with this approach, in a comparative study of membrane surface properties such as hydrophilicity, surface energy etc., is the possibility of changing membrane porosity during modification and also the complex surface composition which results from hydrolysis.

Plasma treatment followed by grafting of hydrophilic monomers such as acrylic acid, 2-hydroxyethyl methacrylate and methacrylic acid on PAN membranes has been shown to improve permeate fluxes for BSA UF (Ulbricht and Belfort, 1996a). Again, it is difficult to control membrane porosity by this approach.

Kobayashi et al (1994) prepared negatively charged ultrafiltration membranes of poly(acrylonitrile-*co*-styrene sulfonate) with stearyl trimethyl ammonium chloride as a counterion. They reported that the separation of dextran over dextran sulfate increases as the styrene sulfonate group content in the membrane increases. This was attributed to repulsive interactions between dextran sulfate and the membrane. Similarly, Miyama et al (1988) prepared negatively charged poly(acrylonitrile)-*graft*-poly(sodium-p-styrene sulfonate) membranes and compared them with poly(acrylonitrile) membranes for the UF separation of BSA-γ-globulin containing solutions. The grafted PAN based membrane gave higher BSA-γ-globulin separation at pH 4.3. They attributed this to attractive interactions between positively charged BSA and negatively charged membrane which led to greater BSA transmission. Hence, both these studies indicate that protein transmission is higher if the solute and membrane are of opposite charges. These studies were done over a limited pH range. Also, the membrane surface charge and hydrophilicity were not

explicitly measured in these studies. Since PAN itself is also negatively charged it would seem desirable to measure the increase in surface charge due to sufonate groups.

Balakrishnan et al (1993) and Balakrishnan and Agarwal (1996a, 1996b) studied ultrafiltration of lysozyme, ovalbumin and myoglobin at various pH, *I* and pressures through Membrex Ultrafilic™ (hydrophilic PAN) membranes. The study was carried out with a rotary module. The membrane surface characteristics were not well defined as this membrane is of a proprietary nature.

Chapter 4

EXPERIMENTAL

The experimental techniques used for the study of the filtration characteristics of polyacrylonitrile based membranes are described in this chapter. The polymer and membrane preparation and characterization methods are described first. This is followed by a description of the preparation of test solutions such as those of standard proteins (BSA, Hb : individual and mixture) and wheys from various sources (acid, cheese and shrikhand). The methodology used in the permeation studies with the above test solutions in order to determine permeate flux, solute rejection, flux recovery and separation factor (in case of mixed proteins) is then described.

The equipment used in this study along with the various model specifications, as applicable, are listed in Table 4.1.

The chemicals used in the this work along with their purity / grade and sources are tabulated in Table 4.2.

4.1. MEMBRANE PREPARATION AND CHARACTERIZATION

4.1.1 POLYMER SYNTHESIS

Poly(acrylonitrile) (PAN) was obtained from Indian Petrochemicals Ltd., India. It was dissolved in dimethyl formamide (DMF) and re-precipitated in methanol and vacuum dried at 70°C for 4 days.

Copolymers of acrylonitrile and acrylamide with varying mole ratios of the two monomers were prepared as follows.

The acrylamide monomer was of electrophoresis grade and was used as received. The acrylonitrile was of commercial grade and was purified as per the procedure of Chiang and Hu (1985). The acrylonitrile was washed with 3% NaOH and then with 3% ortho-phosphoric acid; this was followed by a distilled water wash repeated three times. The washed acrylonitrile was then dried on $CaCl_2$ and subsequently distilled under reduced pressure at 55°C.

In order to prepare the copolymers, acrylonitrile and acrylamide, in various mole ratios, were first dissolved in N,N dimethyl formamide (DMF) at 50% by weight of total monomer concentration. The mole ratios of the two monomers (acrylonitrile : acrylamide) in the initial reaction mixture were varied as 85 :15 (PAN-1), 85 : 15 (PAN-2) and 75 : 25

Table 4.1
List and specifications of equipments used

Equipment / set up	Make
UV-Vis Spectrophotometer (model UV-240)	Shimadzu Corporation, Japan
Scanning Electron Microscope (model Stereoscan 440)	Leica, UK
Elemental analyser (model 1108)	Carlo Erba
Gold sputtering apparatus (model E5000)	Polaron equipment Ltd., Watford, England
Goniometer (model 100-00230)	Rame-Hart Inc., USA
IR Spectrometer (model 683)	Perkin-Elmer, USA
NMR Spectrometer (model 80 / 200 MHz)	Bruker
Digital Conductivity meter (model 1292)	Systronics, India
Digital pH meter (model DPH 500)	Global Electronics, India
Brookfield Viscometer (DV-I)	Brookfield Inc., USA
Bubble Point Apparatus (manual)	Filtech, India
Ultrafiltration Cell (model 52)	Amicon, USA
Electroosmosis set-up	Inhouse fabrication (Figure 4. 2)
Centrifuge machine (model SC 7500)	Eltek, India

Table 4.2

List and specifications of materials used

Material	Grade* / purity	Supplier
Acids		
Acetic acid	LR	S.D. Fine Chem. Ltd., India
Citric acid	AR	S.D. Fine Chem. Ltd., India
Hydrochloric acid	AR	S.D. Fine Chem. Ltd., India
Nitric acid	AR	S.D. Fine Chem. Ltd., India
Orthophosphoric acid	AR	S.D. Fine Chem. Ltd., India
Bases		
Sodium hydroxide	AR	S.D. Fine Chem. Ltd., India
Potassium hydroxide	AR	S.D. Fine Chem. Ltd., India
Tris(hydroxymethyl) methylamine/ (Tris)	LR	S.D. Fine Chem. Ltd., India
N,N,N′,N′ Tetramethyl ethylenediamine	Ultrapure	S.D. Fine Chem. Ltd., India
Miscellaneous chemicals/reagents		
Acrylamide	Electrophoresis	S.D. Fine Chem. Ltd., India
Acrylonitrile	LR	S.D. Fine Chem. Ltd., India
Folin-Ciocalteu's phenol reagent	ExcelaR	Qualigens Fine Chem., India
Iodine	LR	S.D. Fine Chem. Ltd., India
Lactose	LR	S.D. Fine Chem. Ltd., India
Sucrose	AR	S.D. Fine Chem. Ltd., India
N,N′ methylene bisacrylamide	LR	S.D. Fine Chem. Ltd., India
Ammonium persulfate	AR	Loba Chemie, India
Sodium dodecyl sulfate	LR	S.D. Fine Chem. Ltd., India
Coomassie-Brilliant Blue (CBB G-250)	AR	S.D. Fine Chem. Ltd., India
Bromophenol blue	AR	S.D. Fine Chem. Ltd., India
Polymers		
Poly(acrylonitrile)	Commercial	IPCL, India
Poly(ethylene glycol)	Ultrapure	Aldrich, USA

Table 4.2 contd.

Material	Grade* / purity	Supplier
Proteins / enzymes		
Bovine Serum Albumin (Fraction V)	Purified	Hi Media Lab.s , India
Hemoglobin	LR	S.D. Fine Chem. Ltd., India
Urease	Ultrapure	BDH Chemicals Ltd, UK
Salts		
Ammonium sulfate	LR	S.D. Fine Chem. Ltd., India
Barium chloride	AR	S.D. Fine Chem. Ltd., India
Copper sulfate	AR	S.D. Fine Chem. Ltd., India
Disodium hydrogen phosphate	AR	S.D. Fine Chem. Ltd., India
Potassium chloride	AR	S.D. Fine Chem. Ltd., India
Potassium iodide	LR	S.D. Fine Chem. Ltd., India
Sodium carbonate	AR	S.D. Fine Chem. Ltd., India
Sodium chloride	AR	S.D. Fine Chem. Ltd., India
Sodium dihydrogen phosphate	LR	S.D. Fine Chem. Ltd., India
Sodium Potassium Tartarate	LR	S.D. Fine Chem. Ltd., India
Solvents		
Formamide	AR	S.D. Fine Chem. Ltd., India
Isobutyl alcohol	AR	S.D. Fine Chem. Ltd., India
Methyl alcohol	LR	S.D. Fine Chem. Ltd., India
N,N-dimethyl formamide	LR	S.D. Fine Chem. Ltd., India

* AR : Analytical reagent
LR : Laboratory regent

(PAN-3). The 50% monomer solution in DMF was then degassed and flushed with nitrogen. Concentrated HNO_3 (0.0657 moles/l) was added as an initiator and the copolymerization was carried out with stirring at 80°C for 10 hours (Bhadani and Kundu, 1980). The copolymer which was obtained in the form of a viscous mass, was precipitated in methanol. It was redissolved in DMF and re-precipitated in methanol. The copolymer was then vacuum dried at 70°C for 4 days.

4.1.2 POLYMER CHARACTERIZATION

The homopolymer and copolymers were characterized for intrinsic viscosity (η), infra-red spectra (IR), nuclear magnetic resonance spectra (NMR), elemental analysis, hydrophilicity and surface energy. The structures of the homopolymer and copolymer are shown below.

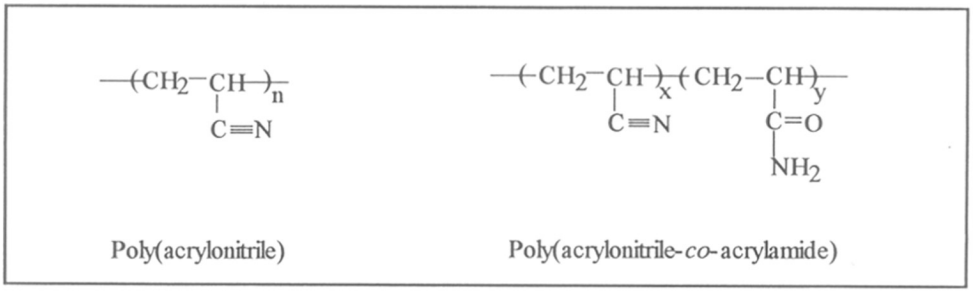

Figure 4.1 : Chemical structures of PAN and copolymers

i) *Elemental analysis* :

The elemental analysis was carried out with dried samples using a Carlo Erba elemental analyzer (model EA-1108). The theoretical elemental copolymer composition was calculated on the basis of the starting reaction mixture composition, assuming 100% yield (see Appendix 1).

ii) *Infra-red Spectroscopy* :

The IR spectra were scanned on polymer films prepared by solvent evaporation of 5% solutions in DMF, at 80°C and then vacuum drying for 8 days at 80°C.

iii) *NMR Spectroscopy* :

The copolymer composition was determined by ^{1}H NMR in DMSO-d_6 using 80 or 200 MHz NMR, following the method of Hu (1994).

iv) *Intrinsic viscosity* :

The intrinsic viscosities (η) were determined by the single point viscosity method (Raju and Yaseen, 1992) with dilute polymer solutions (0.1 g/dl) in DMF at 30°C using an Ostwald viscometer. η was determined from the specific viscosity η_{sp} as :

$$\ln[\eta] = \ln\left(\frac{\eta_{sp}}{C}\right) - K\eta_{sp} \qquad (4.1)$$

where, C is the polymer concentration, η_{sp} is the specific viscosity (= t_s/t_o-1), t_o and t_s are the flow times for solvent and solution respectively and K is a constant (K = 0.14 for η_{sp} < 0.3 and K = 0.12 for 0.3 > η_{sp} < 0.8).

v) *Contact angle measurements* :

The intrinsic hydrophilicity / hydrophobicity of the polymers was determined using a goniometer to measure the polymer / water contact angle by the sessile drop method (Zhang et al, 1989). According to this method, a water droplet of known volume (0.04 ml) was placed on the surface of a polymer film using a microlitre syringe . The angles on both sides of the water droplet were measured after 20 seconds. The angles were repeatedly measured at about 10 different positions to verify surface homogeneity and then averaged.

vi) *Surface Energy* :

The polar and dispersive force components of surface free energy were determined from the measured contact angles of each polymer with water and formamide using the following equation (Owens and Wendt, 1969) :

$$1+\cos\theta = 2\left(\gamma_s^d\right)^{0.5}\left[\left(\gamma_l^d\right)^{0.5}/\gamma_{lv}\right] + 2\left(\gamma_s^p\right)^{0.5}\left[\left(\gamma_l^p\right)^{0.5}/\gamma_{lv}\right] \qquad (4.2)$$

and using the reported surface energy parameters for water and formamide (Fowkes, 1964). In eqn (4.2), θ is the polymer / liquid contact angle, γ_s^p and γ_s^d are the polar and dispersion force components of the polymer surface free energy, γ_l^p and γ_l^d are the corresponding parameters for the test liquid and γ_{lv} is the liquid/air interfacial tension.

The values of relevant parameters for water and formamide are shown below :

	Water	Formamide
γ_{lv} (dynes cm^{-1})	72.8	58.2
γ_l^p (erg cm^{-2})	51	18.5
γ_l^d (erg cm^{-2})	21.8	39.7

4.1.3 MEMBRANE PREPARATION

The polymers were dissolved in dimethyl formamide (DMF) by overhead stirring for 12-16 hours. The viscosities of the polymer solutions were measured at 27°C using a cone and plate viscometer. The polymer concentrations and viscosities of the corresponding polymer solutions used for casting the various membranes are shown in Table 4.3. The solutions were degassed in vacuum and centrifuged at 4000 rpm for 30 minutes before casting. The solutions were then knife coated on a continuously moving porous polyester non-woven backing (Hollytex 3329) of 100 μm thickness. The cast solutions were gelled in water at 27-30°C after a short air dwell time of 7 seconds. The actual membrane thickness (without the thickness of backing) was ≈ 75 μm. The membranes were washed overnight in flowing water, rinsed several times in distilled water and preserved at 10°C until use.

4.1.4 MEMBRANE CHARACTERIZATION :

Membranes were characterized in terms of their average pore size, pore size distribution, morphology and electrostatic surface charge.

Table 4.3

Characteristics of polymer solutions used for casting membranes

Membrane	Polymer Concentration (% wt/wt)	Solution Viscosity* (cps)
PAN	17	650
PAN-1	17	475
PAN-2	17	224
PAN-3	20	1428

* Measured with Brookfield cone-plate viscometer at 27°C and 150 sec^{-1} shear rate

4.1.4.1 *Pore size and pore size distribution* :

Conventionally, pore size and pore size distribution of microfiltration membranes are determined by the well-known bubble point method. In this method, water within the membrane pores is displaced by air. Since the water/air interfacial tension is high (73 dynes/cm), the detection of smaller pores with this method requires correspondingly high pressures, which can result in pore structure damage. Therefore, the UF membranes were characterized by a modified bubble point method (Capannelli et al, 1983), in which two immiscible liquids with very low interfacial tension are used instead of water/air. This allows the determination of smaller pores at relatively low pressures.

The membranes were soaked overnight in distilled water, which was then displaced by water saturated isobutanol (σ^{I}= 1.7 dynes/cm) with a step-wise constant increment (i)

of pressure. The measurements were made on 13.4 cm^2 area membrane pieces. The pore size and pore number density were calculated using Cantor's relation (eqn. 4.3) and Hagen-Poiseuille's equation (eqn. 4.4), respectively, assuming the same effective thickness (≈ thickness of surface skin layer) of 1 μm for all membranes. The assumption of equal effective thicknesses of 1 μm in all cases affects only the estimate of the pore number density. Thus, the pore radius (r_{pi}) was calculated as :

$$r_{pi} = \frac{2\sigma^1 \cos\theta}{P_i} \tag{4.3}$$

where θ is the polymer / water contact angle and P_i is the applied pressure.
The number of pores per unit area (n_i) were calculated as :

$$n_i = \left(J_i - \frac{J_{i-1} P_i}{P_{i-1}} \right) \frac{8\eta l}{\pi P_i r_{pi}^{\ 4}} \tag{4.4}$$

where η is the viscosity of water and l is the pore length which is assumed to be equal to the membrane skin layer thickness. The fluxes J_i correspond to the flux measured at the i^{th} increment where the pressure is P_i.

4.1.4.2 *Neutral Solute rejection* :

To confirm the similarity of pore sizes in these membranes, the ultrafiltration rejections of polyethylene glycol (PEG) (m.w. 9 kD), BSA and urease were measured for each of the above three membranes. The PEG was dissolved in distilled water, while BSA and urease were dissolved in McIlvaine buffer [citric acid (0.1 M)-disodium hydrogen phosphate (0.2 M)] at pH 4.8. This pH corresponds to the isoelectric point of both BSA and urease, at which they have no net charge. The PEG solution contained 0.5% of solute, while the other two solutions contained 0.2% of each protein separately. A stirred cell (13.4 cm^2 area, 600 rpm) assembly (Figure 4.2) operated at a pressure of 200 kPa and 27-29°C was used. The permeate and retentate samples were collected at a volume concentration factor (VCF = V_f / V_r) of 1.67. Unless otherwise mentioned, the same experimental conditions were used for all the UF experiments in this thesis.

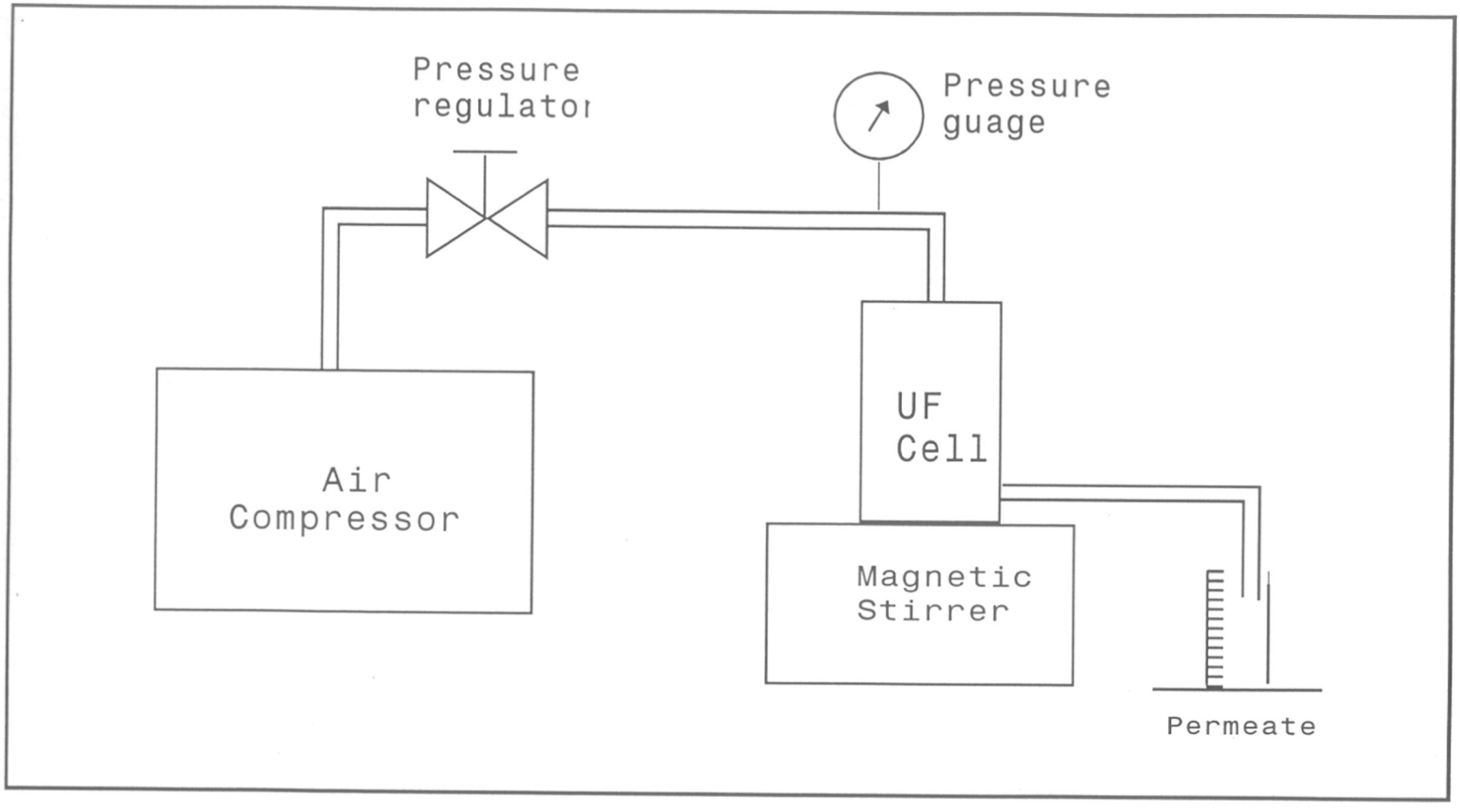

Figure 4.2 : Schematic of ultrafiltration apparatus

The analysis of PEG concentrations in the feed and permeate samples was done by the method of Sims and Snape (1980). According to this method, 4 ml of the PEG containing sample was mixed thoroughly with 1 ml each of reagent A (5% $BaCl_2$ in 1 N HCl) and reagent B (0.127g I_2 + 0.4g KI + 100 ml water). The sample was allowed to stand for 20 minutes followed by measurement of the sample absorbance at 535 nm. The sample absorbance was then compared with a previously obtained calibration plot of absorbance versus the concentration of standard solutions.

The protein concentrations in feed and permeate samples were determined spectrophotometrically by UV absorbance measurements at 280 and 260 nm using the following equation (Jayaraman, 1981) :

$$\text{Protein conc. (mg/ml)} = (1.55 \times \text{Abs.}_{280\ nm}) - (0.74 \times \text{Abs.}_{260\ nm}) \qquad (4.5)$$

All measurements were carried out in duplicate and averaged. The average reproducibility of the rejections ($R = 1 - C_p / C_f$) was 4%.

4.1.4.3 *Pure water permeation* :

The water fluxes were measured in the same cell and at the same conditions as mentioned above. The water used was distilled and filtered.

4.1.4.4 *Membrane morphology* :

Membrane substructure was examined by scanning electron microscopy (SEM). Vacuum dried membrane samples were kept in liquid nitrogen for 1 hr and then cut vertically with a sharp razor to obtain representative cross sections. These samples were gold sputtered for 2 minutes at 0.15 Torr argon pressure and 10 mA (1.4 kV). The samples were scanned at 10^{-6} Torr pressure and 10 kV in a scanning electron microscope.

4.1.4.5 *Surface charge* :

The surface charges on the membranes were determined in terms of their zeta potential (ξ). The zeta potential of each membrane was measured by the electroosmosis

method following the general procedure of Bowen and Clark (1984). The electroosmosis apparatus is shown in Figure 4.3. The membrane (6.6 cm^2 area) was placed in a cell (fabricated inhouse). The cell was placed in an electrolyte medium with the active membrane surface facing the bottom electrode. Both electrodes were made from platinum wires wound tightly in the shape of spiral coils. The electrolyte medium was 0.01 M KCl, with a conductivity of 1.18×10^{-3} S cm^{-1}. The dielectric constant of the medium was assumed to be 78 i.e the same as water. The pH of the medium was adjusted with either 2N HCl or 2N NaOH (2N KOH in case of PAN-1 membrane). The electro-osmotic flux was measured by weight gain on a balance accurate to 10^{-4} gm. Measurements were made at 20 and 30 mA and 50 - 100V, over only the initial 10 minutes to avoid heating of the medium. A fresh medium was used for each measurement. The electrolyte level outside the electroosmosis cell was maintained with a burette as shown in Figure 4.3. All measurements were carried out in duplicate and averaged. The average measurement reproducibility for the electro-osmotic flow rate, J_{eo}, was 6%.

The zeta potential was calculated for each membrane using the Smoluchowski equation (Bowen and Clark, 1984) :

$$\xi = \frac{J_{eo}\eta\lambda_0}{I_a\varepsilon} \tag{4.6}$$

where, η, λ_0 and ε are the viscosity, specific conductivity and permittivity of the electrolyte solution respectively, and I_a is the applied current.

4.2 PERMEATION STUDIES

4.2.1 PREPARATION OF TEST SOLUTIONS

4.2.1.1 *Preparation of BSA and Hb solutions*

Standard protein (BSA and Hb) solutions were prepared in McIlvaine buffer adjusted to various pH values. In single protein UF measurements, the BSA concentration was either 0.1 or 0.2 g/dl, while the Hb concentration was 0.1 g/dl. For binary solution UF measurements, the concentrations of both BSA and Hb were 0.1 g/dl each. All feed solutions were filtered through Whatman paper (No. 1) prior to the UF run.

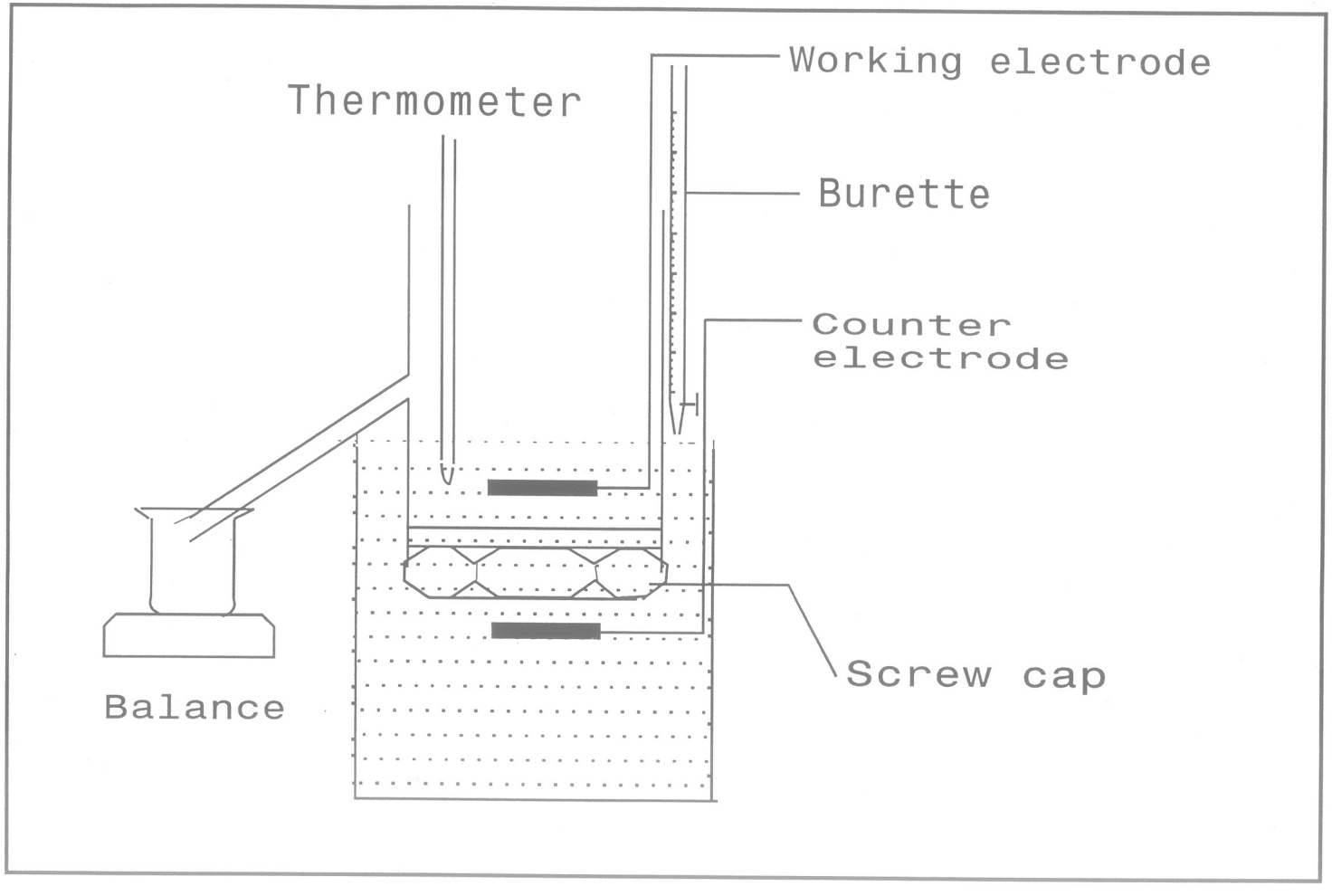

Figure 4.3 : Schematic of electroosmosis apparatus

4.2.1.2 *Preparation of wheys*

Three different types of wheys viz. Acid, Cheese (sweet) and Shrikhand were prepared from pasteurized buffalo milk as follows.

Acid whey (AW) : The pH of the milk kept at 30°C, was adjusted to 4.5 using 2N HCl. The milk was maintained at this pH for 1 hour and then warmed at 40°C for 10 minutes to settle the precipitated casein. The acid whey was separated from casein by filtering through muslin cloth and then by centrifugation at 4000 rpm for 30 minutes.

Cheese whey (CW) : Milk, maintained at 30°C, was stirred with 0.015 % wt/vol $CaCl_2$ and 5% vol/vol curds as the starting culture for 20 minutes. 20 ppm rennet was then added as a coagulant to the mixture. After thorough mixing, the mixture was kept at 30°C for 45 minutes, after which the cheese was cut and kept at 45°C for 15 minutes The whey was separated from the cheese by filtering through muslin cloth and then by centrifugation at 4000 rpm for 30 minutes

Shrikhand whey (SW) : 2 % vol/vol curds was added to the milk and kept at 40°C for 6 hours. The shrikhand whey was obtained by filtering the formed curds through muslin cloth and then by centrifugation at 4000 rpm for 30 minutes.

Each whey was adjusted to various pH values with 2N HCl or 2N NaOH and filtered through Whatman paper (No.1) before the UF run. The whey samples prepared in this manner are referred to as natural whey.

4.2.1.3 *Preparation of clarified wheys*

To prepare clarified wheys, the pH of each of the natural wheys prepared as described above was adjusted to 7.5 with 2N NaOH. On standing, this led to the precipitation of Ca salts (Kuo and Cheryan, 1983) which was removed by filtering through Whatman paper (No.1). The solution pH was then adjusted to the required value with 2N HCl.

4.2.2 ASSAY PROCEDURES FOR TEST SAMPLES

4.2.2.1 *BSA and Hb estimation* :

The concentrations of BSA and Hb in single protein UF were determined spectrophotometrically at 405 nm (Hb) and 280 nm (BSA). BSA has a λmax at 280 nm and absorbs negligibly at 405 nm (λmax of Hb). In the binary solution case, Hb was estimated at 405 nm and BSA was estimated by subtracting the Hb value from the total protein value measured at 280 nm.

4.2.2.2 *Whey protein estimation* :

In the case of whey UF, the total protein concentrations were determined by Lowry's method (Lowry et al, 1951). According to this method, a reagent was prepared, containing 50 ml of 2% Na_2CO_3 in 0.1 N NaOH plus 0.5 ml each of 1% $CuSO_4$ and 2% Na K tartarate. 1 ml of protein sample (5-100 μg/ml) was mixed thoroughly with 5 ml of this reagent and kept for 10 minutes. 0.5 ml of Folin-Ciocalteu's reagent was then added and mixed rapidly and kept for 30 minutes, after which the absorbance was measured at 660 nm. Standard calibration was done with 20-100 μg/ml BSA solutions.

4.2.2.3 *Lactose estimation* :

The lactose content in the whey samples was estimated by the 3,5-dinitro salicylic acid (DNSA) method (Robyt and Whelan, 1972). According this method, the DNSA reagent was prepared from 2.5 g DNSA, 75 g sodium potassium tartarate and 50 ml 2N NaOH dissolved slowly in 125 ml distilled water and then made up to 250 ml with distilled water. 1 ml lactose sample was mixed with 1 ml DNSA reagent and incubated for 5 minutes in a boiling water bath; this was cooled and 10 ml of distilled water was subsequently added. The absorbance was then measured at 540 nm. Standard calibration was done with 0.4 - 2 mg/ml lactose solutions.

4.2.2.4 *Fat estimation* :

Fat content was measured by the Gerber test (Kirk and Sawer, 1991). According to this method, 4 ml water was mixed with 7 ml conc. H_2SO_4 in a butyrometer, followed by addition of 11 ml whey sample. After thorough mixing, this solution was cooled and 1 ml amyl alcohol was added. After complete mixing, this solution was centrifuged at 2000

rpm for 10 minutes The fat content was directly read on the butyrometer as a top black layer.

4.2.2.5 *Ash estimation / conductivity measurements* :

Ash content was determined by the standard gravimetric method using a muffle furnace at 400°C. The conductivity measurements were done at 27°C.

4.2.2.6 *Electrophoresis of whey samples* :

Electrophoresis of milk and natural wheys was carried out in 13 % resolving gel with 3.8% stacking gel. The resolving gel was cast by crosslinking acrylamide (30%) with N,N′ methylene bis acrylamide (0.8%). 1.87 M Tris-HCl (pH 8.85) was used as a resolving gel buffer, while 0.05 M Tris-HCl buffer (pH 6.8) was used for casting the stacking gel. Before loading the sample, a prerun was carried with 0.05 M Tris-glycine buffer for 20 minutes at 10 mA / 60 V. The milk and whey samples (100 µl) were mixed separately with 10 µl of a solution containing glycerol (7%), SDS (20%), 2-mercapto ethanol (0.8%) and bromophenol blue (0.2%). These samples (20 µl each) were loaded with a microlitre syringe. The electrophoresis run was then carried out at 10 mA / 60 V for 7 hr. The gel was fixed in acetic acid : methanol : water (12 : 50 :38) solution for 12 hours. The gel was then washed thrice with distilled water and stained by Commassie brilliant blue solution (0.1% CBB G-250 + 2% phosphoric acid + 10% ammonium sulfate + 20% methanol) for 24 hours. The gel was then preserved in 20% ammonium sulfate solution.

4.2.3 PERMEATION METHODS

4.2.3.1 *Standard protein UF* :

BSA transmission was measured through PAN, PAN-2 and PAN-3 membranes using the stirred cell assembly described in section 4.1.4, at 200 kPa and 27°C. The stirring conditions correspond to laminar flow with a Reynolds number ($Re = \omega r_h^2 / \nu$) of 28000 (Blatt et al, 1970), where ω, r_h and ν are the stirring speed, radius of cell and

kinematic viscosity, respectively. The BSA concentration was 0.2 g /dl in McIlvaine buffer adjusted to various pH values. The experiments were done by 4x concentration of the solution volume. The measurements made at various pH values were replicated three times with a fresh membrane sample used for each run. The permeate fluxes were reproducible to ± 8 % and the BSA rejection values were reproducible to ± 4 %. The BSA rejections ($R = 1\text{-}C_p / C_r$) were calculated from the measured values of C_p and the values of C_r estimated from the initial feed concentration (C_f) and the mass balance given by the following equation :

$$C_r = \left[C_f - (C_p V_p / V_f)\right] / \left[1 - (V_p / V_f)\right] \tag{4.7}$$

where V_f and V_p are feed and permeate volumes, respectively.

At the end of each concentration run, the retentate was replaced by caustic solution (pH 10) and stirred without pressure for 5 minutes. The caustic solution was subsequently replaced by distilled water and again stirred without pressure for 5 minutes. The water flux (J_{wf}) was then measured at 200 kPa and compared with the initial water flux (J_{wi}) measured at the same conditions before the concentration run. The % flux recovery (FR) was then calculated as :

$$\text{FR} = (J_{wf} / J_{wi})\ 100 \tag{4.8}$$

For BSA UF, flux and composition measurements were also made as a function of the VCF ranging from 1 - 5. 50 ml feed was concentrated to 10 ml at each pH value. The permeate flux and composition were measured after the removal of each 10 ml as permeate. By knowing these values and the starting feed volume (V_f) and concentration (C_f), the retentate volume (V_r) and concentration (C_r) could be calculated by a simple mass balance :

$$V_{rn} = V_f - \Sigma V_{pn} \tag{4.9}$$

$$C_{rn} = (V_f C_f - \Sigma V_{pn} C_{pn}) / V_{rn} \tag{4.10}$$

where the index n refers to the increments of permeate (10 ml each) removed. The instantaneous flux as a function of the VCF was calculated from the time required for each permeate increment. The instantaneous rejection was obtained from equation (1.1) using

the experimentally measured $C_{p\,n}$ values and the $C_{r\,n}$ values calculated from equation (4.10).

Hb and BSA-Hb UF were performed under the same experimental conditions with PAN and PAN-1 membranes. BSA UF was also repeated with PAN and PAN-1 membrane under the same conditions for comparison with Hb UF. In these cases, the protein concentrations were 0.1g/dl (BSA or Hb) and 0.1 g/dl of each protein (BSA-Hb). The experiments were done by 2x concentration. The average permeate flux and protein rejection (R) reproducibility was ≈5% and ≈3% respectively.

In the mixture case, the BSA / Hb separation factor was calculated by the following equation,

$$S = \frac{(C_{BSA} / C_{Hb})_{permeate}}{(C_{BSA} / C_{Hb})_{feed}} \qquad (4.11)$$

All UF measurements were carried out in triplicate in a pH range of 4.0 - 7.5 (I = 0.52 - 1.16M). A fresh membrane sample was used for each replication at each pH and the data for that particular pH value were averaged.

The buffer system used in this work is of high ionic strength. In order to investigate the variation in ultrafiltration performance which could be attributed to this change in I, control experiments with BSA (0.1 g/dl) and BSA-Hb (0.1 g/dl of each protein) were done at pH 4.0 and 7.5, where I was fixed at either 0.52 or 1.16M. This was done by adjusting the pH of standard McIlvaine buffer with conc. HCl or 2N KOH. The protein solutions prepared in these media were then ultrafiltered under the same conditions as those used for the pH study.

4.2.3.2 *Whey UF* :

The UF of each whey i.e. wheys derived from acid, cheese and shrikhand processing routes was carried out with PAN and PAN-3 membranes. For each whey sample, the UF measurements were made once for natural wheys and twice for clarified wheys. The experimental conditions were the same as those used for the standard protein UF measurements described above. In the case of natural wheys, the effect of VCF was also studied at each pH value for both PAN and PAN-3 membranes.

The effect of transmembrane pressure on flux and protein retention was also studied at pH 7.5 for each natural whey with PAN and PAN-3 membranes. The feed side pressure was varied in a range from 50-400 kPa.

Flux recovery as a function of pH was determined for each natural whey and each membrane. The procedure to determine flux recovery was similar to that used in the case of BSA UF (section 4.1.2.3), with the only difference being that after the whey UF concentration run, the membranes were washed with distilled water for 10 minutes instead of with caustic and distilled water as in case of BSA UF.

Chapter 5

RESULTS AND DISCUSSION

This chapter presents and discusses the experimental results related to polymer and membrane characterization and the ultrafiltration studies with various protein containing solutions through acrylonitrile homopolymer and copolymer membranes.

5.1 POLYMER CHARACTERIZATION

As described in section 4.1.2, the acrylonitrile homopolymer and copolymers with acrylamide were characterized for intrinsic viscosity, chemical composition, structure, hydrophilicity and surface energy.

i) *Elemental analysis* :

Table 5.1 shows the theoretical and observed elemental composition of acrylonitrile homopolymer and copolymers.

Table 5.1

Elemental composition of acrylonitrile homopolymer and copolymers

Polymer	Elemental composition (weight %)							
	Theoretical				Observed			
	C	H	N	O	C	H	N	O
PAN	67.9	5.7	26.4		66.4	5.9	23.4	4.7
PAN-1	64.6	5.9	25.1	4.3	62.0	6.6	21.0	10.3
PAN-2	64.6	5.9	25.1	4.3	64.8	6.3	16.0	12.9
PAN-3	62.6	6.1	24.3	6.9	60.3	6.5	20.9	12.3

The higher content of H and O observed in the polymers may be due to absorption of moisture from air while handling.

ii) *Infrared spectroscopy* :

The IR spectra for PAN, PAN-1, PAN-2 and PAN-3 are shown in Figures 5.1 - 5.4 respectively. The assignment of various spectral bands in these figures to various chemical functionalities are shown below.

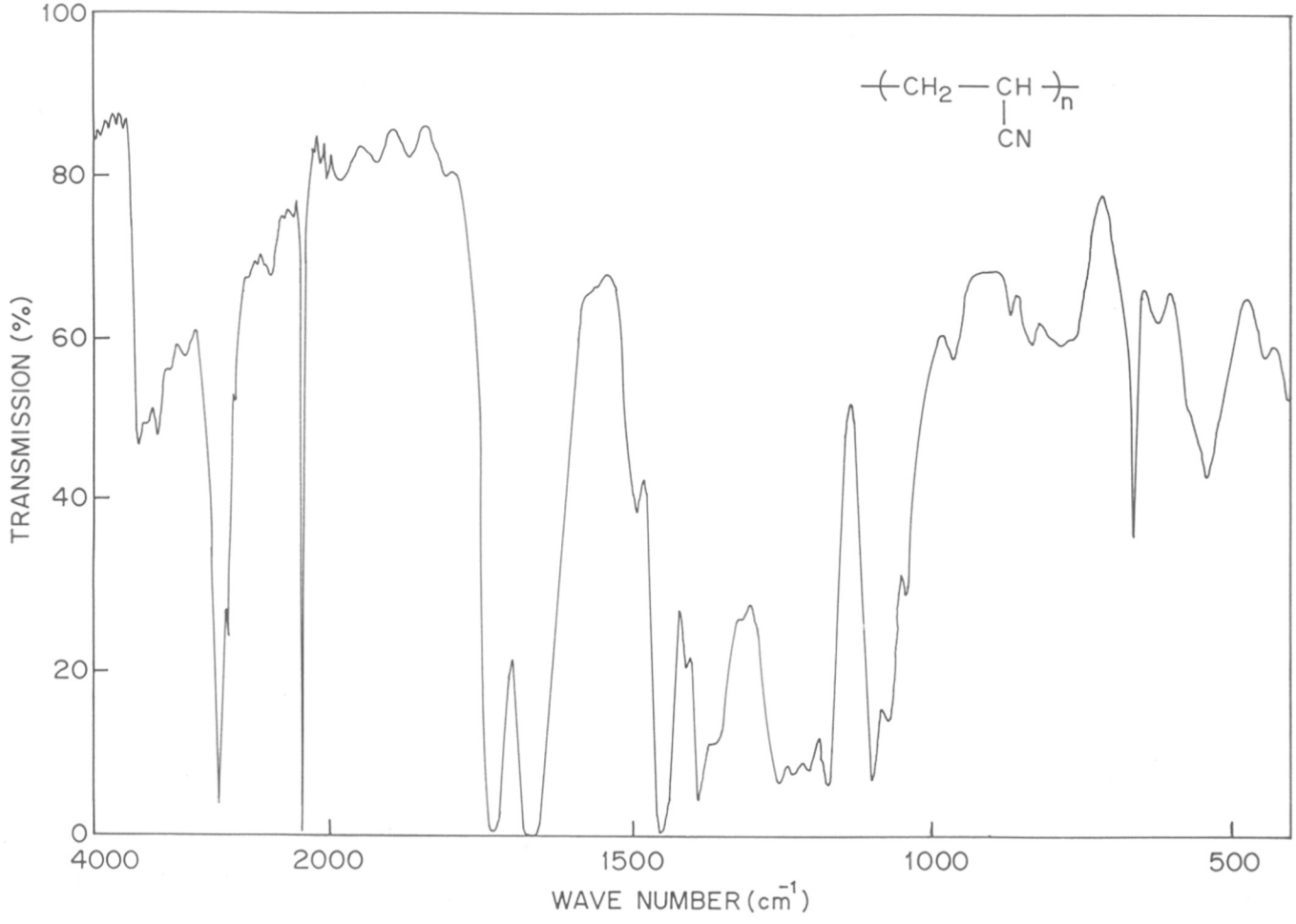

Figure 5.1 IR spectrum of PAN polymer

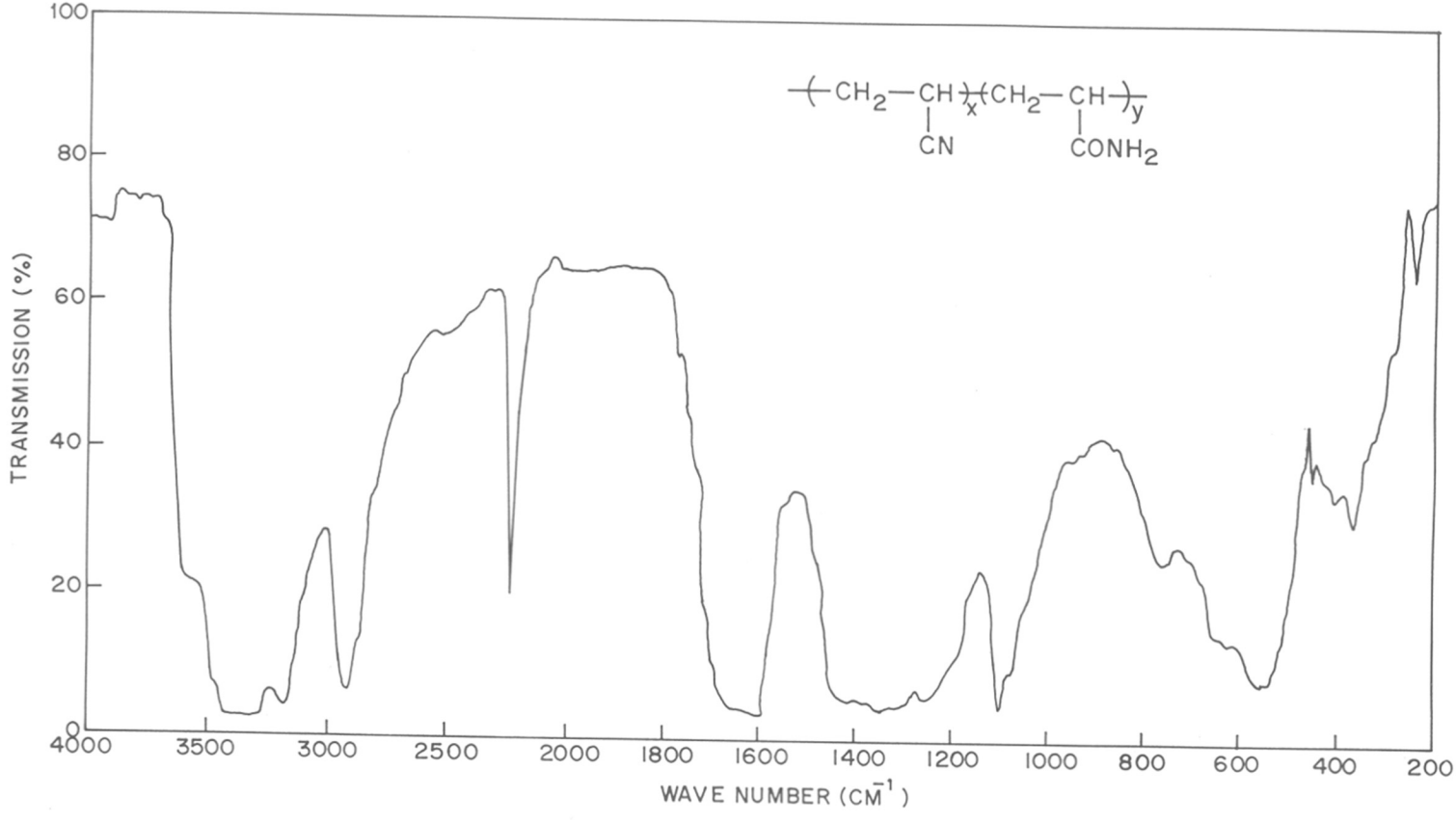

Figure 5.2 IR spectrum of copolymer PAN-1

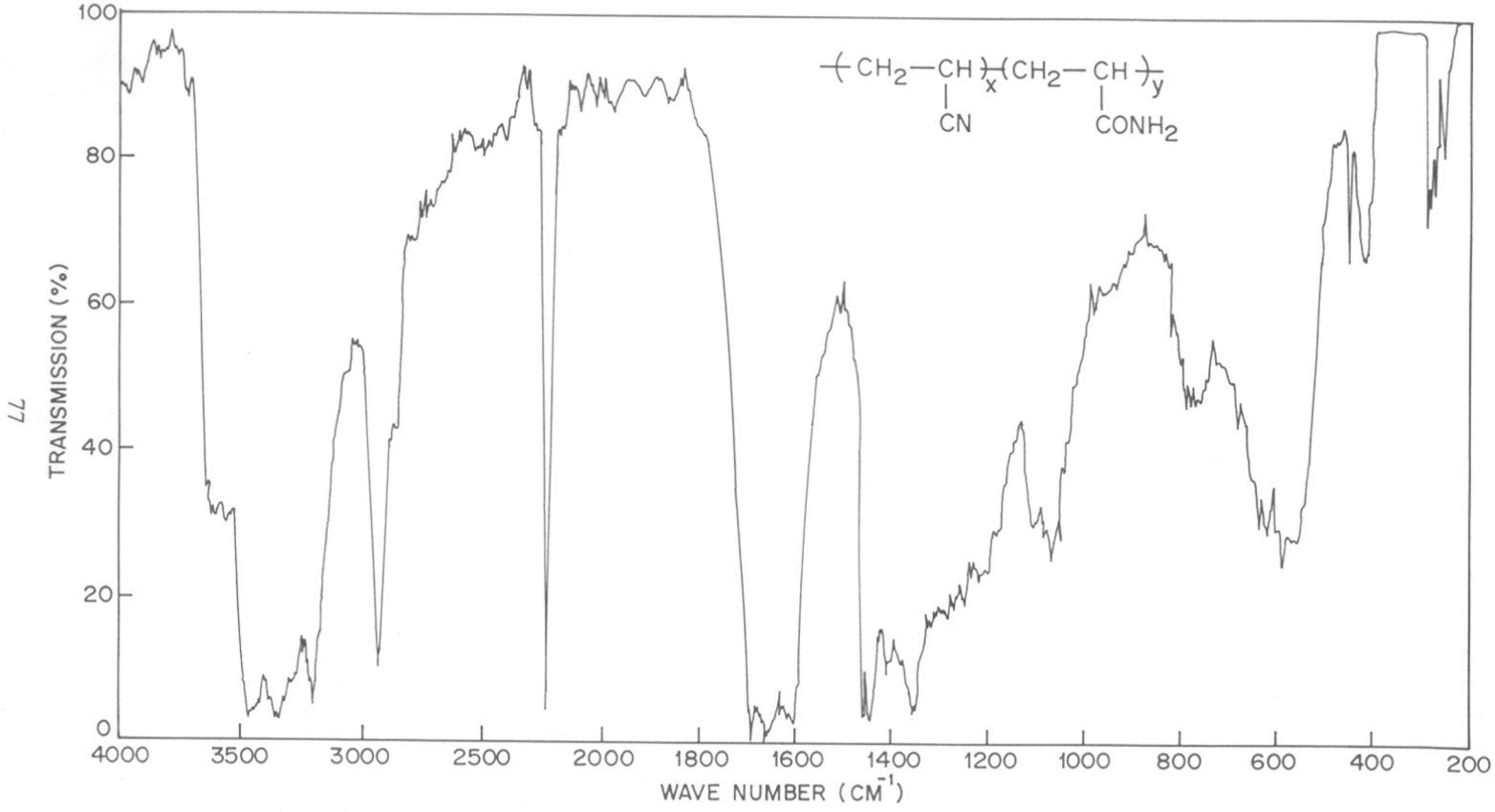

Figure 5.3 IR spectrum of copolymer PAN-2

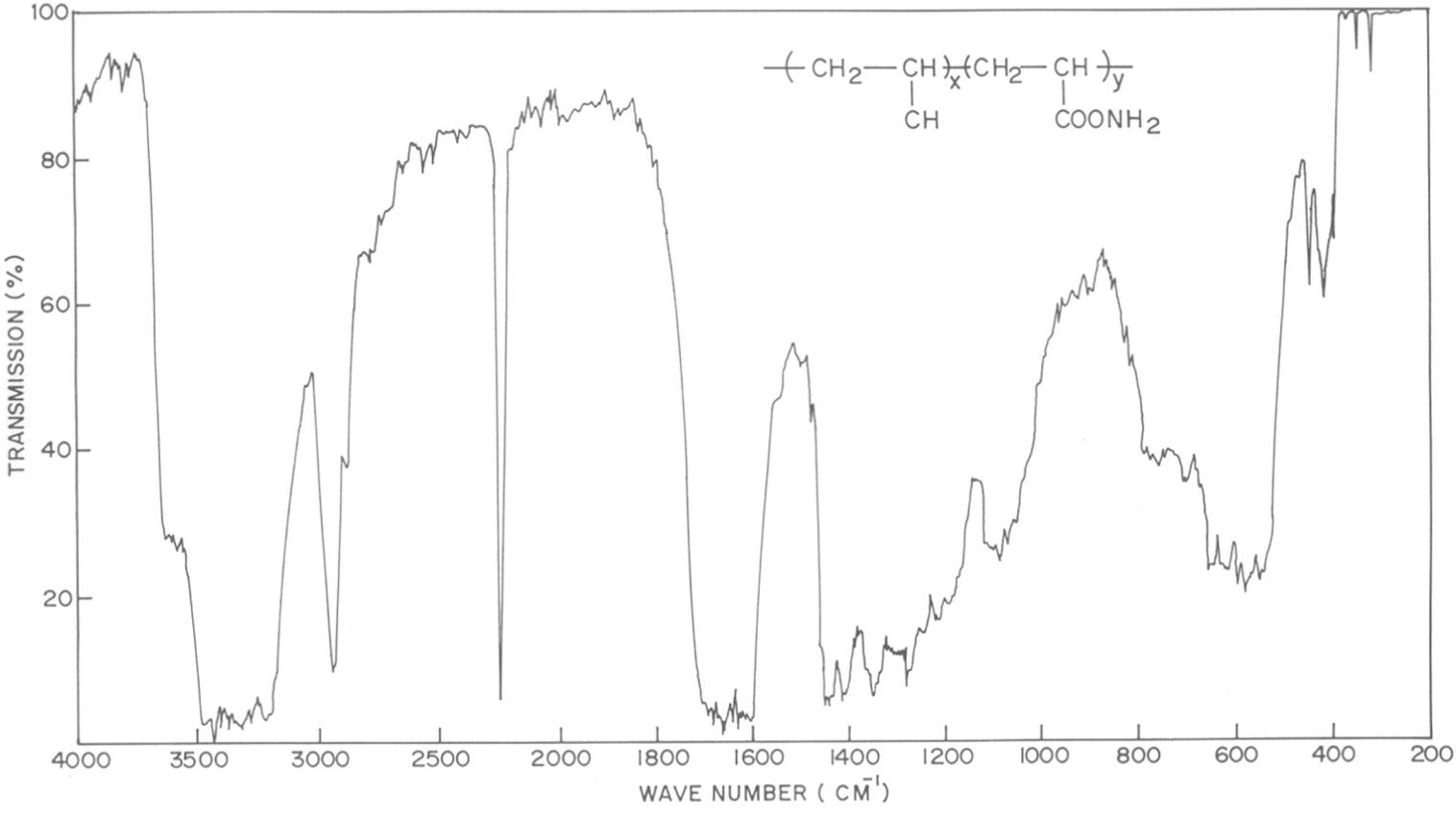

Figure 5.4 IR spectrum of copolymer PAN-3

(a) PAN (Figure 5.1) :

660 cm^{-1}	-C-N bending in residual H-CO-$N(CH_3)_2$
1660 cm^{-1}	-C=O stretching in residual H-CO-$N(CH_3)_2$
1730 cm^{-1}	-C=O stretching in hydrolyzed PAN (-COOH)
2250 cm^{-1}	-C≡N stretching
3520 cm^{-1}	-O-H stretching in hydrolyzed PAN (-COOH)

(b) PAN-1, PAN-2 and PAN-3 (Figures 5.2-5.4) :

1700-1600 cm^{-1}	-C=O stretching in $-CO-NH_2$
2250-2240 cm^{-1}	-C≡N stretching
3200-3180 cm^{-1}	$-NH_2$ stretching
3360-3340 cm^{-1}	$-NH_2$ stretching
3460-3420 cm^{-1}	$-NH_2$ stretching

iii) *NMR Spectroscopy* :

The ^{1}H-NMR spectra for PAN, PAN-1, PAN-2 and PAN-3 are shown in Figures 5.5 - 5.8. The assignment of various peaks to different protons are shown below.

(a) PAN (Figure 5.5) :

2.15 ppm	s, 2H, $-CH_2-$
2.50 ppm	m, Residual protons in DMSO-d_6
2.75 ppm	s, 3H, $-CH_3$ from residual DMF
2.90 ppm	s, 3H, $-CH_3$ from residual DMF
3.10 ppm	s, 1H, -CH-
3.70 ppm	s, Water absorbed by DMSO-d_6

(b) PAN-1, PAN-2 and PAN-3 (Figures 5.6-5.8) :

2.05 ppm	s, 2H, $-CH_2-$
2.50 ppm	m, Residual protons in DMSO-d_6
2.75 ppm	s, 3H, $-CH_3$ from residual DMF
2.90 ppm	s, 3H, $-CH_3$ from residual DMF
3.10 ppm	s, 1H, -CH-
3.3-3.5 ppm	s, Water absorbed by DMSO-d_6
7.15 ppm	s, 1H, -NH2 (cis to -C=O group)
7.75 ppm	s, 1H, -NH2 (trans to -C=O group)
8.0 ppm	s, 1H, H-CO-N$(CH_3)2$ from residual DMF

Thus, IR, NMR spectral analysis (Figures 5.1-5.8) and elemental analysis (Table 5.1) confirm the chemical structures (shown in Figure 4.1) and composition of homopolymer and copolymers.

The amide content in the copolymer was determined as the ratio of the peak area of NH_2 protons to that of $-CH_2-$ protons (Figures 5.5-5.8). The molar composition of the reaction mixture and the final copolymer product are shown in Table 5.2. The degree of hydrolysis of PAN is < 2%.

Table 5.2

Acrylamide content in acrylonitrile-acrylamide copolymers in reaction mixture and product, determined by NMR analysis

Polymer	Acrylamide content in reaction mixture (mole %)	Acrylamide content in product copolymer (mole %)
PAN-1	15	12
PAN-2	15	20
PAN-3	25	30

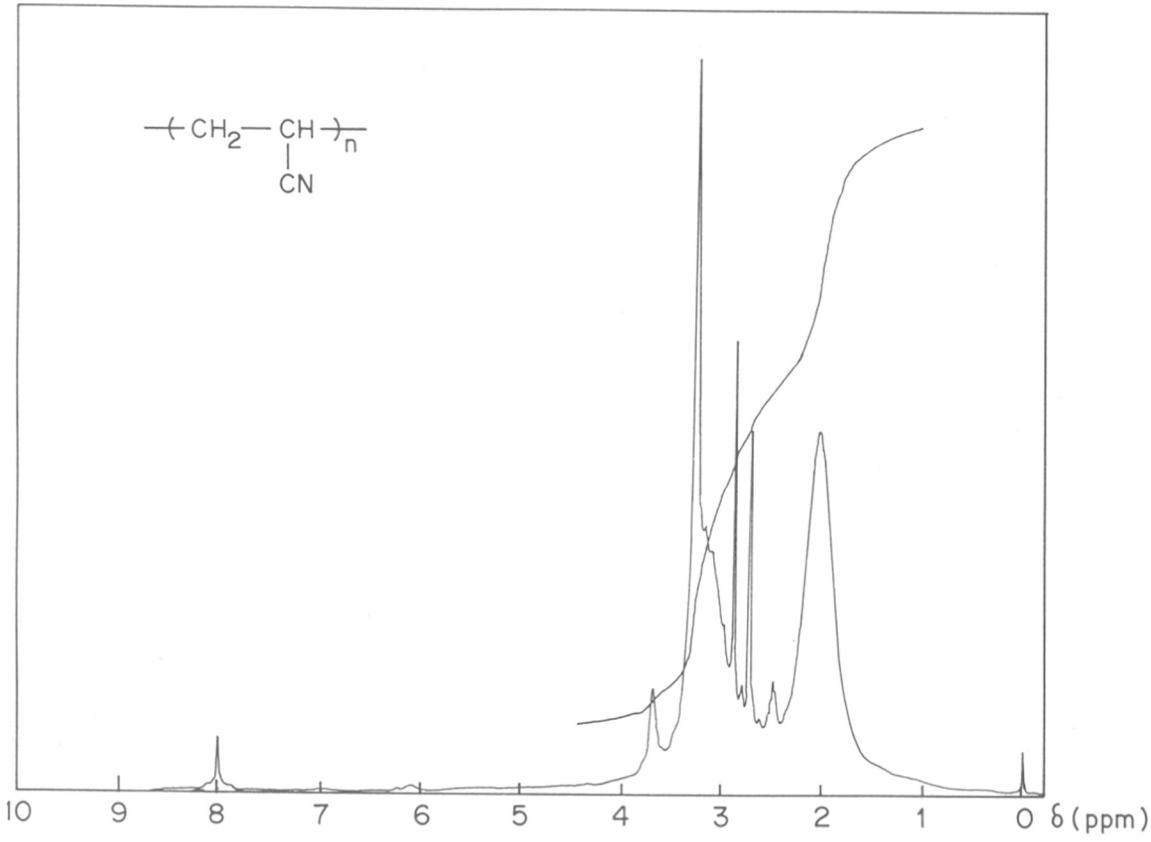

Figure 5.5 NMR spectrum of PAN polymer

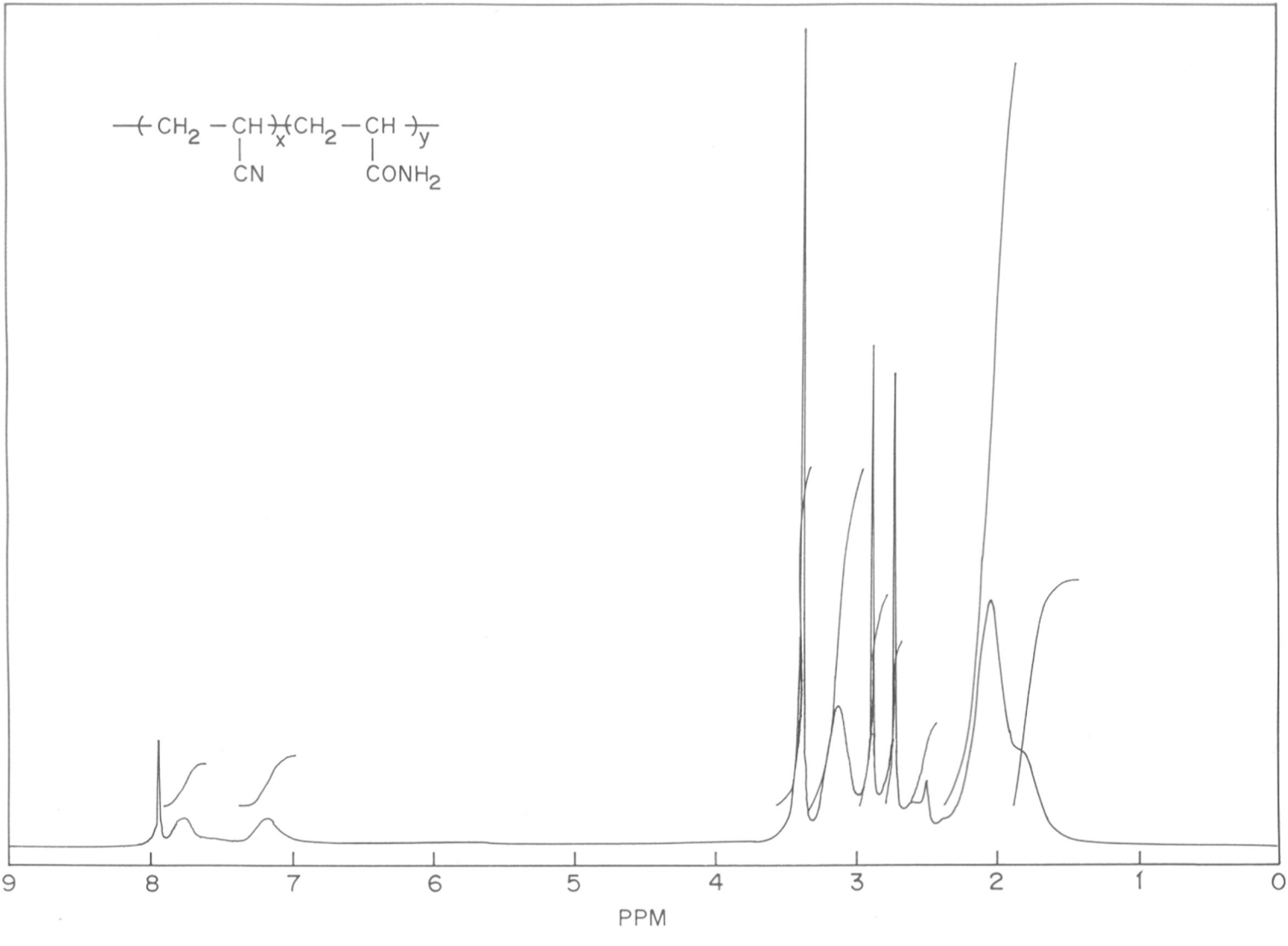

Figure 5.6 NMR spectrum of copolymer PAN-1

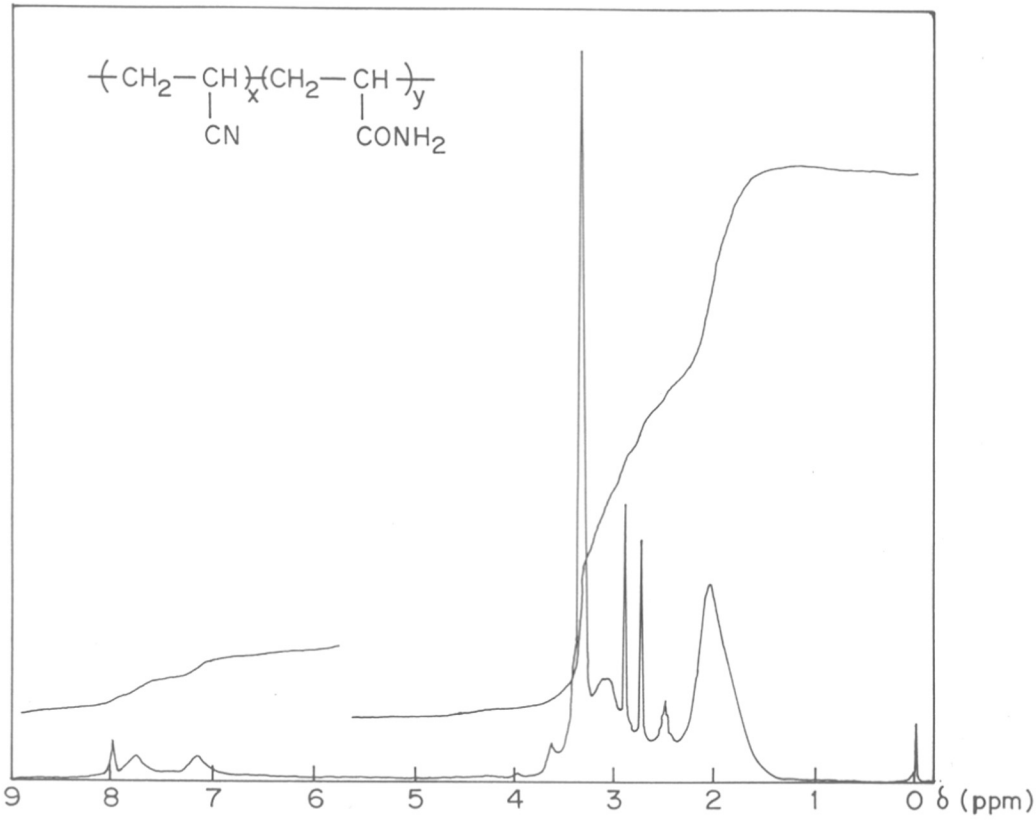

Figure 5.7 NMR spectrum of copolymer PAN-2

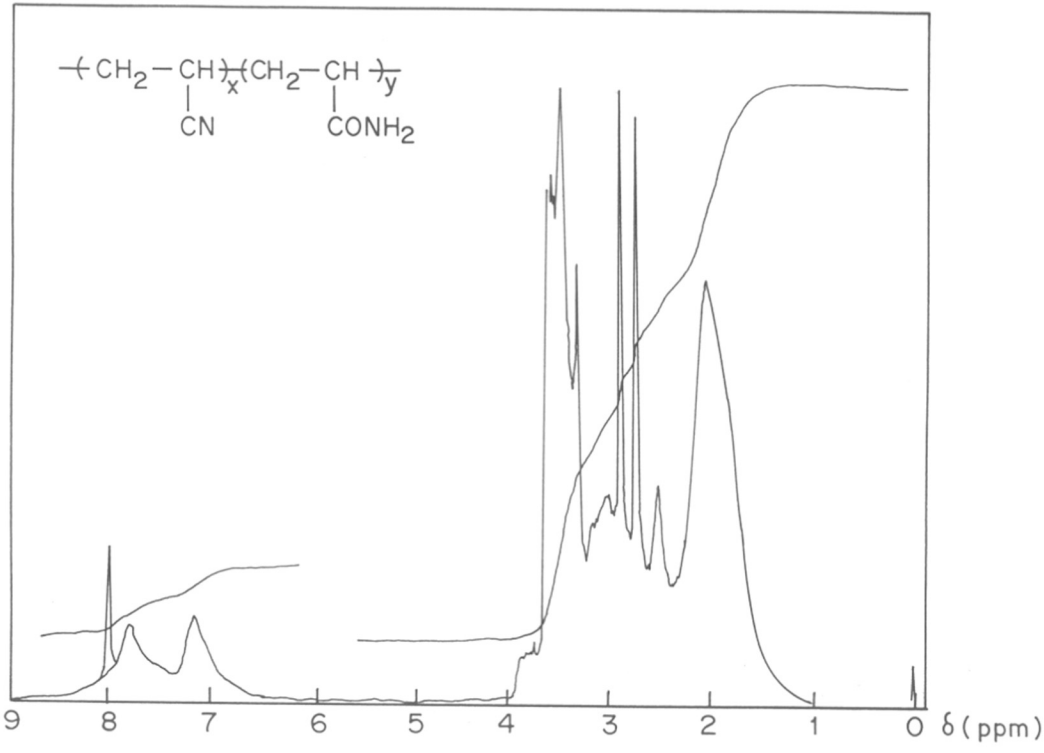

Figure 5.8 NMR spectrum of copolymer PAN-3

Table 5.2 shows that, the acrylamide content in the product is higher than that expected from the reactant mixture for PAN-2 and PAN-3. This may be attributed to partial hydrolysis of nitrile groups caused by the acid catalyst. The slightly lesser acrylamide content in the product compared to the reactant composition in the case of PAN-1 may be an experimental error or incomplete copolymerization. The degree of hydrolysis of PAN is < 2%.

iv) *Contact angle / Surface energy measurements* :

Table 5.3 shows the water and formamide / polymer contact angles and intrinsic viscosity data for PAN and copolymers. The calculated values of γ_s^p, γ_s^d and γ_s (total surface free energy of the polymer), obtained by solving the two simultaneous equations (eqn. 4.2) based on the data obtained with water and formamide, are also listed in Table 5.3.

Table 5.3

Characteristics of acrylonitrile homopolymer and copolymers

Polymer	Intrinsic viscosity (η) (dl/g)	Contact angle (θ) (°)		Surface free energy (erg/cm^2)		
		Water / polymer	Formamide / polymer	γ_s^p	γ_s^d	γ_s
PAN	1.57	73	52	8	31	39
PAN-1	1.03	66	43	14	29	43
PAN-2	0.82	68	58	13	22	34
PAN-3	0.92	56	57	26	13	39

As would be expected from the chemical modification, Table 5.3 shows that the polymer / water contact angles decrease with increase in acrylamide content. The polar component of surface energy increases with increasing acrylamide content; while the dispersion force component decreases with increasing acrylamide content. Thus hydrophilicity increases with increasing acrylamide content in the copolymer.

5.2 MEMBRANE CHARACTERIZATION

The membranes were characterized for their pore size distribution, surface morphology and surface charge. This basic information can be used to interpret the ultrafiltration data.

5.2.1 PORE SIZE AND PORE SIZE DISTRIBUTION

As described in section 4.1.4, the pore size of these membranes was determined by the modified bubble point method, neutral solute rejection and pure water permeability.

The modified bubble point measurements (Figure 5.9) indicate that the majority of the pores in all these membranes are of similar size (20 20 nm); however, PAN-2 has a bimodal pore size distribution with a few larger pores (~ 40 nm) than the other membranes. Since the entire pore size profile could not be determined due to equipment pressure limitations, the fraction of these larger pores could not be quantified.

The pure water fluxes and the average rejections of neutral solutes for these membranes are shown in Table 5.4. The pure water fluxes for all four membranes were averaged over 8-10 measurements at 200 kPa.. The standard deviation of the pure water flux measurements corresponds to 20-30% of the mean flux values. This table shows that the rejection of PAN-2 for BSA at the IEP is less than that of PAN; however the rejection of the larger urease protein is identical and the water fluxes are the same within experimental error.

Since PAN-2 has a small fraction of larger pores, this membrane could be expected to have slightly higher flux / lower rejection than the other membranes, based only on pore size considerations.

Since the pore size distribution, neutral solute rejection and water permeabilities of PAN, PAN-1 and PAN-3 membranes are similar, it is expected that steric effects on the transport through membrane pores will also be similar for these membranes. Differences in flux and rejection behavior can thus be attributed primarily to the differences in surface chemistry for these three membranes.

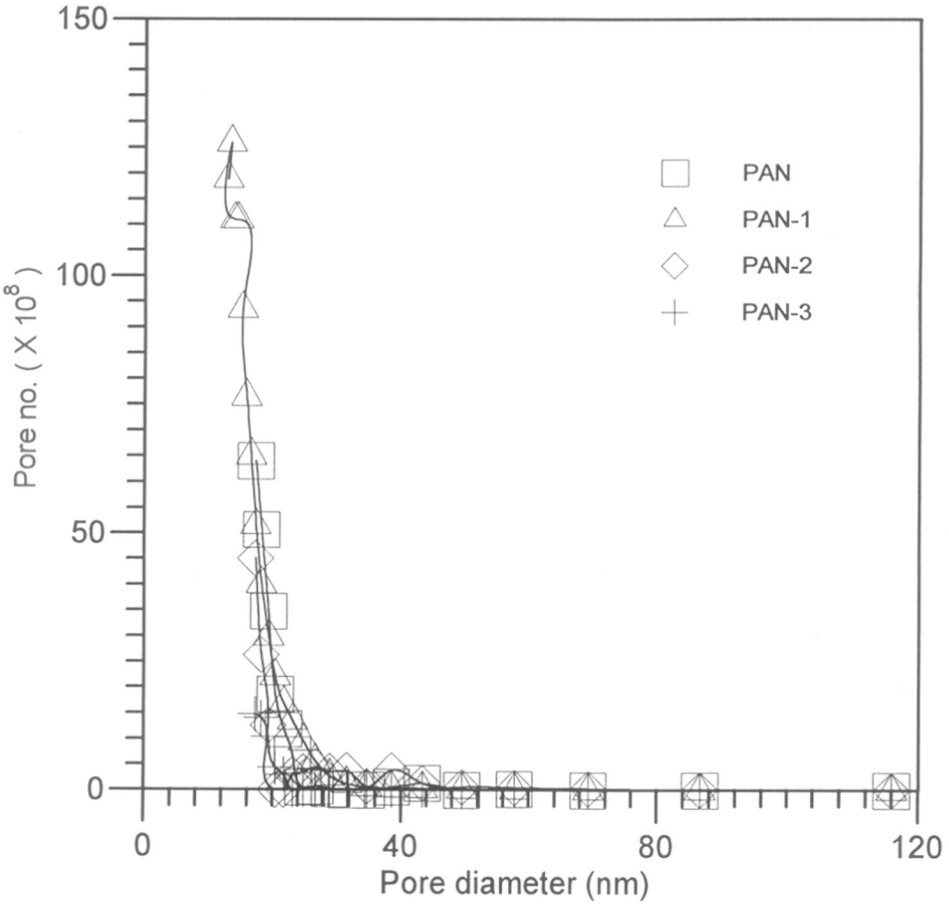

Figure 5.9 Pore size distribution of PAN and copolymer membranes by the modified bubble point method.

Table 5.4

Pure water flux and rejection of standard solutes*

Membrane	Pure water flux ($lm^{-2}h^{-1}$)	Rejection (%)		
		PEG-9	BSA	Urease
PAN	232	13	90	100
PAN-1	200	ND	60	ND
PAN-2	183	28	60	100
PAN-3	207	30	80	100

* Measured at 200 kPa and 27-29°C

ND : Not determined

5.2.2 MEMBRANE MORPHOLOGY

As can be seen from Figure 5.10 (a and b), both PAN and copolymer (PAN-2) membranes show a typical asymmetric structure with a skin layer of thickness ≈ 8 μm and a porous substructure of ≈ 100 μm. The true thickness of the skin layer could not be ascertained because of poor resolution caused by electron charging effects during SEM examination. For the same reason, no pores could be seen on the surface of any of the membranes, even at high magnifications (80kx). Large microvoids are seen in the substructure of both membranes. The figures also show considerable penetration of polymer solution in the polyester nonwoven support (Hollytex 3329).

5.2.3 SURFACE ELECTROSTATIC CHARGE

Figure 5.11 shows a typical plot of electro-osmotic flow rate (J_{eo}) as a function of applied current (I_a). Zeta potentials, calculated using eqn. (4.6) are shown for all the membranes at various pH values in Figure 5.12. In common with many polymeric membranes, all the PAN based membranes show a negative zeta potential in the pH range of 4.0 - 7.5 (Figure 5.12). However, comparison of the zeta potentials measured for the

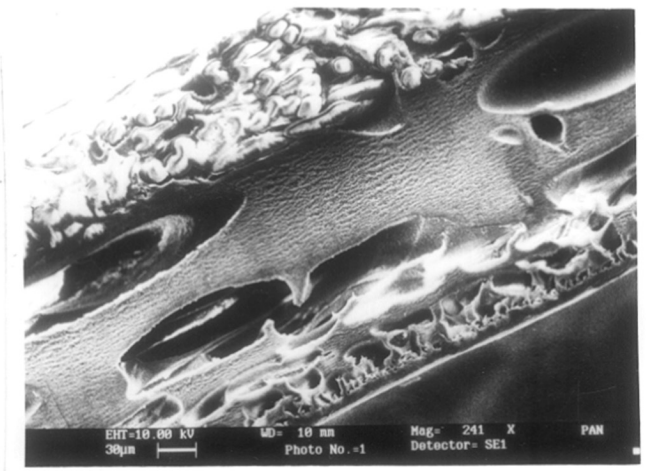

(a)

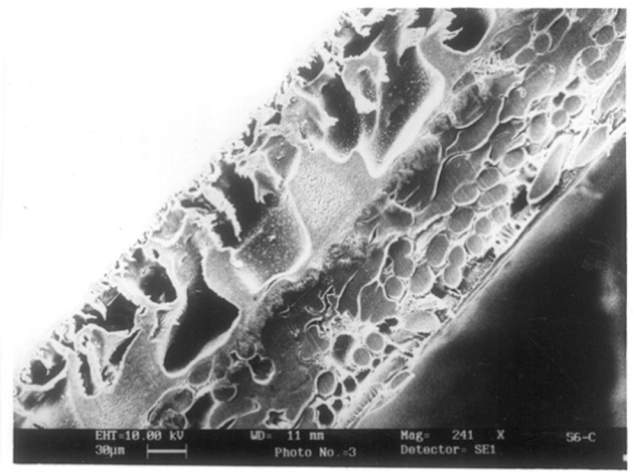

(b)

Figure 5.10 : Scanning electron micrographs of cross sections of (a) PAN and (b) PAN-2 membranes at 10 kV and 241x magnification

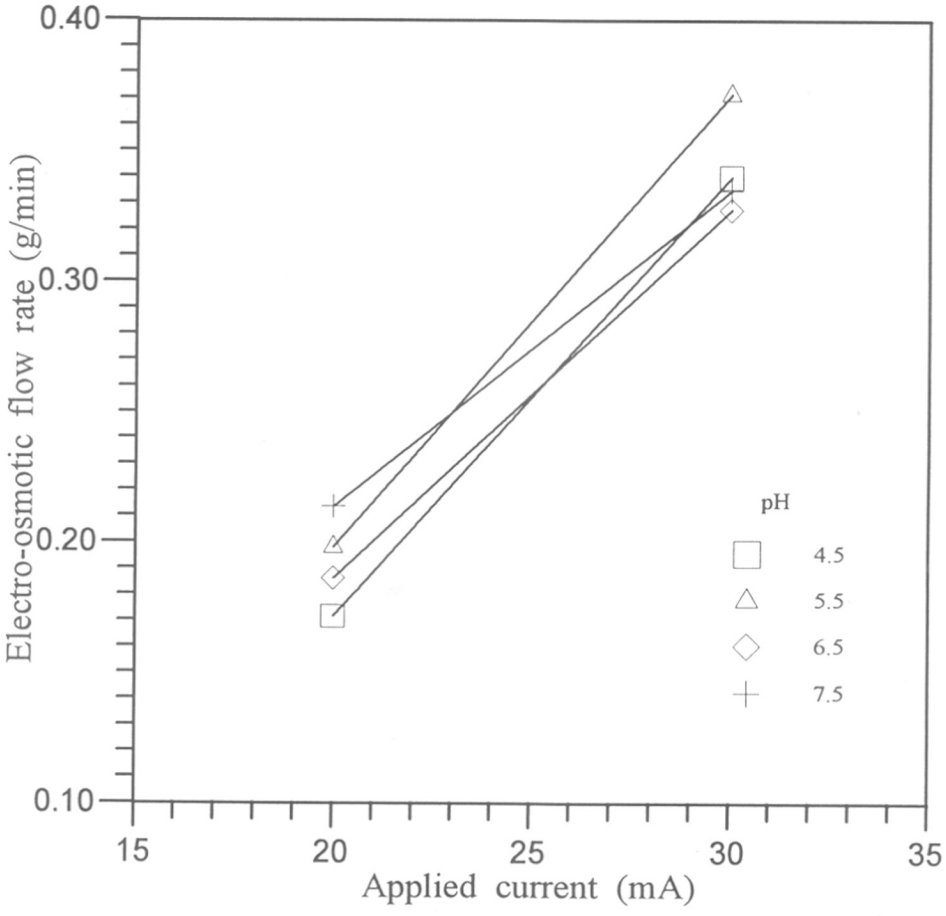

Figure 5.11 Typical plot of electroosmotic flow rate (J_{eo}) vs applied electric current (I_a) for PAN

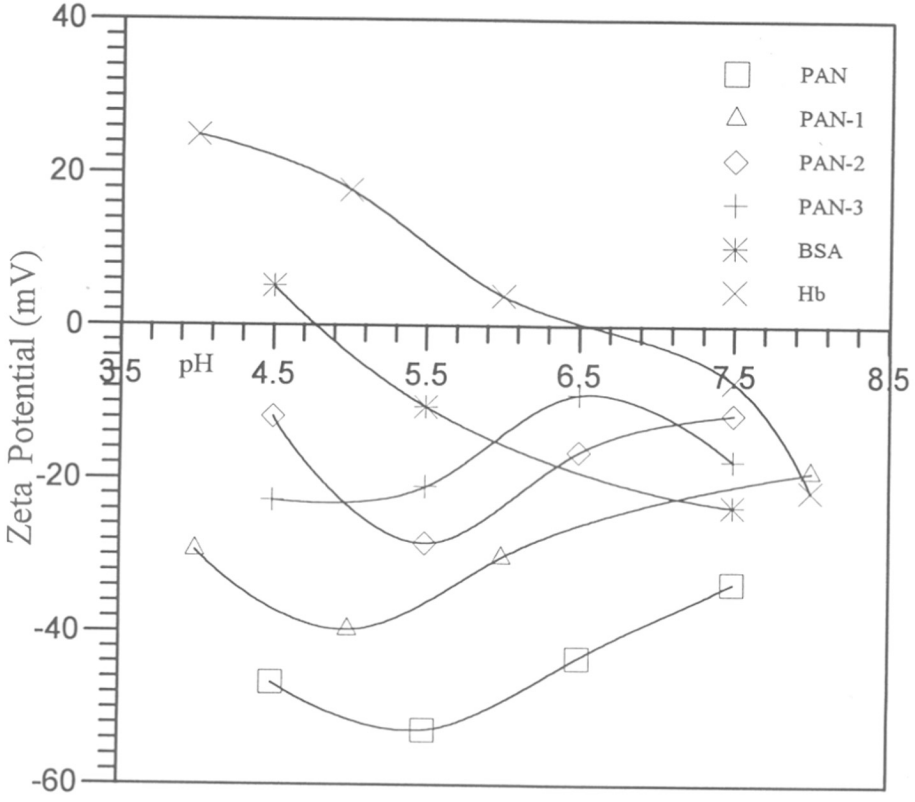

Figure 5.12 Effect of pH on zeta potential (ξ) for PAN and copolymer membranes and surface potential of BSA (Vilker et al, 1981a) and surface charges on Hb (Overbeek and Bungenberg De Long, 1949)

copolymer membranes vis-a-vis PAN shows that the acrylamide insertion reduces the surface negative charge by a factor of ≈ 2 - 3. All the copolymer membranes have similar surface characteristics even though the acrylamide content varies from 12 to 30%.Figure 5.12 also shows the surface potential of BSA (Vilker et al, 1981b) and surface charges on Hb (equivalents / mol) (Overbeek and Bungenberg De long, 1949). Below a pH of 4.8 (6.8 for Hb), there is an attractive electrostatic force between the proteins and the membranes, while with increasing pH, the electrostatic force becomes increasingly repulsive. The magnitude of these electrostatic forces between these proteins and the copolymer membranes is smaller than that between the proteins and the homopolymer membrane.

5.3 UITRAFILTRATION STUDIES

The permeation properties of the PAN and copolymer membranes were measured first with BSA solutions. The trends in flux, rejection and flux recovery seen with varying pH were confirmed and extended by UF studies with Hb and BSA-Hb mixture. UF data obtained with these standard proteins can be used to interpret the complex UF data with various wheys.

The membrane characterization data shows that PAN, PAN-1 and PAN-3 have similar pore size distribution. The copolymer based membranes have reduced negative surface charge and increased hydrophilicity in comparison to PAN. This makes it possible to delineate hydrophilicity from electrostatic effects during protein UF. This is in contrast to previous studies (Miyama et al, 1988; Kobayashi et al, 1994) with modified PAN membranes where the sulfonate group incorporation would be expected to simultaneously increase both simultaneously increase both hydrophilicity and negative surface charge

5.3.1 ULTRAFILTRATION OF STANDARD PROTEINS

Poly(acrylonitrile) based membranes were used for ultrafiltration of standard proteins (BSA and Hb : individual and mixture). BSA and Hb are of similar size but their IEPs are different. BSA has an IEP at pH 4.8 while Hb is positively charged upto pH 6.8

and Hb is more hydrophobic than BSA. A comparison of the physical characteristics of BSA and Hb is shown in Table 5.5.

Table 5.5

Comparison of BSA and Hb characteristics

Characteristics	BSA[a]	Hemoglobin[b]
Size related parameters		
Molecular weight (kD)	66-68	64-67
Equivalent Ellipsoidal Dimensions (nm)	4×4×14	6.4×5.5×5
Diffusion Coefficient (10^{-7} cm^2/s)	5.9	6.4
Partial Specific Volume (10^{-4} m^3/kg)	7.34	7.5
Electrostatic parameters		
Net charge (at pH 7.4)	-22	-7.2
Isoelectric Point	4.8	6.8
Hydrophilicity / phobicity [c]		
Hydrophobic amino acids content (g/100 g protein)	44.07	54.16
Hydrophilic amino acids content (g/100 g protein)	56.16	43.13

a) Data from Kupcu et al (1993) and van den Berg and Smolders (1989)

b) Data from Overbeek and Bungenberg De Long (1949) and Barisas (1986)

c) Calculated from the amino acids composition (Haurowitz, 1963)

5.3.1.1 *BSA ultrafiltration*

BSA ultrafiltration was carried out with all four membranes. Initially the results are discussed for BSA UF with PAN, PAN-2 and PAN-3 membranes. This data was obtained with at a BSA feed concentration of 0.2 g/dl. The BSA UF data at 0.1 g/dl with PAN and PAN-1 is discussed later during the comparison with Hb UF data.

At pH 4.0, BSA is positively charged; consequently, there is a small attractive electrostatic interaction between all membranes and BSA (Figure 5.12). The permeate

flux, rejection (R) and flux recovery for BSA UF are shown in Figures 5.13 - 5.15 respectively. These figures show that the flux is lowest, the rejection (R) is highest, and the flux recovery is poorest at pH 4.0, even in comparison to the results at the isoelectric pH of 4.8. These results indicate strong protein adsorption at pH 4.0. In addition to the attractive electrostatic interaction between BSA and the membranes, the high adsorption may also be attributed to conformational changes in BSA which occur at acidic pH (Loeb and Scheraga, 1956).

Figure 5.14 shows that above pH 4.8, R for the PAN membrane is relatively constant, while that for both PAN-2 and PAN-3 drops markedly. It may be recalled from section 5.2.1 that PAN and PAN-3 have similar pore size distribution while PAN-2 has a small fraction of larger pores. Since the pore size distributions of PAN and PAN-3 are similar, the lower BSA rejection of PAN-3 in relation to PAN at these higher pH values may be explained on the basis of the differences in their surface chemistry. The lower hydrophilicity and higher dispersive surface energy of PAN would allow more protein adsorption and consequent pore size reduction. In addition, the increasing electrostatic repulsion between PAN and BSA above pH 4.8, where both are negatively charged (Figure 5.12), would inhibit BSA passage through the pores. On the other hand, the improved hydrophilicity / surface energy characteristics of the copolymers would inhibit the reduction of the pore size. Also, the reduced electrostatic repulsion would allow BSA to penetrate the pores, thus resulting in increased protein transmission.

The above explanation would be consistent with the results of both Miyama et al (1986) (electrostatic effect) as well as Higuchi et al (1993) (hydrophilic effect). Miyama et al reported less protein transmission with increasing sulfonate group incorporation. Higuchi et al (1993) measured BSA transmission at pH 7.2 and 9.0 for polysulfone and propylene oxide modified polysulfone membranes. While the rejection of the unmodified membrane increased with increase in pH, the rejection of the modified (hydrophilic) membrane decreased.

The interaction between BSA and the membrane surface discussed above obviously affects the permeate fluxes as well. As can be seen from Figure 5.13, PAN-2

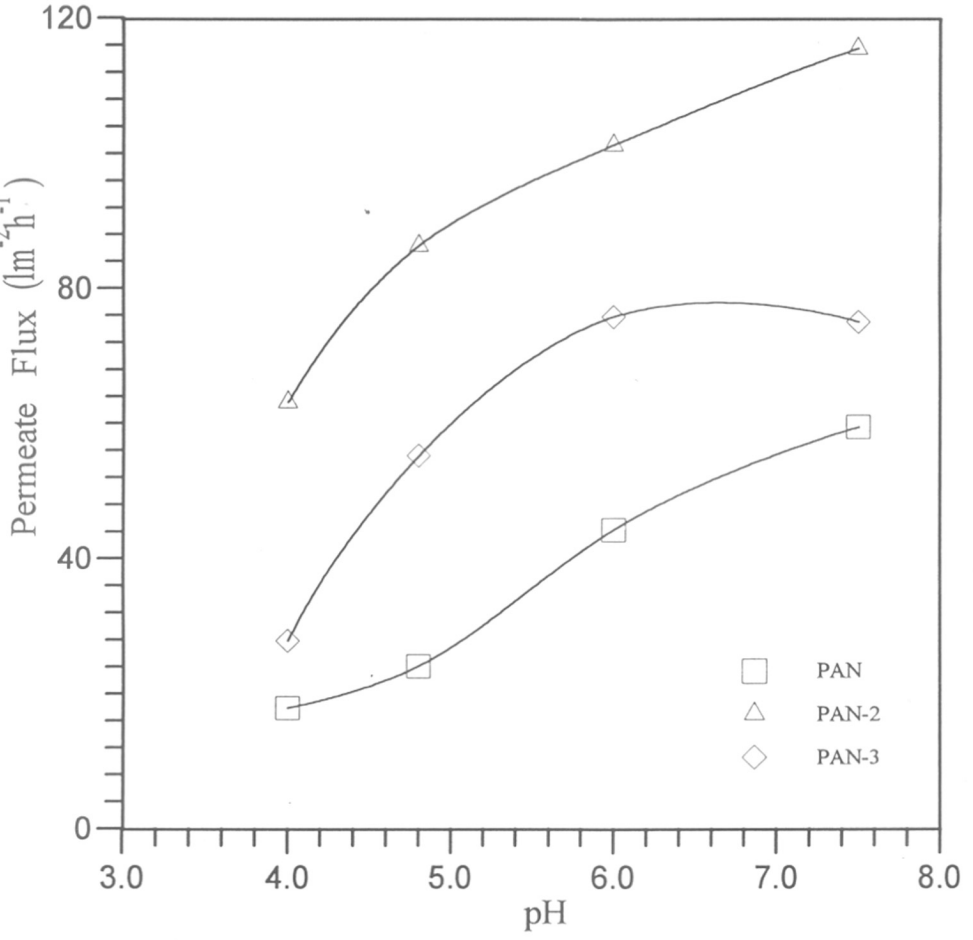

Figure 5.13 Effect of pH on permeate flux at 1.25 VCF; 600 rpm; 200 kPa; 0.2 g/dl BSA for PAN, PAN-2 and PAN-3

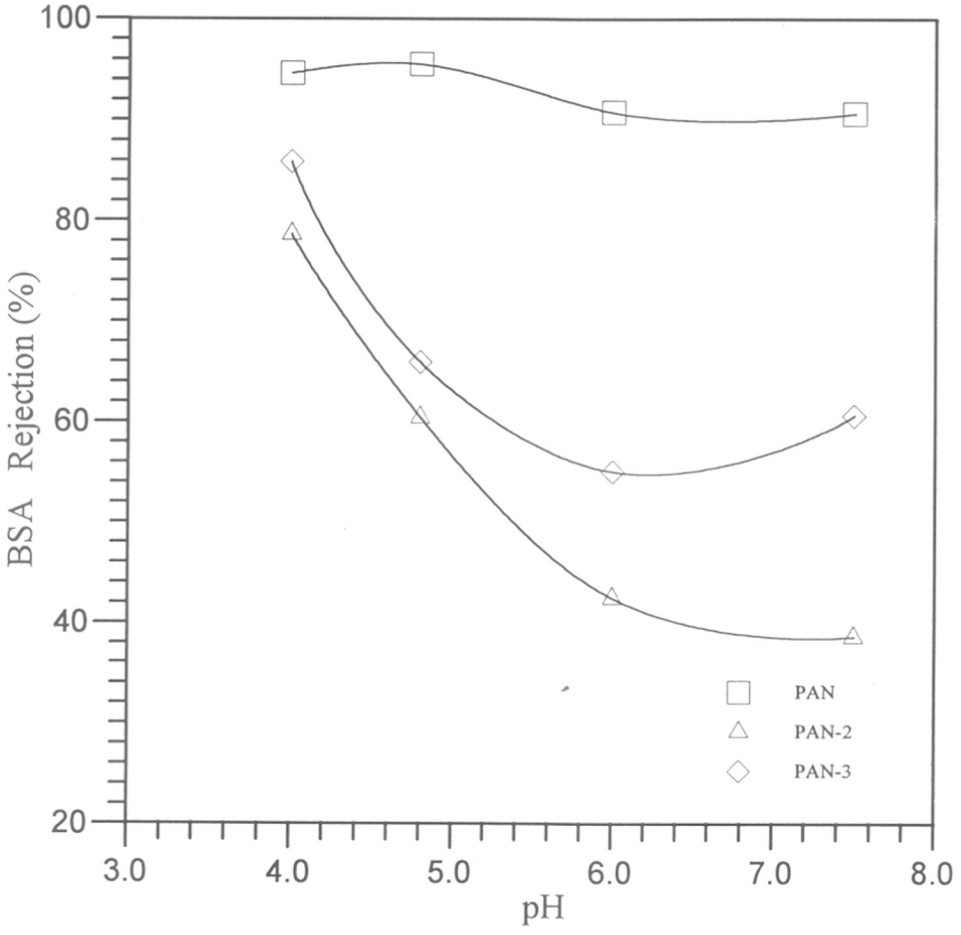

Figure 5.14 Effect of pH on observed BSA rejection (R) (%) at 1.25 VCF; 600 rpm; 200 kPa; 0.2 g/dl BSA for PAN, PAN-2 and PAN-3

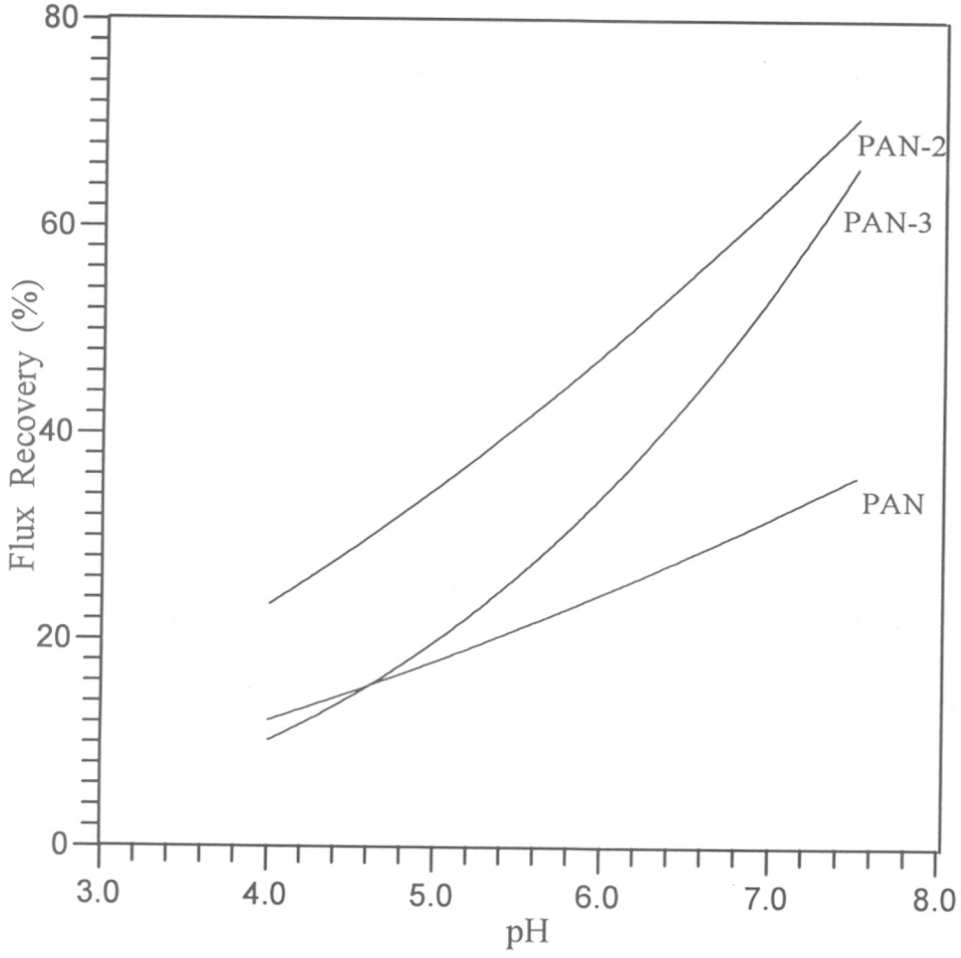

Figure 5.15 Effect of pH on trend in flux recovery (%) at 1.25 VCF; 600 rpm; 200 kPa; 0.2 g/dl BSA for PAN, PAN-2 and PAN-3

and PAN-3 both exhibit higher permeate fluxes than PAN. Also, Figure 5.15 shows that the flux recovery at the same pH values is generally higher for the acrylamide containing membranes. At higher pH values, the lower BSA rejection of PAN-3 in comparison to PAN may be partially responsible for higher flux and higher flux recoveries. However, since these trends hold across all pH values studied (including pH values at 4-4.8 where the rejections of both PAN and copolymer membranes are comparable), they can also be attributed partially to the improved hydrophilicity / reduced dispersive surface energy in the case of acrylamide containing membranes. The higher electrostatic repulsion between PAN and BSA at pH values higher than 4.8 appears to be of less importance than hydrophilic effects when comparing the flux performance of the PAN membrane with those made from the copolymers.

The permeate flux and flux recovery for any given membrane increase with increasing pH. This is related to the decreasing attraction (as pH increases from 4 to 4.8) and increasing repulsion (as pH increases above 4.8) between membrane and BSA.

The repulsive interaction between BSA molecules at pH values other than the IEP could also be an important factor contributing to this trend (Iritani et al, (1991). If such protein-protein repulsive interactions were predominant, one would expect to find a minimum flux at the BSA IEP, as reported by Fane et al (1983a) for BSA UF through polysulfone membranes. The fact that flux increases continuously with increasing pH even at pH 4 - 4.8 indicates that protein-membrane interactions are predominant.

The flux versus concentration data for PAN and PAN-3 were fitted to the boundary layer model (eqn. 3.11).

$$J_v = k.\ln [(C_m - C_p)/(C_r - C_p)] \qquad (3.11)$$

The initial estimate for the k and C_m values was generated from the slope and intercept of a plot of J_v versus $\ln C_r$, assuming C_p to be zero. These parameters were then refined by a standard non - linear regression (Marquardt's method) by fitting the BSA solution flux (J_v) with eqn (3.11) using the actual non-zero values of C_p. These plots for PAN and PAN-3 are shown in Figures 5.16-5.17 respectively.

The C_r values were calculated from the initial feed concentration (C_f) and the solute mass balance equation (eqn. 4.7). The parameters k and C_m for PAN and PAN-3

are summarized in Table 5.6. The mass transfer coefficient estimates have 90 % confidence interval limits of ± 30%, while the estimates for the protein concentration at the membrane surface, C_m , have confidence interval limits of ± 35%. Even at pH 4, where the membrane rejections are comparable, the parameter k is higher and C_m is lower for PAN-3 in comparison to PAN. The lower solute accumulation at the membrane surface may be because of less favorable solute-membrane interactions in the case of the copolymer. The predicted fluxes based on eqn. (3.11) and the parameters in Table 5.6 are also shown in Figures 5.16 - 5.17. According to the boundary layer model, the mass transfer coefficient k depends on hydrodynamic parameters and fluid properties such as viscosity and density. Gekas and Hallstrom (1987) have discussed modified mass transfer correlations taking into consideration the change in these fluid properties under concentration polarization conditions. Thus, the lower C_m values at the membrane surface could translate into a higher observed mass transfer coefficient.

Table 5.6

Mass transfer coefficient, k and solute concentration at the membrane surface, C_m , for BSA UF

pH	$k\times10^4$ (cm s^{-1})		C_m (mg/ml)	
	PAN	PAN-3	PAN	PAN-3
4	1.0	7.5	200	5.0
4.8	1.6	9.1	68	6.1
6	3.0	1.3	61	6.1
7.5	7.4	5.0	47	64

The observed BSA rejections (R) as a function of retentate concentration (C_r) are shown in Figures 5.18 and 5.19 for PAN and PAN-3 respectively. The predicted lines are based on eqn. (5.1) below which is obtained by substituting eqn. (3.13) into eqn. (3.12) and rearranging :

$$\frac{R}{1-R} = \frac{R'}{1-R'}\frac{C_m}{C_r} \qquad (5.1)$$

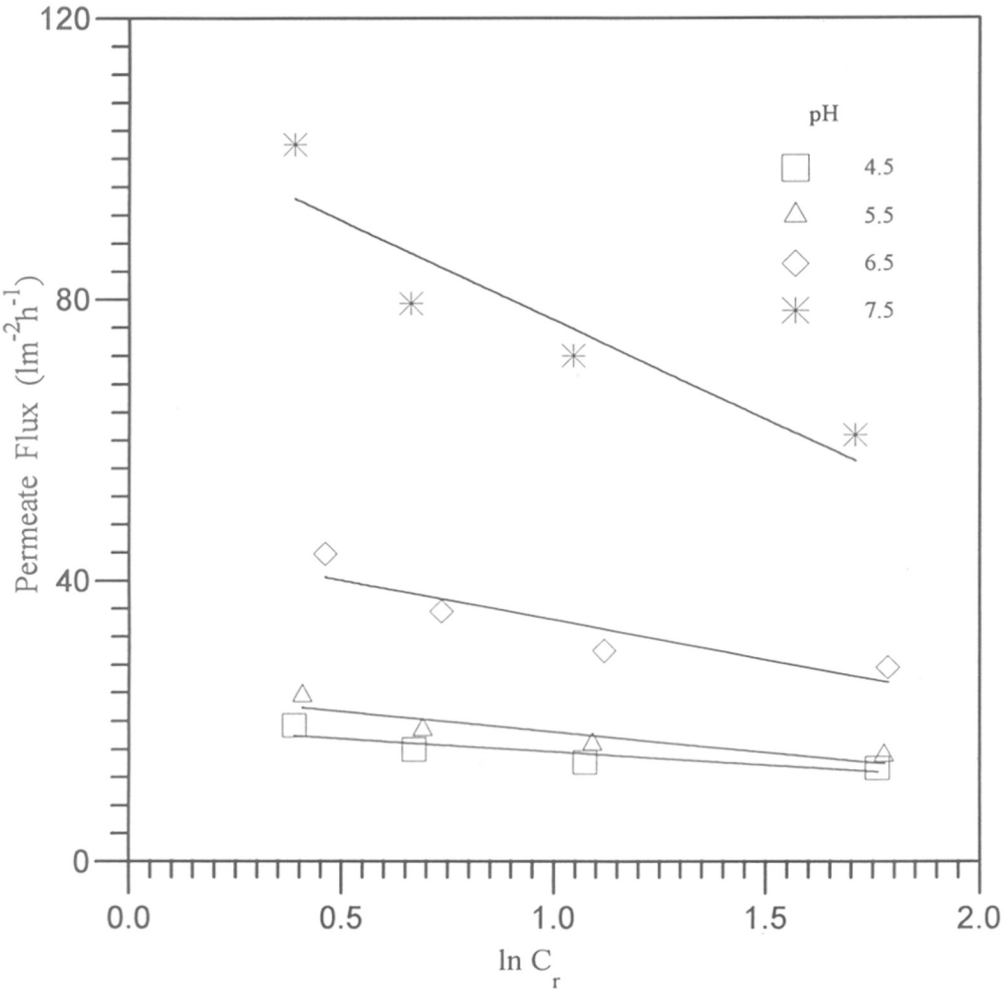

Figure 5.16 Effect of retentate concentration on permeate flux at 600 rpm; 200 kPa; 0.2 g/dl BSA for PAN. (—) represent predictions based on eqn (3.11) and parameters in Table 5.6

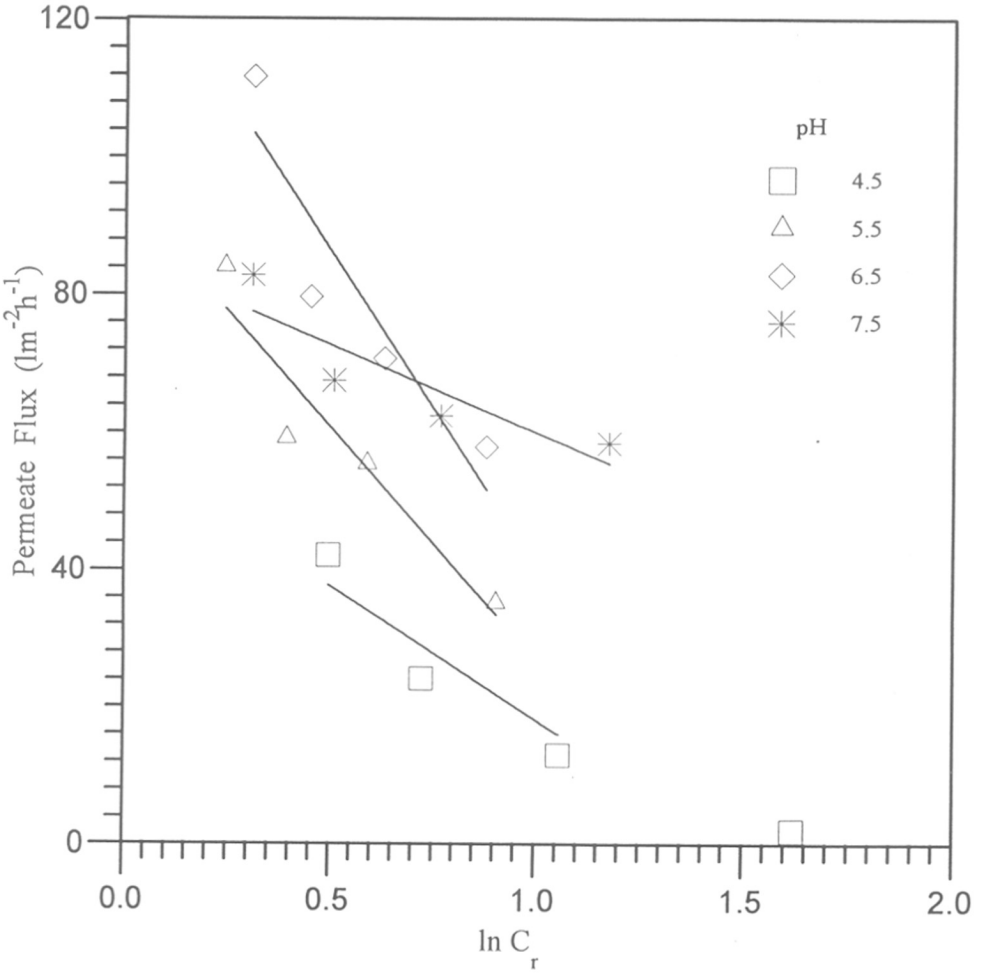

Figure 5.17 Effect of retentate concentration on permeate flux at 600 rpm; 200 kPa; 0.2 g/dl BSA for PAN-3. (—) represent predictions based on eqn (3.11) and parameters in Table 5.6

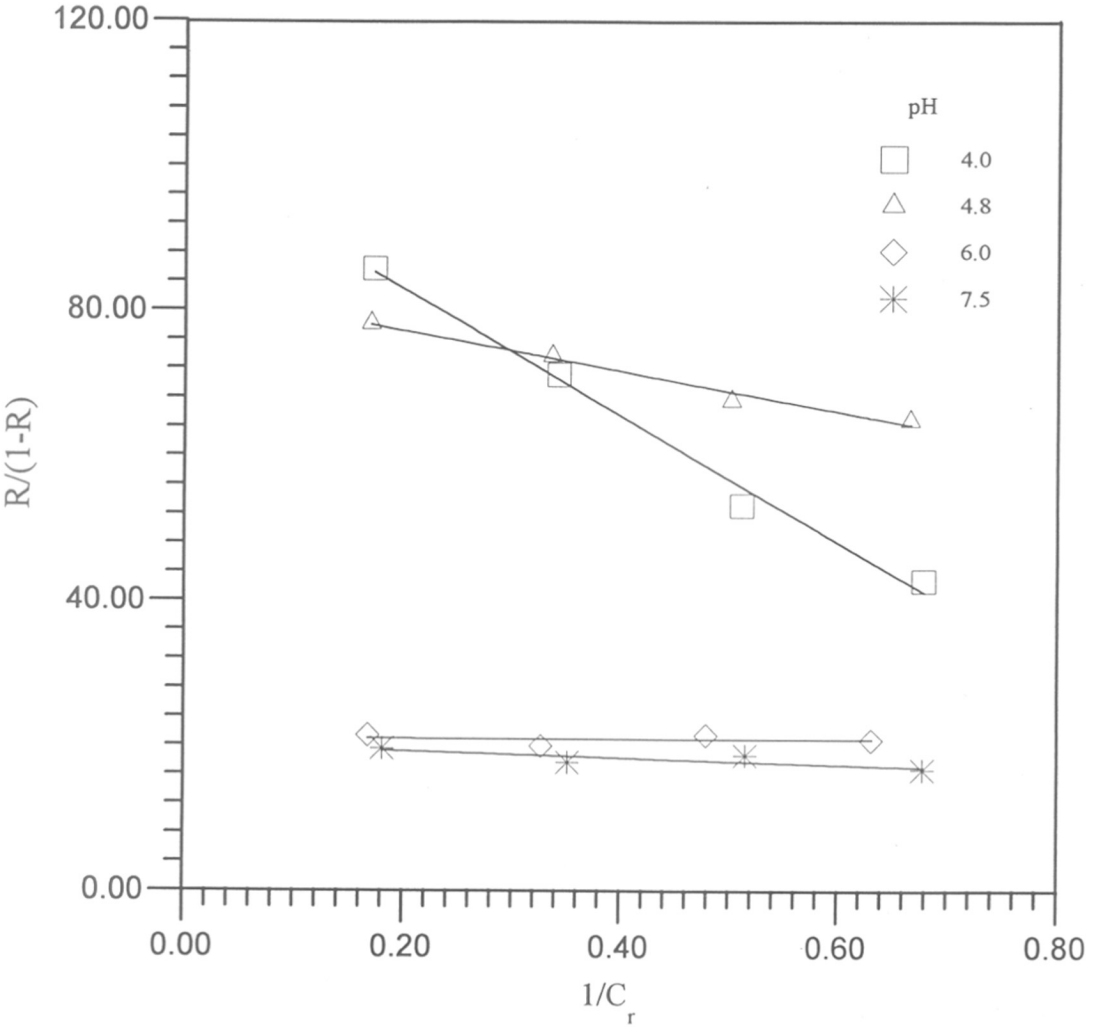

Figure 5.18 Effect of retentate concentration on observed BSA rejection (R) at 600 rpm; 200 kPa; 0.2 g/dl BSA for PAN. (—) represents best fit based on eqn. (5.1)

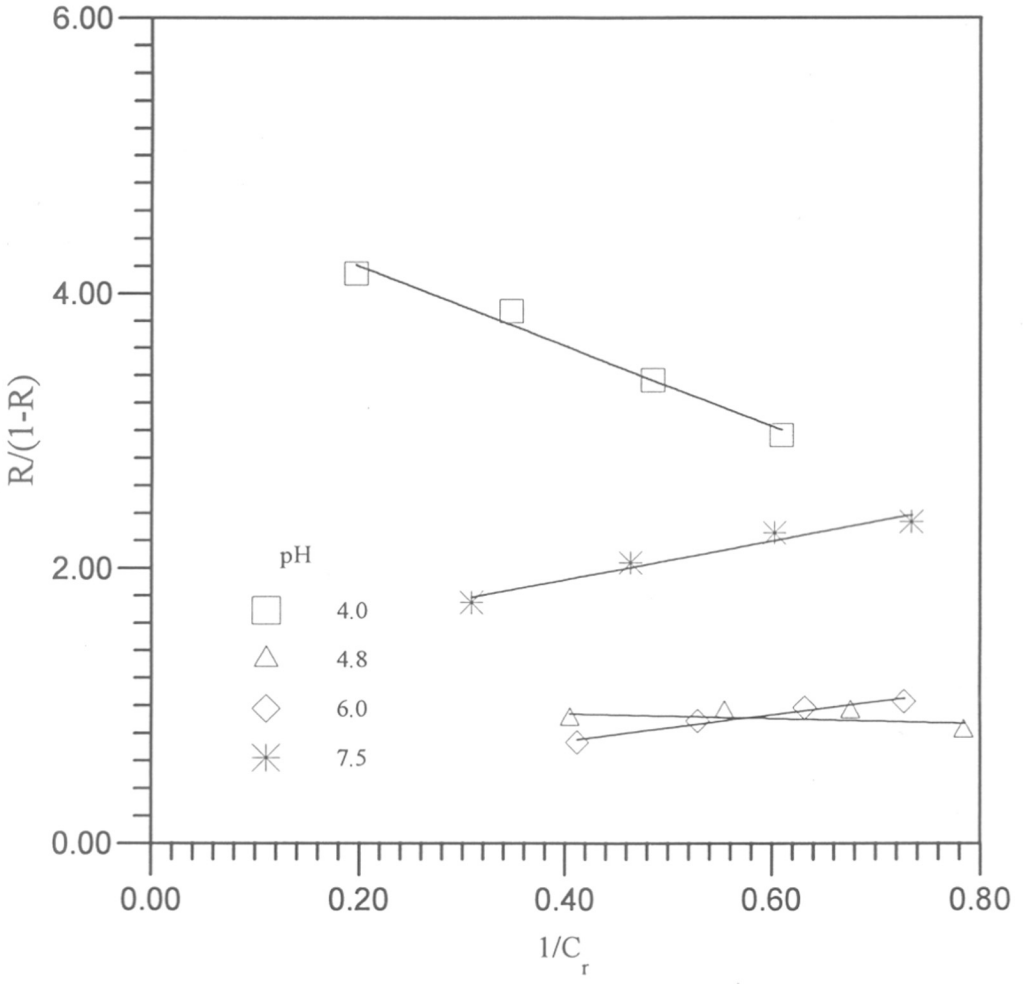

Figure 5.19 Effect of retentate concentration on observed BSA rejection (R) at 600 rpm; 200 kPa; 0.2 g/dl BSA for PAN-3. (—) represents best fit based on eqn. (5.1)

The permeate flux and BSA rejection (R) data for PAN-1 membrane (with 0.1 g/dl BSA) shows similar trends to the data with PAN-3 membrane (obtained with 0.2 g/dl) and are shown in Figures 5.20 and 5.21 respectively. The corresponding data for PAN at 0.1 g/dl BSA feed concentration are also shown in these figures.

A considerable difference between this ultrafiltration study and most others reported previously (Saksena and Zydney, 1994; Eijndhoven et al, 1995; Iritani et al, 1995c) is the high ionic strength (> 0.5M) used here. Due to the buffering system, the ionic strength varies from 0.52M at pH 4.0 to 1.16M at pH 7.5. It is known that changing ionic strength also affects UF performance (Fane et al, 1983a); however, these effect of changing I can be observed only at relatively low I values (I < 0.2M). Doherty and Benedek (1974) indicate that at I > 0.1 M, the diffusivities of BSA with varying electrical charges all tend to the same value. This indicates that varying I in the range of 0.5 -1.16M should have very little effect and the trends seen in flux and rejection can be interpreted in terms of changes in pH rather than changes in I. The effect of varying ionic strength in this range (0.52M < I < 1.16M) is shown for BSA ultrafiltration in Table 5.7. The results show that at either I = 0.52M or 1.16M, the same variation described above in flux and R with pH is seen with both PAN and PAN-1 membranes.

5.3.1.2 *Hb ultrafiltration*

Hb ultrafiltration performance was measured with PAN and PAN-1 membranes at 0.1 g/dl protein concentration in the feed. Hb has an IEP at pH 6.8 while the BSA IEP is at pH 4.8. This means that in comparison to BSA, it was possible to measure Hb UF performance over a wider range of pH values at which the protein is positively charged. While Hb is of similar size as BSA, it is more hydrophobic (see Table 5.5). The Hb UF data (Figures 5.22, 5.23) can be compared with the corresponding BSA data (Figures 5.20, 5.21) measured at the same protein concentration (0.1 g/dl) with the same membranes.

The major differences between Hb and BSA UF can be attributed to the difference in the IEP values of the two proteins; otherwise both proteins show the same basic UF behaviour. Hb also shows lower fluxes and higher rejections when the feed pH is below

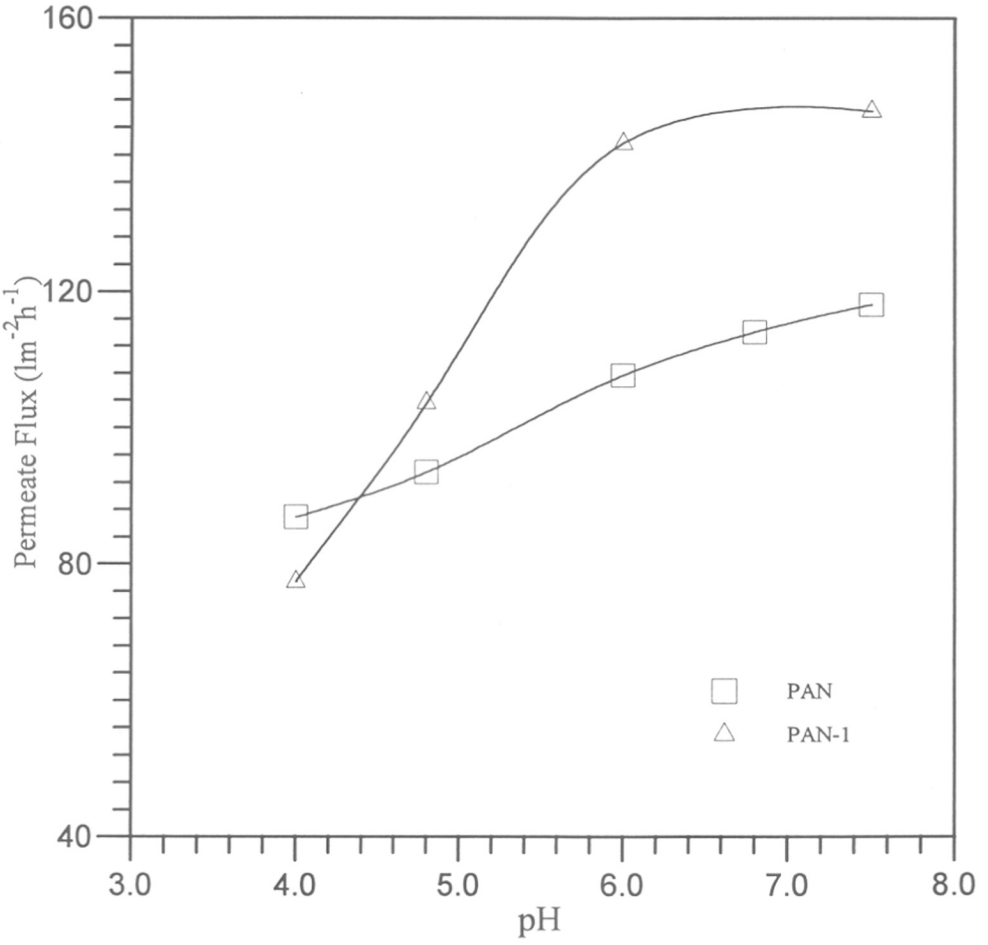

Figure 5.20 Effect of pH on permeate flux at 1.5 VCF; 600 rpm; 200 kPa; 0.1 g/dl BSA for PAN and PAN-1

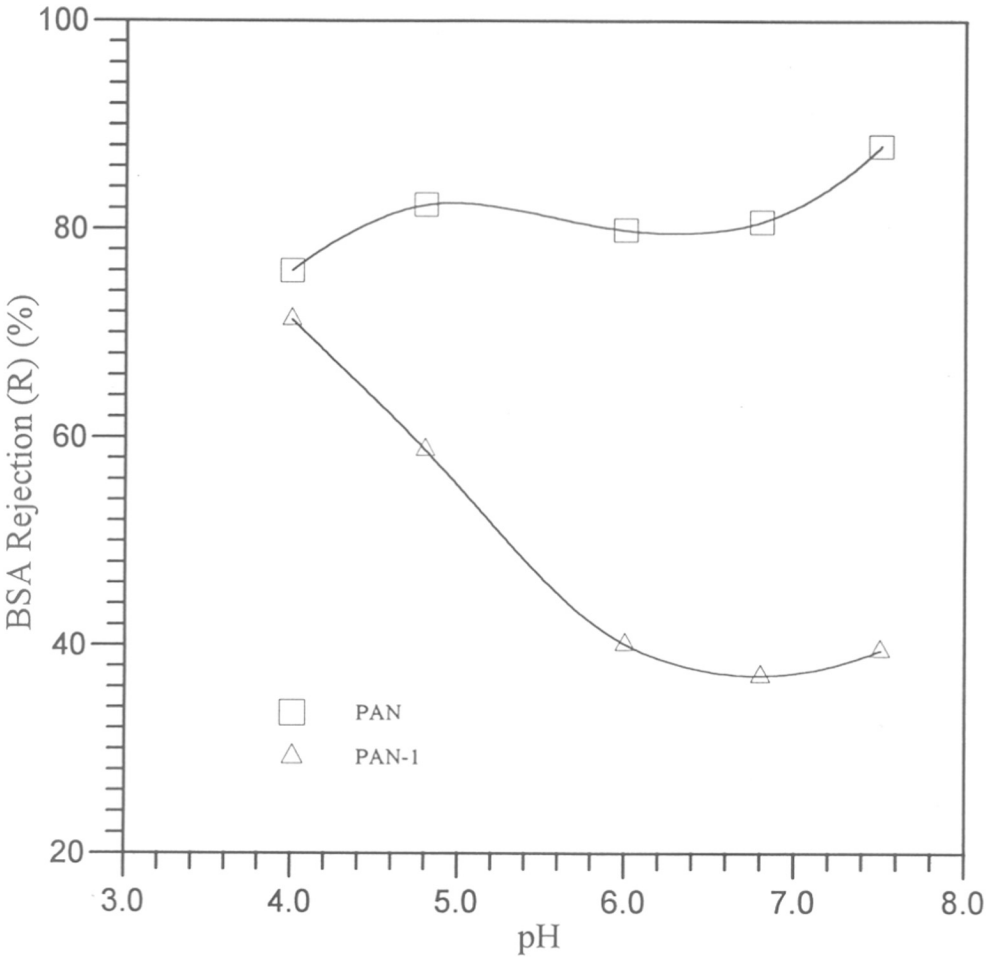

Figure 5.21 Effect of pH on observed BSA rejection (R) (%) at 1.5 VCF; 600 rpm; 200 kPa; 0.1 g/dl BSA for PAN and PAN-1

Table 5.7

Rejection, R and flux at I = 0.52M and 1.16M for BSA and BSA-Hb ultrafiltration

Permeate fluxes ($lm^{-2} h^{-1}$) for BSA UF

	pH 4.0		pH 7.5	
Ionic strength (M)	PAN	PAN-1	PAN	PAN-1
0.52	87	77	108	155
1.16	44	63	118	146

Rejection, R (%) for BSA UF

	pH 4.0		pH 7.5	
Ionic strength (M)	PAN	PAN-1	PAN	PAN-1
0.52	76.0	71.3	96.6	66.6
1.16	79.6	100	88.0	39.5

Permeate fluxes ($lm^{-2} h^{-1}$) for BSA-Hb UF

	pH 4.0		pH 7.5	
Ionic strength (M)	PAN	PAN-1	PAN	PAN-1
0.52	35	44	40	55
1.16	39	60	57	49

BSA rejection, R (%) in BSA-Hb UF

	pH 4.0		pH 7.5	
Ionic strength (M)	PAN	PAN-1	PAN	PAN-1
0.52	68.1	74.4	97.6	97.2
1.16	98.8	67.8	89.4	85.8

Hb rejection, R (%) in BSA-Hb UF

	pH 4.0		pH 7.5	
Ionic strength (M)	PAN	PAN-1	PAN	PAN-1
0.52	83.1	84.4	99.1	98.7
1.16	100	68.0	97.8	95.9

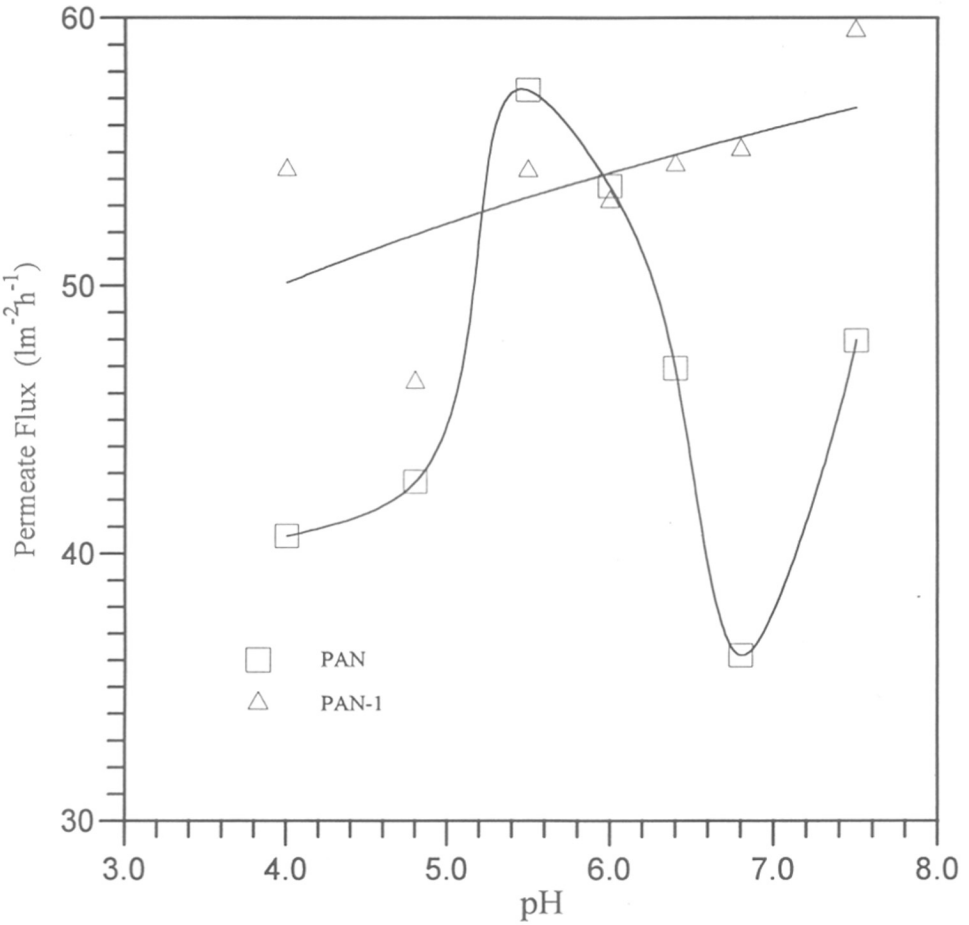

Figure 5.22 Effect of pH on permeate flux at 1.5 VCF; 600 rpm; 200 kPa; 0.1 g/dl Hb for PAN and PAN-1

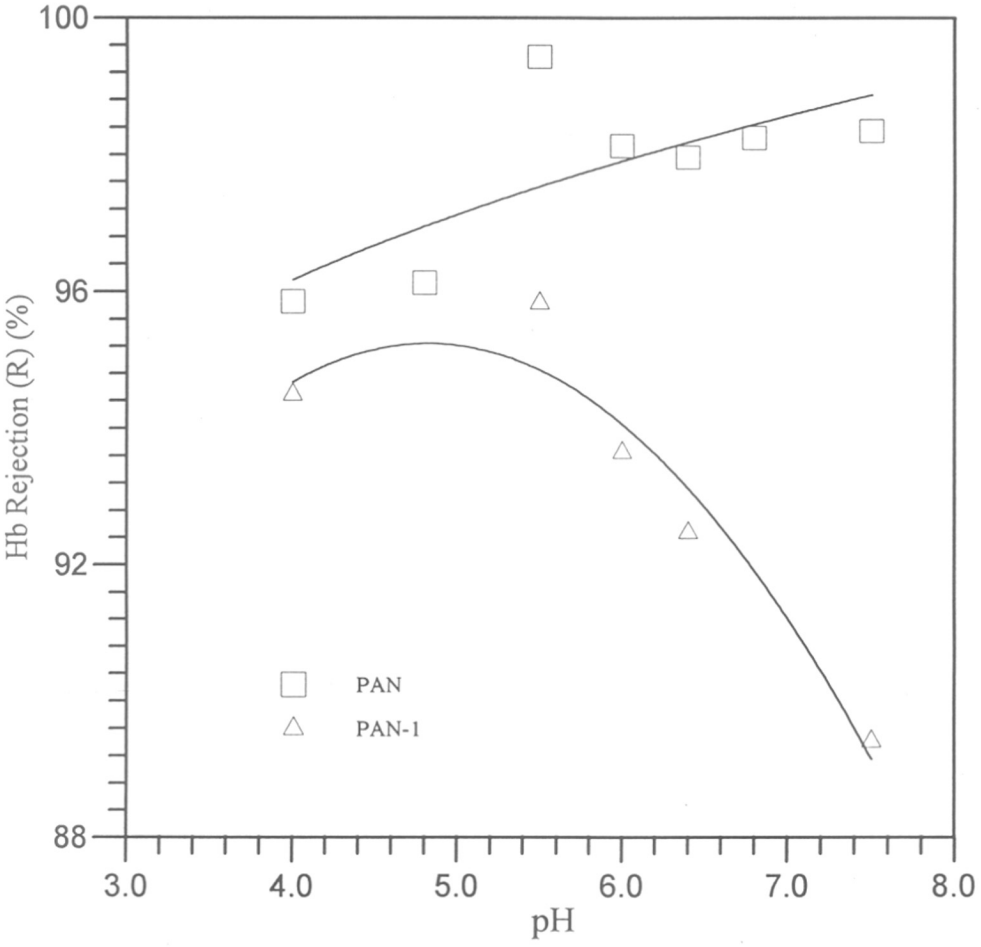

Figure 5.23 Effect of pH on observed Hb rejection (*R*) (%) at 1.5 VCF; 600 rpm; 200 kPa; 0.1 g/dl Hb for PAN and PAN-1

the protein IEP in comparison to higher pH values. As can be seen from the Figures 5.22 and 5.23, the major trends in permeate flux and rejection (R) behaviour for Hb UF are similar to that for BSA (Figures 5.20 and 5.21) and can be explained by the same mechanisms discussed above.

An interesting difference between Hb and BSA UF performance is that the flux data in PAN membrane show a marked minima at the protein IEP which is consistent with the reduced protein-protein repulsive interactions at this pH (6.8). Flux minima at the IEP have also been seen in other UF systems (Nyström, 1989; Hanemaaijer et al, 1989; Fane et al, 1983a). In the case of PAN-1, the increased hydrophilicity of the membrane prevents a minimum in the flux at IEP. As with BSA, Hb rejections are also higher below the IEP where membrane and protein are oppositely charged and decrease above the IEP in the case of the PAN-1 membrane. With the PAN membrane, electrostatic effects are again overcome by hydrophobic adsorption effects and Hb rejections are uniformly high at all pH values.

Repulsive interactions between membrane and protein could have opposing effects. Some experimental evidence (Miyama et al, 1988; Nakao et al, 1988) as well as theoretical models (section 3.1) indicate that repulsive interactions could lead to hindered transmission of the protein through the pore and consequent higher rejections. As per this hypothesis, higher protein rejections should be seen at pH values where both membrane and proteins are negatively charged. However, it has also been indicated that rejection can be increased through protein adsorption on the pore walls and consequent pore size narrowing (Hanemaaijer et al, 1989). Increased rejection and decreased flux as a consequence of pore narrowing is predicted by all transport models (eqn. 3.5) through steric hindrance effects. Adsorptive effects through hydrophobic interactions would be more pronounced at the high ionic strengths used in this study; however, these could be modified by hydrophilic and electrostatic interactions. As per the pore narrowing hypothesis, since repulsive interactions would decrease protein adsorption; one would expect higher fluxes and lower rejections at pH values where the protein and membrane surface would both be negatively charged. The second hypothesis seems to be consistent with the single protein rejection data in Figures 5.21 and 5.23.

Other mechanisms can also be considered for explaining the flux and rejection trends with increasing pH. Light-scattering based studies (Doherty and Benedek, 1974) indicate that the protein diffusivity and consequent mass transfer coefficient (eqn. 3.11) are relatively constant with the net electrostatic charge on BSA at the high ionic strengths used here. Hence changes in the concentration polarization phenomena with increasing pH do not appear to be responsible for these trends.

Another mechanism by which changes in pH could affect the observed flux is by changing the packing characteristics of the retained protein layer at the membrane surface (Iritani et al, 1995c). Such electrostatic interactions between protein molecules would lead to a flux minima at the IEP and increasing fluxes both above and below the IEP as seen by Fane et al (1983a). This mechanism does not appear important for BSA UF in either membrane at the conditions studied here and the transport characteristics at the various pH value can be explained on the basis of the pore narrowing hypothesis alone.

In the case of Hb ultrafiltration also, the flux increases overall with pH for both membranes (Figure 5.22) which is consistent with the pore adsorption / narrowing hypothesis discussed above. However, for Hb UF through the less hydrophilic PAN membrane, a flux minima is seen at the IEP. This minima can be explained by the lower permeability of the Hb deposited on PAN at the IEP.

At any given pH, flux is lower and rejection is higher for Hb UF than for BSA in either membrane. This is attributed to the higher Hb adsorption on the membranes due to its higher hydrophobicity compared to BSA and is consistent with the postulated protein adsorption / pore narrowing hypothesis.

The observed rejection coefficients in Figures (5.21, 5.23) are a consequence of the concentration polarization phenomena and are primarily affected by the flux obtained in the membrane at the various pH values. The rejection coefficients through the membrane, R', were calculated by accounting for the concentration polarized layer of rejected protein on the membrane surface using the boundary layer model of Blatt et al (1970). R' was calculated from the experimentally observed rejections, R, by the equation :

$$R' = R \Big/ \left[R + \exp\left(-J_v / k\right) - R \exp\left(-J_v / k\right) \right] \tag{5.2}$$

The mass transfer coefficient, k, in a stirred cell was estimated from the correlation (Blatt et al, 1970),

$$k = \frac{D}{r_h} 0.253 \left[\frac{\omega r_h^2}{\nu} \right]^{0.55} \left[\frac{\nu}{D} \right]^{0.33} \tag{5.3}$$

where, D is the solute diffusivity, r_h is the stirred cell radius, ω is the stirring speed and ν is the kinematic viscosity. For these calculations, the BSA diffusivity was taken as the value reported for 5% BSA solution at high ionic strengths ($I \geq 0.1$ - 1M) (Doherty and Benedek, 1974). Based on this diffusivity and the values for other parameters (Table 5.8), the mass transfer coefficient, k, was calculated to be 5.2×10^{-4} cm s^{-1}. The value of k is taken to be constant with varying pH. Though in general D and hence k are dependent on pH, at the high ionic strengths (0.5 - 1M) used in this work, D tends to a limiting value. It has been shown (Doherty and Benedek, 1974) that at $I > 0.1$M, the diffusivities of BSA with varying electrical charges all tend to the same value. A similar calculation was done for the Hb data. Figure 5.24 shows R' for both BSA and Hb UF for PAN and PAN-1 membranes. It can be seen from this figure that all the R' values are in the range of 99.5-99.9% for both proteins in both membranes.

Table 5.8

Parameters for calculation of mass transfer coefficient, k

Parameter	Value
Diffusivity of BSA (D)	5.9×10^{-7} cm^2 s^{-1}
Diffusivity of Hb (D)	6.4×10^{-7} cm^2 s^{-1}
Radius of stirred cell (r)	2.13 cm
Kinematic viscosity (ν)	0.01 cm^2 s^{-1}
Stirring speed (ω)	63 radians s^{-1}

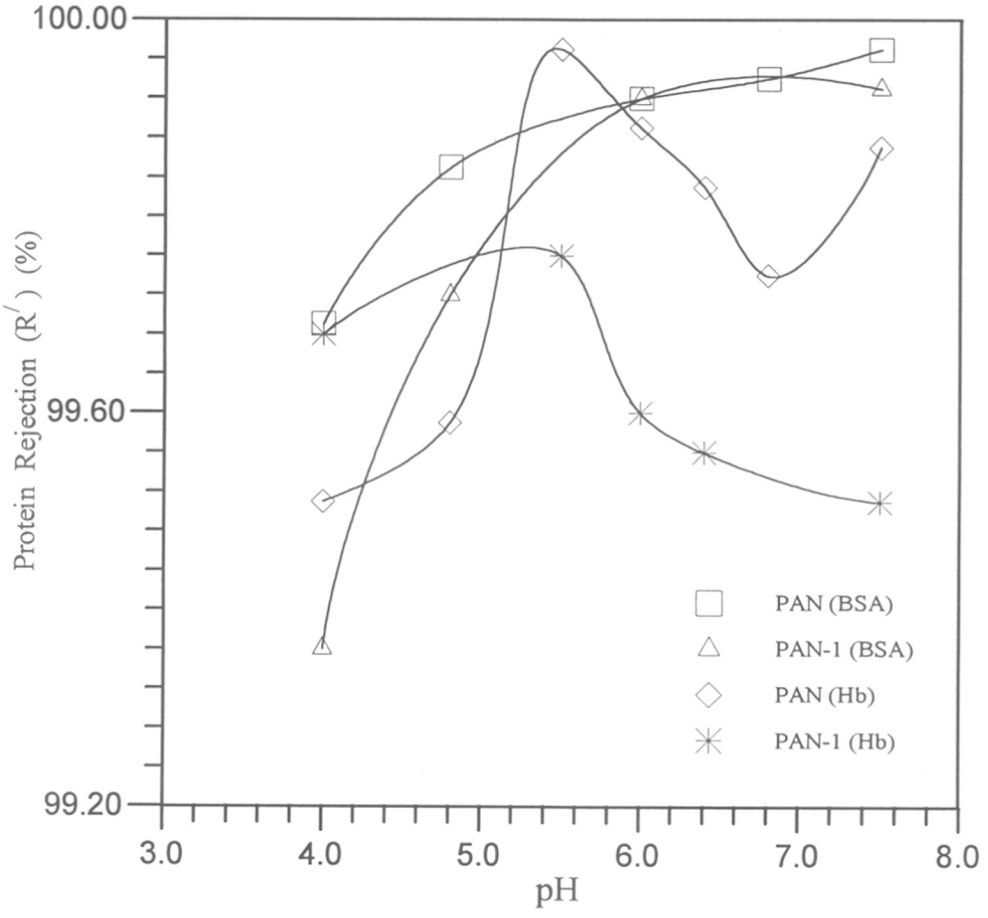

Figure 5.24 Effect of pH on membrane rejections (R') (%) of BSA and Hb at 1.5 VCF; 600 rpm; 200 kPa; 0.1 g/dl BSA or Hb for PAN, PAN-1

5.3.1.3 *Binary solution (BSA-Hb) UF*

BSA-Hb UF performance was measured with PAN and PAN-1 membranes with 0.1 g/dl of each protein. This allows a comparison of the mixed protein UF data with that measured for the individual proteins in each type of membrane. The permeate flux, and BSA and Hb rejections (R and R') for BSA-Hb UF are shown in Figures 5.25-5.29.

With some minor variations, the ultrafiltration fluxes for the binary BSA-Hb solution (Figure 5.25) match the single protein Hb data in both magnitude as well as trends with changing pH. Thus it appears that the mixed BSA-Hb UF performance is dominated by the Hb electrostatic charge and hydrophobicity characteristics.

In the case of PAN-1, the binary solution flux initially increases with increasing pH. This is the same as seen earlier with both pure proteins; however, above pH 6.4 the binary solution flux decreases unlike the case when either Hb or BSA was ultrafiltered alone.

Membrane rejections, R' (Figures 5.26, 5.27) for both BSA and Hb in BSA-Hb UF are lower than those of the single proteins. This may be explained by the pore narrowing mechanism as a function of the electrostatic interactions between the two proteins in combination with the Hb-membrane interactions. Preferential adsorption of Hb on the membrane is expected due to its higher hydrophobicity. This would modify the surface electrostatic characteristics of the membrane. The R' through the Hb adsorbed membranes is lowest at pH 4, where both the proteins are positively charged. Above pH 4.8, where both proteins are oppositely charged; attractive coulombic interactions or association between BSA and Hb on the membrane surface could explain the increased rejection. Association between HSA and Hb has been reported at high ionic strength and at pH values between the IEPs of both proteins by Kontturi et al (1996). R' in the hydrophilic PAN-1 membrane showed a maxima at the Hb IEP indicating the importance of adsorption / pore narrowing effects in this system. At pH 7.5 all three i.e. BSA, Hb and membranes are negatively charged, which allows more protein transmission due to reduced adsorption on the pore walls.

PAN-1 shows generally higher flux and protein transmission than the PAN membrane; also the increase in rejection, R, with increasing pH in the BSA-Hb case is

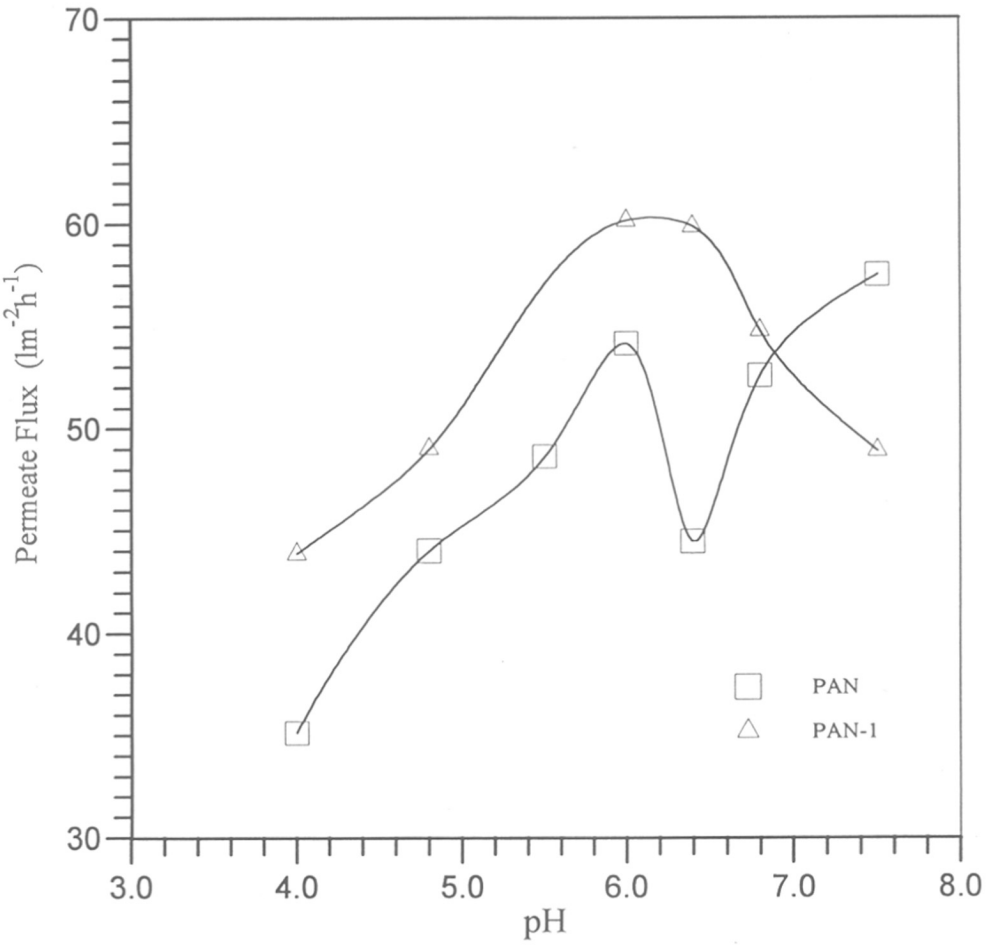

Figure 5.25 Effect of pH on permeate flux at 1.5 VCF; 600 rpm; 200 kPa; (0.1 g/dl BSA + 0.1 g/dl Hb) for PAN and PAN-1

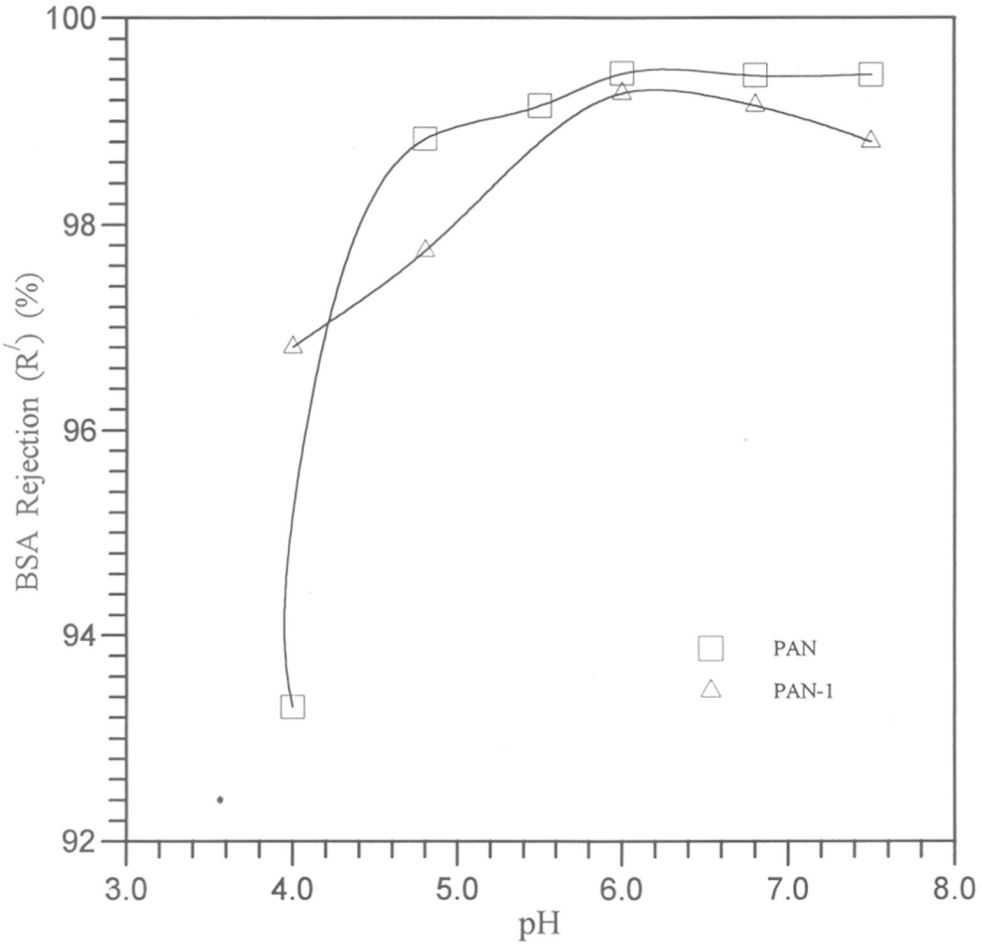

Figure 5.26 Effect of pH on membrane rejection of BSA (R') (%) at 1.5 VCF; 600 rpm; 200 kPa; (0.1 g/dl BSA + 0.1 g/dl Hb) for PAN and PAN-1

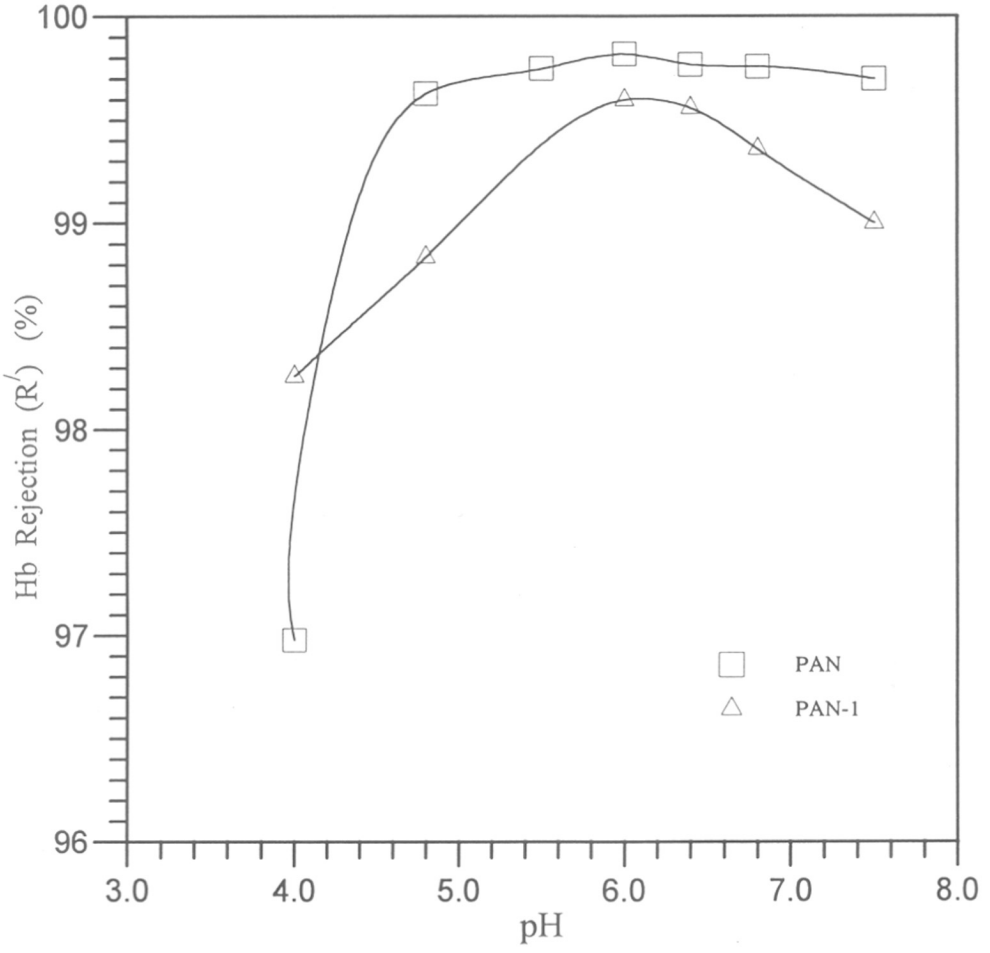

Figure 5.27 Effect of pH on membrane rejection of Hb (R') (%)at 1.5 VCF; 600 rpm; 200 kPa; (0.1 g/dl BSA + 0.1 g/dl Hb) for PAN and PAN-1

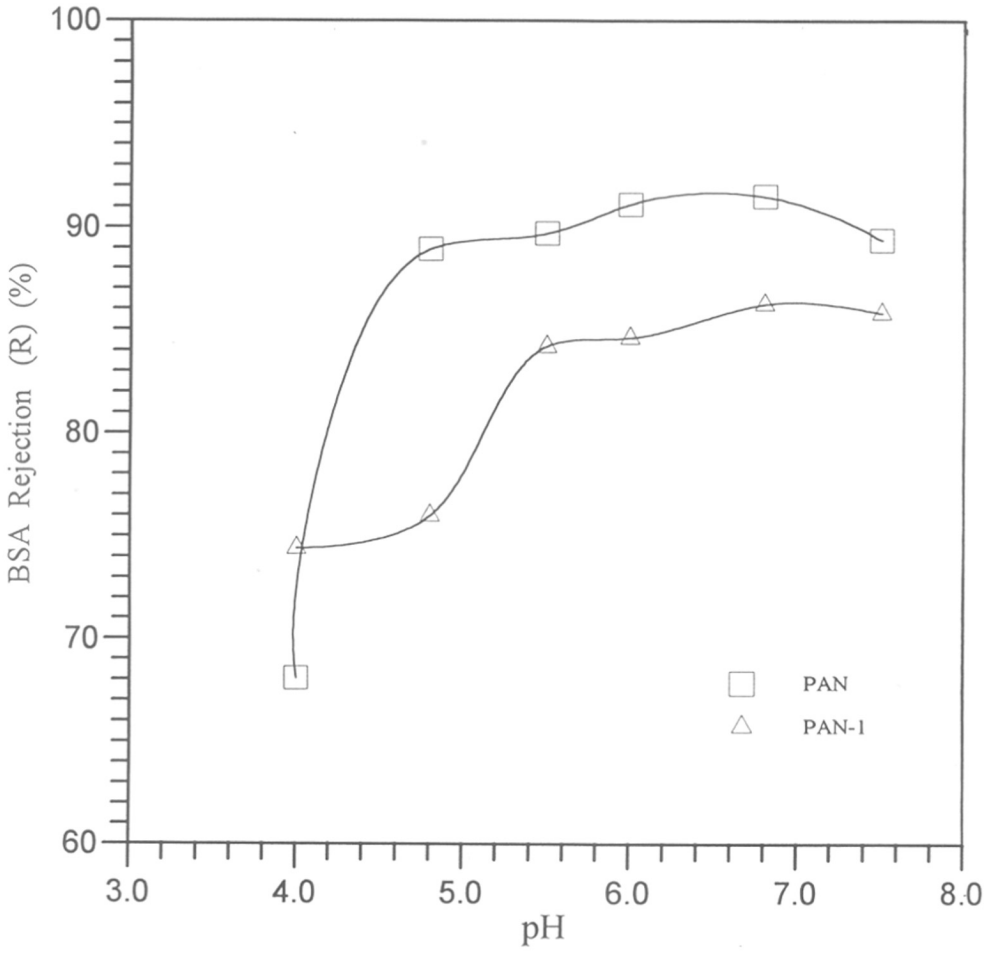

Figure 5.28 Effect of pH on observed BSA rejection (R) (%) at 1.5 VCF; 600 rpm; 200 kPa; (0.1 g/dl BSA + 0.1 g/dl Hb) for PAN and PAN-1

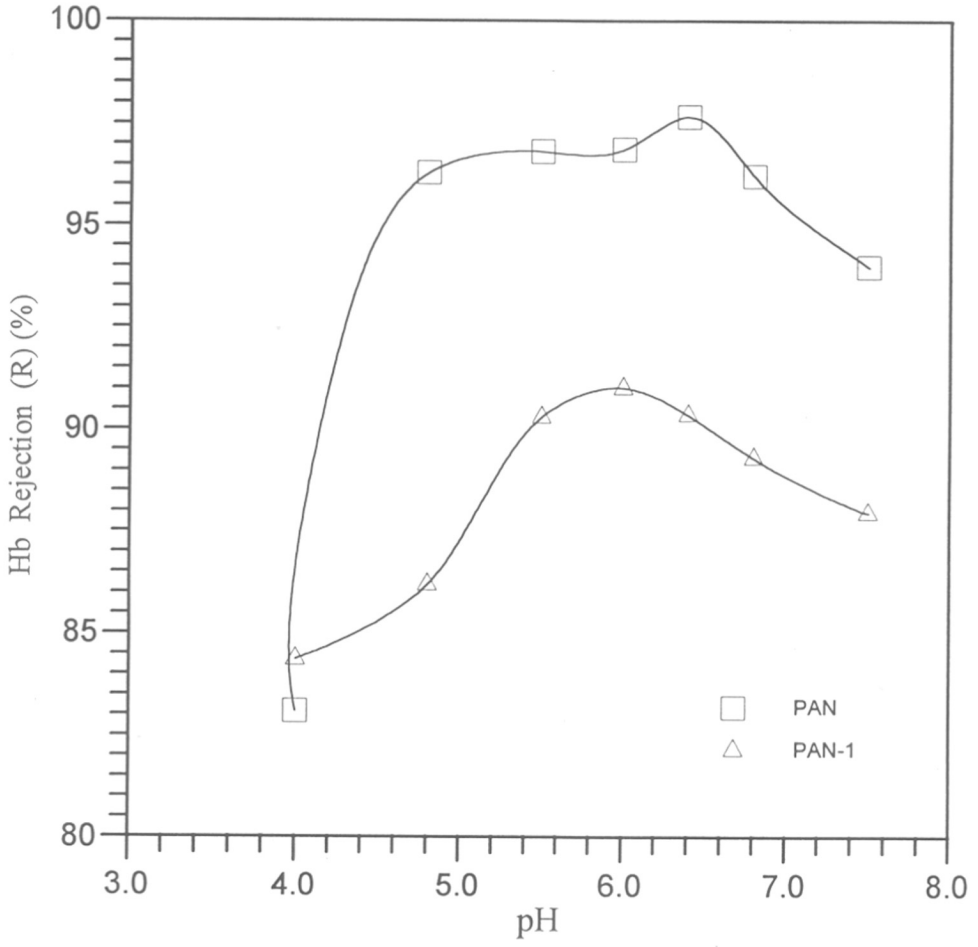

Figure 5.29 Effect of pH on observed Hb rejection (R) (%) at 1.5 VCF; 600 rpm; 200 kPa; (0.1 g/dl BSA + 0.1 g/dl Hb) for PAN and PAN-1

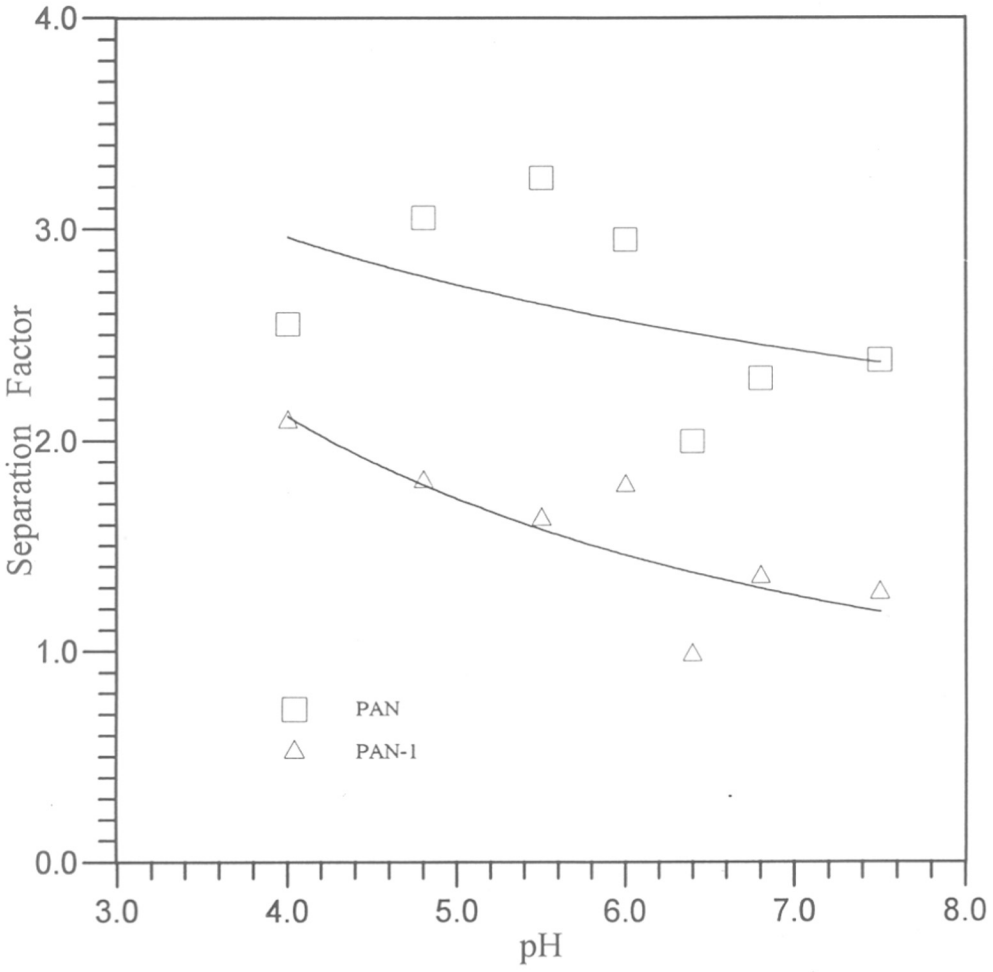

Figure 5.30 Effect of pH on BSA / Hb separation factor at 1.5 VCF; 600 rpm; 200 kPa; (0.1 g/dl BSA + 0.1 g/dl Hb) for PAN and PAN-1. Solid lines represent trend with pH

slightly shifted towards higher pH values (Figures 5.28, 5.29). These differences can be attributed to the higher hydrophilicity, lower dispersive force component of surface energy and less negative electrostatic charge of PAN-1.

The effect of changing I in the range from 0.5-1.16M on the binary solution UF was examined by the same method as discussed at the end of section 5.3.1.1 for BSA UF. Table 5.7 shows that at either I = 0.52M or 1.16M, the same basic variation described above in flux and R with pH is seen with both membranes. The only small exception is seen in the ≈20% higher flux measured for PAN-1 at I = 1.16M at pH 4.0 compared to pH 7.5.

The relative rates of protein transmission are presented in the form of a separation factor (eqn. 4.11) in Figure 5.30. The best separation factors are generally obtained at lower pH and decrease as pH increases. Kontturi et al (1996) also found the best separation between albumin and Hb by convective electrophoresis to occur at low pH.

5.3.2 ULTRAFILTRATION OF ACID, CHEESE AND SHRIKHAND WHEY

The composition of the three wheys studied i.e. acid (AW), cheese (CW) and shrikhand (SW) are listed in Table 5.9. The values for acid and cheese whey compare well with those reported by other investigators (e.g. Kosikowski, 1979). The properties and approximate protein make-up is listed in Table 5.10.

All the three wheys examined contain approximately similar proteins : α-lactalbumin, β-lactoglobulin, BSA and immunoglobulins. Gel electrophoresis (SDS-PAGE) experiments show essentially the same staining pattern for milk and all three wheys (Figure 5.31). α-lactalbumin and β-lactoglobulin are the major whey proteins (accounting for 80% of the total protein content); both are smaller than BSA and have similar IEP (~ 5). Immunoglobulins account for ~ 12% of the total protein; these are larger than BSA and have higher IEP values (pH 7).

Though the protein composition in the 3 wheys appears similar, there are significant differences in pH as well as other components. CW is slightly acidic (pH ~ 5.9) while AW (pH ~ 4.24) and SW (pH ~ 4.78) are formed at more acidic conditions. Natural AW contains 2-3x as much calcium as natural CW (Merin, 1979). Table 5.9 shows that

Table 5.9

Experimentally measured composition and properties of different whey samples used

Constituent	Acid whey		Cheese whey		Shrikhand whey	
	Unclar.	Clarified	Unclar.	Clarified	Unclar.	Clarified
Natural pH	4.24	7.5	5.9	7.5	4.78	7.5
Specific Conductivity ($mS\ cm^{-1}$)	5.0	7.2	3.0	4.9	3.5	7.2
Fat[(a)] (wt %)	0.1	0.1	0.2	0.1	< 0.1	< 0.1
Protein[(b)] (wt %)	0.66	0.59	0.70	0.58	0.70	036
Lactose[(c)] (wt %)	5.65	8.71	4.77	5.70	5.05	6.91
Ash[(d)] (wt %)	0.75	0.38	0.195	0.32	0.80	2.1775
Total solids[(d)] (wt %)	6.97	6.03	6.75	6.42	7.76	5.95
Intrinsic viscosity[(e)](dl/g)	0.022	0.024	0.024	0.026	0.023	0.024

a) The fat content was determined by Gerber test (Kirk and Sawer, 1991)

b) Protein content was determined by the method of Lowry et al (1951)

c) Lactose content was determined by the DNSA method of Robyt and Whelan (1972)

d) determined by gravimetric analysis.

e) measured in aqueous media by the procedure described in section 4.1.2.

the ash content of AW and SW is similar and substantially higher than CW. AW also contains slightly higher lactose than CW and SW. An important difference in SW compared to other wheys is that ~ 7-10% of the lactose has been fermented to lactic acid. While it is well-known that fat content can affect UF fluxes markedly, the fat levels were constant at a low level (~ < 0.1 - 0.2%) in the centrifuged and filtered (Whatman No. 1) whey samples studied here. Hence, no effect of fat content was observed in this study.

Table 5.10

Physical properties of whey proteins*

Characteristics	α-lactalbumin	β-lactoglobulin	BSA	Immunoglobulins
Fraction in whey (%)	0.12	0.33	0.04	0.07
Molecular weight (kD)	14.4	36 (Dimer)	69	155
Equivalent ellipsoidal dimensions (nm)	3.7×3.2×2.5	-	4×4×14	23×4.5×4.5
Partial Specific volume (m^3/kg)	7.35×10^{-4}	-	7.34×10^{-4}	-
Stokes-Einstein radius (nm)	2.02	2.68 (Dimer)	3.64	7.7
Surface area (m^2)	-	-	1.1×10^{-16}	1.94×10^{-16}
Diffusion Coefficient (m^2/s)	10.6×10^{-11}	-	5.9×10^{-11}	-
Sedimentation coefficient (sec)	1.83×10^{-13}	-	4.41×10^{-13}	-
Isoelectric Point	4.8	5.2	4.8	7.0
Net charge (at pH 7.4)	-7	-	-22	-

* Data taken from Kupku et al (1993), van den Berg and Smolders (1989), Norde (1996) and Palecek and Zydney (1994).

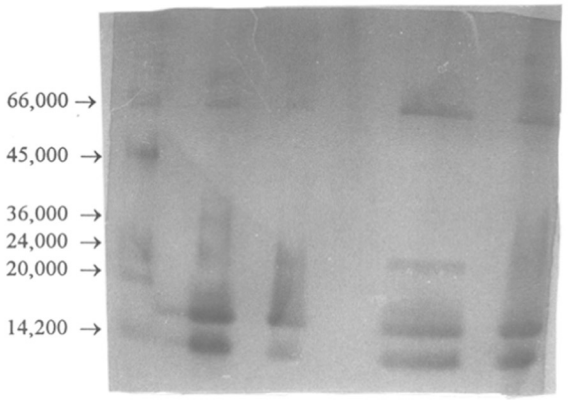

A : SDS-PAGE marker **B** : Milk

C : Acid whey **D** : Cheese whey

E : Shrikhand whey

Figure 5. 31 : Electrophoresis patterns for milk and natural wheys (acid, cheese and shrikhand) along with standard SDS-PAGE markers

Whey UF was carried out with PAN and PAN-3 membranes. The flux and rejection measurements for natural whey UF were made as a function of the VCF. The flux measurements are shown as a function of retentate protein concentration in Figures 5.32-5.37. The corresponding rejections are shown in Figures 5.38-5.43. In order to examine the effect of pH, the flux and rejection data at a constant VCF of 1.67 are plotted as a function of pH for natural wheys in Figures 5.44-5.45 and 5.46-5.47 respectively. All the above measurements were made at a fixed feed side pressure of 200 kPa. Fluxes measured as a function of pressure at the constant conditions of pH 7.5 and VCF of 1.67 are shown in Figures 5.48-5.50 for AW, CW and SW respectively.

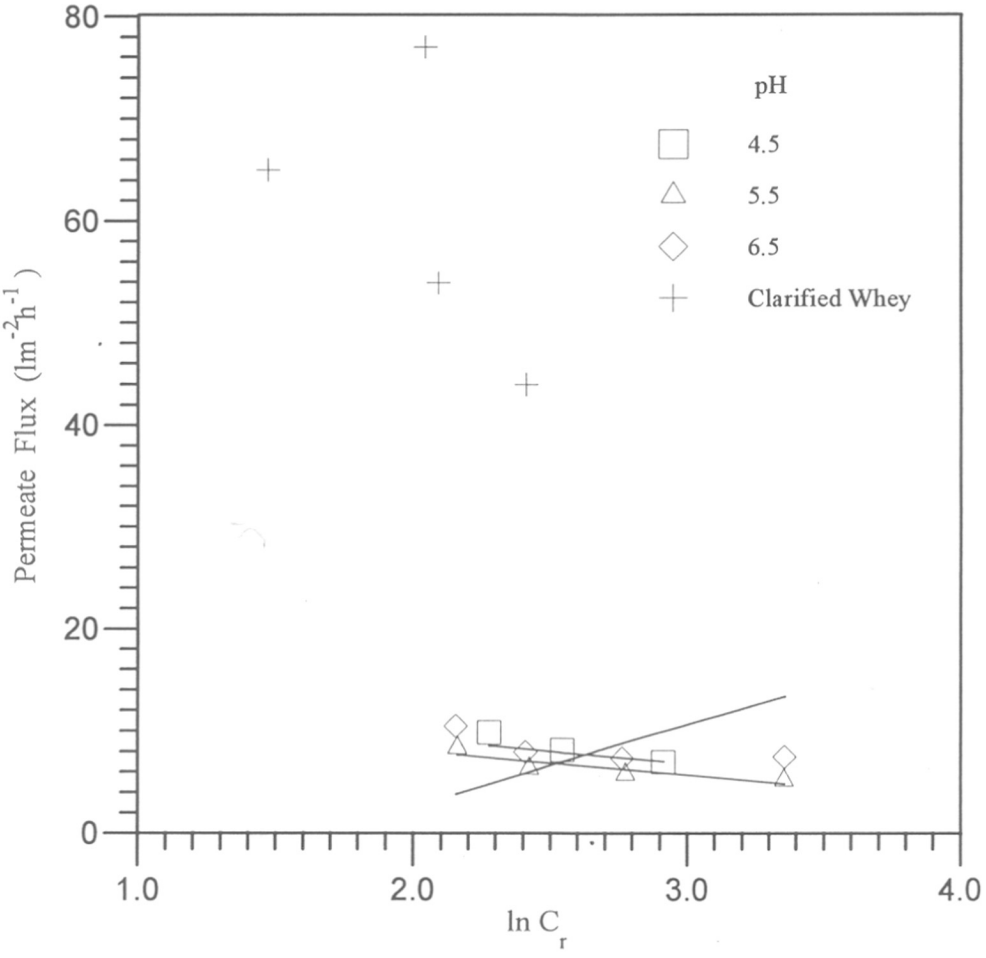

Figure 5.32 Effect of retentate concentration on permeate flux at 600 rpm; 200 kPa for AW with PAN. represent predictions based on eqn (3.11) and parameters in Table 5.11

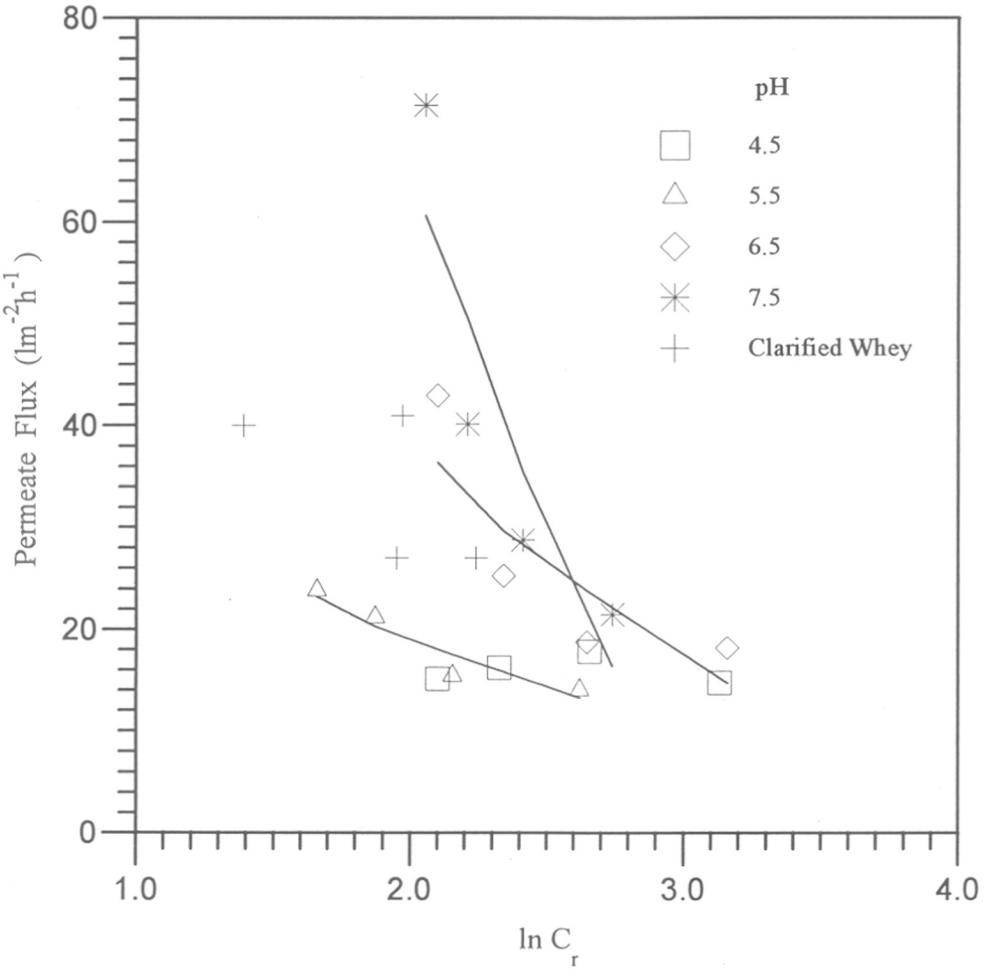

Figure 5.33 Effect of retentate concentration on permeate flux at 600 rpm; 200 kPa for AW with PAN-3. (—) represent predictions based on eqn (3.11) and parameters in Table 5.11

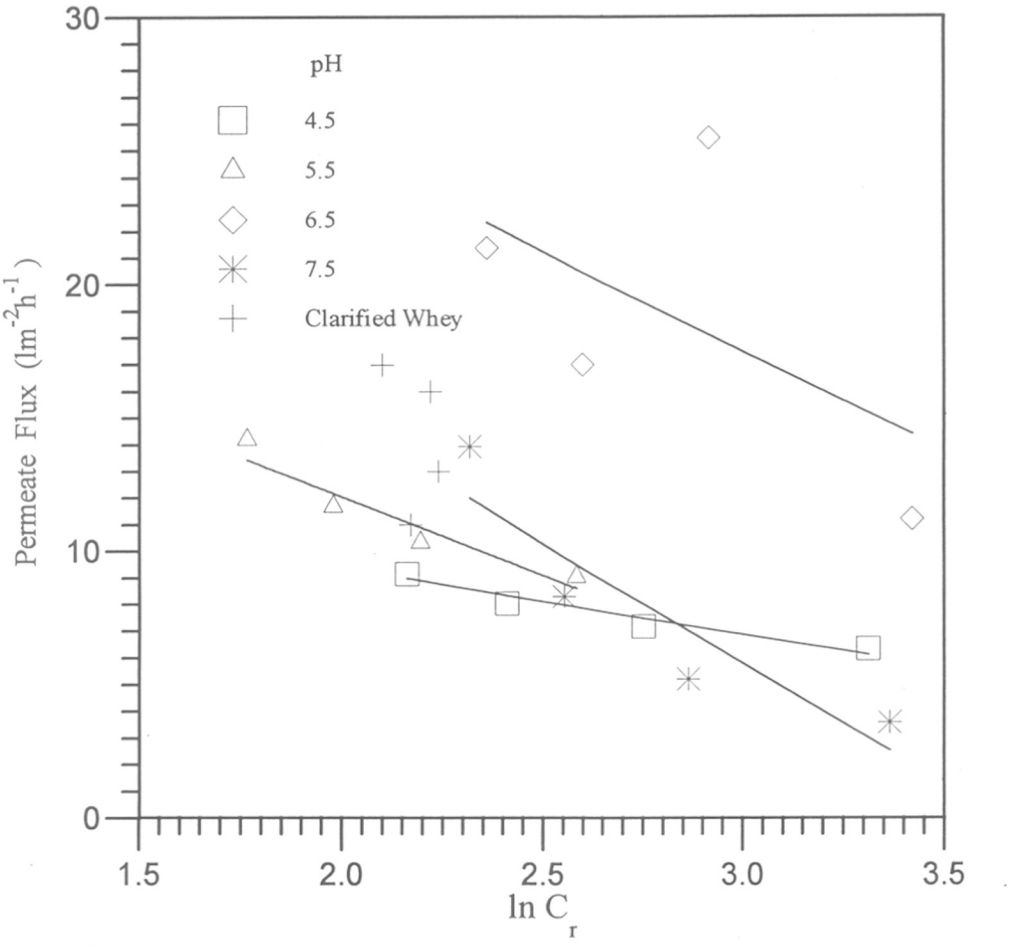

Figure 5.34 Effect of retentate concentration on permeate flux at 600 rpm; 200 kPa for CW with PAN. (—) represent predictions based on eqn (3.11) and parameters in Table 5.11

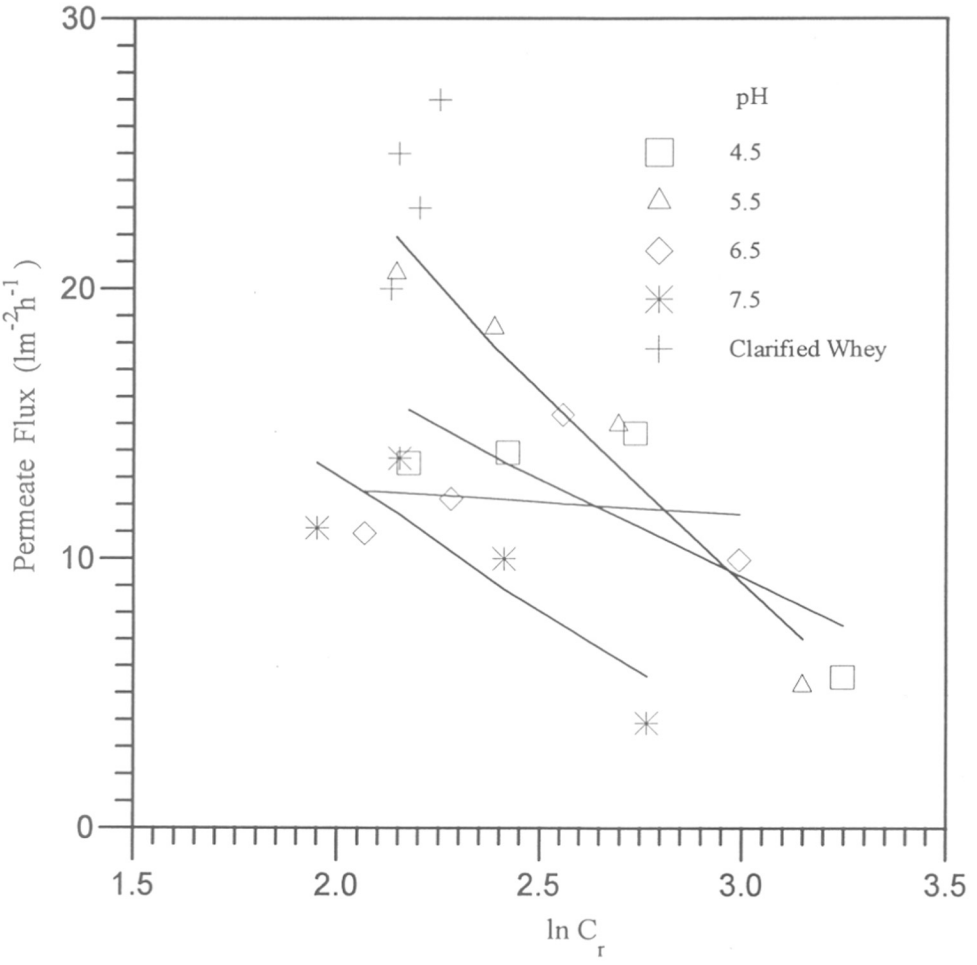

Figure 5.35 Effect of retentate concentration on permeate flux at 600 rpm; 200 kPa for CW with PAN-3. (—) represent predictions based on eqn (3.11) and parameters in Table 5.11

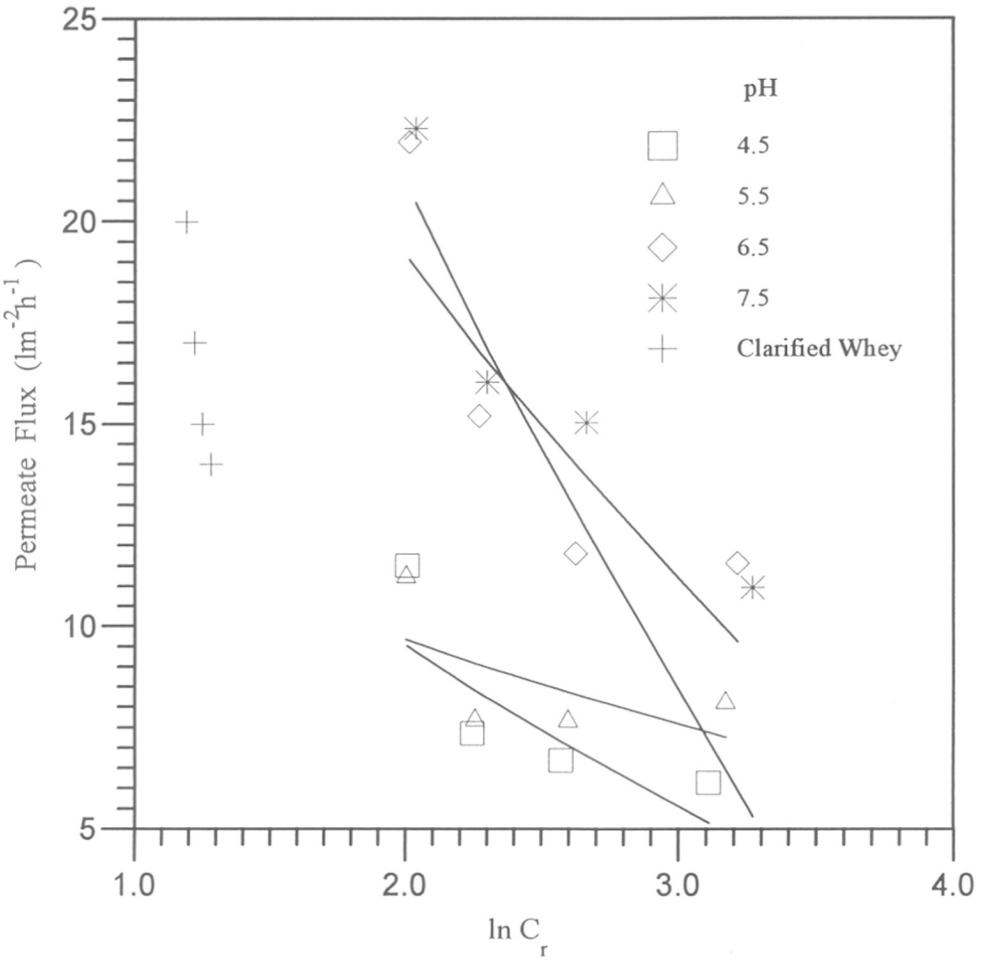

Figure 5.36 Effect of retentate concentration on permeate flux at 600 rpm; 200 kPa for SW with PAN. (—) represent predictions based on eqn (3.11) and parameters in Table 5.11

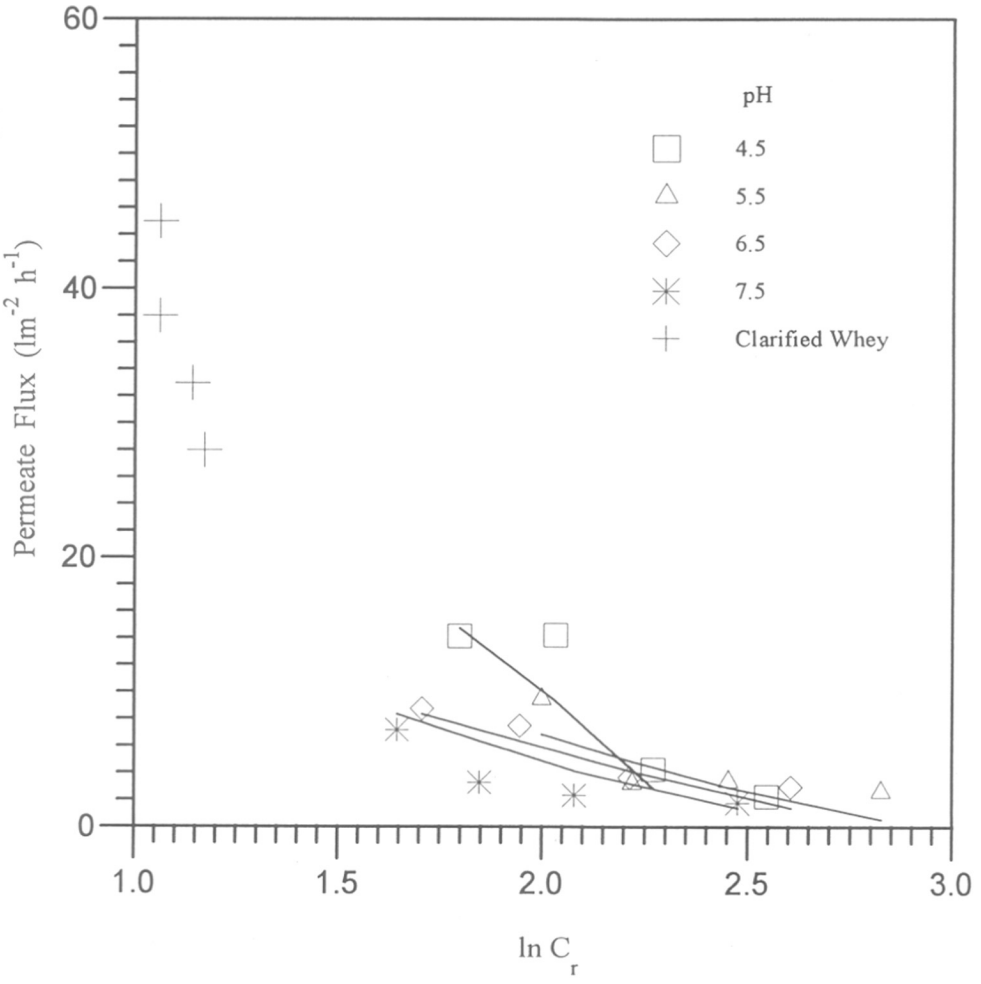

Figure 5.37 Effect of retentate concentration on permeate flux at 600 rpm; 200 kPa for SW with PAN-3. (—) represent predictions based on eqn (3.11) and parameters in Table 5.11

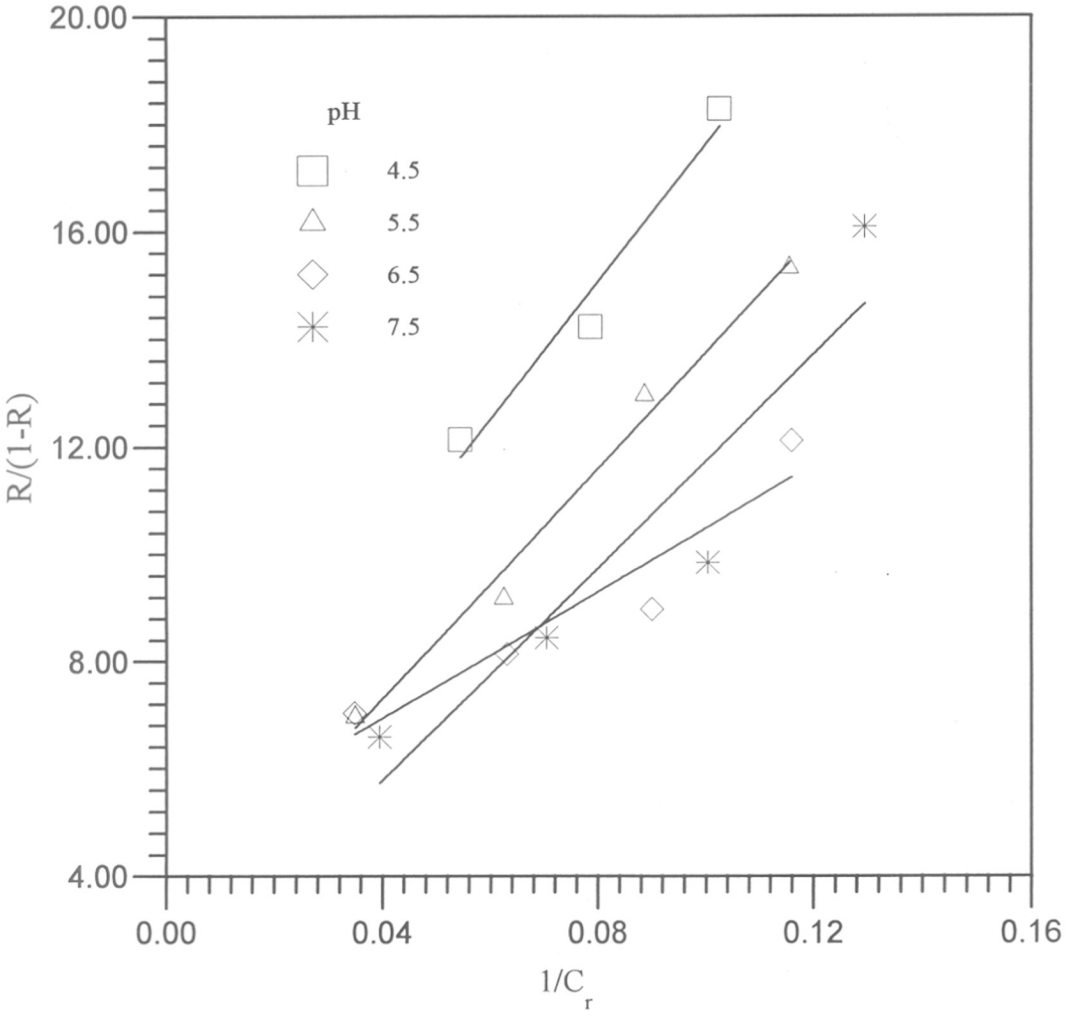

Figure 5.38 Effect of retentate concentration on observed protein rejection (R) at 600 rpm; 200 kPa for AW with PAN. (—) represent best fit based on eqn. (5.1)

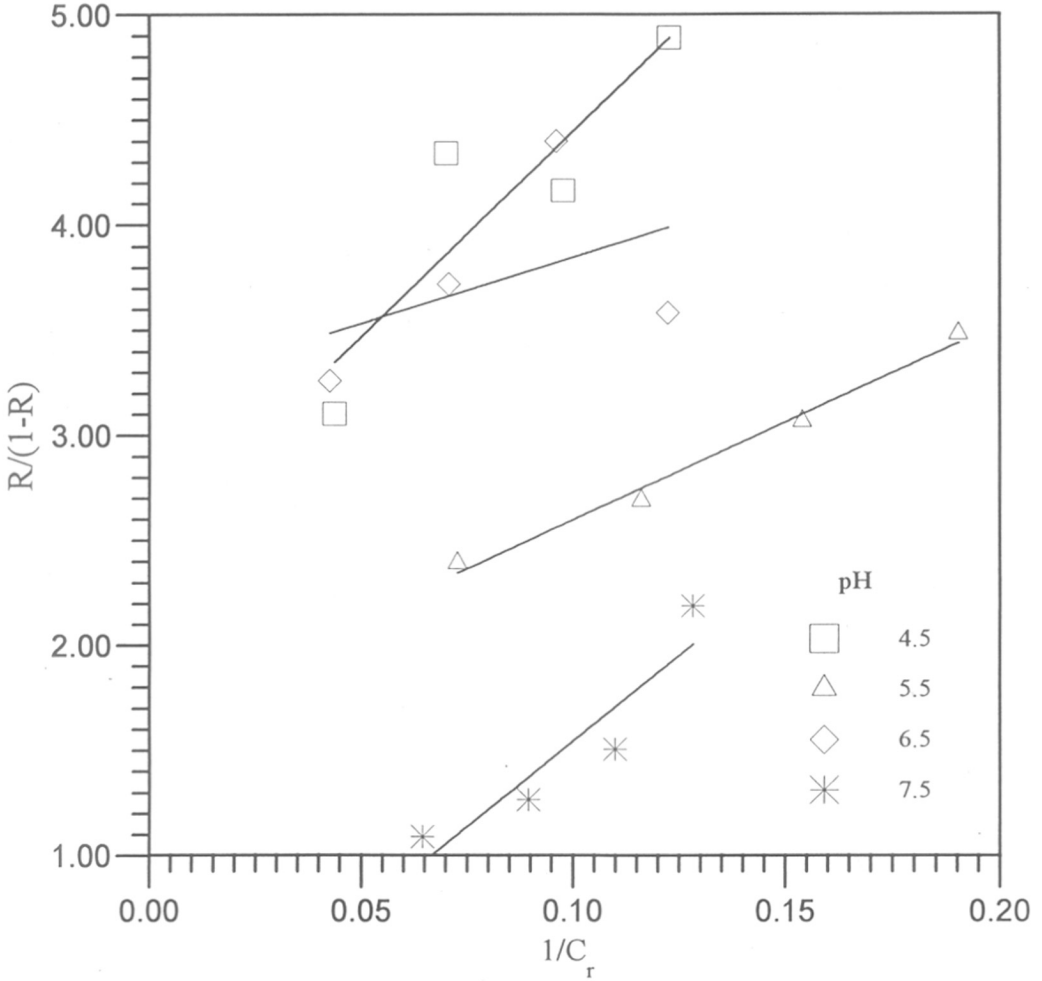

Figure 5.39 Effect of retentate concentration on observed protein rejection (R) at 600 rpm; 200 kPa for AW with PAN-3. (—) represent best fit based on eqn. (5.1)

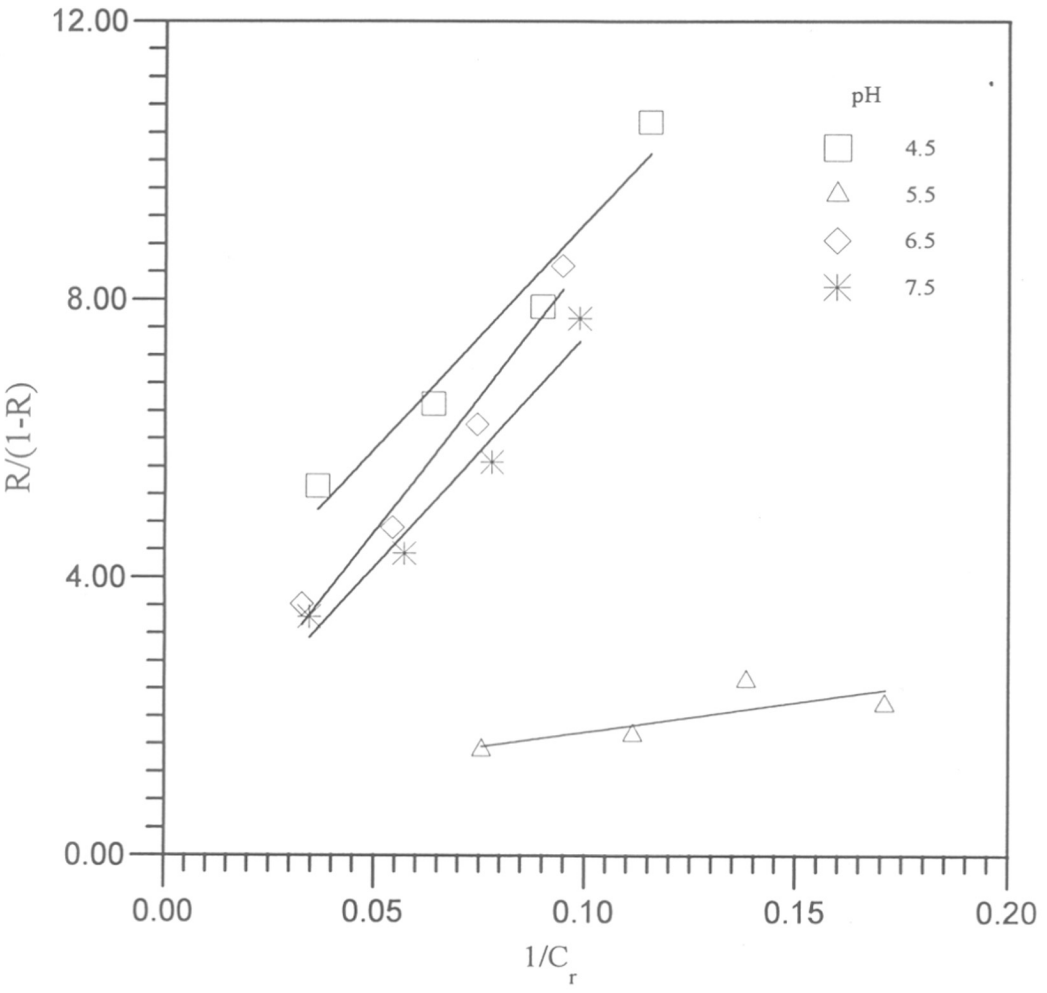

Figure 5.40 Effect of retentate concentration on observed protein rejection (R) at 600 rpm; 200 kPa for CW with PAN. (—) represent best fit based on eqn. (5.1)

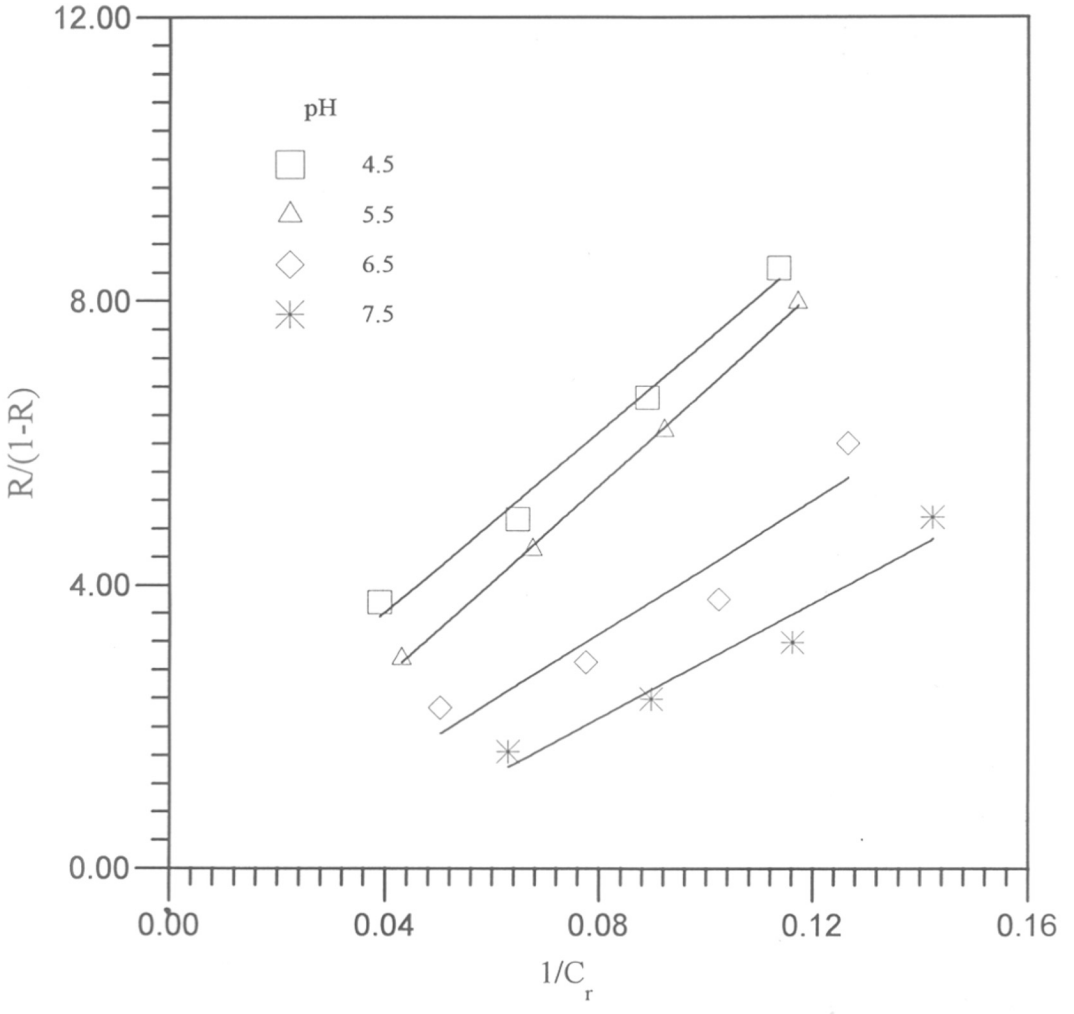

Figure 5.41 Effect of retentate concentration on observed protein rejection (R) at 600 rpm; 200 kPa for CW with PAN-3. (—) represent best fit based on eqn. (5.1)

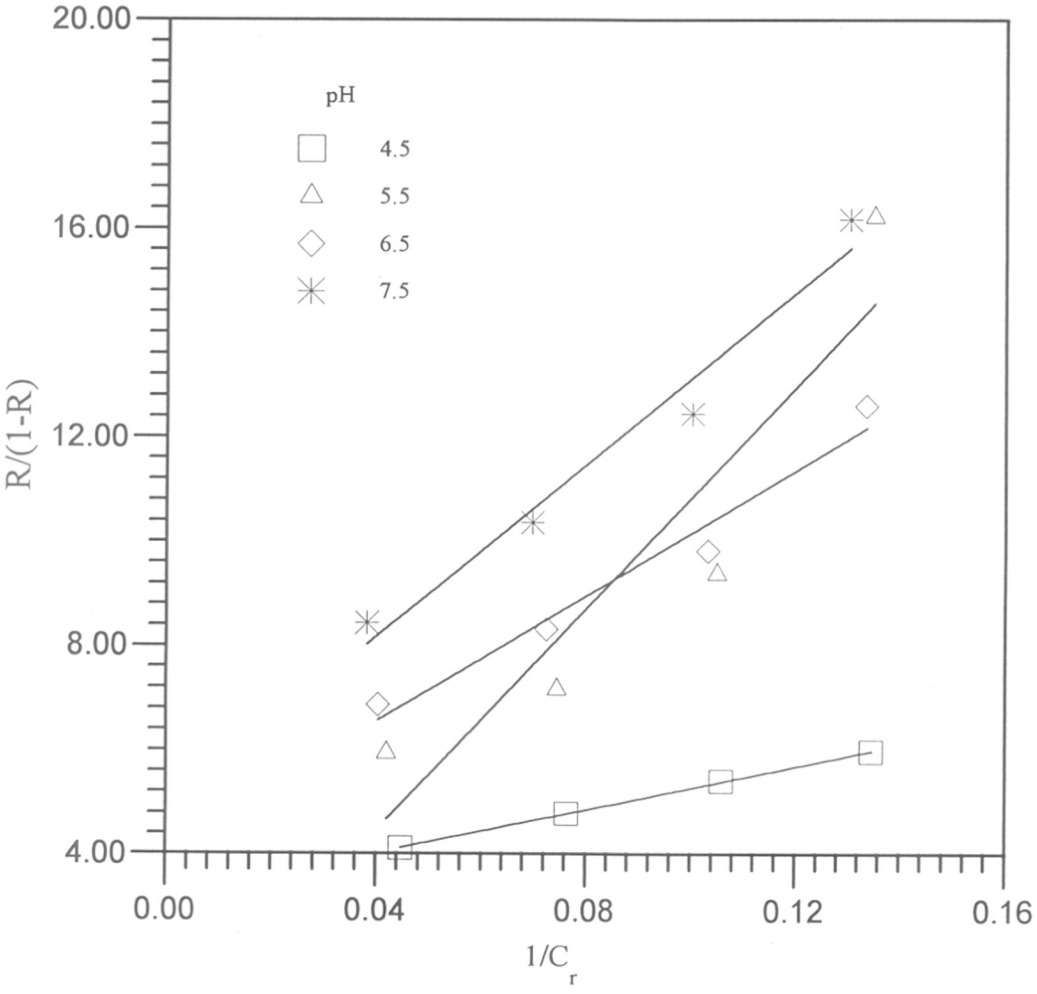

Figure 5.42 Effect of retentate concentration on observed protein rejection (R) at 600 rpm; 200 kPa for SW with PAN. (—) represent best fit based on eqn. (5.1)

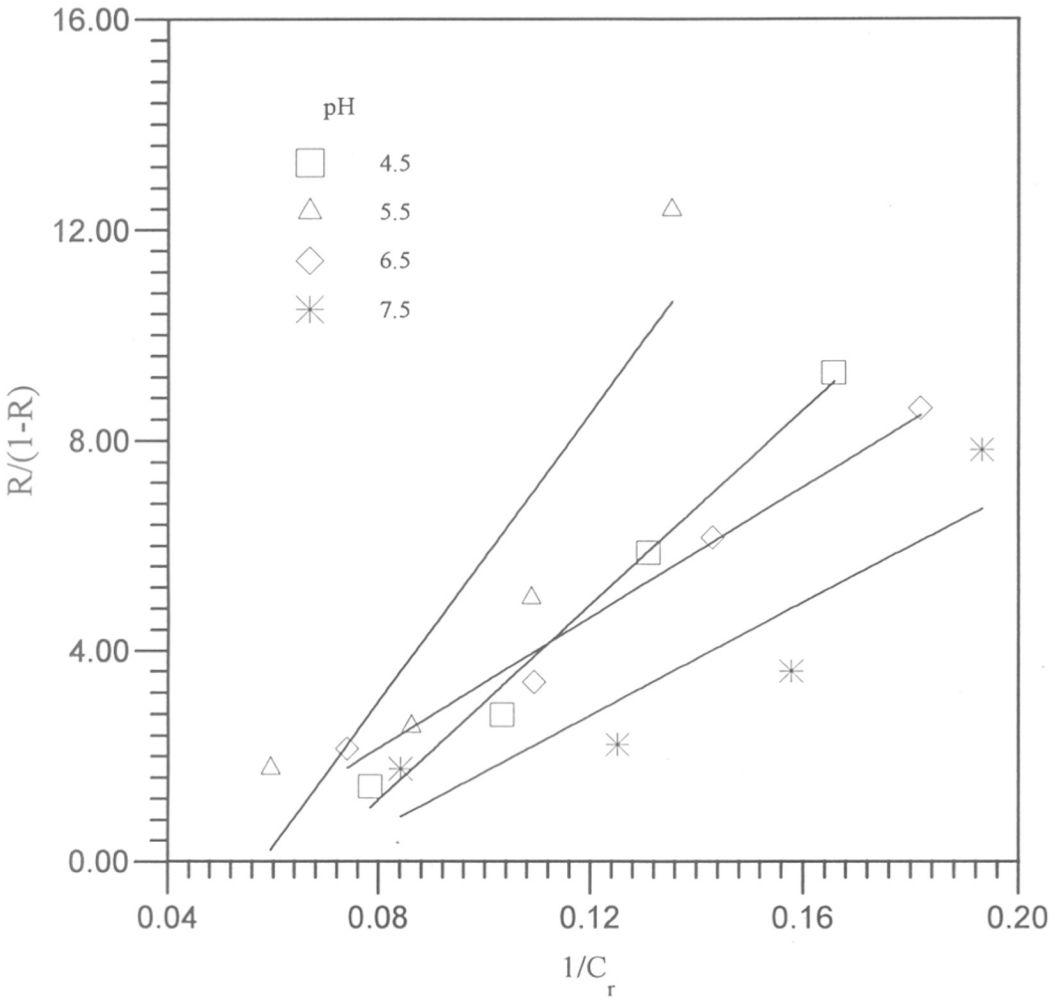

Figure 5.43 Effect of retentate concentration on observed protein rejection (R) at 600 rpm; 200 kPa for SW with PAN-3. (—) represent best fit based on eqn. (5.1)

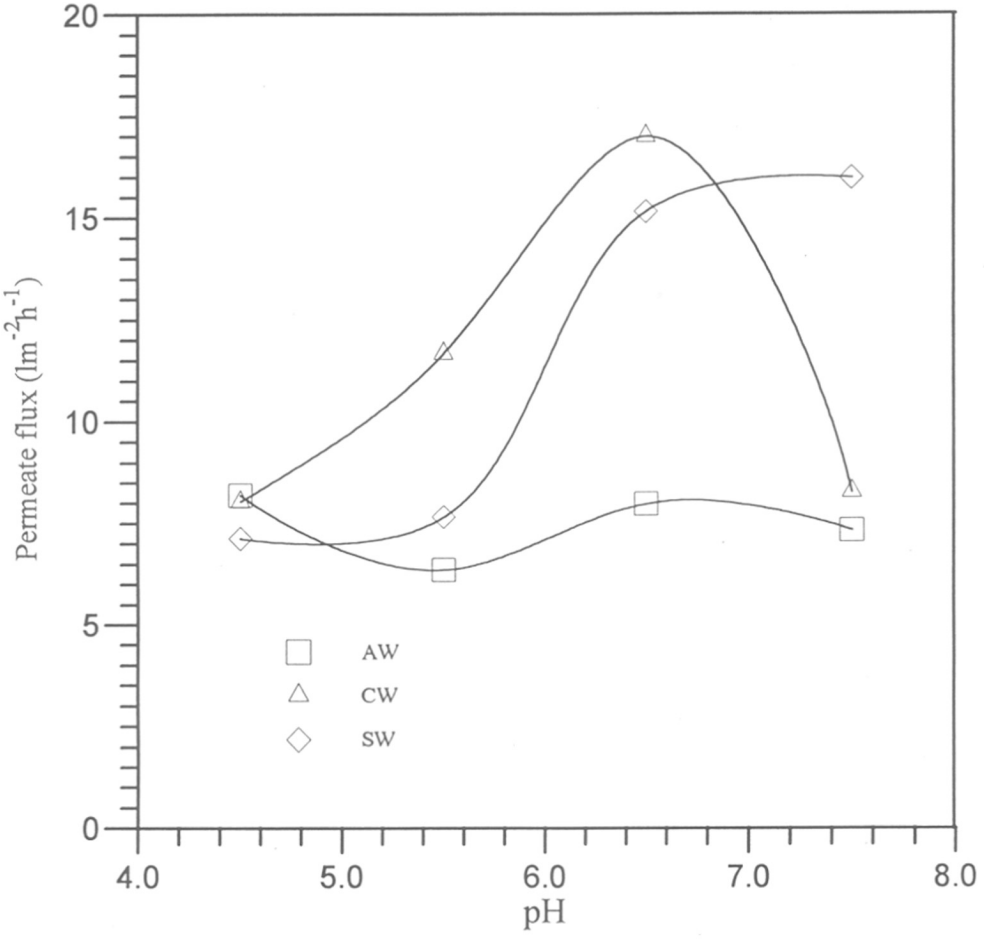

Figure 5.44 Effect of pH on permeate flux of natural wheys at 1.67 VCF, 200 kPa, 600 rpm for PAN

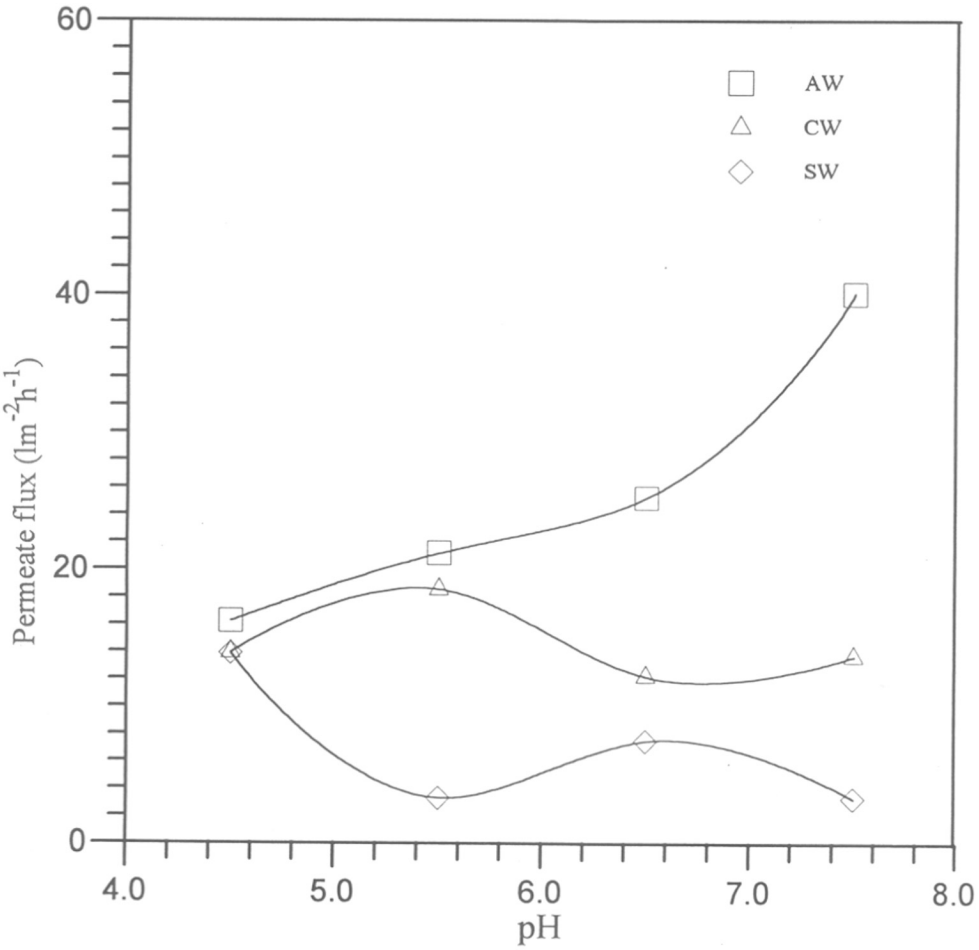

Figure 5.45 Effect of pH on permeate flux of natural wheys at 1.67 VCF, 200 kPa, 600 rpm for PAN-3

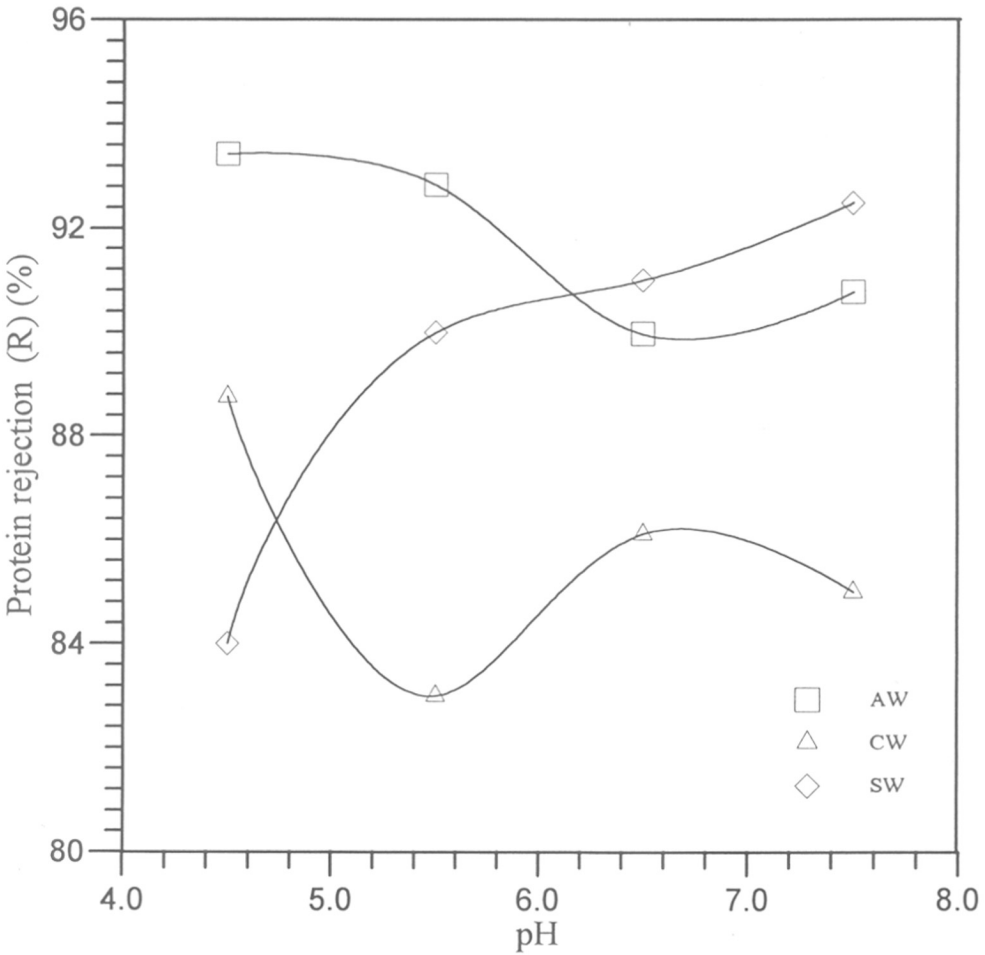

Figure 5.46 Effect of pH on observed protein rejection (R) (%)of natural wheys at 1.67 VCF, 200 kPa, 600 rpm for PAN

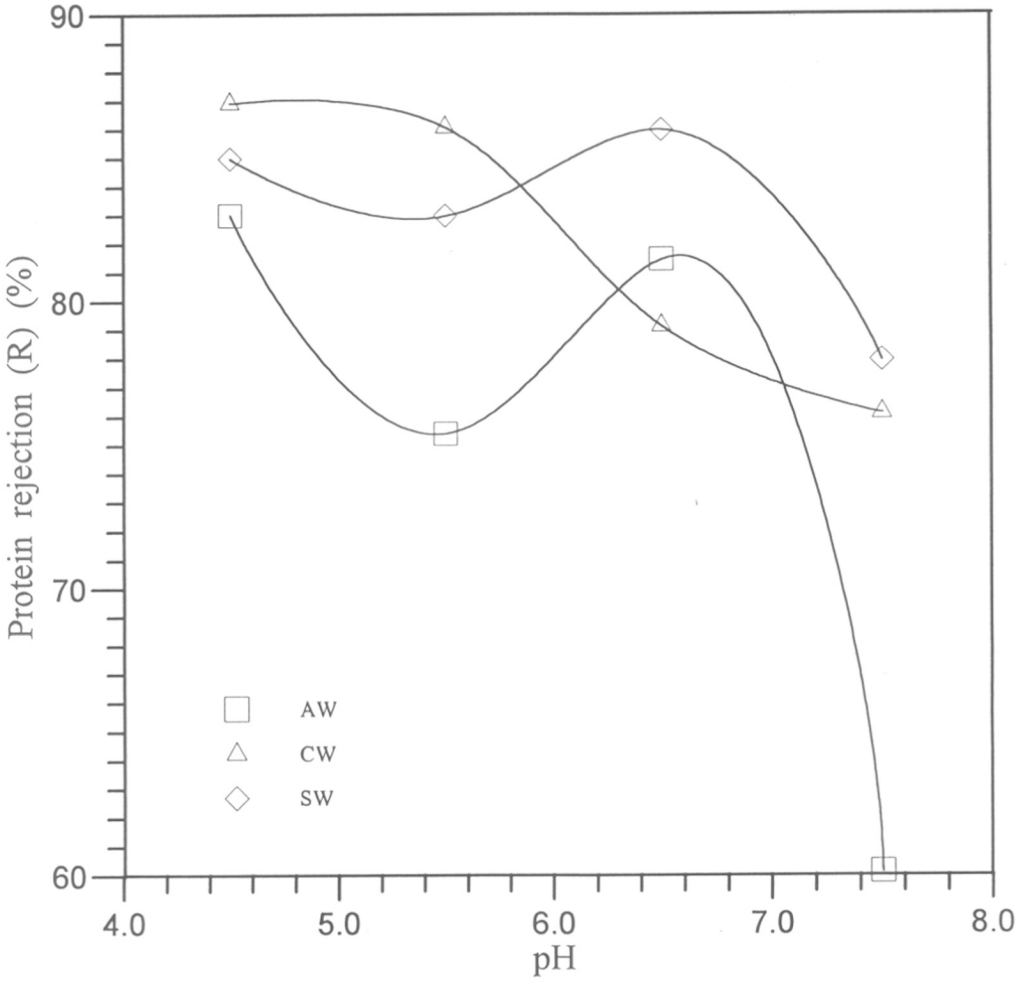

Figure 5.47 Effect of pH on observed protein rejection (R) (%) of natural wheys at 1.67 VCF, 200 kPa, 600 rpm for PAN-3

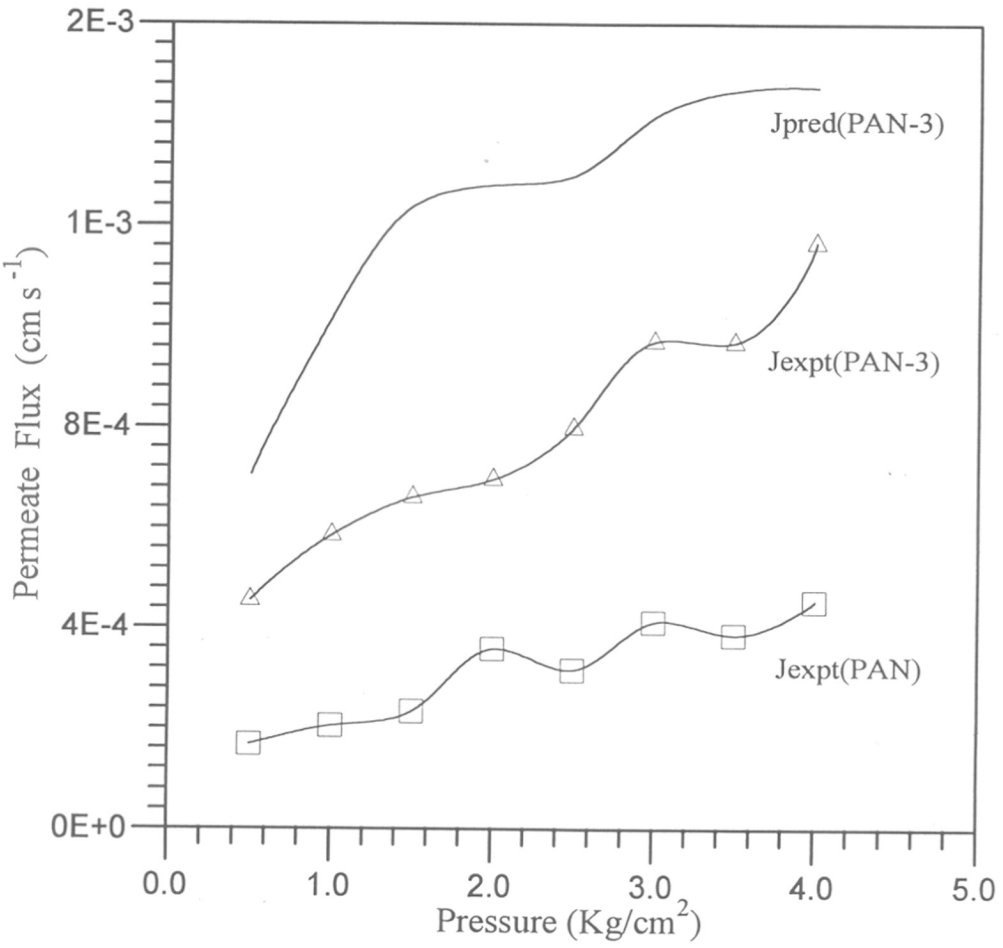

Figure 5.48 Effect of pressure on permeate flux of AW at 1.67 VCF, 200 kPa, 600 rpm for PAN and PAN-3. (—) represents predictions based on eqn (5.3). J(predicted) for Pan is too high to be shown in this plot.

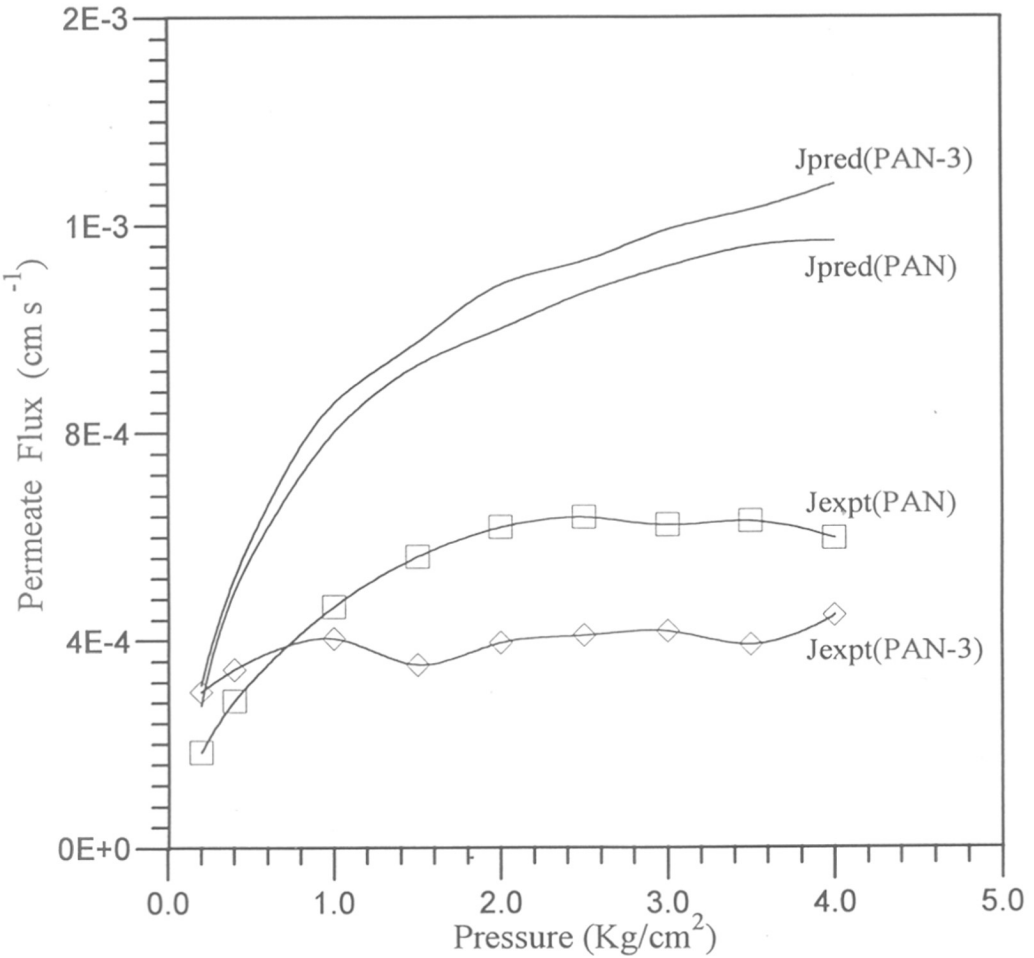

Figure 5.49 Effect of pressure on permeate flux of CW at 1.67 VCF, 200 kPa, 600 rpm for PAN and PAN-3. (--) represents predictions based on eqn (5.3)

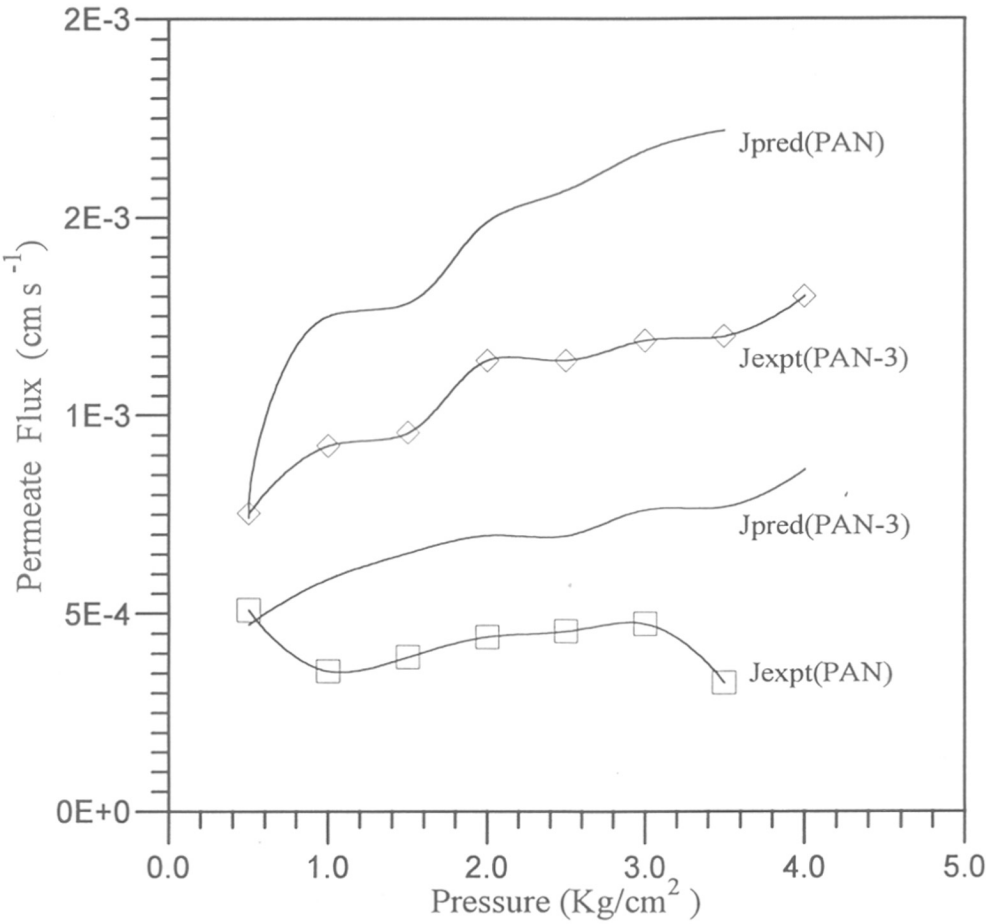

Figure 5.50 Effect of pressure on permeate flux of SW at 1.67 VCF, 200 kPa, 600 rpm for PAN and PAN-3. (--) represents predictions based on eqn (5.3)

The mechanism of flux decline with the wheys was first modelled by estimating the concentration polarization caused by protein rejection. The mass transfer coefficient, k, and the protein concentration at the membrane surface, C_m , were calculated from eqn. (3.11) by non-linear regression (Marquardt's method) as described in section 5.3.1.1. The values of k and C_m calculated by this method are shown in Table 5.11. These values are based on the J_v vs $\ln C_r$ data shown in Figures 5.32-5.37. These figures also show the predicted fluxes based on the k and C_m values in Table 5.11.

Table 5.11

Mass transfer coefficient, k and protein concentration at the membrane surface, Cm for UF of various wheys

pH	Acid whey		Cheese whey		Shrikhand whey	
	$k\times10^4$ (cm s^{-1})	C_m (mg / ml)	$k\times10^4$ (cm s^{-1})	C_m (mg / ml)	$k\times10^4$ (cm s^{-1})	C_m (mg / ml)
PAN						
4.5	1.17	107	1.0	93.0	0.64	374
5.5	0.63	234	0.53	1095	1.19	85.0
6.5	0.54	932	2.02	93.6	1.91	225
7.5	*	*	3.17	42.4	2.24	38.4
PAN-3						
4.5	+	+	4.60	13.9	1.91	72.0
5.5	2.23	66.1	1.67	21.7	3.88	35.3
6.5	4.47	56.3	1.72	19.3	+	+
7.5	1.23	21	1.30	14.7	2.50	26.2

* Data could not be fitted with satisfactory mean square errors; hence the calculated parameters are not reliable.

+ Data fit was satisfactory; however, value of k for best fit was negative. This is attributed to experimental error.

The value of k and C_m can be used to predict the pressure dependence of the permeate flux by the following equation which is based on eqn.s (3.13), (3.24) and (3.26) :

$$J_v = \left\{\Delta P - \sigma\left[RT\left((C_r^n \exp(J_v^n / k)) - C_p^n\right)\right]\right\} \Big/ \eta R_m \qquad (5.4)$$

The value of ηR_m was calculated from water permeability measurements at 200 kPa ($\eta Rm = \Delta P / J_w$). The value of n (index in eqn. 3.24) was assumed to be 1. The values of C_p and C_r at each ΔP and VCF of 1.67 were experimentally measured. The reflection coefficients (σ) were estimated from the C_p and C_m data ($\sigma \approx 1 - C_p / C_m$). The ability of the concentration polarization model to adequately model the flux behaviour observed with each whey / membrane combination can be assessed by comparing the predicted flux dependence on pressure with the experimental data.

The experimentally measured permeate fluxes (J_v) for all three natural wheys at pH 7.5 generally increase with pressure and then show limiting flux behaviour (Figures 5.48 - 5.50). The predicted pressure dependence of J_v using the concentration polarization model (eqn. 5.3) is also shown in Figures 5.48-5.50. The results show that the osmotic pressure-concentration polarization model does not adequately describe the flux vs ΔP data. With one exception (SW in PAN-3), the predicted fluxes are much higher than the experimental fluxes. There could be several reasons for the failure of the concentration polarization model. The simple van't Hoff dependence of osmotic pressure on concentration (eqn. 3.24 with n =1) may not be valid for these non-ideal feed solutions. Alternatively, there may be other flux decline mechanisms which are not addressed by concentration polarization models such as internal fouling by salts (pore blocking by salt precipitation).

While PAN-3 had consistently higher fluxes than PAN during standard protein UF, whey data do not show this difference clearly (compare Figures 5.13, 5.20, 5.22 and 5.44, 5.45). The standard protein measurements were done at lower protein concentrations (0.1-0.2 g /dl) than those present in the wheys (0.6-0.8 g/dl). The higher protein content may overwhelm the increase in fouling resistance seen due to the modification in PAN-3 surface characteristics. While PAN-3 has higher fluxes for AW and CW, the SW flux is

surprisingly low. AW has the lowest flux in the PAN membrane but the highest flux in PAN-3. These differences may be attributable to experimental error.

Literature suggests that fluxes can be increased by raising the pH of whey and filtering the precipitated $CaPO_4$ (Lee and Merson, 1976). This feed pretreatment was investigated from a dual viewpoint of examining this strategy for flux increase as well as identifying the factors controlling the UF flux. The wheys obtained by adjusting the pH to 7.5 and filtering are referred to as clarified wheys. The composition of the clarified wheys are also shown in Table 5.9. There is a reduction in the total solids arising from reduced ash and protein concentrations in the clarified whey. The reduction in ash is particularly marked for AW and SW. Clarified SW also shows a marked reduction in protein content. The intrinsic viscosity is slightly increased in all three wheys after clarification; this may be attributed to the salt removal. The shielding effect of salts would cause contraction of protein molecules in the case of the natural wheys. The apparently increased lactose content in clarified wheys is an artifact due to the Ca sensitivity of the DNSA test (Robyt and Whelan, 1972).

The flux and rejections obtained with each clarified whey with PAN and PAN-3 membranes are shown in Figures 5.51 - 5.54. The data were obtained at 200 kPa and a VCF of 1.67.

Our results indicate that the increase in flux with clarified wheys may be attributable not only to $CaPO_4$ removal as previously thought but also to the reduction in protein levels. Figure 5.55 shows that the clarification procedure reduces the protein content by ~ 11-15% in the case of AW and CW and by as much as ~ 50% in the case of SW. The reason for the large decrease in protein concentration for clarified SW is not known, but may be related to interactions of lactic acid with proteins. Hence, even at the same VCF of 1.67, the retentate protein concentrations are less for the clarified wheys. When the clarified whey flux values are plotted on the same J_v vs ln C_r plots for natural whey (5.32-5.37), it is seen that both sets of data are consistent. The only exception is that of the clarified AW flux through the PAN membrane; this data may be in error. Hence the protein reduction may be equally important as $CaPO_4$ reduction in determining the flux of the clarified wheys vis-a-vis the natural wheys.

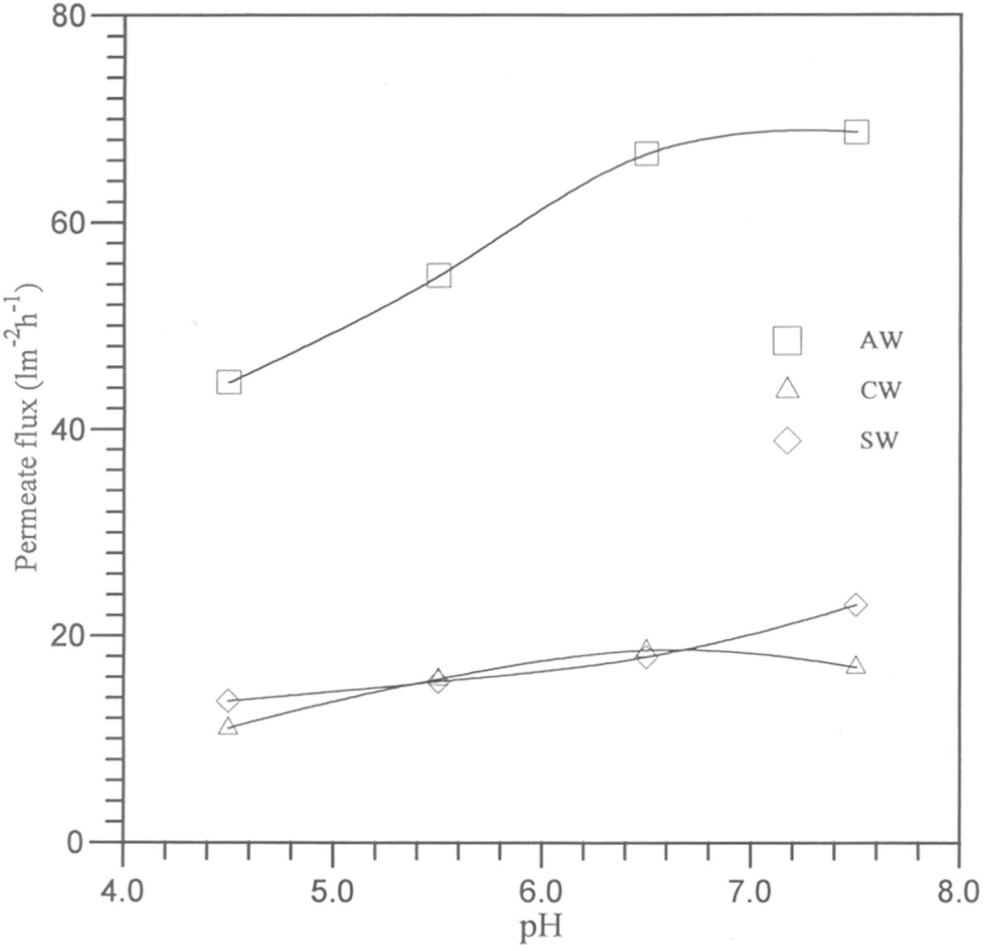

Figure 5.51 Effect of pH on permeate flux of clarified wheys at 1.67 VCF, 200 kPa, 600 rpm for PAN

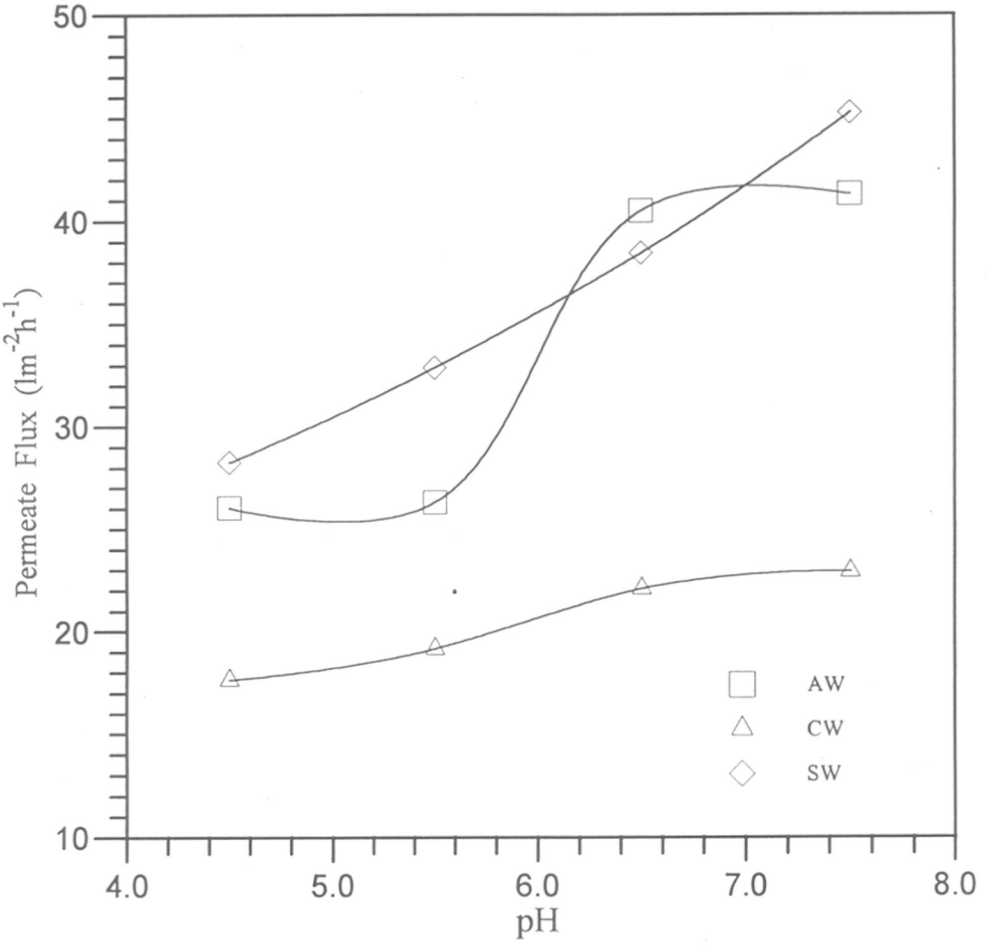

Figure 5.52 Effect of pH on permeate flux of clarified wheys at 1.67 VCF, 200 kPa, 600 rpm for PAN-3

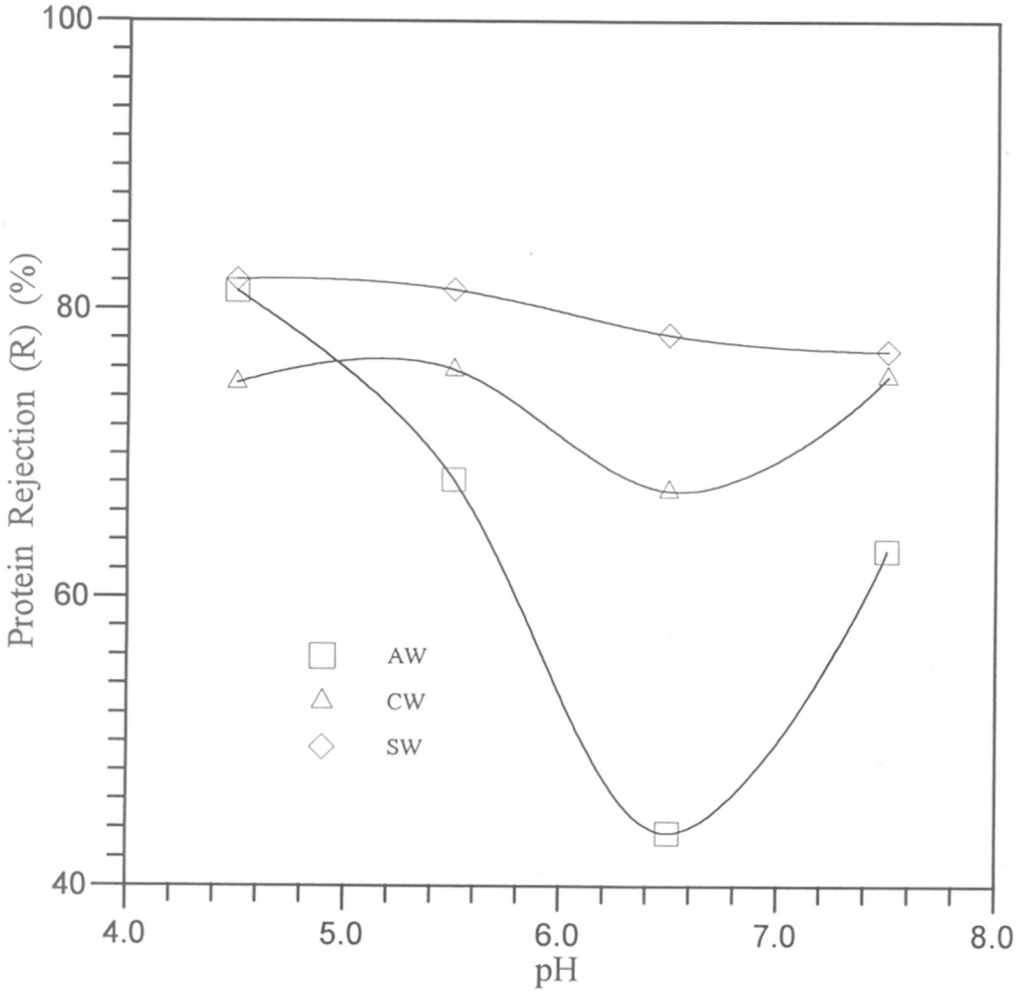

Figure 5.53 Effect of pH on protein rejection (R) (%) of clarified wheys at 1.67 VCF, 200 kPa, 600 rpm for PAN

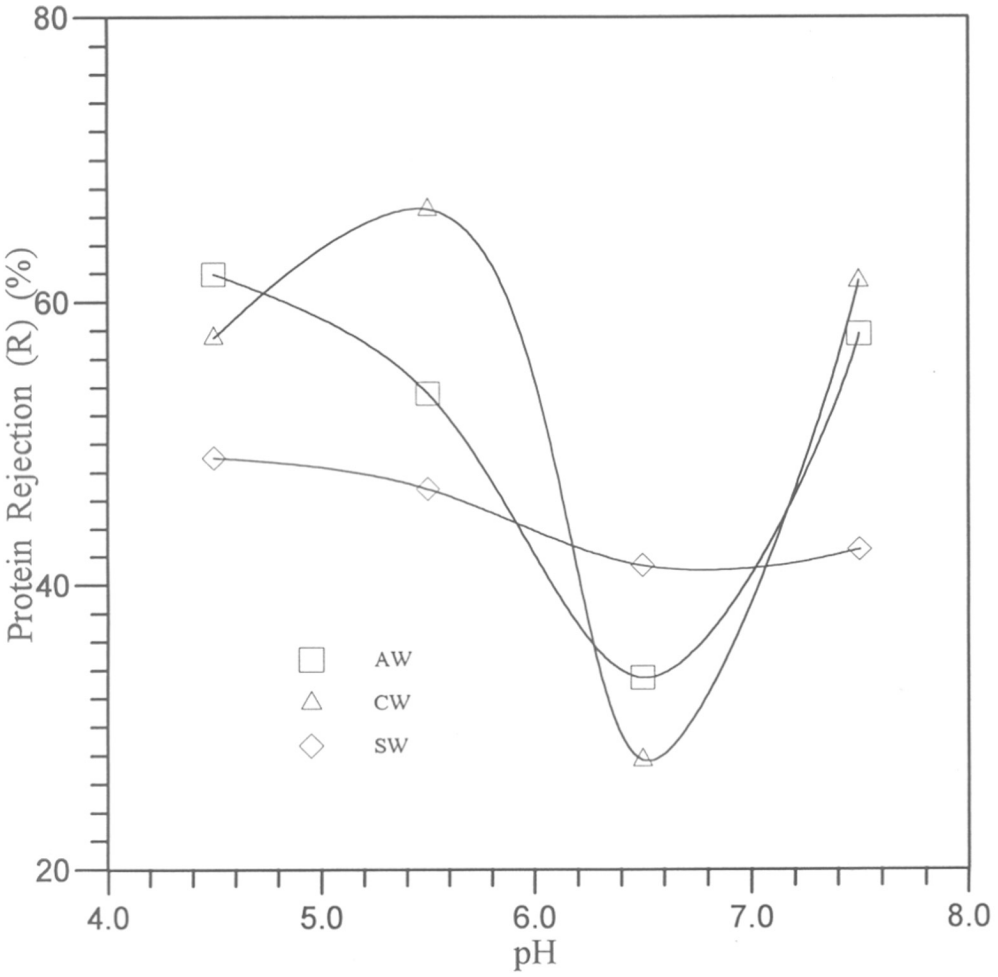

Figure 5.54 Effect of pH on protein rejection (R) (%) of clarified wheys at 1.67 VCF, 200 kPa, 600 rpm for PAN-3

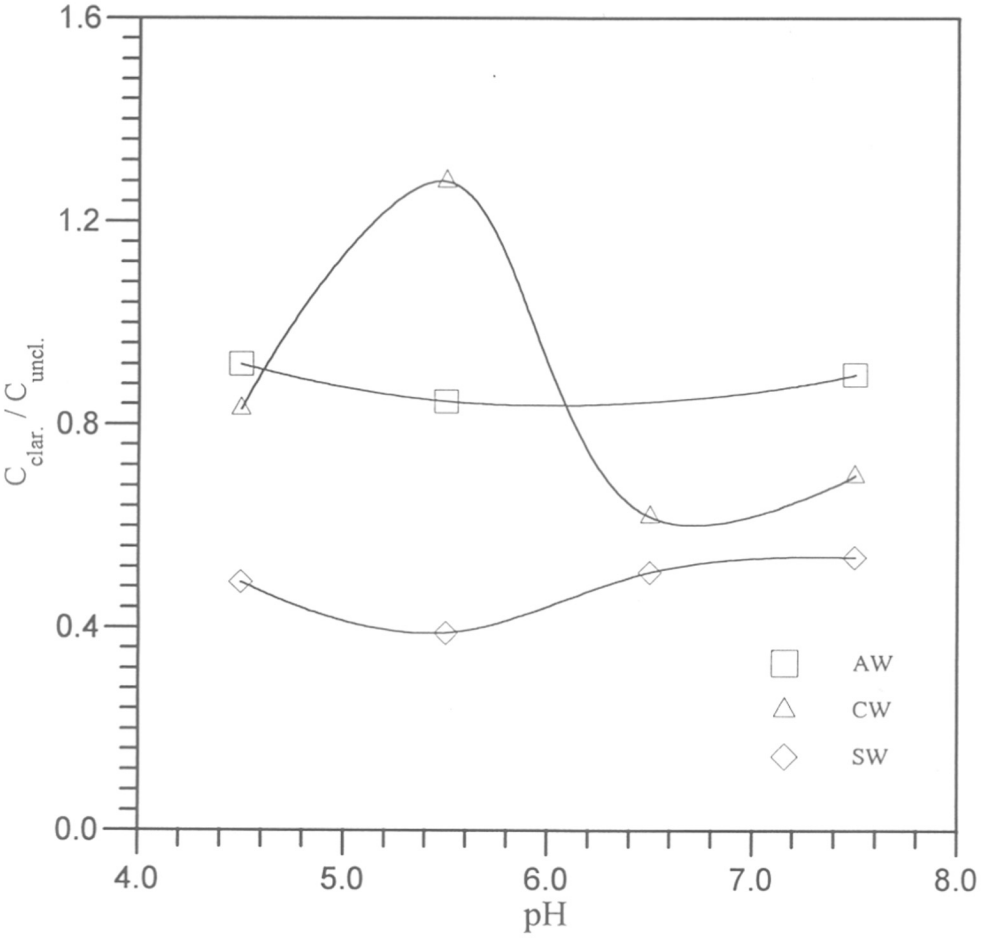

Figure 5.55 Ratio of protein concentrations in clarified : natural wheys used as feed for UF at various pH values

The dependence of flux on pH in the case of natural and clarified wheys also shows some interesting results. Based on the UF data with standard proteins (BSA or Hb), one would expect the whey flux to also increase with increasing feed pH. This is seen to happen consistently only in the case of clarified wheys (Figures 5.51, 5.52). The results with natural wheys show that flux does not necessarily respond to changes in feed pH (Figures 5.44, 5.45) In other words, the clarified whey behaves similarly to the single protein solutions (BSA or Hb) while the natural whey data resemble mixed protein data (BSA-Hb). This may be due to attractive interactions of Ig with other whey proteins at pH values between 5-7. After clarification, which would be expected to precipitate immunoglobulins (IEP = 7) preferentially, the remaining proteins have similar IEPs (pH ~ 5). With increasing pH above pH 5, the repulsive interactions between the remaining proteins (all negatively charged) will be dominant.

Protein Rejection :

The observed rejections (R) for the 3 natural wheys are shown in Figures 5.38-5.43. The dependence of the observed rejection on the retentate concetration is shown by the solid lines which are based on eqn (5.1). These data show the expected trend of increasing R with increasing C_r as predicted by eqn (5.1).

The observed rejections at a constant VCF of 1.67 for the natural and clarified wheys are shown as a function of pH in Figures 5.46, 5.47 and 5.53, 5.54 respectively, while the rejections through the membrane, R' (= 1 - C_p / C_m) are shown for UF of natural wheys in Figures 5.56-5.57. The rejection data at 1.67 VCF as a function of pressure are shown in Figures 5.58-5.59.

Inspite of the smaller sizes of α-lactalbumin / β-lactoglobulin, the R' values in the whey case are similar to those observed with BSA. This may be related to the presence of immunoglobulins which may increase the rejection of these smaller proteins. A large increase in the rejection of a smaller protein (BSA) after addition of a larger protein (γ-globulin) in the feed solution have been observed by Blatt et al (1970) and Higuchi et al (1991).

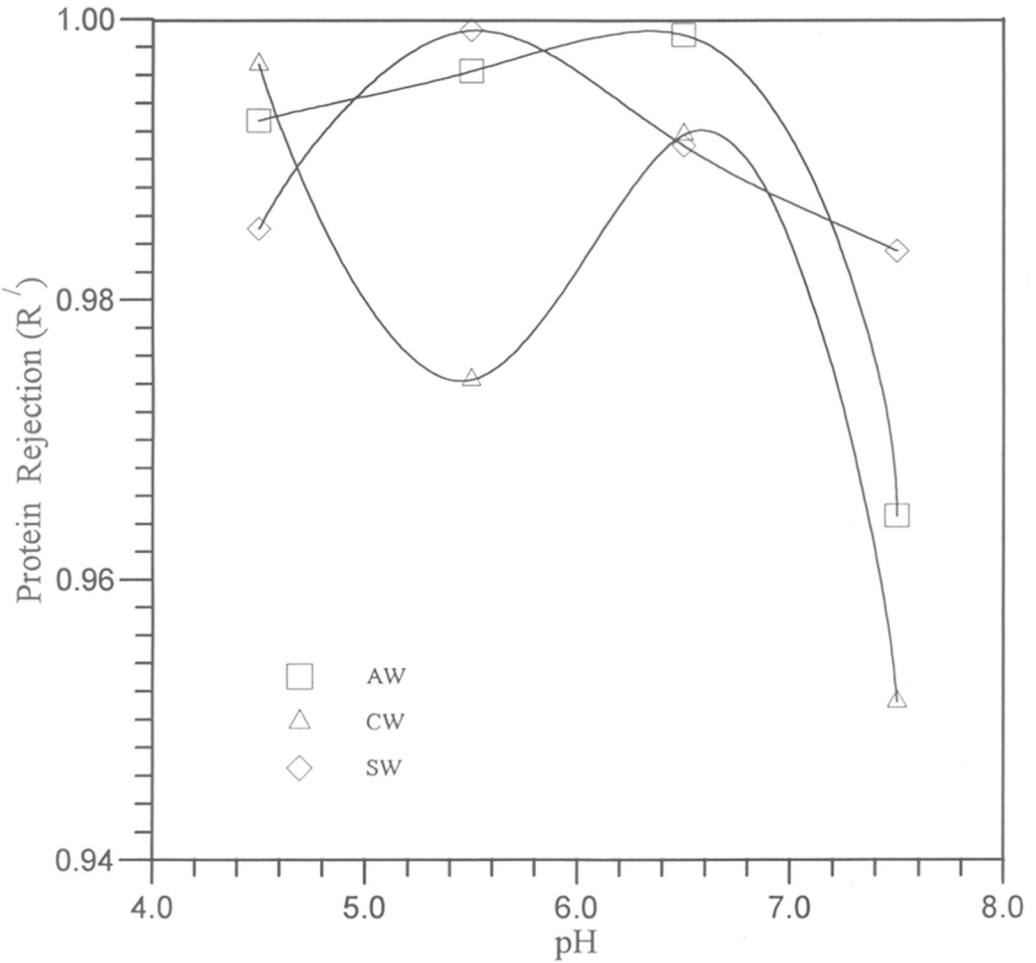

Figure 5.56 Effect of pH on membrane protein rejection (R')of natural wheys at 1.67 VCF, 200 kPa, 600 rpm for PAN

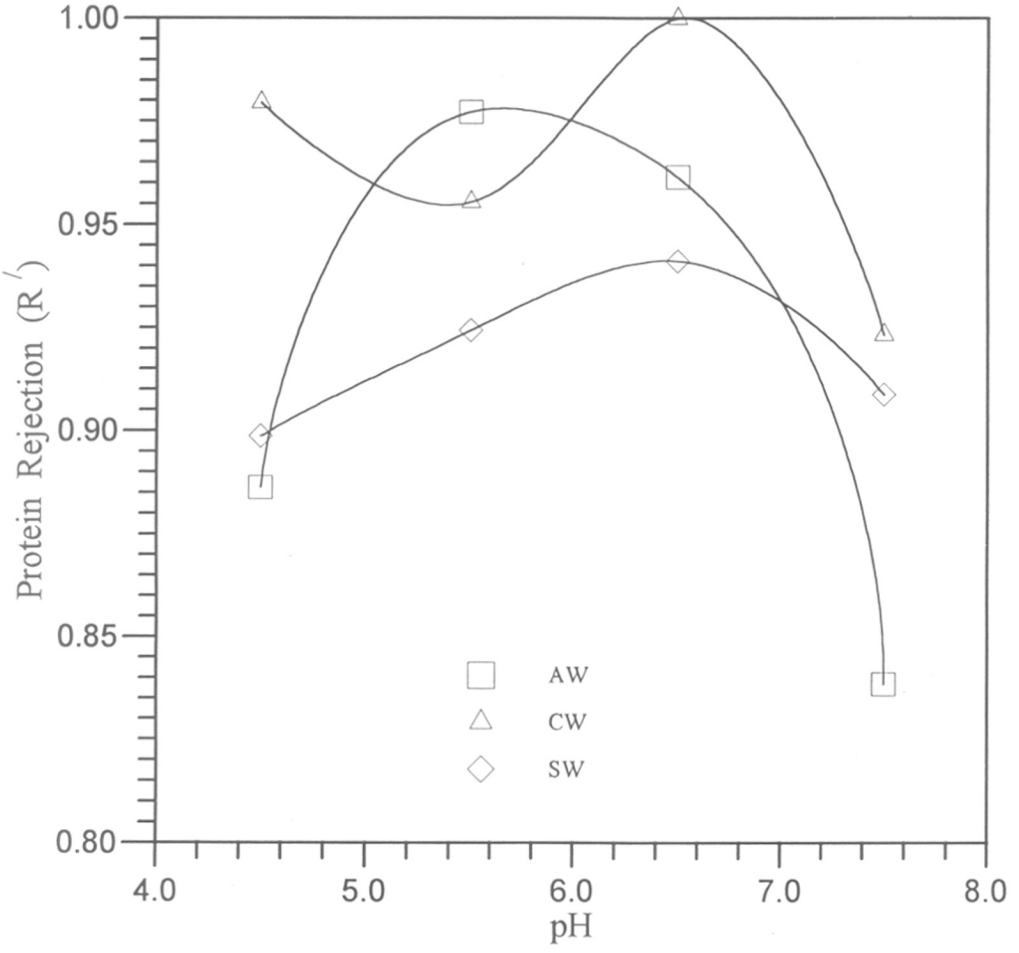

Figure 5.57 Effect of pH on membrane protein rejection (R')of natural wheys at 1.67 VCF, 200 kPa, 600 rpm for PAN-3

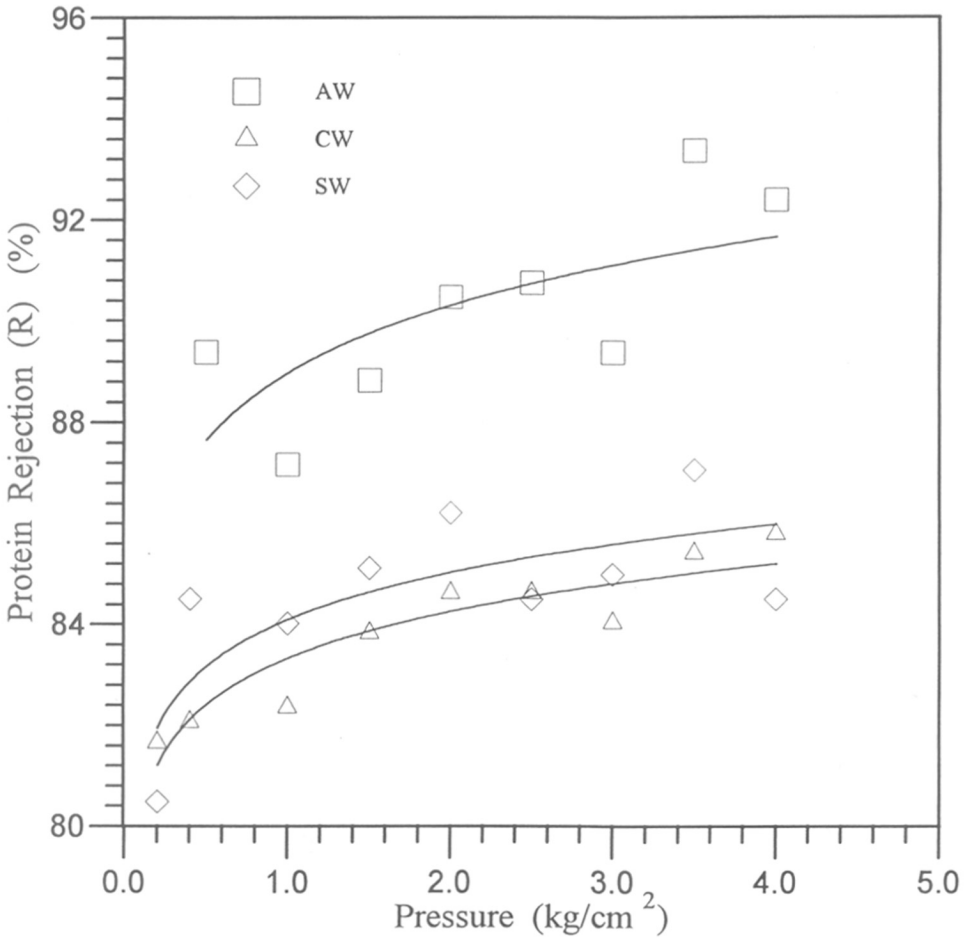

Figure 5.58 Effect of pressure on observed protein rejection (R) (%) for UF of natural wheys at 200 kPa, 600 rpm for PAN

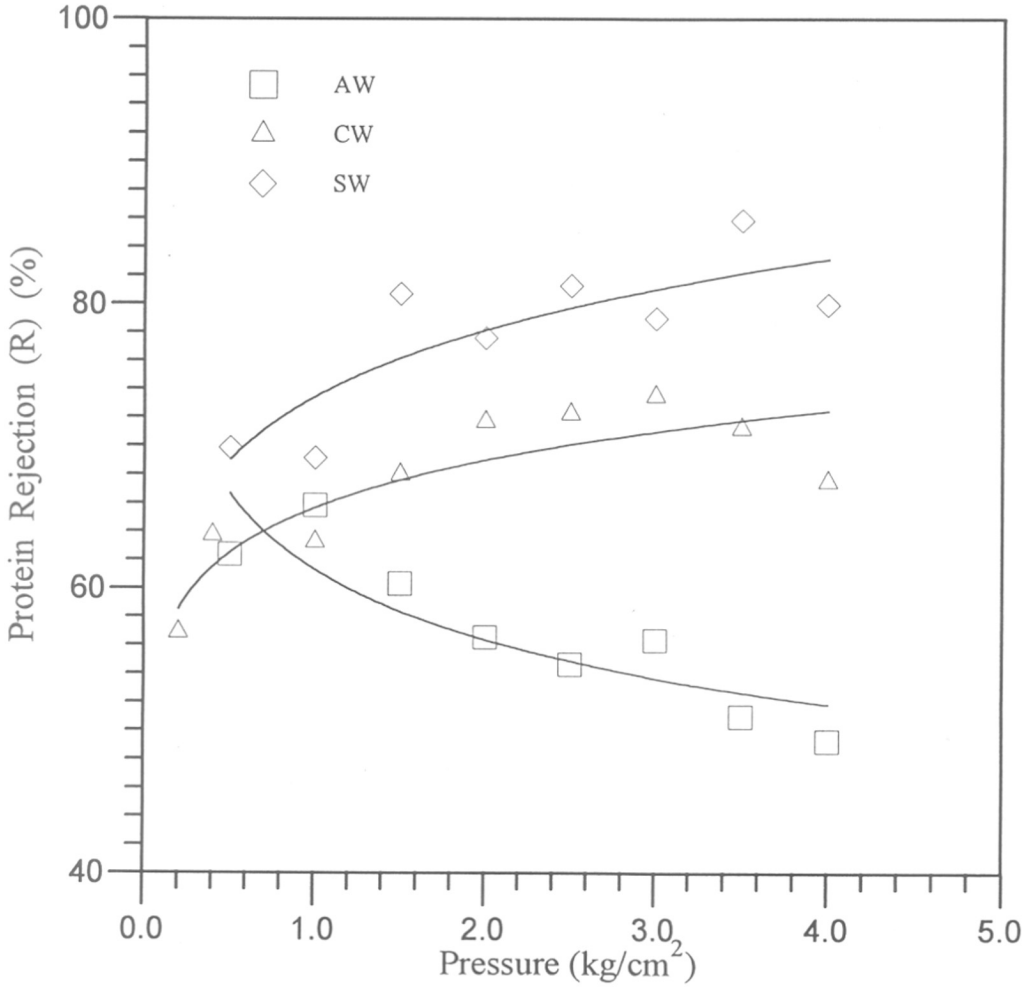

Figure 5.59 Effect of pH on observed protein rejection (R) (%) for UF of natural wheys at 200 kPa, 600 rpm for PAN-3

In case of PAN-3, the overall protein transmissions are more than that in PAN due mainly to its hydrophilicity, lower negative charge and lower dispersive surface energy. Increased transmission in the hydrophilic PAN-3 membrane compared to the hydrophobic PAN membrane is consistent with BSA and Hb UF data described in section 5.3.1.1 and 5.3.1.2 and can be explained similarly.

Figure 5.46 and 5.47 show that the observed protein rejection (R) for UF of natural wheys in the membranes do not show a clear trend with varying pH. This may be attributed to constant protein adsorption due to protein-membrane hydrophobic interactions. The relatively constant R values are consistent with the flux being insensitive to pH (i.e. the concentration polarization effect remains same) and the uniformly high R' values shown in Figure 5.56, 5.57. SW shows the highest rejection while CW shows the lowest rejection.

In the case of the clarified wheys, observed rejections (R) (Figures 5.53-5.54) do decrease with increasing pH upto pH 6.5. This is consistent with concentration polarization effects due to increasing flux with increasing pH for clarified wheys. The rejection (R) again increases at pH 7.5; the reason for this is not known.

The rejections with the clarified wheys are less than those with the natural wheys. This effect would be consistent with both salt reduction as well as with Ig removal during clarification. Clarified AW shows more transmission than clarified CW and SW, which indicates that the higher protein rejection for AW in case of natural whey UF is due to fouling of the membrane by $CaPO_4$.

Lactose and salt rejections were typically less than 20-30%. No trends can be seen in this data beyond that attributed to experimental error.

Flux recovery :

The flux recovery increases with pH for all three types of natural wheys for both PAN (Figure 5.60) and PAN-3 (Figure 5.61) membranes, similar to the data obtained with BSA UF (section 5.3.1.1). With the PAN membrane (Figure 5.60), all three wheys show similar flux recoveries, while with the PAN-3 membrane (Figure 5.61), AW shows higher flux recovery than the other two wheys. The flux recovery increases with pH due to

decreased electrostatic attraction between the major whey proteins and the membranes upto pH 5 and increase in electrostatic repulsion above pH 5. Because of its hydrophilic nature, PAN-3 has slightly higher flux recoveries than PAN, as seen previously for BSA UF (section 5.3.1.1). As was also the case for comparison of fluxes, this advantage in the case of PAN-3 was not consistent.

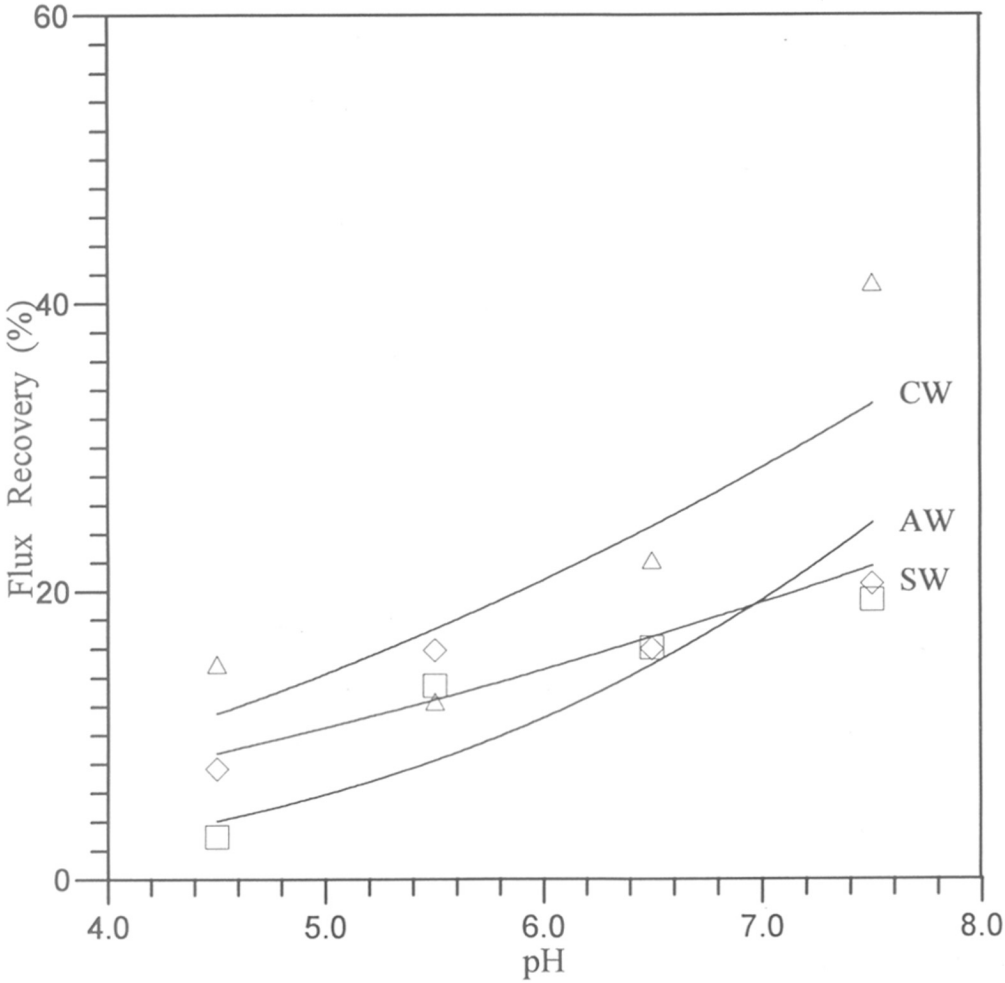

Figure 5.60 Effect of pH on flux recovery for UF of natural wheys at 200 kPa, 600 rpm for PAN

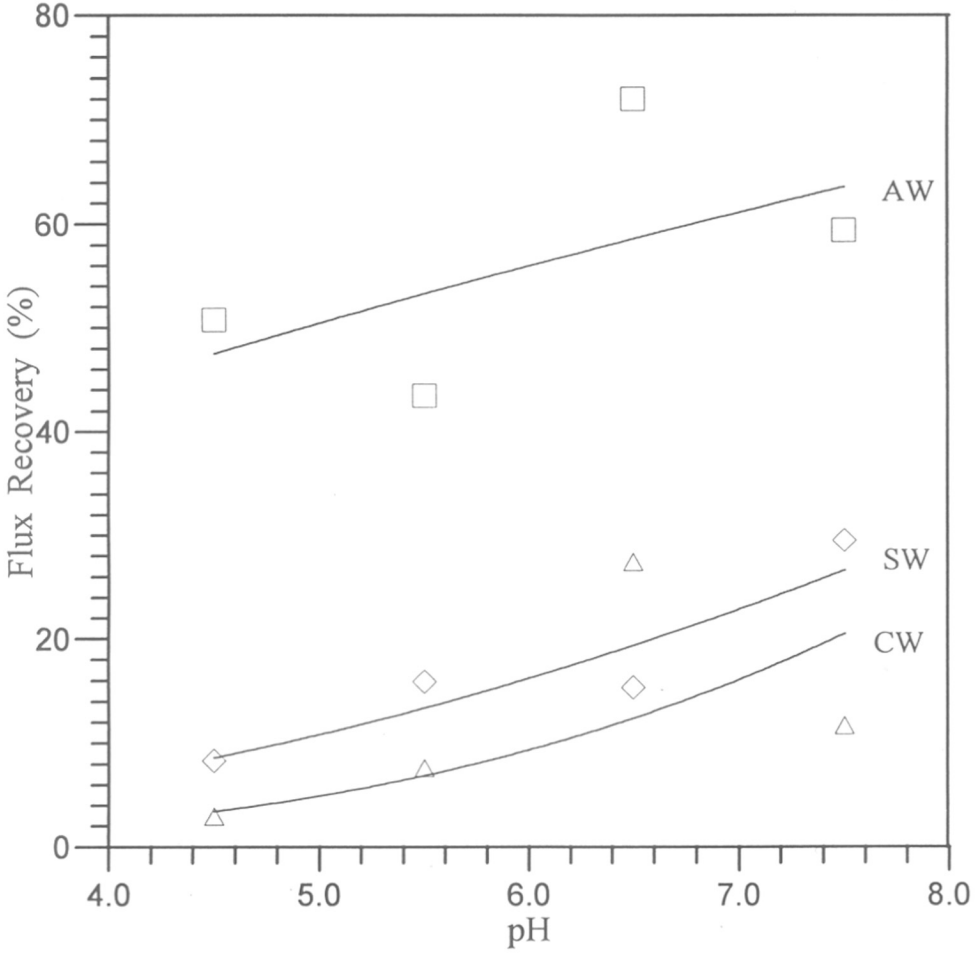

Figure 5.61 Effect of pH on flux recovery for UF of natural wheys at 200 kPa, 600 rpm for PAN-3

Chapter 6

CONCLUSIONS AND RECOMMENDATIONS FOR FUTURE WORK

This chapter summarizes the experimental observations and the mechanisms responsible for the various UF data obtained. Suggestions for further work are also included.

6.1 GENERAL:

The main objectives of this thesis were to study the membrane performance in terms of membrane surface chemistry (hydrophilicity, surface energy and electrostatic surface charge) and solution environment (pH and solute concentration). As explained in chapter 2, variables such as pH have the potential to affect UF performance in different or even contradictory ways. Also, it is generally difficult to assign the relative importance of hydrophilic and electrostatic interactions during the UF of protein containing solutions.

In this study, flux, rejection, and flux recovery data were gathered with standard proteins (BSA, Hb and BSA-Hb mixture) and with various types of wheys (acid, cheese and shrikhand). The data were examined on the basis of concentration polarization and fouling models. The effect of hydrophilicity / surface energy was examined mainly by comparing the UF performance of PAN membranes with those based on the acrylonitrile-acrylamide copolymers. The electrostatic effects were examined mainly by comparing the UF performance of these membranes as a function of varying feed pH.

It was found possible to correlate the UF performance in terms of the following basic mechanisms:

Pore size narrowing : The changes in membrane UF performance could be correlated with the potential for higher or less solute adsorption / deposition within the membrane pores.

Hydrophobic interactions between solute and membrane : Less solute adsorption occurs in the case of more hydrophilic membranes and proteins.

Electrostatic interactions between solute and membrane : Solute adsorption may be enhanced or decreased depending on whether the protein-membrane interactions are attractive or repulsive.

Electrostatic interactions between proteins : These may be repulsive at pH values other than the IEP in the case of single proteins, or attractive at intermediate pH values in the case of proteins with different IEPs.

The relative importance of these mechanisms in the specific cases studied are summarized in the remainder of this chapter.

6.2 MEMBRANES

The PAN based membranes were prepared from poly(acrylonitrile) and poly(acrylonitrile-*co*-acrylamide) with varying acrylonitrile : acrylamide ratios. The IR and NMR spectral analyses (Figures 5.1 - 5.8) and elemental analysis (Table 5.1) confirmed the polymer compositions. NMR analysis (Table 5.2) was the most useful in determining the actual acrylamide content in the copolymers.

The contact angle measurements (Table 5.3) showed that the acrylamide insertion increases the membrane hydrophilicity. Surface energy studies (Table 5.3) also indicated that the dispersion force component of surface energy decreases and the polar component increases after insertion of acrylamide in poly(acrylonitrile). Thus, copolymers are shown to be more hydrophilic and polar than PAN. The zeta potential measurements (Figure 5.12) showed that membranes based on both the acrylonitrile homopolymer and the copolymers are negatively charged over the pH range studied (4 - 7.5). The magnitude of the negative charge of poly(acrylonitrile) is reduced by a factor of ~3 by incorporation of acrylamide. The above characteristics did not change substantially with acrylamide content in the copolymer in the range from 10-30% acrylamide.

The membrane characterization data show that PAN, PAN-1 and PAN-3 have similar pore size distribution (Figure 5.9). Since steric effects are comparable, the changes in the UF characteristics of the copolymer based membranes vis-a-vis PAN can be attributed to their reduced negative surface charge and increased hydrophilicity.

6.3 SINGLE PROTEIN UF

Single protein UF using the above membranes was carried out with the standard proteins, BSA and Hb. BSA and Hb are of similar size but the IEP of BSA is at pH 4.8, while Hb is positively charged upto pH 6.8. Also, Hb is more hydrophobic than BSA.

The permeate flux during BSA or Hb UF increases with increasing feed pH for all membranes (Figs 5.13, 5.20, 5.22). This may be partly attributed to the decreasing

electrostatic attraction (as pH increases from 4.0 to the IEP value) and increasing electrostatic repulsion (above the IEP) between the protein and the membrane surface. In case of Hb UF with the PAN membrane a flux minima is observed at the IEP (Figure 5.22). This minima is attributable to reduced protein-protein repulsive interactions and hence increased aggregation at this pH. However, this minima was not observed in the case of BSA UF with either membrane (Figures 5.13, 5.20); this may be due to the lower hydrophobicity of BSA compared to Hb.

At any given pH, a comparison of permeate fluxes (Figures 5.13, 5.20, 5.22) and flux recoveries (Figure 5.15) indicates less fouling in the case of the acrylamide containing membranes, compared to PAN. The protein transmission through the membranes (Figures, 5.14, 5.21, 5.23) is also higher for the copolymer based membranes. These effects indicate that fouling by pore narrowing is reduced in the case of the copolymer membranes. This increased fouling resistance of the copolymer membranes is observed inspite of the reduced electrostatic repulsion and may be attributable to the improved hydrophilicity / reduced dispersive surface energy. The higher hydrophilicity of the copolymer membranes inhibits protein adsorption on the pore walls. The reduced charge repulsion of the proteins in the copolymer membranes compared to PAN would also allow higher protein transmission.

At pH values below the IEP, all the membranes have low fluxes as well as low BSA or Hb transmission. This is due to high adsorption resulting from attractive electrostatic interactions between the positively charged protein and the negatively charged membranes.

The increase in observed protein transmission with increasing pH in the case of the copolymer membranes can be explained by concentration polarization. The validity of this model is shown by the flux vs $\ln C_r$ data (Figures 5.16, 5.17). The mass transfer coefficient, k increases and the protein concentration at the membrane surface, C_m decreases with increasing pH (Table 5.6). The BSA accumulation at the membrane surface is less for the copolymer membranes compared to PAN even when the protein rejections are comparable. The protein rejections through the membranes themselves are uniformly high (Figure 5.24).

Table 6.1 summarizes the trends in flux and observed rejection for each protein (BSA or Hb) in each membrane (PAN or copolymer). These trends can be explained by protein adsorption / pore narrowing as a result of hydrophobic and electrostatic interactions. Electrostatic interactions between protein and the negatively charged membranes would promote less protein adsorption / pore narrowing and a corresponding increase in flux and decrease in protein rejection as pH is increased above the IEP. These trends in flux and rejection are seen most clearly with the more hydrophilic copolymer based membranes. For Hb ultrafiltration through the PAN membrane, where hydrophobic interactions would be strongest, the rejection is relatively constant and the flux exhibits a minimum at the IEP.

Table 6.1
Trends in observed rejection (R) and flux with increasing pH for UF of single protein solutions

Protein	PAN (Hydrophobic)	Copolymer (Hydrophilic)
Hb (Hydrophobic)	Rejection remains constant Flux generally increases but shows a minima at IEP	Rejection decreases after IEP Flux increases monotonically
BSA (Hydrophilic)	Rejection remains constant Flux increases monotonically	Rejection decreases after IEP Flux increases monotonically

Thus, the UF data with the single proteins can be correlated with hydrophobic / hydrophilic interactions and electrostatic interactions between the protein and membrane surface. Electrostatic interactions are important with the hydrophilic copolymer membrane surfaces and with the more hydrophilic protein (BSA). In the case of Hb UF through the PAN membrane, hydrophobic interactions dominate the electrostatic effects.

6.4 MIXED PROTEIN UF

The flux and protein rejection trends observed during single protein UF are different when both BSA and Hb are ultrafiltered together. This is mainly due to the possibility of protein-protein attractive electrostatic interactions. In the case of single protein UF, protein-protein electrostatic interactions are always repulsive, except at the

IEP, where the proteins are neutral. In the case of the mixed protein UF, protein-protein electrostatic interactions are attractive at pH values between the IEPs of BSA and Hb.

Being more hydrophobic and opposite in charge to the membrane over most of the pH range, Hb is expected to be preferentially adsorbed on the membrane surface. The permeate flux data for BSA-Hb UF (Figure 5.25) is similar to the pure Hb UF data (Figure 5.22) indicating the importance of Hb-membrane interactions.

The membrane protein rejections (both R' and R) (Figures 5.26-5.29) are higher when BSA and Hb are oppositely charged and lower when BSA and Hb are similarly charged. This clearly indicates the importance of protein-protein electrostatic interactions.

The trends in flux and observed rejection for mixed protein UF are summarized in Table 6.2.

Table 6.2
Trends in observed rejection (R) and flux with increasing pH
for BSA-Hb mixed protein UF

Characteristic	PAN	PAN-1
Hb Rejection	Minimum at pH 4.0 High at pH 4.8-6.8 Decreases after pH 6.8	Minimum at pH 4.0-4.8 High at pH 4.8-6.4 Decreases after pH 6.8
BSA Rejection	Minimum at pH 4.0 Higher at higher pH	Minimum at pH 4.0-4.8 Higher at higher pH
Flux	Generally increases but shows minima near pH 6.4	Increases upto pH 6.4 and then decreases

The trends summarized in Table 6.2 can be explained by preferential Hb adsorption and consequent pore narrowing and by BSA-Hb electrostatic interactions. The trends in UF performance, summarized above, are specifically attributed to the these mechanisms as summarized in Table 6.3.

Table 6.3

Mechanistic explanation of mixed protein UF performance

Characteristic	Observed trend	Explanation
BSA or Hb Rejection	Minimum at pH 4.0 High between BSA and Hb IEPs	BSA-Hb electrostatic interactions
Permeate flux PAN	Generally increases but shows a minima near pH 6.4 for PAN	Hb-membrane electrostatic and hydrophobic interactions
Permeate flux PAN-1	Increases upto pH 6.4 and then decreases for PAN-1	Hb-membrane electrostatic interactions

Thus, the mixed protein data can be explained by the same mechanisms operational for pure Hb data in combination with BSA-Hb attractive interactions at pH values between the IEPs of BSA and Hb.

6.5 WHEY UF

The UF performance with AW, CW and SW is complex as a result of the many components present in these solutions. The inability of the osmotic pressure-concentration polarization model to fit the flux dependence on ΔP with a simple van't Hoff relationship (Figures 5.48 - 5.50) shows the non-ideal nature of these feed solutions. Both AW and SW contain more ash content than CW (Table 5.9). SW contains a significantly higher amount of lactic acid (~ 7 - 10%) than the other two wheys. All three wheys contain similar proteins with α-lactalbumin and β-lactoglobulin comprising a major fraction (~ 80%) of the total protein (Table 5.10). These proteins are smaller than BSA and have similar IEP values (~pH 5), while immunoglobulins are larger in size than BSA and have a higher IEP at pH 7.

The relative insensitivity of flux to feed pH in the case of natural whey (Figures 5.44-5.45) is similar to mixed protein (BSA-Hb) UF (Figure 5.25). This may be due to

the electrostatic interactions between the whey proteins with IEP values about pH 5 and the immunoglobulins at IEP 7.

The natural whey protein rejections (R and R') are high considering their smaller size with respect to BSA (comparison of Figures 5.14, 5.21, 5.24 and 5.46, 5.47, 5.56, 5.57). These higher values may also be attributed to the effect of Ig. These rejections are relatively insensitive to pH.

The fluxes and flux recoveries with the copolymer membranes in the case of the natural wheys are not markedly higher than those with PAN (compare Figures 5.44, 5.60 and 5.45, 5.61). Though the R' values for the copolymer membrane were less than those for PAN, the observed protein rejections (R) between the two membranes are similar over the entire pH range (compare Figures 5.46, 5.56 and 5.47, 5.57). This discrepancy vis-a-vis the standard protein results may be attributed to the higher protein concentrations in the whey case.

No single type of whey consistently showed higher or lower fluxes or rejections than the others across the various pH, pressure or membrane variations (Figures 5.44 - 5.50). It appears that the effect of the different salt content / compositions in the AW and SW cases was not as important as the other effects mentioned above.

Clarified wheys prepared by raising the pH of natural wheys to 7.5 and filtering, had reduced amount of proteins and ash than the original wheys (Table 5.9). The ash content of AW and SW is markedly reduced by this clarification. SW clarification also results in a marked loss of protein (~ 50%). This may be due to interactions of lactic acid with proteins at higher pH.

Clarified wheys generally had higher fluxes than the natural wheys (compare Figures 5.51, 5.52 with 5.44, 5.45). This increase was consistent with the reduced protein content as shown by cross plotting the clarified and natural whey fluxes as a function of retentate protein concentration (Figure 5.32 - 5.37). Within experimental error, no synergistic effect of ash reduction was seen.

Immunoglobulins are most prone to precipitate at the clarification pH. Thus, in clarified wheys, protein-protein electrostatic interactions are only repulsive (the remaining proteins have similar IEPs) and the flux dependence on pH (Figure 5.51, 5.52) is similar to

pure protein (BSA) UF. The protein rejections in the clarified whey case also tend to decrease with increasing pH (Figures 5.53, 5.54) similar to BSA UF.

6.6 AREAS FOR FURTHER WORK

This thesis focuses on the importance of various membrane characteristics such as hydrophilicity, surface energy and surface electrostatic charge and solution properties such as pH and solute concentration on the UF membrane performance i.e. flux, rejection and fouling characteristics. The results indicate that by proper adjustment / combination of the above parameters one can manipulate the desired separation / purification of proteins by mechanisms other than sieving.

It would be interesting to develop membranes with further increased hydrophilicity / charge. Polyelectrolyte complex membranes with varying surface charges would be good candidates for further study. These can be prepared with varying molar ratios of the polyanion and polycation.

In the present study, the BSA, Hb or BSA-Hb UF was carried out at high ionic strengths, at which the effect of electrostatic charge is suppressed to some extent. It would be interesting to study such effects at low ionic strengths, typically below 0.1 M.

The studies on single protein UF give an insight for the studies on multicomponent natural feeds such as wheys. Therefore, more UF studies on single proteins which are part of some of the natural feeds would give a better understanding of the fouling mechanisms in the membrane filtration of complex mixtures such as blood or dairy fluids.

REFERENCES

Ahner N., Gottschlich D., Narang S., Roberts D., Sharma S. and Ventura S., Piezoelectrically assisted UF, Sep. Sci. Technol. **28**(1-3) (1993) 895

Aimar P., Taddei C., Lafaille J.-P. and Sanchez V., Mass transfer limitations during ultrafiltration of cheese whey with inorganic membranes., J. Memb. Sci. **38** (1988) 203

Akhtar S., Hawes C., Dudley C., Reed I. and Stratford P., Coatings reduce the fouling of MF membranes, J. Memb. Sci. **107** (1995) 209

Altena F.W. and Belfort G., Lateral migration of spherical particles in porous flow channels : Application to membrane filtration, Chem. Eng. Sci. **39** (1984) 343

Anderson J.L. and Quinn J.A., Restricted transport in small pores : Model for steric exclusion and hindered particle motion, Biophys J. **14**(2) (1974) 130

Arroyo G. and Fonade C., Use of intermittent jets to enhance flux in cross-flow filtration, J. Memb. Sci. **80** (1993) 117

Asenjo J.A. and Patrick I., Large scale protein purification , in Harris E.L.V. and Agal S. (Eds)., Protein purification applications, a practical approach., IRL Press, Oxford, 1990, p 1.

Attia H., Bennasar M. and Tarodo de la Fuente B., Study of the fouling of inorganic membranes by acidified milks using scanning electron microscopy and electrophoresis. II. membrane with pore diameter 0.8 µm, J. Dairy Sci. **58** (1991b) 51

Attia H., Bennasar M. and Tarodo de la Fuente B., Study of the fouling of inorganic membranes by acidified milks using scanning electron microscopy and electrophoresis. I. membrane with pore diameter 0.2 µm, J. Dairy Sci. **58** (1991a) 39

Attia H., Bennasar M. and Tarodo de la Fuente B., Ultrafiltration on a mineral membrane of biologically or chemically acidified milk (with varying pH) and of lactic coagulum, Le Lait **68** (1988) 13

Baker R.J., Fane A.G., Fell C.J.D. and Yoo B.H., Factors affecting flux in crossflow filtration, Desalination **53** (1985) 81

Balakrishnan M. and Agarwal G.P., Protein fractionation in a vortex filter. II. Separation of simulated mixtures, J. Memb. Sci. **112**(1) (1996b) 75

Balakrishnan M. and Agarwal G.P., Protein fractionation in a vortex filter. I. Effect of system hydrodynamics and solution environment on single protein transmission, J. Memb. Sci. **112**(1) (1996a) 47

Balakrishnan M., Agarwal G.P. and Cooney C.L., Study of protein transmission in ultrafiltration., J. Mem. Sci. **85** (1993) 111

Balman H. De, Aimar P. and Sanchez V., Membrane partition and mass transfer in ultrafiltration, Sep. Sci. Technol. **25** (1990) 507

Bansal A. et al, A quantitative investigation of membrane fouling by proteins using energy dispersive spectroscopy, Key Eng. Mater.**61/62** (1991) 503

Barisas B.G., Hemoglobin, in H-J. Hinz (Ed.), Thermodynamic data for biochemistry and biotechnology, Springer-Verlag, Berlin, 1986

Baudet J., US Patent 3,993,816 (1976)

Bauser H., Chmiel H., Stroh N. and Walitza E., Control of concentration polarization and fouling in medical, food and biotechnical applications, J. Memb. Sci. **27** (1986) 195

Bauser H., Chmiel H., Stroh N. and Walitza E., Interfaial effects with microfiltration membranes, J. Memb. Sci. **11** (1982) 321

Belfort G. and Nagata N., Fluid mechanics and cross-flow filtration : Some thoughts, Desalination **53** (1985) 57

Bellara S.R., Cui Z.F. and Pepper D.S., Gas sparging to enhance permeateeate flux in UF using hollow fibre membranes, J. Memb. Sci. (1996) (Communicated)

Bennasar M., Rouleau D., Mayer R. and Tarodo de la Fuente B., J. Soc. Dairy Technol. **35** (1982) 43

Bennett C. and Myers J., Momentum heat and mass transfer, McGraw-Hill, NY, 1982, pp560-587

Bentham A.C., Ireton M.J., Hoare M., Dunnil P., Protein precipitate recovery using microporous membranes, Biotech. Bioeng. **31**(9) (1988) 984

Bhadani S.N. and Kundu S., Acid initiated copolymerization of acrylamide with acrylonitrile, Macromol. Chem., Rapid Commun., **1** (1980) 281

Bhattacharjee S. and Bhattacharya P.K., Flux decline behaviour with low MW solutes during ultrafiltration in an unstirred batch cell, J. Memb. Sci. **72** (1992) 149

Bhattacharyya D., Jumawan A.B., Grieves R.B. and Harris L.R., Ultrafiltration characteristics of oil-detergent-water systems : Membrane fouling mechanisms, Sep. Sci. Technol. **14**(6) (1979) 529

Bixler H.J., Nelsen L.M. and Bluemle Jr. L.W., Trans. Am. Soc. Artificial Int. Organs **14** (1968) 99

Blatt W.F., Dravid A., Michaels A.S. and Nelsen L.M., Solute polarization and cake formation in membrane ultrafiltration : Causes, consequences and control techniques, in Flinn J.E. (Ed.) Membrane science and technology, Plenum press, NY, 1970, pp 47

Bowen W.R. and Clark R.A., Electro-osmosis at microporous membranes and the determination of zeta potential, J. Colloid Interface Sci., **97** (1984) 401

Bowen W.R. and Gan Q., Properties of microfiltration membranes : Flux loss during constant pressure permeation of bovine serum albumin, Biotech. Bioeng. **38** (1991) 688

Bowen W.R. and Hughes D.T., Properties of microfiltration membranes. Part 2. Adsorption of bovine serum albumin at aluminium oxide membranes, J. Memb. Sci. **51** (1990) 189

Bowen W.R., Kingdon R.S. and Sabuni H.A.M., Electrically enhanced separation processes : The basis of in situ intermittent electrolytic membrane cleaning (IIEMC) and in situ electrolytic membrane restoration (IEMR), J. Memb. Sci. **40** (1989) 219

Breslau B.R., Agranat E.A., Testa A.J., Messinger S. and Cross R.A., Hollow fibre ultrafiltration, Chem. Eng. Prog. **71** (1975) 74

Brian P.L.T., Concentration polarization in RO desalination with variable flux and incomplete rejection, Ind. Eng. Chem. Fundam. **4** (1965) 439

Brink L.E.S. and Romijn, D.J., Reducing the protein fouling of polysulfone surfaces and polysulfone ultrafiltration membranes : Optimization of the type of presorbed layer, Desalination, **78** (1990) 209

Brink L.E.S., Elbers S.J.G., Robbertsen T. and Both P., The anti-fouling action of polymers preadsorbed on UF and MF membranes, J. Memb. Sci. **76** (1993) 281

Brites A.M. and de Pinho M.N., A new approach to the evaluation of the effects of protein adsorption onto a polysulfone membrane, J. Memb. sci., **78** (1993) 265

Brun C. and Angleraud R., US Pat. No. 5 14 55 83, 1992 (see also WPI Acc No.s 71-410115 / 24 and 91-202140 / 28)

Capannelli G., Vigo F. and Munari S., Ultrafiltration membranes-characterization methods, J. Memb. Sci., **15** (1983) 289

Chang Y.A., Kulkarni S.S. and Funk E.W., US Pat. No. 4,595,507, 1987

Chen M.-H., Chiao T.-C. and Tseng T.-W., Preparation of sulfonated polysulfone/polysulfone and aminated polysulfone/polysulfone blend membranes, J. Appl. Poly. Sci. **61**(7) (1996) 1205

Chen V., Fane A.G. and Fell C.J.D., The use of anionic surfactants for reducing fouling of UF membranes : Their effects and optimization, J. Memb. Sci. **67** (1992) 249

Cheryan M., Ultrafiltration handbook, Technomic Publishing Co. Inc., Lancaster, 1986

Chiang W.Y. and Hu C.-M., Studies of reactions with polymers. II. The reaction of maleic anhydride with acrylonitrile onto PVA and the properties of the resultant, J. Appl. Polym. Sci., **30** (1985) 4045

Clark W.M., Bansal A., Sontakke M. and Ma Y.H., Protein adsorption and fouling in ceramic ultrafiltration membranes, J. Memb. Sci. **55** (1991) 21

Colman D.A. and Mitchell W.S., Enhanced mass transfer for membrane processes, IChE. Symp. Ser. **118** (1990) 87

Colman D.A. and Mitchell W.S., Enhanced mass transfer for membrane processes, Food Bioprod.Proc. **69** C (1991) 91

Cross S.N., Membrane fouling and cleaning, in Turner M.K. (Ed.) Effective industrial membrane processes : Benefits and opportunities, Elsevier Appl. Sci., London, 1991 p 61

Cui Z.F., Wright K.I.T., Flux enhancements with gas sparging in downwards crossflow ultrafiltration : performance and mechanism, J. Memb. Sci. **117**(1-2) (1996) 109

Dal-Cin M.M., Striez C.N., Tweddle T.A., Capes C.E., McLellan F. and Buisson H., Effect of adsorptive fouling on membrane performance : Case study with a pulp mill effluent, Desalination **101** (1995) 155-167

Daufin G., Labbe J.-P., Quemerais A. and Michel F., Fouling of an inorganic membrane during Ultrafiltration of defatted whey protein concentrates, Neth. Milk. Dairy J., **45** (1991b) 259

Daufin G., Merin U., Labbé J.P., Quémerais A. and Kerhervé F.L., Cleaning of inorganic membranes after whey and milk UF, Biotech. Bioeng. **38** (1991a) 82

Daufin G., Michel F. and Merin U. Ultrafiltration of defatted whey : influence of some physiochemical characteristics, The Aust. J. Dairy Technol., **47** (1992) 7

Davis R.H., in Ho Winston W.S. and Sirkar K.K. (Eds), Membrane Handbook, Van Nostrand Reinhold, NY, 1992, Chapter 33

De Boer R., Zomerman J.J., Hiddink J., Aufderheyde J., Van Swaay W.P.M. and Smolders C.A., Fluidized beds as turbulence promoters in the concentration of food liquids by reverse osmosis, J. Food Sci. **45**(6) (1980) 1522

Deen W.M., Hindered transport of large molecules in liquid-filled pores, AIChE J. **33** (1987) 1409

Defrise D. and Gekas V., Microfiltration membranes and the problem of microbial adhesion, Proc. Biochem. **23** (1988) 105

Dejmek P. and Nilsson J.L., Flux-based measures of adsorption to ultrafiltration membranes, J. Memb. Sci. **40** (1989) 189

Dejmek P. et al, Turbulence promoters in UF of whey protein concentrate, J. Food Sci. **39**(5) (1974) 1014

Dejmek P., PhD Thesis, Lund Institute of Technolgy, Sweden, 1975

Delaney A.M. and Donnelly J.K., Applications of reverse osmosis in the dairy industry, in Sourirajan S. (Ed.) Reverse Osmosis and synthetic membranes, Ottawa, Canada, Natl. Res.Council, Canada. 1977, pp 417

Deverex N. and Hoare M., Membrane separation of protein precipitates : Studies with crossflow in hollow fibers, Biotech. Bioeng. **28** (1986) 422

Doherty P. and Benedek G.B., The effect of electric charge on the diffusion of macromolecules, J. Chem. Phys. **61**(12) (1974) 5426

Drew D.A, Schonberg J.A. and Belfort G., Lateral migration of a small sphere in fast laminar flow through a membrane duct, Chem. Eng. Sci. **46** (1991) 3219

Dudley L.Y., Stratford P., Akhtar S., Hawes C., Reuben B., Perl O. and Reed I.M., Coatings for the prevention of fouling of MF membranes, Chem. Eng. Res. Des. **71**(A3) (1993) 327

Dumon S. and Barnier H., UF of protein solutions on ZrO_2 membranes. The influence of surface chemistry and solution chemistry on adsorption, J. Memb. Sci. **74** (1992) 289

Eijndhoven R.H.C.M. van, Saksena S. and Zydney A.L., Protein fractionation using electrostatic interactions in membrane filtration, Biotech. Bioeng. **48** (1995) 406

Fane A.G. and Fell C.J.D., A review of fouling and fouling control in ultrafiltration, Desalination, **62** (1987) 117

Fane A.G. and Kim. K.J., Prospects for improved ultrafiltration membranes, Proceedings IMTEC'88, *International membranes technology conference*, 15-17 Nov., Sydney, 1988, K10-K14

Fane A.G., Fell C.J.D and Waters A.G., Ultrafiltration of protein solutions through partially permeable membranes, J. Memb. Sci., **16** (1983b) 211

Fane A.G., Fell C.J.D. and Kim K.J., The effect of surfactant pretreatment on the UF of proteins, Desalination **53** (1985) 37

Fane A.G., Fell C.J.D. and Suki A., Effect of pH and ionic environment on the ultrafiltration of protein solutions with retentive membranes, J. Memb. Sci. **16** (1983a) 195

Fane A.G., in Wakeman R.J. (Ed.), Progress in filtration and separation, Elsevier, Amsterdam, 1986, pp 101

Fane A.G., Ultrafiltration of suspensions, J. Memb. Sci. **20** (1984) 249

Fell C.J.D., Kim K.J., Chen V., Wiley D. and Fane A.G., Factors determining flux and rejection of UF membranes, Chem. Eng. Process **27** (1990) 165

Ferry J.D., Ultrafiltartion membranes and ultrafiltration, Chem. Rev. **18** (1936) 373

Field R.W., Wu D., Howell J.A. and Gupta B.B., Critical flux concept for MF fouling, J. Memb. Sci. **100**(3) (1995) 259

Finnigan S.M. and Howell J.A., The effect of pulsatile flow on UF fluxes in a baffled tubular membrane system, Chem. Eng. Res. Des. **67**(3) (1989) 278

Flora J.R.V., Stochastic approach to modeling surface fouling of ultrafiltration membranes, J. Memb. Sci. **76** (1993) 85

Fowkes F.M., Attractive forces at interfaces, Ind. Engr. Chem., **56** (1964) 40

Futselaar H., PhD Thesis, University of Twente, 1993

Garg D.H., Lenk W., Berwald S., Lunkwitz, Simon F. and Eichhorn K.-J., Hydrophilization of microporous polypropylene Celgard® membranes by the chemical modification technique, J. Appl. Poly. Sci. **60**(12) (1996) 2087

Gatenholm P., Peterson S., Fane A.G. and Fell C.J.D., Performance of synthetic membranes during cell harvesting of *E. coli*, Proc. Biochem. **23** (1988) 79

Gekas V. and Hallström B., Mass transfer in the membrane concentration polarization layer under turbulent crossflow. 1. Critical literature review and adaptation of existing Sherwood correlations to membrane operations, J. Memb. Sci., **30** (1987) 153

Gekas V. and Hallström B., Microfiltration membranes, cross-flow transport mechanisms and fouling studies, Desalination **77** (1990) 195

Gésan G., Daufin G., Merin U., Labbé J.-P. and Quémerais A., Fouling during constant flux crossflow microfiltration of pretreated whey. Influence of transmembrane pressure gradient, J. Memb. Sci., **80** (1993) 131

Glover F.A. and Brooker B.E., The structure of the deposit formed on the membrane during the concentration of milk by reverse osmosis, J. Dairy Res. **41** (1974) 89

Godjevargova T. and Dimov A., Permeateeability and protein adsorption of modified charged acrylonitrile copolymer membranes, J. Memb. Sci. **67** (1992) 283

Goel V. and McCutchan J.W., Colorado river desalting by reverse osmosis, Proc. 5th Int. Symp. Fresh water from sea, Alghero, May 16-20, 1976, 4, 143-56

Gölander C.-A. and Kiss E., Protein adsorption on functionalized and ESCA-characterized polymer films studied by ellipsometry, J. Colloid Interface Sci. **121** (1988) 240

Goldinger W., Rebsamen E., Brandi E. and Ziegler H., Dynamic micro-and ultrafiltration in biotechnology, Sulzer Technical Review **3** (1986)

Goldsmith R.L., Macromolecular ultrafiltration with microporous membranes, Ind. Eng. Chem. Fundam. **10** (1971) 113

Gourley L., Britten M., Gauthier S.F. and Pouliot Y. Characterization of adsorptive fouling on ultrafiltration membranes by peptide mixtures using contact angle measurements, J. Memb. Sci. **97** (1994) 283

Grabbe E.S., Total internal reflection fluorescence with energy transfer : A method for analysing IgG adsorption on nylon thin films, Langmuir **9** (1993) 1574

Green G. and Belfort G., Fouling of ultrafiltration membranes : lateral migration and the particle trajectory model, Desalination **35** (1980) 129

Gupta B.B. Use of hydrodynamic methods for pressure driven membrane operations, Ind. J. Chem. Technol. **3**(3) (1996) 156

Gupta B.B., Howell J.A., Wu D., and Field R.W., A helical baffle for cross-flow microfiltration, J. Memb. Sci. **102** (1995) 259

Gupta B.B., Wu D., Field R.W. and Howell J.A., in Vansant E.F. (Ed.) Separation Technology, Elsevier Science B.V. Amsterdam, 1994a, p 559

Gupta B.B., Wu D., Field R.W. and Howell J.A., Permeate flux enhancement using a baffle in microfiltration with mineral membranes, Proc. Technol. Proc. **11** (1994b) 559

Hallström B. and López-Leiva, Description of a rotating ultrafiltation module, Desalination **24** (1978) 273

Hanemaaijer J.H., Microfiltration in whey processing, Desalination **53** (1985) 143

Hanemaaijer J.H., Robbertsen T., van den Boomgaard Th., Olieman C., Both P. and Schmidt D.G., Characterization of clean and fouling ultrafiltration membranes, Desalination **68** (1988) 93

Hanemaaijer J.H., Robertsen T., van den Boomgaard Th. and Gunnink J.W., Fouling of ultrafiltration membranes. Role of protein adsorption and salt precipitation , J. Memb. Sci. **40** (1989) 199

Haurowitz F., The chemistry and function of proteins, 2nd ed., Academic Press, NY, 1963, p 164, 190

Hayes J.F., Dunkerley J.A., Muller L.L. and Griffin A.T., Studies on whey processing by ultrafiltration .II. Improving permeation rates by preventing fouling, Aus. J. Dairy Technol. **29** (1974) 132

Heinemann P., Howell J.A. and Bryan R.A., Microfiltration of protein solutions : Effect of fouling on rejection, Desalination **68** (1988) 243

Hiddink J., Kloosterboer D. and Bruin S., Evaluation of static mixers as convection promoters in the UF of dairy liquids, Desalination **35** (1980) 149

Higuchi A. and Nakagawa T, Surface modified polysulfone hollow fibres .III. Fibres having a hydroxide group, J. Appl. Poly. Sci. **41** (1990) 1973

Higuchi A., Mishima S. and Nakagawa T., Separation of proteins by surface modified polysulfone membranes, J. Memb. Sci. **57** (1991) 175

Higuchi A., Y. Ishida, T. Nakagawa, Surface modified polysulfone membranes : Separation of mixed proteins and optical resolution of tryptopha, Desalination 90 (1993) 127

Hong J. and Lee C.K., Membrane separation coupled with electrophoresis, Ann. N.Y. Acad. Sci. **469** (1986) 131

Howell J.A. and Velicangil Ö, Protein ultrafiltration : Theory of membrane fouling and its treatment with immobilized proteases, in Cooper A.R. (Ed.), Poly. Sci. Technol., vol. 13, NY, 1980, pp 217

Hu D.S.-G., Synthesis and dielectric characterization of poly(acrylonitrile-co-acrylamide-co-acrylic acid) terpolymer gels, Macromol. Chem. Phys., **195** (1994) 3629

Hvid K.B., Nielsen P.S. and Stengaard F.F., Preparation and characterization of a new ultrafiltration membrane, J. Memb. Sci. **53** (1990) 189

Ilias S. and Govind R., Potential applications of pulsed flow for minimizing concentration polarization in ultrafiltration, Sep. Sci. Technol. **25**(13-15) (1990) 1307

Iritani E., Mukai Y, Tanaka Y. and Murase T., Flux decline behaviour in dead-end microfiltration of protein solutions, J. Memb. Sci. **103** (1995b) 181

Iritani E., Mukai Y. and Murase T., Properties of filter cake in dead-end ultrafiltration of binary protein mixtures with retentive membranes, Chem. Eng. Res. Des., **73** (1995a) 551

Iritani E., Mukai Y. and Murase T., Upward dead-end UF of binary protein mixture, Sep. Sci. Technol. **30**(3) (1995c) 369

Iritani E., Nakatsuka, Hisanao A.and Murase T., Effect of solution enviroment on unstirred dead-end ultrafiltration characteristics of proteinaceous solutions, J. Chem. Eng. Jpn., **24** (1991) 177

Iritani E., Watanabe T. and Murase T., Effects of pH and solvent density on dead-end upward UF, J. Memb. Sci. **69** (1992) 87

Jaffrin M.Y., Gupta B.B. and Paullier P., Energy saving pulsatile mode flow cross-flow filtration, J. Memb. Sci. **86**(3) (1994) 281

Jagannadh S.N. and Murlidhara H.S., Electrokinetic methods to control membrane fouling, Ind. Eng. Chem. Res. **35**(4) (1996) 1133

Jayaraman J., Laboratory manual in biochemistry, John wiley and sons Increases., NY, 1981, pp80

Jeffree M.A., Peacock J.A., Sobey I.J. and Bellhouse B.J., Gel layer limited hemofiltration rates can be increased by vortex mixing, Clin. Exp. Dial. Aspheresis **5** (1981) 373

Johnsson G., Boundary layer phenomena during ultrafiltration of dextran and whey protein solutions, Desalination **51** (1984) 61

Karakelle M. and Zdrahala R.J., Membranes for biomedical application : Utilization of plasma polymerization for dimensionally stable hydrophilic membranes, J. Memb. Sci. **41** (1989) 305

Kedem O and Katchalsky A, Thermodynamic analysis of the permeateeability of biological membranes to non-electrolytes, Biochim. Biophys. Acta **27** (1958) 229

Kim K.J. and Fane A.G., Performance evaluation of surface hydrophilized novel ultrafiltration membranes using aqueous proteins, J. Memb. Sci. **99** (1995) 149

Kim K.J., Fane A.G. and Fell C.J.D., The effect of Langmuir-Blodgett layer pretreatment on the performance of ultrafiltration membranes, J. Memb. Sci. **43** (1989) 187

Kim K.J., Fane A.G. and Fell C.J.D., The performance of UF membranes pretreated by polymers, Desalination **70** (1988) 229

Kim K.J., Fane A.G., Fell C.J.D. and Joy D.C., Fouling mechanisms of membranes during protein ultrafiltration, J. Memb. Sci. **68** (1992) 79

Kim K.J., Sun P., Chen V., Wiley D.E. and Fane A.G., The cleaning of UF membranes fouled by protein, J. Memb. Sci. **80** (1993) 241

Kim M., Kiyohara S., Konishi S., Saito K. and Sugo G., Ring opening reaction of poly-GMA chain grafted onto a porous membrane, J. Memb. Sci. **117**(1-2) (1996) 33

Kim M., Kojima J., Saito K. and Furusaki S., Reduction of nonselective adsorption of proteins by hydrophilization of MF membranes by radiation induced grafting, Biotechnol. Prog. **10** (1994) 114

Kirk R.S. and Sawer R., *Pearson's composition and analysis of foods*, Longmans Scientific and Technical Books, Essex, UK, 1991, p537

Knops F.N.M., Futselaar H. and Rácz I.G., The transversal flow MF module. Theory, design, realization and experiments, J. Memb. Sci. **73** (1992) 153

Kobayashi T., Miyamoto T., Nagai T., and Fujii N., Negatively charged UF membranes of polyacrylonitrile having amphiphilic quaternary ammonium counter ions, J. Memb. Sci, **90** (1994) 141.

Kontturi A.-K., Kontturi K. and Vuoristo M., Separation of proteins of nearly the same size but having different isoelectric points by convective electrophoresis, Acta Chemica Scandinavica, **50** (1996) 102

Kosikowski F.V., Whey utilization and whey products, J. Dairy Sci. **62** (1979) 1149

Kozinski A.A. and Lightfoot E.N., Protein ultrafiltration : A general example of boundary layer filtration, AIChE J., **18**(5) (1972) 1030

Krause S, in Paul D.R. and Newmans S., (Eds) Polymer blends, Academic press, NY, 1978

Kroner K.H. and Nissinen V., Dynamic filtration of microbial suspensions using an axially rotating filter, J. Memb. Sci. **36** (1988) 85

Kroner K.H., Nissinen V. and Ziegler H., Bio. Technology **5** (1987) 921

Kulkarni S.S., Funk E.W. and Li N.N., in Ho W.S.W. and Sirkar K.K. (Eds), Membrane Handbook, Van Nostrand Reinhold, NY, 1992a, Chapter 26

Kulkarni S.S., Funk E.W. and Li N.N., in Ho W.S.W. and Sirkar K.K. (Eds), Membrane Handbook, Van Nostrand Reinhold, NY, 1992b, Chapter 27

Kulkarni S.S., Funk E.W. and Li N.N., in Ho W.S.W. and Sirkar K.K. (Eds), Membrane Handbook, Van Nostrand Reinhold, NY, 1992c, Chapter 29

Kulkarni S.S., Funk E.W. and Li N.N., in Ho W.S.W. and Sirkar K.K. (Eds), Membrane Handbook, Van Nostrand Reinhold, NY, 1992d, Chapter 30

Kuo K.-P. and Cheryan M., Ultrafiltration of acid whey in a spiral wound unit : Effect of operating parameters on membrane fouling, J. Food Sci. **48** (1983) 1113

Küpcü S, Margit S and Sleytr U.B., Influence of covalent attachment of low molecular weight substances on the rejection and adsorption properties of crystalline proteinaceous ultrafiltration membranes, Desalination, **90** (1993) 65

Kuruzovich J.N. and Piergiovanni P.R., Yeast cell MF : Optimization of backwashing for delicate membranes, J. Memb. Sci. **112**(2) (1996) 241

Labbé J.-P., Quémerais A., Michel F. and Daufin G., Fouling of inorgnic membranes during whey ultrafiltration : Analytical methodology, J. Memb. Sci. **51** (1990) 293

Lai J.Y. and Chao. Y.C., Plasma treated nylon 4 membranes for reverse osmosis desalination, Proc. IMTEC'1988 International membrane technology conference, 15-17 Nov. 1988, Sydney, J44-J47

Larsson K., Interfacial phenomena-Bioadhesion and biocompatibility, Desalination **35** (1980) 105

Le M.S., Spark L.B. and Ward P.S., The separation of aryl acrylamide by crossflow microfiltration and the significance of enzyme / cell debris interaction, J. Memb. Sci. **21** (1984) 219

Le Roux J., Paul D.R. and Pinnau I., Surface fluorination of polysulfone membranes, Proc. of the fifth annual meeting of the north american membrane society, Lexington, Kentucky, USA, 1992

Lee C.K. and Hong J., Characterization of electric charges in micropores membranes, J. Memb. Sci. **39** (1988) 79

Lee C.K. and Hong J., Enzyme reaction in a membrane cell coupled with electrophoresis, Ann. N.Y. Acad. Sci. **506** (1987) 499

Lee C.K., Chang W.G. and Ju Y.H., Air slugs entrapped crossflow filtration of bacterial suspensions, Biotech. Bioeng. **41**(5) (1993) 525

Lee D.N. and Merson R.L., Chemical treatment of cottage cheese whey to reduce fouling of ultrafiltration membranes, J. Food Sci. **41** (1976) 778

Lee D.N. and Merson R.L., Examination of cottage cheese whey proteins by scanning electron microscopy : Relationship to membrane fouling during ultrafiltration, J. Dairy Sci. **58**(10) (1975) 1423

Lee S.H. and Ruckenstein E., Adsorption of proteins onto polymeric surfaces of different hydrophilicities. - A case study with bovine serum albumin, J. Colloid Interface Sci. **125** (1988) 365

Lee S.S., Burt A., Russotti G. and Buckland B., Microfiltration of recombinant yeast cells using a rotating disc dynamic filtration system, Biotech. Bioeng. **48**(4) (1995) 386

Lentsch S., Aimar P. and Orozco J.L., Enhanced separation of albumin-poly(ethylene glycol) by combination of UF and electrophoresis, J. Memb. Sci. **80** (1993) 221

Loeb G.I. and Scherga H.A., Hydrodynamic and thermodynamic properties of bovine serum albumin at low pH, J. Am. Chem. Soc., **60** (1956) 1633

Lowe E. and Durkee E.L., Dynamic turbulence promotion in reverse osmosis processing of liquid foods, J. Food Sci. **36** (1971) 31

Lowry O.H., Rosenrough N.J., A.L. Farr and R J Randall, Protein measurement with Folin-Phenol reagent, J. Biol. Chem. **193** (1951) 265

Marshall A.D., Munro P.A. and Trägårdh G., The effect of protein fouling in microfiltration and ultrafiltration on permeate flux, protein retention and selectivity : A literature review, Desalination, **91** (1993) 65

Marshall K.R., Industrial isolation of milk proteins : whey proteins, " Developments in Dairy Chemistry, London : Applied Science Publishers, 1982, pp 339

Mateus M. and Cabral J.M.S., Recovery of 6-α-methylprednilosolone from biotransformation medium by membrane filtration, Downstream Proc. Biotech. II (1989) 3.21

Matsumoto Y., Nakao S. and Kimura S., Int. Chem. Eng. **28** (1988) 677

Matsuura T. and Sourirajan S., Interfacial parameters governing RO for different polymer material-solution systems through gas and liquid chromatography data, Ind. Eng. Chem. Process Des. Dev. **20** (1981) 273

Matthiasson E., Molecular adsorption and fouling in UF and their relationships to concentration polarization, PhD Thesis, University of Lund, 1984

Matthiasson E., The role of macromolecular adsorption in fouling of ultrafiltration membranes, J. Memb. Sci., **16** (1983) 23

Maubois J.-L., Pierre A., Fauquant J. and Piot M., Industrial fractionation of main whey proteins. Trends in whey utilization, Int. Dairy Fed. Bull. **212** (1987) 381

Maubois J.L., Pierre A., Fauquant J. and Piot M., Industrial fractionation of main whey proteins, IDF Bull. **212** (1987) 154

McDonogh R.M. Bauser H., Stroh N. and Chmiel H., Concentration polarization and adsorption effects in crossflow ultrafiltration of proteins, Desalination **79**(2-3) (1990) 217

McGregor W.C (Ed), Membrane separations in biotechnology, Marcel Dekker Inc., NY, 1986

Meireles M., Aimar P. And Sanchez V., Albumin denaturation during ultrafiltration : Effects of operating conditions and consequences on membrane fouling, Biotech. Bioeng. **38** (1991) 528

Merin U., A study of the mechanism of fouling of ultrafiltration membrane, PhD Thesis, University of Illinois, Urbana Champaign, Illinois (USA) 1979

Michaels A.S. and Matson S. L., Membranes in biotechnology : state of the art, Desalination, **53** (1985) 231

Michaels A.S., New separation technique for the CPI, Chem. Eng. Prog. **64**(2) (1968) 31

Millesime L., Amiel C. and Chaufer B., Ultrafiltration of lysozyme and bovine serum albumin with polysulfone membranes modified with quaternized polyvinylimidazole, J. Memb. Sci. **89** (1994) 223

Miyama H., Yoshida H and Nosaka Y., Negatively charged poly(acrylonitrile) graft copolymer membrane for permeation and separation of plasma proteins, Makromol. Chem., Rapid Commun., **9** (1988) 57

Mohr C.M., Engelau, Leeper S.A. and Charboneau (Eds) , Membrane applications and research in food processing, Noyes data corporation, Perk Ridge, New Jersey, USA, 1989

Montlohuc G., Tarodo de la Fuente B. and Rios G.M., Transfer de matiere entre un lit fluidise homogene et une paroi poreuse, Entropie **124** (1985) 24

Moulin P., Rouch J.C., Serra C., Clifton M.J. and Aptel P., Mass transfer improvement by secondary flows : Dean vortices in coiled tubular membranes, J. Memb. Sci. **114**(2) (1996) 235

Mueller J. and Davis R.H., Protein fouling of surface-modified polymeric microfiltration membranes, J. Memb. Sci. **116**(1) (1996) 47

Mulder M., Nature of membranes, in Howell J.A., Sanchez V. and Field R.W. (Eds.), Membranes in bioprocessing : Theory and applications, Chapman and Hall, NY, 1993, Chapter 2

Mulder M.H.V., Polarization phenomena and membrane fouling, in Noble R.D. and Stern S.A. (Eds.) Membrane separations technology : Principles and applications, 1995, pp 45

Muller L.L., Hayes J.F. and Griffin A.T., Studies on whey processing by ultrafiltration. Comparison of various ultrafiltration modules on whey from hydrochloric acid whey and cheddar cheese, Aus. J. Dairy Technol. **28**(2) (1973) 70

Munoz-Aguado M.J., Wiley D.E. and Fane A.G., Enzymatic and detergent cleaning of a polysulfone UF membrane fouled with BSA and whey, J. Memb. Sci. **117**(1-2) (1996) 175

Murlidhara H.S. and Huffman, Paper presented at sixth Ann. Memb. Technology / planning Conf. Cambridge, MA, 1988

Najarian S. and Bellhouse B.J., Enhanced MF of bovine blood using a tubular membrane with a screw-threaded insert and oscillatory flow, J. Memb. Sci. **112**(2) (1996) 249

Nakanishi K. and Kessler H.-G., Rinsing behaviour of deposited layers formed on membranes in ultrafiltration, J. Food Sci., **50** (1985) 1726

Nakao S., Osada H., Kurata H., Suru T and Kimura S., Separation of proteins by charged ultrafiltration membranes, Desalination, **70** (1988) 191

Nakao S.I., Nomura T. and Kimura S., Characteristics of macromolecular gel layer formed on ultrafiltration tubular membranes, AIChE J. **25** (1979) 615

Nel R.S., Oppenheim S.F. and Rodgers V.G.J., Effects of sorption properties of solute and permeate flux in Bovine serum albumin- IgG Ultrafiltration, Biotechnol Prog. **10** (1994) 539

Nikolov N.D., Mavrov V. and Nikolova J.D., Ultrafiltration in a tubular membrane under simultaneous action of pulsating pressures in permeate and feed solution, J. Memb. Sci. **83** (1993) 167

Norde W, Driving forces for protein adsorption at solid surfaces, Macromol. Symp. **103** (1996) 5

Nyström M. and Howell J.A., Flux enhancement, in Howell J.A., Sanchez V. and Field R.W. (Eds.) Membranes in bioprocessing : Theory and applications, 1993, chapter 7

Nyström M. and Lindström M., Optimal removal of chlorolignin by ultrafiltration achieved by pH control, Desalination **70** (1988) 145

Nyström M., Fouling of unmodified and modified polysulfone ultrafiltration membranes by ovalbumin, J. Memb. Sci., **44** (1989) 183

Oldani M. and Schock G., Characterization of ultrafiltration membranes by IR, ESCA and contact angle measurements, J. Memb. Sci. **43** (1989) 243

Opong W.S. and Zydney A.L., Diffusive and convective protein transport through asymmetric membranes, AIChE J. **37** (1991) 1497

Oppenheim S.F., Buettner G.R., Dordick J.S. and Rodgers V.G.J., Applying electron paramagnetic resonance (EPR) spectroscopy to the study of fouling in protein ultrafiltration, J. Memb. Sci. **96**(3) (1994) 289

Osada Y., Honda K. and Ohta M., Control of water permeability by mechanochemical contraction of poly(methacrylic acid) grafted membranes, J. Memb. Sci. **27** (1986) 327

Overbeek J.Th.G. and Bungenberg De Long H.G., Sols of macromolecular colloids with electrolyte nature, in H.R. Kruyt (Ed.), Colloid Science, vol II, Elsevier Publ. Com. Inc., NY, 1949, p 191

Owens D.K. and Wendt R.C., Estimation of the surface free energy of polymers, J. Appl. Poly. Sci., **13** (1969) 1741

Palecek S.P. and Zydney A.L., Intermolecular electrostatic interactions and their effect on flux and protein deposition during protein filtration , Biotechnol. Prog. **10** (1994) 207
Chudacek M.W. and Fane A.G., The dynamics of polarization in unstirred and stirred ultrafiltration, J. Memb. Sci. **21** (1984) 145

Palecek S.P., Mochizuki S. and Zydney A.L., Effect of ionic environment on BSA filtration and the properties of BSA deposits, Desalination **90** (1993) 147

Pall D.B., US Pat. No. 4,340,479, 1982

Parkin M.F. and Marshall K.R., N.Z.J. Dairy Technol. **11** (1976) 107

Patocka J. and Jelen P., Calcium chelation and other pretreatments for flux improvement in ultrafiltration of cottage cheese whey, J. Food Sci. **52** (1987) 1241

Persson K.M., Capannelli G., Bottino A. and Trägårdh G., Porosity and protein adsorption of four polymeric MF membranes, J. Memb. Sci. **76** (1993) 61

Piot M., Maubois J.-L., Schaegis P., Veyre R. and Luccioni A., Microfiltration en flux tangential Desalination lactosérums de fromagerie, Le Lait **64** (1984) 102

Piot M., Vachot J.-C., Veaux M., Maubois J.-L. and Brinkmann G.-E., La Tech. Laitiere **1016** (1986) 42

Porter M.C., Concentration polarization with membrane ultrafiltration, Ind. Eng. Chem. Prod. Res. Dev., **11** (1972) 234

Porter M.C., in Schweitzer P. (Ed.) Handbook of separation techniques for chemical engineers, 2nd Ed., McGraw-Hill, NY, 1988, pp 2.3-2.103

Pouliot M., Pouliot Y., Britten M. and Ross N., Effects of pH and ionic environment on the permeability of rejective properties of an alumina microfiltration membrane for whey proteins, J. Memb. Sci. **95** (1994) 125

Pritchard M., The influence of rheology upon mass transfer in crossflow membrane filtration, Ph.D. Thesis, University of Bath, Great Britain, 1990

Probstein R.F., Shen J.S. and Leung W.F., Ultrafiltration of macromolecular solution at higher polarization in laminar channel flow, Desalination **24** (1978) 1

Raju K.V.S.N. and Yaseen M., A new equation for estimating [η] from single viscosity measurement in dilute solution, J. Appl. Poly. Sci. **45** (1992) 677

Rautenbach R. and Schock G., Ultrafiltration of macromolecular solutions and cross-flow microfiltration of colloidal suspensions. A contribution to permeate flux calculations, J. Memb. Sci., **36** (1988) 231

Razavi S.K.S., Harris J.L. and Sherkat F., Fouling and cleaning of membranes in the UF of the aqueous extract of soy flour, J. Memb. Sci. **114**(1) (1996) 93

Rebsamen E. and Ziegler H., Dynamic microfiltration and ultrafiltraton in biotechnology, Proc. 4th World filtration congress, Ostend, Belgium (1986) 31

Reihanian H., Robertson C.R. and Michaels A.S., Mechanism of polarization and fouling of ultrafiltration membranes by proteins, J. Memb. Sci., **16** (1983) 237

Renner E. and Abd El-Salam M.H., Application of ultrafiltration in the dairy industry, Elsevier Applied Science, London, 1991

Riesmeier B., Kroner K.H. and Kula M.-R., Harvest of microbial suspensions by microfiltration, Desalination **77** (1990) 219

Rios G.M, Rakotoarisoa H. and Tarodo de la Fuente B., Basic transport mechanisms of UF in the presence of fluidized particles, J. Memb. Sci. **34** (1987) 331

Robertson G.H., Olieman J.J. and Farkas D.F, Concentration polarization reduction in a centrifugally driven membrane separator, AIChE Symp. Ser. **78**(218) (1982) 129

Robinson C.W., Siegel M.H., Condemine A., Fee C., Fahidy T and Glick B.R., Pulsed electric field crossflow UF of BSA, J. Memb. Sci. **80** (1993) 209

Robyt J.F. and Whelan W.J., Reducing value methods for maltodextrins : I. Chain-length dependence of alkaline 3,5-dinitrosalicylate and chain-length independence of alkaline copper, Anal. Biochem. **45** (1972) 510

Rodgers V.G.J. and Sparks R.E., Effect of transmembrane pressure pulsing on concentration polarization, J. Memb. Sci. **68** (1992) 149

Rodgers V.G.J. and Sparks R.E., Effects of solution properties on polarization redevlopment and flux in pressure pulsed ultrafiltration, J. Memb. Sci. **78** (1993) 163

Rodgers V.G.J. and Sparks R.E., Reduction of membrane fouling in the ultrafiltration of binary protein mixtures, AIChE J., **37**(10) (1991) 1517

Roesink H.D.W., Ph.D. Thesis, University of Twente, 1989

Rolchigo P.M., Raymond W.A. and Hildebrandt J.R., Improved control of ultrafiltration using vorticular hydrodynamics and hydrophilic membranes, Proc. Biochem. **24** (1989) Pro-Bio Tech iii-vii.

Saksena S. and Zydney A.L., Effect of solution pH and ionic strength on the separation of albumin from immunoglobulins (IgG) by selective filtration, Biotech. Bioeng. **43** (1994) 960

Schulz G. and Ripperger S., Concentration polarization in cross-flow microfiltration, J. Memb. Sci. **40** (1989) 173

Scopes R.K., Protein purification. Principles and practice, Springer-Verlag, NY, 1987

Scott J.A., Application of crossflow filtration to cider fermentations, Proc. Biochem. **23** (1988) 146

Sedath R.H., Taylor D.R. and Li N.N., Reduced fouling of UF membranes via surface fluorination, Sep. Sci. Technol., **28**(1-3) (1993) 255

Sheldon J.M., Reed I.M. and Howes C.R., The fine structure of UF membranes. II. Protein fouled membranes, J. Memb. Sci. **62** (1991) 87

Shoji T., Nakajima M., Nabetani H., Ohtani T. and Watanabe A., J. Agri. Chem. Chem. Soc. Jpn. **62** (1988) 1055

Silva L.K., Klein E., Ward R.A. and Hagan E.A., New synthetic membranes from acrylonitrile copolymers for dialysis and ultrafiltration, in Proceedings of 'ICOM 90', Chicago, USA, 1990, pp1143

Silva M., Zaniquelli M.E.D. and Galembeck F., Parallel electric field in flux restoration during UF, Sep. Sci. Technol. **26**(6) (1991) 831

Sims G.E.C. and Snape T.J., A method for the estimation of polyethylene glycol in plasma protein fractions, Anal. Biochem. **107** (1980) 60

Smith F.G. and Deen W.M., Electrostatic double layer interactions for sperical colloids in cylindrical pores, J. Colloid Interface Sci. **78** (1980) 44

Smith K.R. and Bradley Jr. R.L., J. Dairy Sci. **70** (1987) 243

Spiazzi E., Lenoir J. and Grangeon A., A new generator of unsteady-state flow regime in tubular membranes as an antifouling technique : A hydrodynamic approach, J. Memb. Sci. **80** (1993) 49

Stengaard F.F., Characterization and performance of new types of UF membranes with chemically modified surfaces, Desalination **70** (1988) 207

Taddei C., Aimar P., Daufin G. and Sanchez V., Etude du transfert de matière lors del' ultrafiltration de lactosérum doux sur membrane minérale, Le Lait **66** (1986) 371

Taddei C., Aimar P., Daufin G. and Sanchez V., Factors affecting fouling of an inorganic membrane during sweet whey ultrafiltration, Le Lait **68**(2) (1988) 157

Tam T.M. and Tweddle T.A., Kutowy O. and Hazlett J.D., Polysulfone membranes. II. Performance comparison of polysulfone-poly(N-vinyl-pyrrolidone) membranes, Desalination **89** (1993) 275

Tarleton E.S. and Wakeman R.J., Understanding flux decline in crossflow microfiltration . Part 1. Effects of particle and pore size, Chem. Eng. Res. Des. **71**(A) (1993) 399

Teymans D. and Lenges J., Belg. J. Food Chem. and Biotech. **44**(6) (1989) 233

Tobler W., Dynamic filtration : Principle and application of shear filtration in an annular gap, Filtr. Sepn. **19** (1982) 329

Trettin D.R. and Doshi M.R., Limiting flux in ultrafiltration of macromolecular solutions, Chem. Eng. Commun. **4** (1980) 507

Tutunjian R.S., Dev. Ind. Microbiol., **2** (1984) 415

Ulbricht M. and Belfort G., Surface modification of ultrafiltration membranes by low temperature plasma. II. Graft polymerization onto polyacrylonitrile and polysulfone , J. Memb. Sci. **111**(2) (1996a) 193

Ulbricht M., Matsuschewski H., Oechel A. and Hicke H.-G., Photo-induced graft polymerization surface modifications for the preparation of hydrophilic and low-protein adsorbing UF membranes, J. Memb. Sci. **115**(1) (1996b) 31

Urase T., Yamamoto K. and Ohgaki S., Effect of pore structure of membranes and module configuration on virus retention, J. Memb. Sci. **115**(1) (1996) 21

Urbain V., Benoit R and Manem J., Membrane bioreactor : a new treatment tool, J. Am. Wat. Works Assoc. **88**(5) (1996) 75

van Boxtel A.J.B., Otten Z.E.H. and van der Linden H.P.L.J., Evaluation of process models for fouling control of reverse osmosis of cheese whey, J. Memb. Sci. **58** (1991) 89

van den Berg G.B. and Smolders C.A., Concentration polarization phenomena during dead-end ultrafiltration of protein mixtures : The influence of solute-solute interactions, J. Memb. Sci., **47** (1989b) 1

van den Berg G.B. and Smolders C.A., Flux decline in ultrafiltration processes, Desalination **77** (1990) 101

van den Berg G.B. and Smolders C.A., The boundary layer resistance model for unstirred ultrafltration. A new approach, J. Memb. Sci. **40** (1989a) 149

van der Horst H.C. and Hanemaaijer J.H., Crosflow microfiltration in the food industry. State of art, Desalination **77** (1990) 235

van der Waal M.J. and Rácz I.G., Mass transfer in corrugated-plate membrane modules. I. Hyperfiltration experiments, J. Memb. Sci. **40** (1989a) 243

van der Waal M.J., Stevanovic S. and Rácz I., Mass transfer in corrugated-plate membrane modules.II. ultrafiltration experiments, J. Memb. Sci. **40** (1989b) 261

van Gassel T.J. and Ripperger S., Crossflow microfiltration in the process industry, Desalination, **53** (1985) 373

Vetier C., Bennasar M. and Tarodo de la Fuente B., Study of the fouling of a mineral microfiltration membrane using scanning electron microscopy and physicochemical analysis in the processing of milk, J. Dairy Res. **55** (1988) 381

Vigo F., Nicchia M. and Uliana C., Poly(vinyl chloride) ultrafiltration membranes modified by high frequency discharge treatment, J. Memb. Sci. **36** (1988) 187

Vigo F., Uliana C. and Ravina E., The vibrating ultrafiltration module. Performance in the low frequency region, Sep. Sci. Technol. **25** (1-2) (1990) 63

Vilker V.L., Colton C.K. and Smith K.A., Concentraion polarization in protein ultrafiltration.II. Theoretical and experimental study of albumin ultrafiltered in an unstirred cell, AIChE J. **27** (1981a) 637

Vilker V.L., Colton C.K. and Smith K.A., The osmotic pressure of concentrated protein solutions : effects of concentration and pH in saline solutions of bovine serum albumin, J. Colloid Interface Sci., **79** (1981b) 548

Wakeman R.J. and Tarleton E.S., An experimental study of electroacoustic crossflow microfiltration , Chem. Eng. Res. Des. **69** (1991) 386

Whittaker C., Ridgway H. and Olson B.H., Evaluation of cleaning strategies for removal of biofilms from reverse-osmosis membranes, Appl. Environ. Microbiol. **48**(2) (1984) 395

Wijmans J.G., Nakao S.I. and Smolders C.A., Flux limitations in ultrafiltration : Osmotic pressure model and gel layer model, J. Memb. Sci. **20** (1984) 115

Wijmans J.G., Nakao S.I. van den Berg J.W.A., Troelstra F.R. and Smolders C.A., Hydrodynamic resistance of concentration boundary layers in ultrafiltration, J. Memb. Sci. **22** (1985) 117

Winzeler H.B., A novel separation unit with big performance and low energy input, Food Biotech **4**(1) (1990) 287

Wolff J., Steinhauser H. and Ellinghorst G., Tailoring of ultrafiltration membranes by plasma treatment and their application for the desalination and concentration of water soluble organic substances, J. Memb. Sci. **36** (1988) 207

Wyatt J.M., Knowles C.J. and Bellhouse B.J., A novel membrane module for use in biotechnology that has high transmembrane flux rates and low fouling. Proc. Int. Conf. Biorectors and Biotransformations, Moody G.W. and Baker P.B. (Ed.), Gleneagles, Scotland, 1987, p 166

Yamagiwa K., Kobayashi H., Onodera M., Ohkawa A., Kamiyama Y. and Tasaka K., Surfactant pretreatment of a polysulfone ultrafilter for reduction of antifoam fouling, Biotech. Bioeng. **43** (1994) 301

Yang M.C. and Cussler E.L., Designing hollow-fibre contactors, AIChE J. **32** (1986) 1910

Zeman L. and Wales M., Polymer solute rejection by UF membranes. in, Turbak A.F. (Ed.), Synthetic membranes. Vol. II. Hyperfiltration and ultrafiltration uses, ACS Symp. Ser. No. 154, Washington DC, Am. Chem. Soc., 1981 pp. 412

Zhang W., Wahlgren M. and Sivik B., Membrane characterization by the contact angle technique. II. Characterization of UF membranes and comparison between the captive bubble and sessile drop as methods to obtain water contact angles, Desalination **72** (1989) 263

Appendix 1

Determination of theoretical elemental composition of copolymers

For PAN-1, the quantities taken for copolymerization were :

Acrylonitrile : 2.375 moles

Acrylamide : 0.4196 moles

Thus, each repeat unit of copolymer chain contains 0.1766 moles of acrylamide for each mole of acrylonitrile.

Then,

No. of H atoms in repeat unit = (3x1) + (5x0.1766) = 3.883

No. of C atoms in repeat unit = (3x1) + (3x0.1766) = 3.5298

No. of O atoms in repeat unit = 1x0.1766 = 0.1766

No. of N atoms in repeat unit = 1+0.1766 = 1.1766

and

Molecular weight of H atoms in repeat unit = 3.883x1.00797 = 3.9139

Molecular weight of C atoms in repeat unit = 3.5298x12.01115 = 42.3969

Molecular weight of O atoms in repeat unit = 0.1766x15.9994 = 2.8254

Molecular weight of H atoms in repeat unit = 1.1766x14.0067 = 16.4802

Thus, mole fraction of H in repeat unit = 3.9139/(3.9139+42.3969+2.8254+16.4802)

= 0.0596

Similarly, mole fraction of other elements can be calculated.

List of Publications / Patents / Presentations

1.Fouling Reduction in Poly(Acrylonitrile-co-acrylamide) Ultrafiltration Membranes, **D.A. Musale** and S.S. Kulkarni; **J. Memb. Sci.** 111(1) (1996) 49

2.Relative rates of protein transmission through modified poly(acrylonitrile) membranes **D.A. Musale** and S.S. Kulkarni; **J. Memb. Sci.** (communicated)

3.Membrane Separations in Biotechnology **D.A. Musale** and S.S. Kulkarni; **Hindustan Antibiotics Bulletin ,** 36(3-4) (1994) 157

4.Flux Decline in Reverse Osmosis and Ultrafiltration : Causes and Solutions, **D. A. Musale** and S. S. Kulkarni; **Indian Membrane Society Bulletin,** 7(1+2) (1995) 6

5.An improved process for the manufacture of ultrafiltration membranes based on poly(acrylonitrile) and its copolymers, S.S. Kulkarni, M.H. Shinde and **D.A. Musale, Indian Pat.Appl.** (applied)

6.Comparative study of acid, cheese and shrikhand whey ultrafiltration, **D. A. Musale** and S. S. Kulkarni (in preparation)

7.Role of synthetic membranes in food, dairy and beverage industry : A critical review, **D.A. Musale**, A. Badrinarayanan, A.M. Bodhe and S.S. Kulkarni (in preparation)

8.Protein Transmission Through Modified Polyacrylonitrile Membranes, **D.A. Musale** and S. S. Kulkarni; Paper presented at an **Indo-French International meet** and XIIIth National Conference of **Indian Membrane Society**, Feb. 28, Mar.1, 1995, Dharwad, India

9.Relative rates of protein transmission through modified poly(acrylonitrile) membranes, **D.A. Musale** and S.S. Kulkarni; Paper presented at 14th National conference of **Indian Membrane Society**, on 'Membranes in chemical and biochemical industries', Indian Instt. of Technology, New Delhi, Feb. 16-17, 1996